DALHOUSIE UNIVERSITY

FACULTY OF GRADUATE STUDIES

The undersigned hereby certify that they have read and recommended to the Faculty of Graduate Studies for acceptance a thesis entitled "Alteration of Opaque Minerals and the Magnetization and Magnetic Properties of Volcanic Rocks in a Drill Hole from an Active Geothermal Area in the Azores."

by Osama Y. Abdel-Aal

in partial fulfillment of the requirements for the degree of Doctor of Philosophy.

Dated January, 1978

External examiner ____

Research Supervisor ____ _____

Examining Committee ____ _____

____ _____

____ ____

_____

_____

DALHOUSIE UNIVERSITY

Date May 2, 1978

Author Osama Youssef Abdel-Aal

Title Alteration of Opaque Minerals and the Magnetization and Magnetic Properties of Volcanic Rocks in a Drill Hole From an Active Geothermal Area in the Azores.

Department or School Geology

Degree Ph.D. Convocation Spring Year 1978

Permission is herewith granted to Dalhousie University to circulate and to have copied for non-commercial purposes, at its discretion, the above title upon the request of individuals or institutions.

Signature of Author

TABLE OF CONTENTS

ABSTRACT

Two hundred and thirty-two polished sections representing ninety-four flow units, three agglomerates and three intrusions from a 981 m borehole drilled in the northern flank of the active volcano Agua de Pau were studied. Opaque minerals were found to be titanomagnetite and ilmenite and their alteration products. Mineralogical and microprobe studies show that both titanomagnetite and ilmenite were subjected to high temperature oxidation and hydrothermal alteration of different degrees in most of the drill core. A new classification for hydrothermal alteration of titanomagnetite and ilmenite in active geothermal areas is proposed.

One hundred and eleven samples were used for rock and paleomagnetic studies. The high Curie temperatures in the drill core indicate a high degree of overall oxidation and alteration. The variation in the magnetic parameters were related to the effect of oxidation and alteration on the magnetic phases. All the magnetic inclinations were normal, indicating a magnetization during Brunhes polarity. The possibility of self-reversal in the drill core was discussed and rejected.

LIST OF FIGURES

LIST OF TABLES

LIST OF PLATES

ACKNOWLEDGEMENTS

The author is greatly indebted to his supervisor Dr. J. M. Hall for his valuable guidance, encouragement, advice and support. To the supervising and examination committee: Professor E. M. Cameron, Dr. D. B. Clarke, Dr. G. K. Muecke, Dr. M. Zentilli, Dr. P. H. Reynolds and Dr. J. Peirce; the author highly appreciated your suggestions and judgment.

Many thanks are extended to M. J. Clark, R. MacKay and S. Parikh for their technical assistance, and to Dr. H. P. Johnson, D. Plasse and P. Rice for their discussions of the paper with the author.

Many people have given me great help and assistance and I am grateful to them all, in particular:

My family who constantly and repeatedly gave me the encouragement to work with enthusiasm to reach my goal,

My friend D. Wightman for all the help given me during difficult times,

The Cultural and Educational Bureau of Egypt, Washington, for renewing my study leave every year.

The author received a Dalhousie Graduate Study Fellowship and additional funds were kindly provided by Dr. J. M. Hall.

During the course of this research, the author was on leave from his post at the Faculty of Engineering, Cairo University, Egypt.

CHAPTER 1

INTRODUCTION

Opaque minerals are minor components of volcanic rocks, but their presence can yield information regarding the history of rocks in which they occur. These opaque minerals include iron-titanium oxides and iron-copper-nickel sulfides.

The magnetic properties of volcanic rocks are highly sensitive to the mineralogy of their iron-titanium oxides. Therefore the study of mineralogy of the system $FeO-Fe_2O_3-TiO_2$ is of prime importance. A wide variety of minerals can be located within this system but the three most important groups are those of the solid solution series: magnetite-ulvospinel, ilmenite-hematite and pseudobrookite-ferropseudobrookite.

1. Mineralogy of the $FeO-Fe_2O_3-TiO_2$ ternary system

The mineralogy of this system has been subjected to extensive investigations by many scientists. Elsdon (1975), gives an excellent review of the literature and the progress in this field. The system, figure 1, includes the following series:

1.1. Magnetite-ulvöspinel series ($FeO \cdot Fe_2O_3-2FeO \cdot TiO_2$): This is known as the β series. It shows complete solid solution above 600°C (Vincent et al. 1957) and Basta (1960), figure 2. The two end members possess

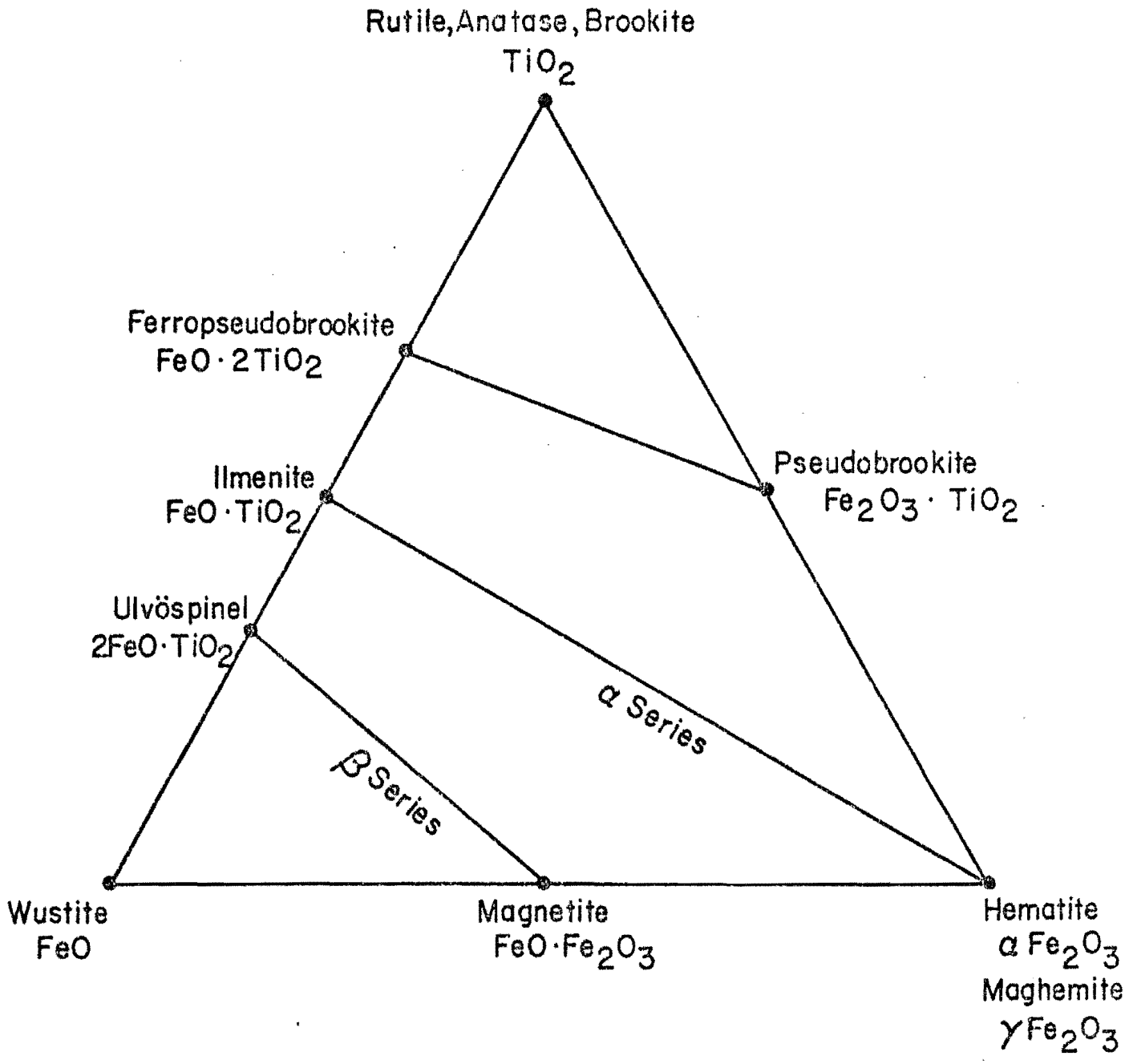

Figure 1. FeO-Fe_2O_3-TiO_2 ternary diagram of the composition of iron-titanium oxides.

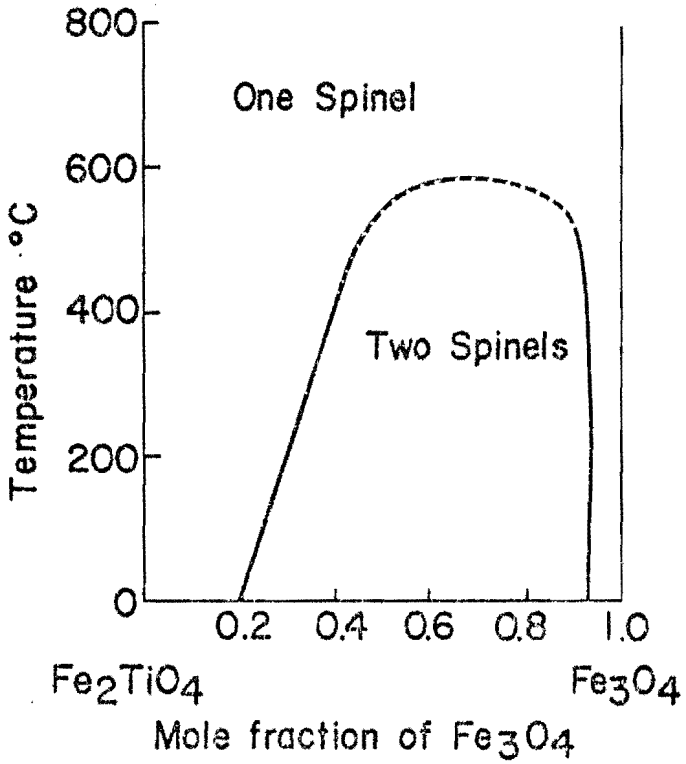

Figure 2. Possible form of the solvus in the magnetite-ulvöspinel series. After Basta (1960) from Nagata (1961).

inverse spinel structure. In magnetite, Fe^{2+} and half Fe^{3+} ions occupy the octahedral sites while the remaining Fe^{+} ions are in the tetrahedral sites. The introduction of Ti^{4+} into the magnetite lattice increases the cell dimension from a = 8.395Å to a = 8.535Å (O'Reilly 1976). Banerjee et al. (1967), Stephenson (1969), Bleil (1971) and Jensen and Shive (1973) studied the cation distribution for intermediate compositions in the series. They concluded that, in contrast with Fe_3O_4, both Fe^{2+} and Fe^{3+} ions are present in the tetrahedral sites throughout most of the series. Ti^{4+} has a strong preference for the octahedral sites.

Magnetite often contains small amounts of Al^{3+}, V^{3+} and Cr^{3+} in substitution for Fe^{3+} and Mg^{2+}, Ca^{2+}, Mn^{2+} and Co^{2+} for Fe^{2+}. The variations in minor elements in the magnetite-ulvospinel series and their role in the properties of the series have been examined by many researchers. Vincent and Phillips (1954) and Ade-Hall (1964) detected small amounts of Si in magnetite, but this may represent contamination. Oshima (1971), on his study of dacites from Haruna volcano, Japan, has shown that in magnetite that crystallized before and after eruption, while Fe, Al and Mg decreased, Ti, V and Mn increased as crystallization proceeded. In addition, Prevot and Mergoil (1973), described successive crystallization of magnetite from alkali basalt at Saint-Clement, France, with large increases in Ti, a slight rise in Mn and falling Al and Mg as crystallization proceeds. The same trend, with the absence of Mn, has been observed by Abdel-Aal et al. (1976) in a study of basalts from Mid-Atlantic Ridge (MAR) at 37°N. The increase in titanium is attributed to decreasing oxygen fugacity in the magma during its ascent.

Experimental work on the stability of Fe-Ti oxides has shown that in the presence of oxygen, ulvöspinel is unstable with respect to ilmenite. Although unmixing is extremely slow at ambient temperature in the magnetite-ulvöspinel series, intergrowths of magnetite and ulvöspinel have been reported by Vincent and Phillips (1954), Anderson (1966) and Ramdohr (1969).

1.2. Hematite-Ilmentite series (Fe_2O_3-$FeO{\cdot}TiO_2$): This is referred to as the α series by Verhoogen (1962). The series shows complete solid solution above 950°C but unmixing occurs at lower temperatures. The members of the series possess rhombohedral structure, in hematite, Fe^{3+} fills two-thirds of the octahedral sites within the hexagonally close-packed oxygen lattice, while in ilmenite, the oxygen positions are slightly irregular. The cell dimensions increase with Ti content (a = 5.427Å in hematite and a = 5.534Å in ilmenite). Carmichael (1967) and Elsdon (1972) have shown that substitution of Mg and Mn for Fe and Ti in ilmenite occurs. Small amounts of Fe^{2+} and Mn are usually present in hematite (Elsdon 1975).

Various experimental studies have been carried out to deduce the shape of the solvus for the hematite-ilmenite solid solution, figure 3, (Nicholls 1955, Uyeda 1958, Carmichael 1960, Ramdohr 1969 and Lindh 1972). The results of these investigators are rather contradictory and none agree well with the predictions of thermodynamic analysis (Rumble 1972). Rumble predicted that rutile + magnetite is stable with respect to hematite + ilmenite. However, the former assemblage is less common

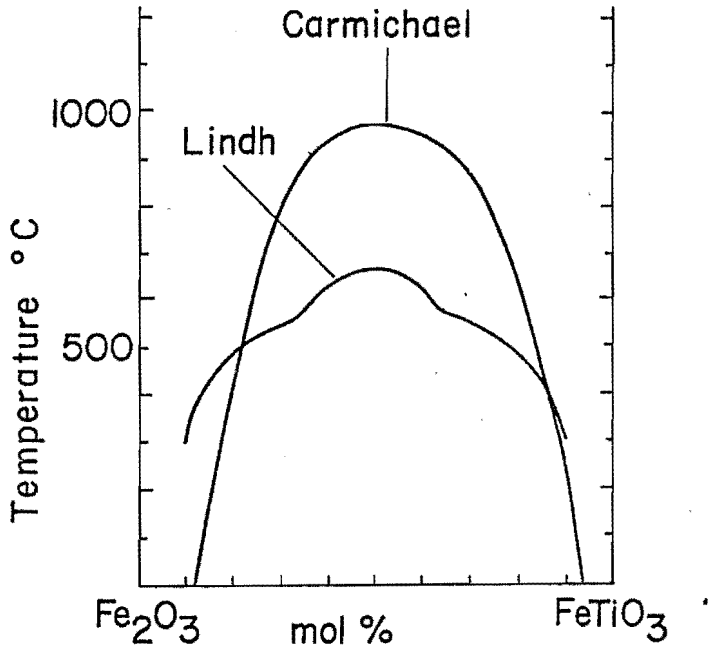

Figure 3. Two possible forms of hematite-ilmenite solvus curve as deduced by Carmichael (1960) and Lindh (1972), from Elsdon (1975).

in nature than the latter.

1.3. Pseudobrookite-Ferropseudobrookite ($Fe_2O_3 \cdot TiO_2$-$FeO \cdot 2TiO_2$) series: Pseudobrookite has an orthorhombic structure. The structure of ferropseudobrookite has been described by Lind and Housley (1972) as related to pseudobrookite. Ti^{4+} ions occupy the octahedral sites while Fe^{2+} and Mg^{2+} ions are randomly distributed over the tetrahedral sites. Ferropseudobrookite is not known to occur in terrestrial rocks. It has been described in lunar rocks by Haggerty (1973b). Solid solution between pseudobrookite and ferropseudobrookite is complete above 1150°C (Akimoto et al. 1957, Haggerty and Lindsley 1969) figure 4 , but ferropseudobrookite decomposes at 1140°C and pseudobrookite breaks down at 585°C (Haggerty and Lindsley 1969). Considerable variation in composition of the naturally occurring members of this series has been reported by Otteman and Frenzel (1965).

1.4. Polymorphs of TiO_2: Rutile, anatase and brookite are polymorphs of TiO_2. Rutile is the most common and is stable over a wide range of pressure and temperatures (Dachille et al. 1968). The inversion anatase $\rightarrow$ rutile depends on pressure (Dachille et al. 1968), temperatures (Schröder 1928) and chemical environment (Iida and Ozaki 1961 and Shannon 1964). Brookite is formed preferentially in the presence of traces of Fe_2O_3 and low oxygen fugacity (Shannon and Pask 1964 and Heald and Weiss 1972).

Although these minerals are formed as the product of oxida-

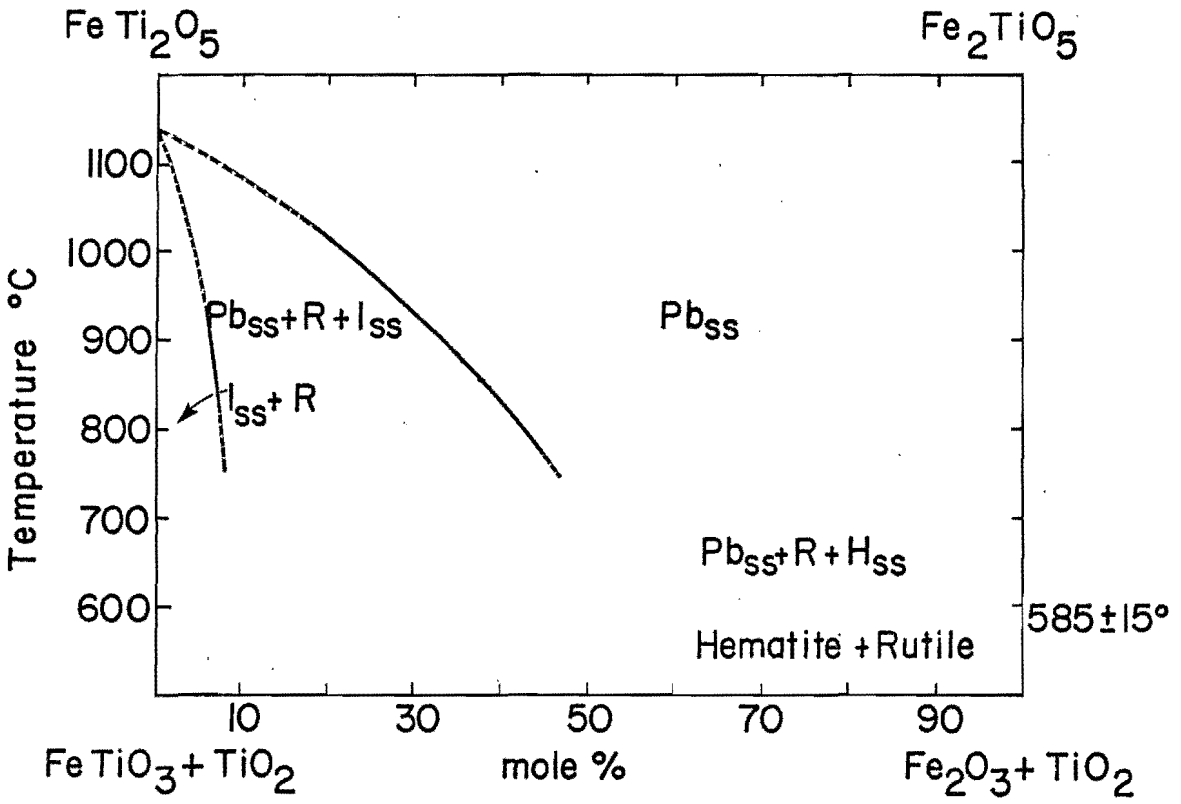

Figure 4. Stability relations in the pseudobrookite-ferropseudobrookite series. (After Haggerty and Lindsley 1969).

tion of iron-titanium minerals in basalts, they are also formed as primary minerals under a considerable range of conditions (Lerz 1968, Ramdohr 1969 and Elsdon 1975).

1.5. Wüstite (FeO): Wüstite has a cubic structure (Walenta 1960). The stability field for this mineral in the system Fe-O is such that the formation of the mineral is very unlikely under geologic conditions (Ramdohr 1968). However, Walenta (1960) has identified wüstite which was formed in a tuff products of volcanic activity in Stuttgart. Rapid cooling produced and preserved this wüstite.

1.6. Cation deficient phases ($Fe_aTi_b\square_cO_4$, a+b+c = 3 and $\square$ denotes vacancy: This series has a spinel structure and is called titanomaghemite. Vacancies are present on the octahedral sites (Hagg 1935). This conclusion was verified by the x-ray work of Verwey (1935) and measurements of saturation magnetization (Ozima and Sakamoto 1971, Readman and O'Reilly 1972 and O'Donovan and O'Reilly 1977a). Properties of titanomaghemite have been determined using synthetic materials. At atmospheric pressure the upper temperature limit to the stability field of titanomaghemites is about 350-400°C (Hauptman 1974). Heating titanomaghemites to above 350°C in vacuum produces a variety of inversion products depending on the composition of the spinel phase prior to inversion (O'Reilly 1976). Studies of natural occurrences demonstrate that the normal mode of formation is by oxidation of titanomagnetite (Katsura and Kushiro 1961, Prévot et al. 1968, and others in the study of deep sea drilling pro-

ject materials). However, Harrison and Peterson (1965), described a occurrence of primary titanomaghemite in deep-sea cores from the Indian Ocean.

2. Oxidation and alteration of iron-titanium oxide minerals:

The composition of the magma and the conditions of cooling, determine the iron-titanium oxide formation. Quenching the melt from above 1000°C, results in the crystallization of homogeneous titanomagnetites ($Fe_{3-X}\ Ti_X\ O_4$, $0 < x < 1$). When the rate of cooling becomes slow, the iron-titanium system equilibrates with the oxygen fugacities pressure corresponding to each temperature. At high temperatures (above 600°C), intergrowths of oxides of spinel and rhombohedral structure will form. This process is known as deuteric oxidation. At low temperatures (< 300°C) oxidation of titanomagnetite results in the formation of titanomaghemite, sphene and hematite. A mixture of both types of oxidation may take place between 300-600°C (intermediate temperatures).

2.1. Oxidation at high temperatures: The oxidation of titanomagnetites is a complex process. It has received intensive study during the last decade because of its importance in rock magnetism and its use as geological thermometer. Deuteric oxidation of titanomagnetite is classified into successive stages of increasing degree of oxidation by Wilson and Haggerty (1966), Watkins and Haggerty (1967), Ade-Hall et al. (1968a) and Wilson et al. (1968). The classification depends

on the formation of a sequential series of a Fe-Ti oxide assemblage in which ilmenite, rutile and hematite are intermediate stages and pseudobrookite solid solutions are end products. However, Haggerty and Lindsley (1969) have studied experimentally the stability of pseudobrookite and concluded that pseudobrookite is unstable with respect to rutile + ilmenite - hematite solid solution at low temperatures (< 585°C).

The oxidation of ilmenite at high temperatures has been classified into six stages by Haggerty (1971). In his classification: rutile + titanohematite is an intermediate stage while pseudobrookite solid solutions are end products. The evidence for his classification was derived from vertical traverses through Icelandic lavas (Watkins and Haggerty 1967) and from variable oxidation zones in Makaopuhi lava lake, Hawaii (Sato and Wright 1966).

Many researchers have studied the stability field of the iron-titanium oxide phases and their temperature of formation. Verhoogen (1962), suggested that spinel and rhombohedral phases may be stable at high temperatures in the presence of reducing magmatic gas phases. The work by Vincent et al. (1957), Akimoto et al. (1957), Webster and Bright (1961), Carmichael and Nicholls (1967), Haggerty and Lindsley (1969), Haggerty (1971) and others, indicated that deuteric oxidation assemblages are functions of temperature (above 600°C) at high oxygen fugacity. If the oxidation products of oxide minerals do not include pseudobrookite, oxidation very likely took place below 600°C.

The mechanism by which deuteric oxidation occurs is not fully understood. However, some light has been thrown on this problem by Sato and Wright (1966). They suggest that high temperature oxidation may take place when part of the cooling lava behaves as a semi-permeable membrane, permeable to hydrogen but not to oxygen. Then dissociated water vapour would lose its hydrogen so leaving the remaining oxygen free to react with the Fe^{2+} of titanomagnetite, ilmenite and olivine.

2.2. Oxidation at low temperatures: The second type of oxidation of Fe-Ti oxides described in the literature, involves the formation of a cation deficient material of spinel structure at low temperatures (< 300°C). In this type of oxidation, titanomagnetites may react in the lava with residual, oxygen rich, liquids or later with ground water so that their bulk composition, but not structure, changes toward the ilmenite-hematite series. This low temperature oxidation of titanomagnetite yields non-stoichiometric titanomagnetites of general composition $Fe_a\ Ti_b\ \square_c\ O_4$ where a+b+c = 3 and $\square$ indicates a vacant lattice site occupied in a stoichiometric spinel.

A mechanism for the production of cation deficient iron-titanium spinel oxides has been suggested by Readman and O'Reilly (1970). They suggested that prolonged oxidation of titanomagnetite at low temperatures (< 300°C) may be the process responsible for the formation of cation deficient titanomagnetite. The evidence for their mechanism came from the discovery of such materials in little altered continental and submarine igneous rocks.

The composition of the original titanomagnetite, temperature of oxidation, degree of oxidation, rate of cooling and the presence of foreign ions as stabilizers all play an important role in the type of intermediate mineral produced.

The inversion of titanomaghemites takes place by heating to temperatures above 350°C (O'Reilly 1976). The products of inversion depend largely on the composition of the spinel phase prior to inversion. Any Fe^{2+} in titanomaghemite appears in an iron-rich spinel phase. Depending on the degree of oxidation, Ti^{4+} goes towards the formation of ilmenite or, in more highly oxidized samples, anatase, TiO_2 or pseudobrookite, $Fe_2\ TiO_5$. Hematite is a constituent of the inversion products of more highly oxidized compositions.

Low temperature oxidation of titanomagnetite has been observed also in the cold, deep ocean environment. The process is actually a chemical exchange between lava and sea floor at temperatures close to 0°C. Ade-Hall et al. (1976a) in their work on Deep Sea Drilling Project (DSDP) samples, Leg 34 and other legs have described changes in titanomagnetites such as color lightening, reflectivity increase, volume change cracks and replacement of titanomagnetite by a grey phase with very fine grain size. These features have been observed also by others, Hall and Fischer (1977) and Johnson (in press) and were related to halmyrolytic alteration process of the whole rock (Hart 1973).

The oxidation of magnetite to maghemite $\gamma\ Fe_2O_3$ is a special case of cation deficient oxidation type, in which Fe^{2+} occurs only in

octahedral sites of magnetite and thus vacancies occur only in octahedral sites of maghemite. The question of whether magnetite will be oxidized to maghemite or hematite is still unresolved. It has been studied by many workers but contrasting results obtained. Earlier, Geith (1952) and Schmidt and Vermaas (1955) have shown that natural (impure) magnetite is oxidized directly to hematite with no intermediate formation of maghemite. However, David and Welch (1956) have shown in the laboratory that oxidation product depends on the reaction conditions. They performed "dry (no moisture)" oxidation experiments which yielded, with difficulty, hematite by a single-stage reaction ($2Fe_3O_4 + O_2 \rightarrow 3 \alpha Fe_2O_3$), while under wet conditions maghemite formed with relative ease. The two stage reaction has been suggested by Lepp (1957) and confirmed by Davis et al. (1968). Lepp has demonstrated experimentally that when natural magnetite is heated in air, in the range 200° to 275°, maghemite is formed. Above 550°C hematite is the product of oxidation, while at intermediate temperatures magnetite is changed to maghemite which then inverts to hematite. Later, Basta (1959) concluded that there are two different processes in the oxidation of magnetite; a continuous process which results in the formation of maghemite and a discontinuous process which forms hematite and is called the martitization process. Colombo et al. (1968) argued on the basis of their experiment that hematite is never formed directly from magnetite unless hematite nuclei are already present. Recently, Johnson and Merrill (1972) have successfully produced maghemite and hematite by

oxidizing pure magnetite at temperatures of between 50°C and 200°C, depending on the water content of the initial material. In conclusion, it seems that the conditions governing the oxidation of magnetite to either maghemite or hematite are not fully studied. More work is needed. The instability of maghemite at moderate temperatures (400°C) suggests that hematite rather than maghemite might form as a result of oxidation of magnetite. However, impurities may play an important role in raising the stability of maghemite to higher temperatures.

The oxidation of ilmenite has been in dispute for many years. Most of the previous workers (Lynd et al. 1954, Bailey et al. 1956, Flinter 1959, Temple 1966 and Grey and Reid 1975) are agreed that ilmenite undergoes alteration (oxidation and leaching) during which, iron is removed from the structure, resulting in a relative enrichment in TiO_2. The nature of alteration product has not yet decided. The very fine grain size of alteration products make positive identification extremely difficult. Lynd et al. (1954) indicated that the alteration products are either a mixture of ilmenite and hematite or rutile. Bailey et al. (1956) reported the progressive breakdown of the ilmenite lattice in weathering to an amorphous material identified by them as leucoxene. X-ray studies of two different leucoxenes, brown and white, gave a rutile pattern. However, they also recorded both brookite and anatase in leucoxene from the black sands of Mozambique. Flinter (1959) studied the alteration of ilmenite and concluded that rutile is the product of alteration. He used the term "diffuse rutile" to prevent any confusion with primary rutile. Three different types of leucoxenes

have been studied by Karkhanavala et al. (1959). Type 1, white leucoxene, consisted of rutile and only small numbers consisted of rutile and anatase. On the other hand brown and black leucoxene contained a pseudobrookite as the main constituent. Teufer and Temple (1966) introduced pseudorutile as a new mineral intermediate between ilmenite and rutile. This led Temple (1966) to suggest that rutile and pseudorutile are the end products of ilmenite alteration. Grey and Reid (1975) agreed with Temple and they proposed a mechanism for alteration of ilmenite to rutile with pseudorutile as an intermediate mineral. In spite of all these various studies, the stages of alteration of ilmenite still need more investigation. The stability of the various phases as well as the role of water in ilmenite alteration and the removal of iron from ilmenite to form rutile, all are important factors which must be taken into consideration for any proposed mechanism of ilmenite alteration.

2.3. Oxidation at intermediate temperatures: This type of oxidation has not fully been considered in the literature. In this type, which takes place between 600-300°C, a mixture of high and low temperature oxidation of Fe-Ti oxides may take place. Verhoogen (1962) has concluded on thermodynamic grounds that none of ilmenite, ulvöspinel or magnetite are stable with respect to oxidation by magmatic gases at temperatures of less than 600°C. Rutile and hematite are the only stable phases. Haggerty and Lindsley (1969) have reported the breakdown of pseudobrookite to rutile and hematite at temperatures $< 585°C$. Oxidation of magnetite to hematite may occur in this intermediate

stage. However, the overlap and the mix between low and high temperature oxidation may be the reason for the lack of study in this range of temperatures.

2.4. Combined action between regional hydrothermal alteration and other oxidation processes: This combined action comes from reheating of the Fe-Ti oxides as a result of the burial of lavas by subsequent flows. Heated ground water is the major factor in regional hydrothermal alteration. Ade-Hall et al. (1971) have described a combined action of two alteration processes, deuteric oxidation and regional hydrothermal alteration on basaltic lava at a maximum temperature of 300°C and pressure of 1 kb. They described the variations in titanomagnetite and ilmenite features due to this combined action. However, some parts of their classification need to be revised. The necessity for revision comes from the instability at low temperatures in the presence of water of some of the phases identified by them.

3. The relation between magnetization and the mineralogy of iron-titanium oxides:

3.1. Introduction: A small number of magnetic minerals are responsible for the magnetization of rocks during their formation or later by the action of oxidation and alteration processes. Measurements of the remanent magnetization of these minerals are used in determining the nature of the ancient geomagnetic field, while other magnetic studies describe the alteration history of the rocks containing these minerals.

The properties of the most important magnetic minerals, the titanomagnetites have been established mainly using synthetic minerals. Magnetite is ferrimagnetic due to the unbalanced Fe^{2+} in its octahedral lattice. The change in composition from magnetite towards ulvöspinel is marked by an increase in size and distortion, but still cubic, of the unit cell. Ulvöspinel itself is antiferromagnetic as it has equal amounts of Fe^{2+} in both sub-lattices. However, the Curie temperature, the temperature above which a magnetic mineral loses its magnetism, of the ferrite solid solution falls to below room temperature before the composition ulvöspinel is reached. The presence of greater strains, imperfections and impurities, other than titanium, in natural minerals generally slightly lower their Curie temperature and reduce their saturation moments (Tarling 1971). Ilmenite and hematite have the same amount of iron in each antiparallel crystal lattice and therefore basically antiferromagnetic. Hematite carries a weak, but very hard, parasitic ferromagnetism. The origin of this parasitic ferromagnetism could be explained as the oppositely magnetized Fe^{3+} ions in the two sub-lattices are canted at small angle (McElhinny 1973). A great deal of variation is found in the reported magnetic properties of hematite (Jacobs et al. 1971) and thus only generalization about the magnetic properties of hematite is possible (O'Reilly 1976). Figure 5 shows the system $FeO-Fe_2O_3-TiO_2$ with magnetic parameters for end members.

The opaque mineralogy of basalts has been correlated with such magnetic properties as stability, intensity and polarity of natural remanent magnetization (NRM), saturation magnetization and Curie temperatures.

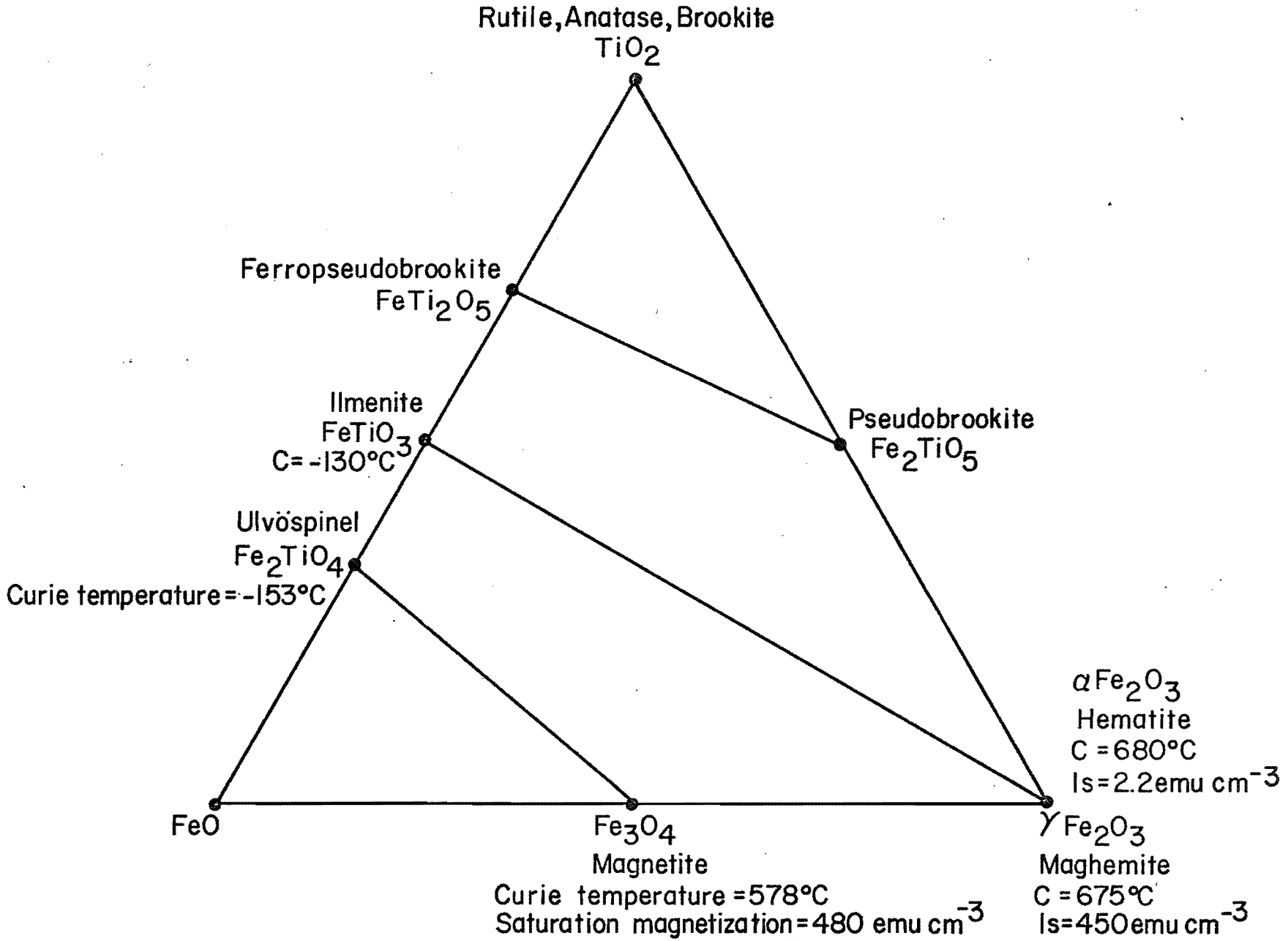

Figure 5. Curie temperatures and saturation magnetization of magnetic minerals in the ternary system FeO-Fe_2O_3-TiO_2. (Data from McElhinny 1973).

3.2. Opaque mineralogy and stability of remanence: The relationship between the alteration of titanomagnetite and the stability of the remanence has been established since Graham (1953) suggested that alteration could result in increased coercive force. This has been confirmed by the work of Watkins and Haggerty (1965), Larson et al. (1966), Strangway et al. (1968b), Ade-Hall et al. (1968b) and Ade-Hall (1969). These workers related the increase in stability with oxidation to the development of sub-solidus exsolution of ilmenite lamellae following oxidation of primary ulvöspinel rich titanomagnetite. This exsolution model has been criticized by Stacey and Banerjee (1974). They suggested that the observed high stability of NRM in rocks could be due to hematite and not subdivided magnetite. Watkins and Haggerty (1965) suggested that the strong stable remanence may be associated with small magnetite particles produced by oxidation of ferromagnesian silicates. However, Hargraves and Ade-Hall (1975) concluded, from their study on unoxidized and oxidized Icelandic basalts, that the natural remanence is associated with original Fe-Ti oxide grains and not with the breakdown products of ferromagnesian silicates. Whether titanomagnetite granulation influences remanence stability, is answered by Ade-Hall (1969). He stated that titanomagnetite granulation when unusually highly developed seems to increase the stability of the remanence. It seems that the problem of stability involves other factors than grain division by oxidation. Merrill (1975) listed these factors as: grain shape, grain volume, saturation magnetization, exchange energy and the grain environment. All these factors must be properly evaluated in any viable explanation of change in stability with oxidation.

3.3. Opaque mineralogy and the intensity of NRM: This relation has been studied by many scientists. High remanence intensity always being associated with initial deuteric oxidation of titanomagnetite (Watkins and Haggerty 1965, 1967, Wilson et al. 1968, Ade-Hall et al. 1968b, Gromme et al. 1969 and Lawley and Ade-Hall 1971). On the other hand, the effect of low temperature oxidation of titanomagnetite on the intensity of NRM is still in debate. Many investigators have shown that low temperature oxidation of titanomagnetite reduces the intensity of remanence (Ozima and Larson 1968, Carmichael 1970, Irving et al. 1970, Marshall and Cox 1971b, Ozima et al. 1974, Johnson and Atwater 1977 and others). However, other workers have reported contrasting results. Marshall and Cox (1971a) indicated experimentally that oxidation of titanomagnetites near 200°C actually increased the intensity of NRM. Later Johnson and Merrill (1972, 1973, 1975) have shown in laboratory that the intensity of titanomagnetite is reduced on oxidation at low temperatures (50°C or below), but that is increased at 150°C or so. One possible explanation could be the nature of oxidation products. At low temperatures (50°C or below) only cation deficient phases (γ) appears as product of oxidation which have shown by Ade-Hall et al. (1976a) and others to decrease the NRM intensity. At temperatures $\simeq$ 150°C, γ phases, titanohematite phases and other non-magnetic oxides formed.

3.4. Opaque mineralogy and the polarity of NRM: Many rocks are magnetized in the opposite direction to that of the Earth's present

magnetic field. This means that either the geomagnetic field reverses its polarity or the magnetization in the rock can be acquired in a direction opposite to that of the ambient field. It has been argued that there is a correlation between magnetic polarity and oxidation state. A strong correlation has been found in several igneous rock sequences between the polarity and the degree of oxidation of their iron-titanium oxides (Wilson 1966, Wilson and Watkins 1967, Watkins and Haggerty 1968 and Ade-Hall and Wilson 1969), where reverse polarity samples were associated with high oxidation state. Conversely, Larson and Strangway (1966), Watkins and Haggerty (1968) and Ade-Hall and Watkins (1970) in other samples have shown no correlation between opaque minerals and the NRM polarity in basaltic rocks. Although there is experimental evidence of self-reversal in minerals (Ozima and Larson 1968, Peterson and Bleil 1973, Ryall and Ade-Hall 1975 and Hoffman 1975), only few cases have been found in nature. It appears that further work is necessary to approach satisfactory conclusion and to assess the meaning and importance of relationship between opaque mineralogy and natural remanence polarity.

3.5. Opaque Mineralogy and Saturation Magnetization and Curie temperatures: The relation between opaque mineralogy and magnetic properties of rocks have been established since Ade-Hall et al. (1965) correlated the oxidation of titanomagnetite with all the features of Curie temperatures distribution. High strong-field Curie points have always been found associated with high deuteric oxidation of titano-

magnetite (Wilson et al., 1968 , Ade-Hall et al., 1968b , Grommé et al., 1969 and Lawley and Ade-Hall 1971). The relationship between mineralogy and magnetic properties of non-stoichiometric (cation deficient) titanomagnetite has been examined experimentally by Readman and O'Reilly (1972). They found that Curie temperature increases with degree of oxidation. They construct contours of equal cell edge and Curie temperature for spinels in the FeO-Fe_2O_3-TiO_2 system, figure 6. The contours are useful in the identification of naturally occurring cation deficient phases, provided they don't contain appreciable amounts of other impurity cations. Ade-Hall et al. 1976b and Ryall et al. (1977) have shown, on the study of DSDP samples, that all magnetic properties change by oxidation of titanomagnetite at low temperatures. The Curie temperature increased and the saturation magnetization decreased when the parameter z (degree of oxidation of titanomagnetite) increased.

In order to separate the effects of deuteric oxidation and regional hydrothermal alteration, Ade-Hall et al. (1971) have examined the Curie point curves for some basaltic lavas. Both processes produced marked changes from the single-low-Curie point thermomagnetic curve of recently erupted basalts. Extreme action of both processes results in indistinguishable single high-Curie point curves. Double Curie points in partly deuterically oxidized samples are taken as an indication of an intermediate degree of alteration by the deuteric process. Regional hydrothermal alteration results in single-Curie point curves; the Curie point being proportional to the degree of alteration.

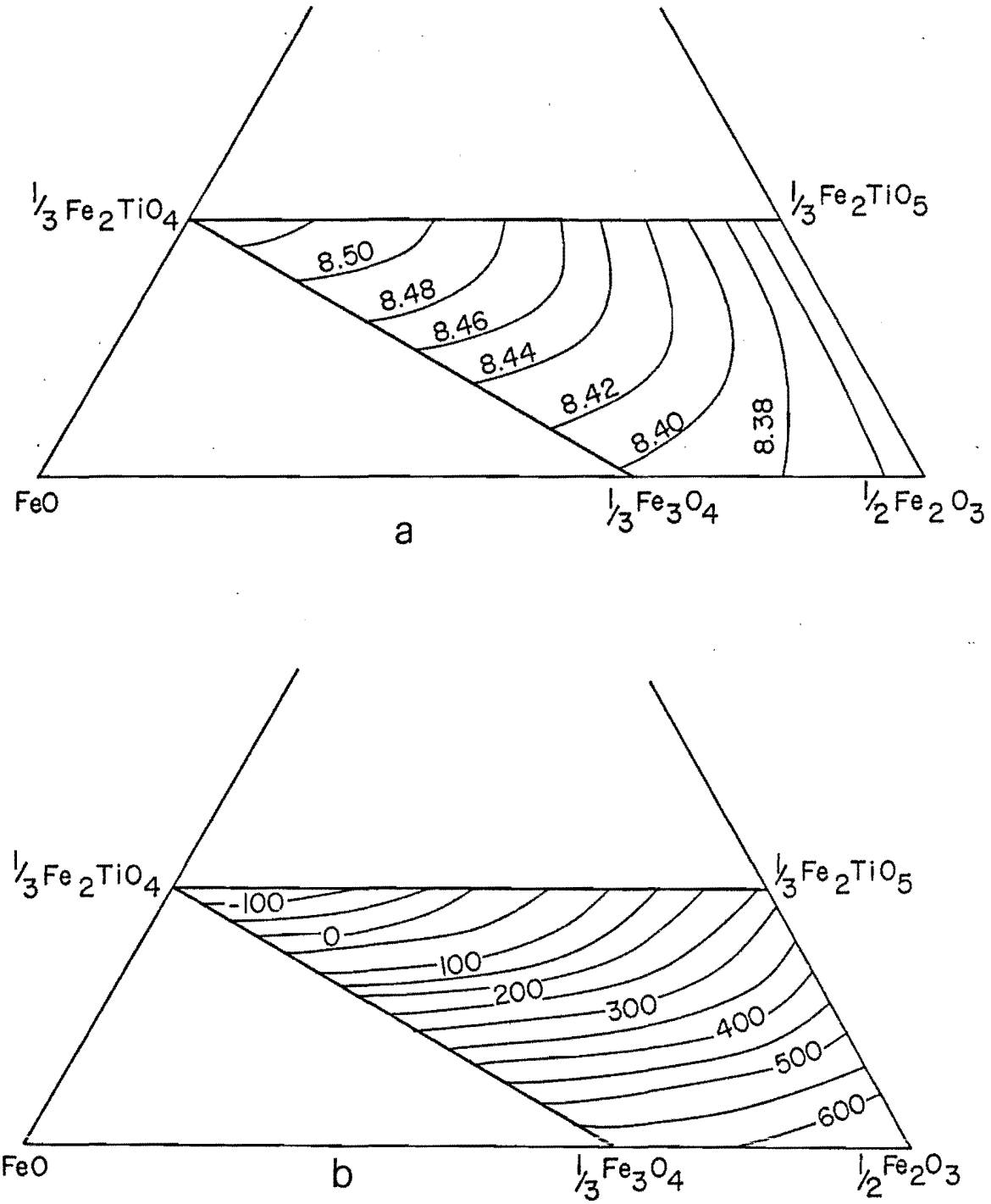

Figure 6. Contours of equal cell edge and Curie temperature for spinels in the FeO-Fe_2O_3-TiO_2 system (after Readman and O'Reilly 1972).

4. Analytical methods and other techniques in the study of Fe-Ti oxides:

Ade-Hall (1964), has pointed out that ordinary chemical analyses of naturally occurring magnetic phases should be abandoned due to the difficulties in obtaining pure extracts. He used the electron probe micro-analyzer to obtain the weight percent of elements present in the area of few microns. Creer and Ibbetson (1970) used a combination of micro-probe and magnetic studies of non-stoichiometric titanomagnetites in basaltic rocks. They defined the compositional point of titanomagnetite as the point of intersection between oxidation line and a Curie point contour. Gidskehaug (1975) adopted a method to determine the degree of non stoichiometry of iron-titanium oxides using electron probe micro-analyses. His method provides a new way to study the effects of oxida-tion and forms the basis of a procedure to test the phase uniformity of optically homogeneous cation deficient spinels. Recently, Hoblitt and Larson (1975) described a combination of techniques for determina-tion of the ultrafine structure of magnetic minerals. A variety of submicroscopic inclusions and structures have been observed in etched magnetite using scanning electron microscope and up to 50,000 X magnification.

5. Sulfide minerals in basalts:

Sulfides are minor opaque minerals in basalts. Although their presence could add more information about the history of the rocks in which they occur, they have been neglected in the literature. Since

the excellent work by Desborough et al. (1968) and Skinner and Peck (1969) no valuable information has been added. Several sulfide minerals have been described by Abdel-Aal et al. (1976), Ade-Hall et al. (1976a) and MacLean (1977) but the origin of these phases has not fully been discussed. Desborough et al. (1968) described polymineralic sulfide grains composed principally of Fe, Cu, S and small amount of Ni in tholeiitic basalts of Kilauea volcano, Hawaii. The grains appear to represent a once-immiscible sulfide droplets in a basaltic crystal mush or a glass that was partially crystallized during rapid cooling after the lavas were extruded. Skinner and Peck (1969), identified "solid sulfide globules" from lava lake in Hawaii. These globules were characterized by a lack of magnetite and by pyrrhotite and chalcopyrite with more Ni than the "immiscible sulfide liquid" globules. Enrichment in sulfur of the interstitial material from the lava lake could be the reason.

Except for pyrrhotite, most sulfide minerals are non-magnetic. Pyrrhotite has been investigated by Bhimasankaram (1964) and Schwartz and Vaughan (1972). As mentioned by Tarling (1971), pyrrhotite can spontaneously self-reverse in extremely weak fields if it contains appropriate variations in vacancy distribution within its lattice to give different Curie temperatures in different locations within the same structure.

However, more study on sulfide mineralogy and their magnetic properties are needed.

6. Aim of the present work:

The study of rocks from an active geothermal system is of interest because of the analogies that may be drawn between these and the well-known hydrothermal ore-forming systems. The rocks in hydrothermal areas are altered with many secondary minerals, the nature of which depends on the chemical composition of the rock, temperature, water composition, rate of water flow and the availability of gases. Some of these are known for the 1973 Azores drill hole in the island of Sao Miguel.

The differences in petrology and geochemistry between island rocks and deep ocean crustal rocks and the geophysical data suggest that special processes operate beneath oceanic islands. The information from deep drilling is essential to understand the process of island formation and its relation to the ocean floor spreading process. The study of 981 m core of subaerial and submarine lavas, pyroclastic and volcanic sediments from the Azores has given an insight of the process of island formation.

The importance of an opaque mineralogy study of the Azores rock is to follow alteration in an active geothermal system--a situation which has not been studied before, and to relate the variation in mineralogical phases to known temperatures and pressures instead of guessing at past temperatures. An essential part of the alteration study is the identification of low temperature phases, which are relatively poorly known in experimental petrology. The comparison between the oxidation state of opaque phases and the state of silicate alteration (unpublished report

by Sarkar 1976 and McGraw 1976) is an assessment in understanding the alteration history of the Azores rocks, since silicates provide conventional hydrothermal alteration indicators. The behavior of the minor elements in the opaque phases during hydrothermal alteration and the partitioning of these elements during phase splitting following deuteric oxidation, are further aims of the opaque mineralogy study. In addition this study includes the use of quantitative reflectivity technique to measure the reflectivity of mineral phases at certain wavelengths and correlate these measurements with oxidation state. This is the first application of this technique to oxidized samples in geothermal areas. Sulfide minerals, their absence or presence, are interesting as hydrothermal alteration indicators. Their absence may indicate that sulfur has suffered considerable redistribution subsequent to the initial crystallization of their host rocks, or that sulfur may have escaped as gases, or sulfides have been subjected to extreme action of hydrothermal alteration.

This study also adds more information to our knowledge of the relation between opaque mineralogy and magnetic properties of rocks and may assist in better understanding of this relation in hydrothermally altered areas.

From all these studies a general model for the crystallization and alteration of a volcanic sequence in active geothermal areas is proposed.

CHAPTER 2

GEOLOGY OF THE AREA

1. Introduction and literature review:

The Azores archipelago consists of nine islands aligned broadly in the NW-SE direction. Their alignment intersects the MAR at 39°N, figure 7. The islands are divided by the MAR into two groups: Corvo and Flores on the west flank of the ridge and Santa Maria, São Miguel, Terceira, Graciosa, São Jorge, Pico and Faial on the eastern side of the ridge.

Morphologically, the Azores platform, of which the islands are the subaerial expression, appears to represent a broadening of the MAR. Machado (1959 and 1969) suggested that the trends of most of the islands were controlled by the Azores-Gibraltar Alpine contraction belt. LePichon (1968) pointed out that the Azores region may represent the junction of the European, African and North American plates. Banghar and Sykes (1969) and Dewey and Bird (1970) indicated the possibility that Alpine contraction might be replaced by expansion from over the Azores islands segment of the Azores-Gibraltar line. Krause and Watkins (1970) identified five features which they say must be taken in consideration if any model of the genesis of the Azores is to be constructed (figure 8). These are: (i) the seismically active East Azores Fracture Zone (EAFZ) extending from Gibraltar to the MAR; (ii) the transverse island chain of the Azores which trends southeast-

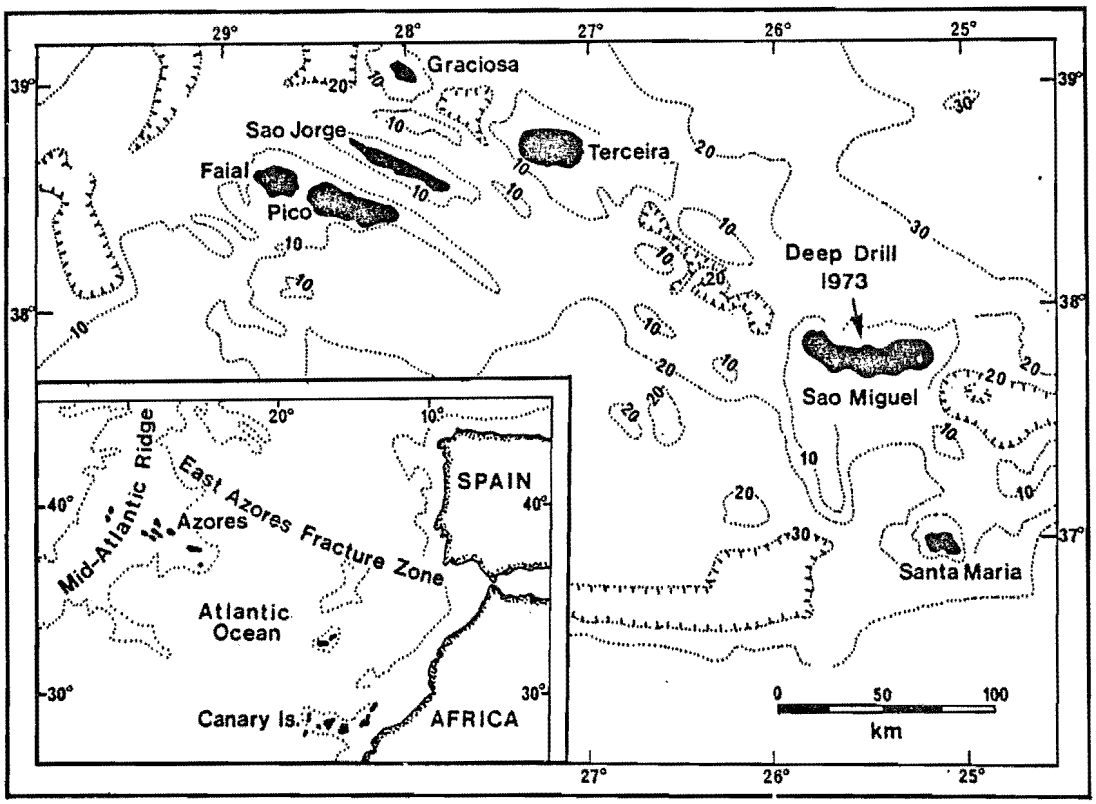

Figure 7. Location map of Deep Drill 1973. Site coordinates 25° 31.4'W, 37° 48.9°N at 5 km from the caldera wall of Agua de Pau volcano, São Miguel. 1,000 m bathymetric contours are shown. (After Muecke et al. 1974).

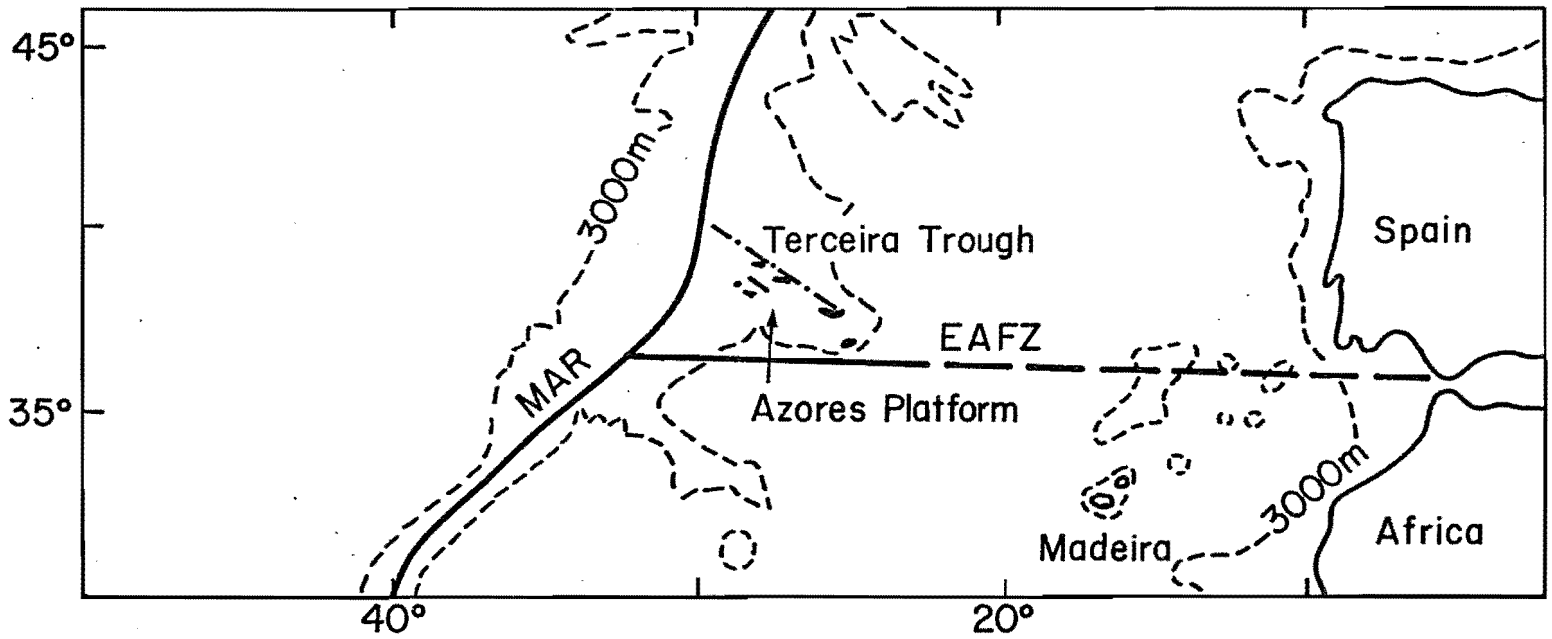

Figure 8. Tectonic features of the Azores area.

northwest across the MAR; (iii) the marked change in direction of the MAR at 38°N from northeast-southwest to north-south (iv) the broadening of the MAR to the east; and (v) the seismically inactive West Azores Fracture Zone (WAFZ) which is off northwards from the trend of the EAFZ. However, there is no evidence to support the existence of WAFZ and Krause (1977)(quoted in Schilling 1977 personal communication) no longer believe that it exists.

Various models to describe the genesis of the Azores have been proposed (Cloos 1939, Krause and Watkins 1970, Morgan 1971, 1972, McKenzie 1972, Machado et al. 1972, Ridley et al. 1974 and Schilling 1975a). Earlier, Cloos (1939) has attributed the tectonic features of the Azores to a series of folds developed across the MAR. Recently, the development of crustal plate tectonic models has led Krause and Watkins (1970) to characterize the tectonic evolution of the Azores area as a triple junction. In their model, the two principal MAR segments trending N-S and SW, act as major spreading centers, whereas the Terceira Trough plays the role of a secondary spreading center. The complexity of the Krause and Watkins model has been critized by McKenzie (1972). He suggested a much simpler triple-junction system, resulting from ignoring both the existence and northward offset of the WAFZ. Morgan (1971, 1972) proposed that the Azores region is underlain by a rising mantle "plume". Another model has been proposed by Machado et al., (1972). They envisage the MAR to be locally offset to the east by a series of eight major east-west transform faults, so

that the islands occupy oxial positions over the offset ridge segments. However, Ridley et al. (1974) disagree with both McKenzie and Machado et al. models. Ridley et al. in critizing McKenzie's model, consider it essential that any model provides a triggering mechanism to bring the secondary spreading center into existence. Ridley et al. indicated that Machado et al. model requires the MAR to be absent between Flores and Graciosa and Faial, but the ridge axis is actually present and there is no evidence to support the preferred ridge configuration of Machado et al. Ridley et al. prefered another model, which consists of a ridge migrating eastward as its own crustal spreading rate. This is followed by a change in the direction of crustal spreading which leads to the development of a leaky transform fault with the resulting growth of a secondary spreading center along the Terceira Trough. Schilling (1975) presented rare-earth abundance data to support the presence of a major plume upwelling under the Azores. The data also suggest two distinct mantle sources and an intermediate zone of mixing. Schilling proposed that the appearance of a plume beneath the Azores region and its doming effect on the lithosphere may have generated the triple junction.

In general, none of the models for the excess topography of the Azores platform, triple junction, secondary spreading centers, change of direction and distinct spreading rate history north and south of the Azores, took into account the rare-earth data and the two distinct mantle sources for basalts. There is no convincing model that has been proposed yet.

2. Geology of São Miguel Island

São Miguel consists of four volcanoes, figure 9. Three volcanoes, Agua de Pau, Furnas and Sete Cidades are dormant while Povaação is supposed to be extinct.

Age determinations for Sao Miguel have been carried out using K-Ar method by Abdel-Monem et al. (1968) and Muecke et al. (1974). Abdel-Monem et al. date the oldest exposed lava as 4.01 m.y. and the youngest flows of the andesite series as 0.95 m.y. More recently Muecke et al. gave an age of (117 ± 24) x 10^3 yr for a sanidine sample concentrated from a fresh subaerial trachytic flow located at 57 m depth in the drill core from Agua de Pau. A second sample of a relatively fresh submarine lava from the 950 m level has an apparent whole rock age of (280 ± 140) x 10^3 yr. From paleomagnetic measurements on the drill core rocks, the normally magnetized rocks suggest an upper age limit of 0.69 m.y. for the formation of the rock sequences (Muecke et al. 1974).

Petrological study has been carried out on São Miguel by Assunção and Canilho (1970), Boone and Fernandez (1971), Schmincke and Weibel (1972), Schmincke (1973), Fernandez (1973) and McGraw (1976). Most of the analyses of the Azorean rocks indicate that they belong to an alkaline olivine-basalt series. This is different from Iceland where both the tholeiitic and the alkaline series are present. However, Assunção and Canilho (1970) reported in São Miguel a tholeiitic differentiation trend besides the predominant alkaline olivine-basaltic one. Boone and Fernandez (1971) studied the olivine in different rocks in

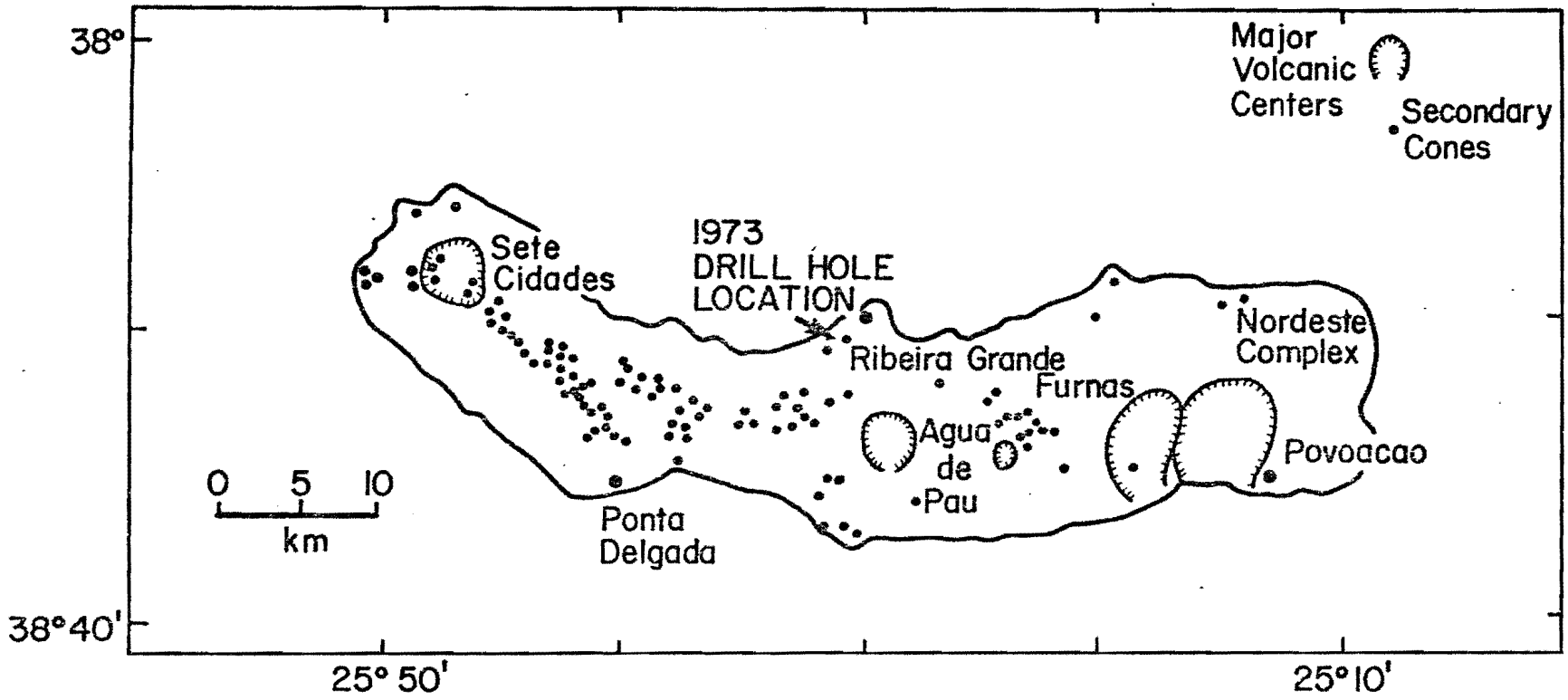

Figure 9. Volcanoes on São Miguel (after Ridley et al. 1974).

São Miguel. They recognized an overlap in olivine compositions between nodules, ankaramites and alkali olivine-basalts, but all were more iron-rich than typical olivine in Hawaiian lherzolites. They suggested a shallow-level origin for all the olivine-bearing samples on the basis of low Ni and high Ca contents and distinct zonation in all the olivine samples. Schmincke and Weibel (1972) and Schmincke (1973) analysed ankaramites, alkali olivine-basalts, trachytes and comenditic trachytes from Sao Miguel. The analyses indicate that the Azores volcanics are all strongly alkaline. Fernandez (1973) studied the Nordeste Complex in São Miguel and concluded that the alkali basalt-trachyte series of Nordeste Complex results from a fractional crystallization of plagioclase + titanomagnetite ± Ti-Al clinopyroxene ± olivine. The presence of mildly alkaline, sub-alkaline and alkali basalts suggests varying degrees of partial melting within the mantle produced this spectrum of basaltic rocks. McGraw (1976) described the petrology and chemistry of the drill core from the flank of Agua de Pau volcano. Basalts, trachybasalts and trachytes were identified and analysed. In the basalts, Al_2O_3, Nb and Zr increased with depth in the drill core while CaO, TiO_2 and MgO all decreased. McGraw suggested an alkaline magmatism for the area and related the tholeiitic nature of some of the rocks to the effect of hydrothermal alteration.

The magnetic anomalies map of São Miguel, figure 10, shows the central area between long. 25°20' and 25°40' west is an area of positive anomaly. On either side, there are equally large areas of negative

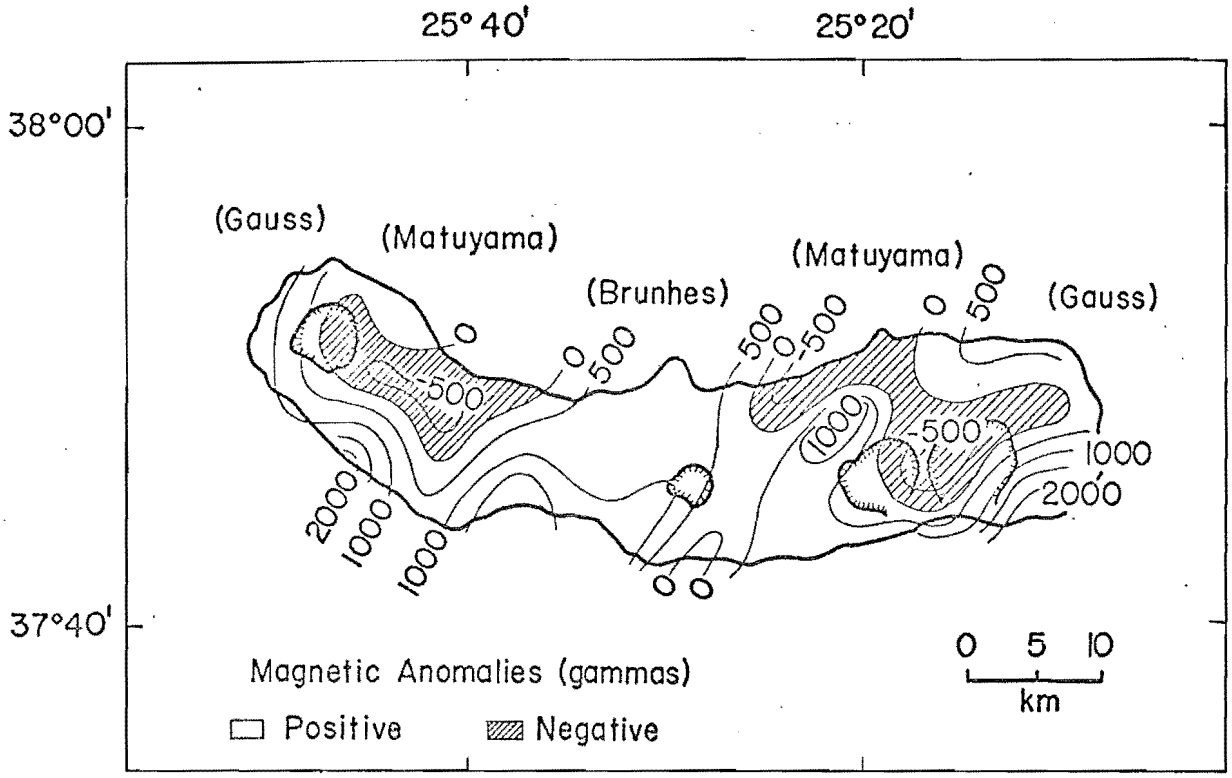

Figure 10. Magnetic anomalies over São Miguel (after Machado et al. 1972).

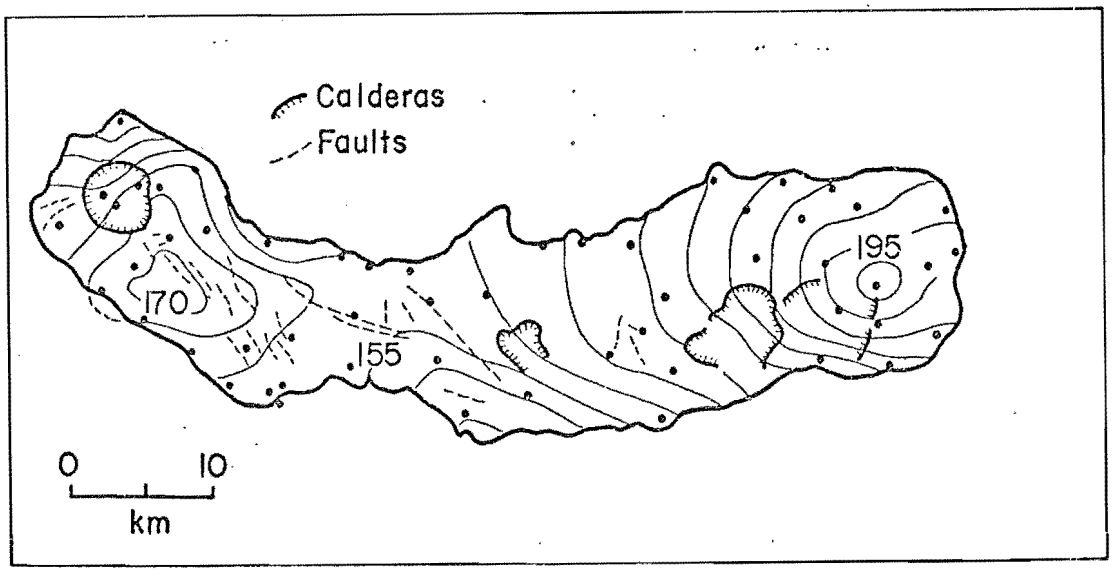

Figure 11. Bouguer anomaly map for São Miguel. Contour interval is 5 mgal. Filled circles are individual gravity stations. (After Ridley et al. 1974).

anomaly which are followed both to the east and west by strong positive areas which continue offshore on the eastern end. The magnetic anomaly map is based on the geomagnetic survey by Quintino (1962).

Ridley et al. (1974) present a Bouguer anomaly gravity map for São Miguel, figure 11. In this map, two centers of high positive Bouguer gravity are aligned in an approximately east-west direction. The larger center is located near the extinct volcano Povoacão and has a maximum value of 203 m gal. In the west, a positive anomaly is centered to the southeast of the volcano Sete Cidades. Ridley et al. (1974) suggested that the low Bouger anomaly across the west center of the island may represent a northwest-southeast trending fracture zone. Such a possibility is in agreement with the topographic and fault trends and with numerous adventive cones in this area.

3. Source of the rocks used in the present study

In 1972, a joint program was initiated by Dalhousie University and the Lamont-Doherty Geological Observatory. The aim of the program was to drill into the oceanic islands to aid in the discovery of the processes of their formation and the role they play in the sea-floor spreading process. The project started in 1972 with a 800 m drillhole on the island of Bermuda in the western Atlantic. This was followed in 1973 by a drillhole on the island of São Miguel, in the Azores.

The drillhole was located at 37°48.9'N and 25°31.4'W on the lower northern flank of the dormant volcano Agua de Pau, figure 9. The vol-

cano rises to a maximum height of 950 m above sea level and has a diameter at sea level of approximately 15 km. Trachytic ash and associated basaltic lavas, intercalated with occasional trachytic extrusives occur at the surface in the vicinity of the drillhole. Several hot springs are located on the flanks of the volcano. The rig floor was at 72 m above sea level and drilling terminated at depth of 981 m below the rig floor following steam production. The recovered core consisted of subaerial and submarine lavas and pyroclastic materials. The present study deals with the opaque mineralogy and magnetic properties of the recovered rocks.

CHAPTER 3

EQUIPMENT AND TECHNIQUES

In this work, 232 polished surfaces of rocks from the Azores drill core were prepared for opaque mineralogy study. Fifty-one polished sections were selected for microprobe analysis. Ninety-six mini-core sub-samples and 111 chip samples were taken for paleomagnetic and rock magnetism studies. The preparation of the samples, analytical techniques and equipment used for the various studies are described below.

1. Opaque mineralogy

1.1. Preparation of samples: Polished surfaces of the rock samples were prepared in four steps; cutting, mounting, grinding and polishing. First a small slice was cut from the original sample using a diamond saw. Then, the specimens were mounted using cold-setting quick mount resin. Grinding was carried out in two stages using 15 μ alumina in water as abrasive. When a satisfactory flat and smooth surface was obtained, the final step of sample preparation took place. In this final step, the specimens were polished in two stages using respectively 6 μ and 1 μ diamond abrasive in kerosene. Specimens were usually polished for 10 hours before they were ready for examination. In all grinding and polishing stages, cleanliness is essential before transferring from coarse to fine abrasive stages. The specimens were cleaned with diluted soap in an ultrasonic cleaner. The polished surface

were extra-polished by hand before reflectivities were measured. Alumina polishing suspension of 1.0, 0.3 and 0.05 microns were used.

1.2. Equipment: The assembly for opaque mineralogy study, plate 1(a) consists of a zetopan polarized reflected light microscope, manufactured by the Reichert company of Austria, for examination of polished surfaces. The microscope is supplied with an air 28X and oil 90X objectives. A 10X eye piece was used, throughout the present work, providing a total magnification of 420 and 1350 diameters in air and oil respectively. An Ultraphot II Carl Zeiss microscope, plate 1(b), with an oil 100X objective provides a total magnification of 2500 diameter, was also used. Both microscopes are provided with 35 mm cameras. For measuring the reflectivity of opaque minerals, a microphotometer is fitted behind the eye piece of the Zetopan microscope. The microphotometer consists of a magnifying lens system, wedge filter, aperture diaphragm and a Phillips type 150 AVP photomultiplier for which the spectral sensitivity curve is shown in figure 12. The photomultiplier is attached by a cable to the control unit which is also connected to an 120 V a.c. supply. The control unit contains a step transformer which supplies the voltage for the LUX FNI low-voltage illuminator of the microscope. This arrangement achieves more constant light intensity than does a regulating transformer whose sliding contact may cause variations in the operating current. The control unit is connected to a chart recorder which has a range of 10 mv. Figure 13, shows a schematic layout of the reflectivity measuring system.

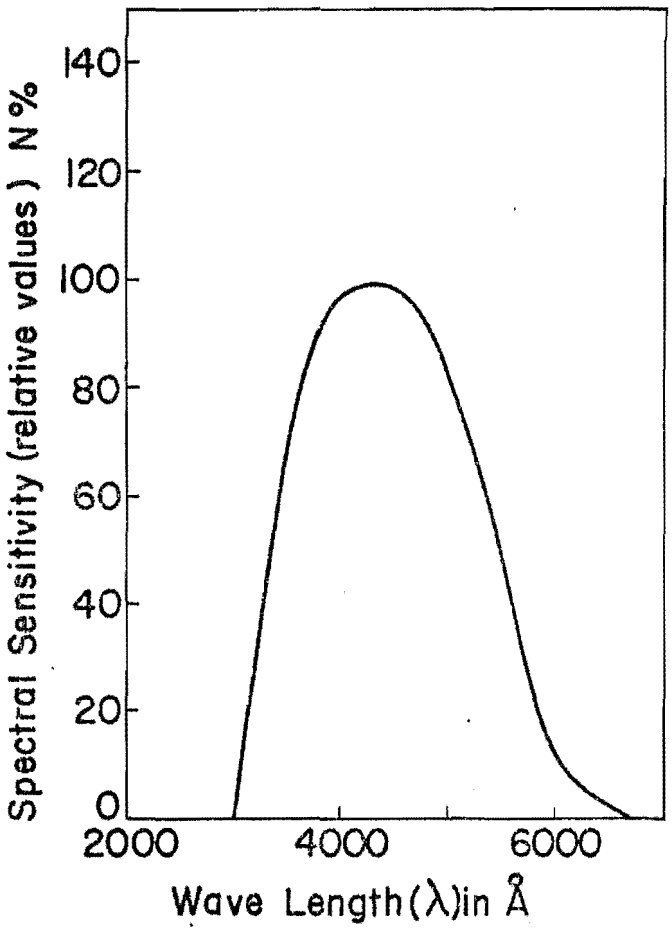

Figure 12. Spectral senstivity of photomultiplier 150 AVP. Wavelength (λ) in Å

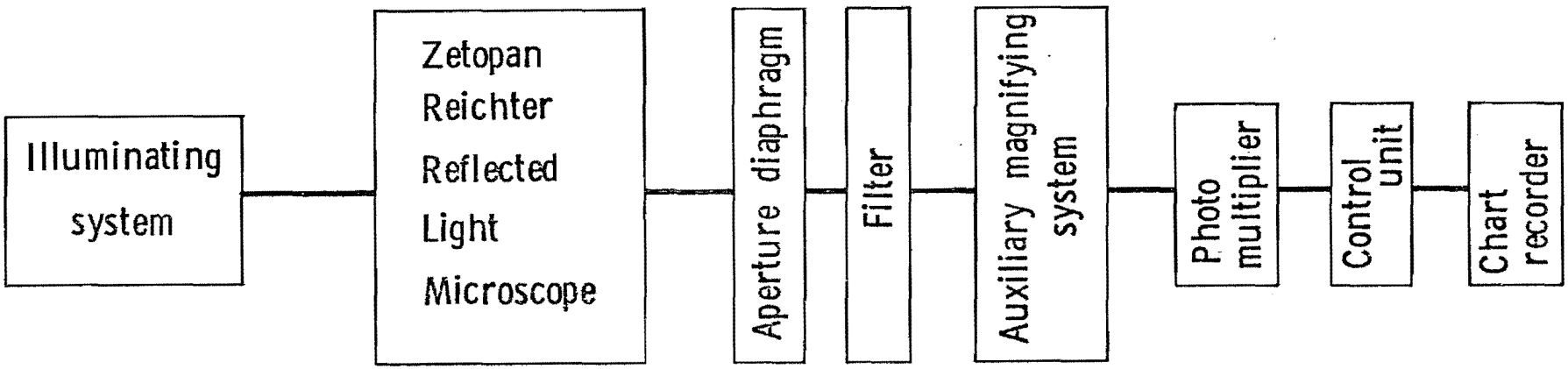

Figure 13. Schematic layout of the reflectivity measuring system.

1.3. Instrumental factors in reflectivity measurements: Standardization of the apparatus used in determining reflectivity of opaque minerals is very important. Abdel-Aal (1973) studied the effect of instrumental factors on the accuracy of the apparatus. These factors are:

i) Angle of incidence and the numerical aperture of the objective

ii) Linearity of the apparatus during the warm-up period

iii) Spectral characters and wave length

iv) Size of the aperture

Tests on these factors were carried out in the present study and the apparatus was used in all reflectivity measurements under the following standardized conditions:

i) Plane-polarized light with the polarizer in 45° position, 28X and 90X objectives in air and oil respectively were used.

ii) Apparatus was allowed 30 minutes to warm-up before any measurements were taken.

iii) All reflectivity values reported in this research were measured in air at wave length 546 nm.

iv) Aperture used was equal to 1.0 mm.

1.4. Reflectivity measuring procedure: The procedure used involved measurements of an unknown specimen between two sets of measurements on standards of known reflectivities. There was a negligible variation when measuring at different points on each standard. The mean value of

five readings has been found to be sufficient for an accurate estimation of the standard deflection. The unknown specimens had less homogeneous surfaces than the standard, so the accuracy of the calculated reflectivity value is partly a function of the number of determinations made on the specimen. It has been found that 10 readings are usually the appropriate number of determinations required for accurate estimation of the deflection of unknown specimen (Abdel-Aal 1973). Measurements were carried in blocks of 10 readings on unknown samples interspersed by 5 measurements on the standards.

The reflectivity of the unknown is determined by the direct comparison with standards of known reflectivity. The following equation is applied:

$$R_u = R_s \times \frac{\mu}{s}$$

where R_u = unknown reflectivity value of specimen

R_s = known reflectivity value of standard

u and s are scale deflections for unknown and standard measured in units of chart recorder respectively.

1.5. Standards in reflectivity measurements: Three standards were used in the present study. They are black glass, black silicon-carbide and tungsten-carbide. These are the only standards acceptable to the Commission for Ore Microscopy of the International Mineralogical Association (COM/IMA). The spectral calibration data for each standard (as supplied by the manufacturer) is shown in figure 14.

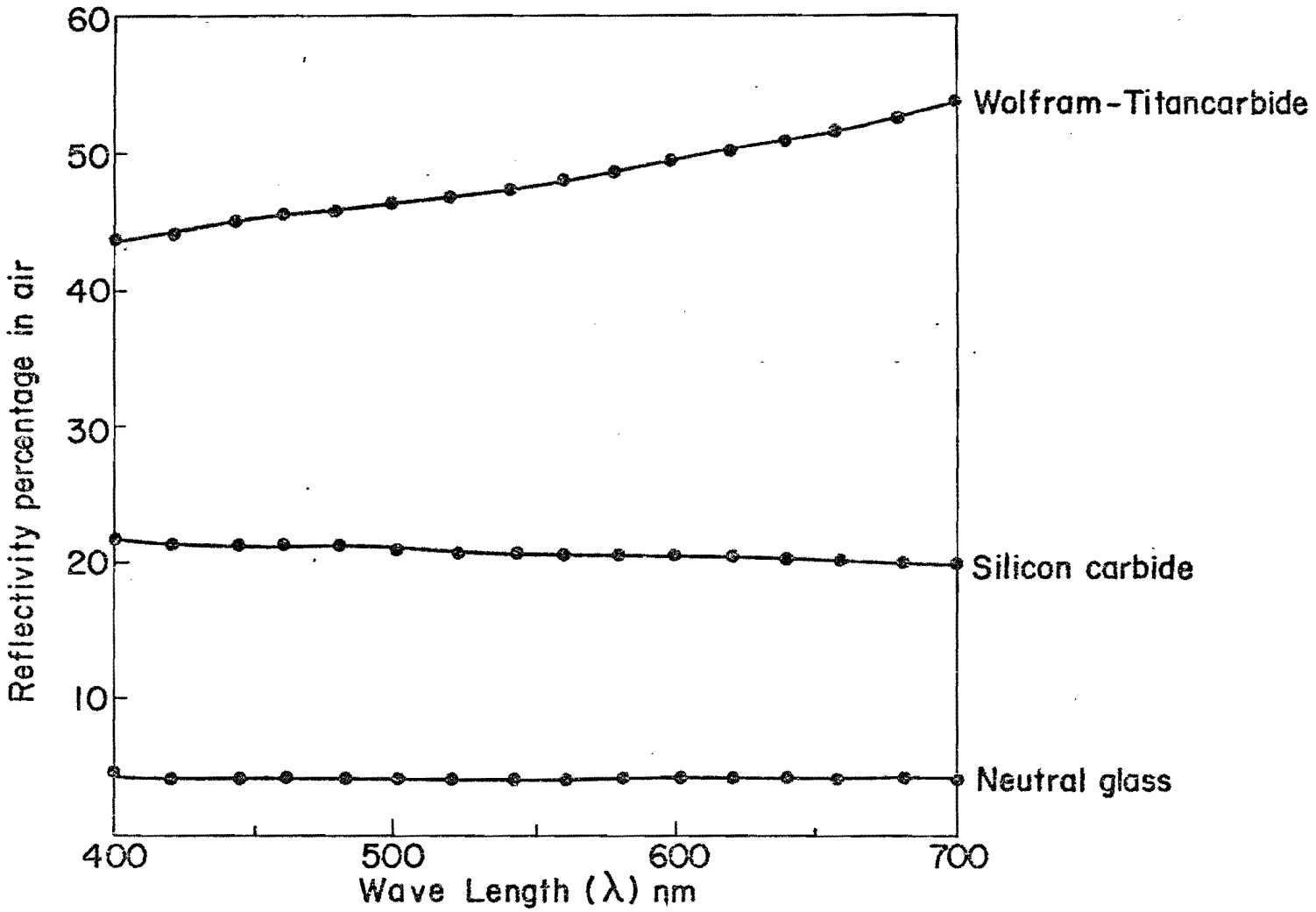

Figure 14. Spectral calibration data for standards, neutral-glass, silicon-carbide and Wolfram-Titancarbide.

1.6. Errors and accuracy of reflectivity measurements: Regardless of the method of reflectivity measurement used, there are some sources of error that affect the accuracy of results. These errors are:

i) systematic errors which include instrumental errors, variation in composition of the sample and errors due to polishing technique.

ii) non systematic errors, which are the variation in the reflectivity value of the same area of a grain from repeated measurements.

iii) errors in the standard values.

These errors and their effect on the accuracy of reflectivity measurements, have been studied in detail by Abdel-Aal (1973). Precautions were taken to minimize these errors in the present measurements. A relative accuracy of 1% is assumed throughout the present measurements and calculated as follows. The relative standard deviation in measurements of the unknown varies from 0.3% to 0.5%. Assuming normal distribution of the variation, the confidence interval at the 95% level for the mean value of 10 measurements is almost equal to $\pm \sigma$ (σ = standard deviation). Taking into account the resulting reflectivity values of more than one grain, a relative precision of the order of $\pm$ 0.5% seems probable. Pillar (1972) measured the variation in reflectivity in SiC standards and found that the relative standard deviation from the macroscopically calibrated value was of the order of $\pm$ 0.4%. The relative accuracy, taken as 2σ, is $\pm$ 0.8%. The relative accuracy of the reflectivity measurements = resultant nonsystematic error + error in the standard value + systematic errors. Assume that the systematic

error = ± 0.5% (Abdel-Aal 1973), the relative accuracy = ± (0.5^2 + 0.8^2 + 0.5^2) = 1.1%.

2. Paleomagnetism and Rock Magnetism

2.1 Preparation of samples: For paleomagnetic studies and initial susceptibility measurements, mini-core sub-samples were prepared by using a diamond crowned coring bit of 1" (2.54 cm) inside diameter. The cores were cut to a maximum of 1" (2.54 cm) length using the diamond saw, then the samples were oriented for paleomagnetic studies.

To measure Curie temperatures and saturation magnetization, a small chip from each sub-sample was used.

2.2. Equipment and Techniques: The natural remanence magnetization (NRM), inclination and declination for each sample were measured using a Schonstedt SSM 1A spinner magnetometer.

An alternating field demagnetizer capable of reaching peak fields of 1300 oe was used for samples demagnetization.

A MS-3 magnetic susceptibility bridge was used for measuring the initial susceptibility of the samples.

Saturation magnetization and Curie temperature were measured using a Cahn R-100 electrobalance for 10-30 mg. rock chip taken from each sample. The apparatus was modified by Ryall (1974) and Clark (personal comm., 1976). The sample was placed in a quartz bucket suspended

between the pole pieces of 7 kG electromagnet. The force measured by the balance was the sum of the sample weight and the downwards directed magnetic force due to the magnetic field gradient acting on the sample. The magnetic force (ordinate) was plotted against temperature (abscissa) on a BBN 815 M x-y plotter to produce a magnetization-temperature curve for the sample. Heating can be done up to 700°C using a nichrome furnace element.

3. Microprobe analysis

The selected polished surfaces were coated with carbon, then the minerals were analysed by a Cambridge MK V electron microprobe using synthetic and natural standards. Measured X-ray intensities were corrected for atomic number, fluorescence and absorption effects by correction program EMPAD VII (Rucklidge 1967). The use of microprobe analyses allowed the analyses of grains as small as 5 μ. Some alteration and exsolution phases were less than 3 μ in their grain size so contamination with other minerals had occurred and resulted in a high calculation of these phases. Other than that, there was no doubt about the nature of minerals being analysed as most of the grains were in 20-80 μ size range. The analyses of different titanomagnetite and ilmenite grains in a sample were found to contain very similar major and minor elements, so the calculated compositions of the grains are likely to represent the whole sample.

CHAPTER IV

OPAQUE MINERALOGY

In this chapter, the description of opaque mineral phases, their structures and textures are given. The variations in chemical composition in the opaque phases and its effect on other parameters such as reflectivity are discussed. An attempt to follow the paragenesis of the various opaque minerals, whenever possible, is given.

1. Description of the core log

The rocks of the 981 m drill core are described in detail in the core log (Scientific party, 1973). McGraw (1976), added more observations and interpretations to the core log from her study of petrology and geochemistry of drill core rocks.

Five different letters in the core log refer to a specific rock type. AUL (lava flow), AUA (pyroclasticts), AUG (agglomerates), AUB (breccias) and AUS (intrusive).

Muecke et al. (1974) have studied the drill core and found that extrusive lavas constitute 72% of the drill core. They occur in 140 separate flow units. The flows are massive basaltic or trachytic rock units. They are usually separated from one another by ash beds or brecciated tops. Pyroclastic deposits represent 22% of the core and they include ignimbrites, which are common in the depth interval 262 m

to 508 m. The pyroclastics consist of fine-grained to medium-grained ash materials. The agglomerate units composed of fragments of trachytic or basaltic rock in fine grained ash. The few intrusives are fine grained and frequently contain large feldspar phenocrysts. Basaltic breccias consist of angular basalt fragments in chloritic, calcitic, hematitic and clayey matrixes.

Muecke et al. (1974) recognized the division of the core into five major parts, figure 15, subaerial sequence III, 0 - 268.4 m, subaerial sequence II, 268.4 - 428.6 m, subaerial sequence I, 428.6 - 762.8 m, transition sequence, 762.8 - 856.8 m and subaqueous sequence 856.8 - 980.5 m. However, as described later the presence of some subaerial types of titanomagnetite in the subaqueous sequence in the present study, suggests an increase in the thickness of transition sequence.

2. Opaque Mineral Phases

Examination of 232 polished sections of the drill core rocks indicates that various iron-titanium oxide phases are present. The mineral phases in the core were subjected to both deuteric oxidation and hydrothermal alteration. A detailed mineralogical description of each polished section is given in Appendix I.

2.1. Primary opaque oxide phases: Although most of the rocks in the drill core were subjected to various degrees of oxidation and hydro-

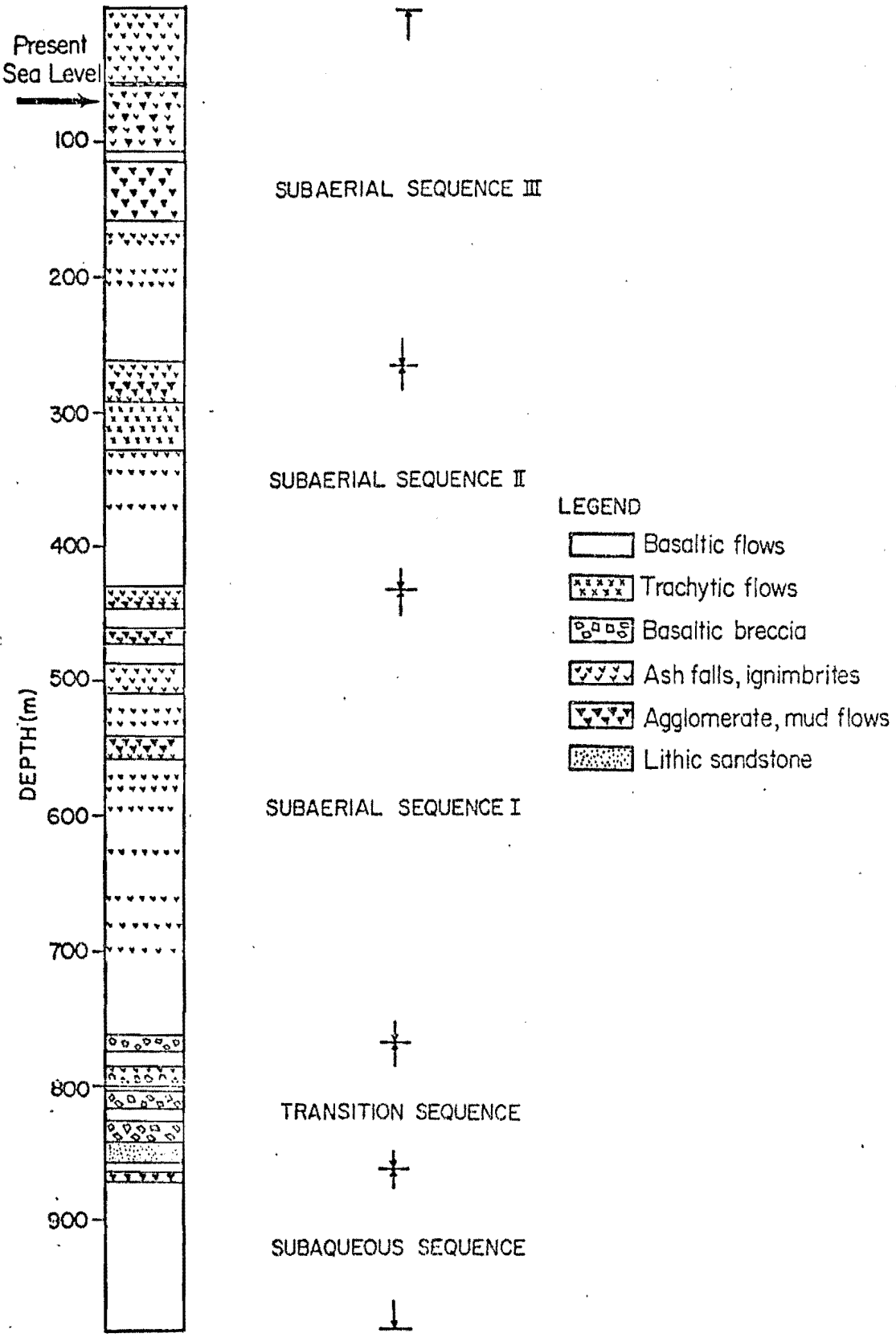

Figure 15. Lithologic variations in the São Miguel drill core (after Muecke et al. 1974).

thermal alteration, some unaltered primary opaque phases were recognized at many levels in the core. Primary oxide phases comprise titanomagnetite, ilmenite and spinel.

2.1.1. Titanomagnetite: Titanomagnetite with its alteration products is the dominant opaque phase in the core. Three types of titanomagnetite were identified which varied in size, color and composition. Plate 2 shows an example of each type and a brief description of each is given below.

(1) Titanomagnetite type 1: This type includes large euhedral to subhedral grains larger than 50 μ. It is randomly distributed in the core. The grains are all homogeneous and either included in clinopyroxene phenocrysts or occur separately in the groundmass. The large groundmass crystals show peripheral corrosion, plate 2(d). Microprobe data of five samples of titanomagnetite type 1 indicates that titanium (Ti) represents between 12.0-16.0 by weight of the total elements. Table 1 gives microprobe data, together with reflectivity percentage measured in air at wavelength 546 nm for this type of titanomagnetite. Relations between the various elements in titanomagnetite type 1, reflectivity and the molecular proportion of ulvöspinel in titanomagnetite are given in figures 16 and 17. From the study of Table 1 and figures 16 and 17, (i) it seems that titanomagnetite included in clinopyroxene phenocrysts has a higher reflectivity value than titanomagnetite in the groundmass, (ii) it is clear from figures 16 a and b, that Al and Mg

Table 1: Microprobe and reflectivity data of titanomagnetite type 1.

SAMPLE	Depth in m	Fe	Ti	Al	Mg	Cr	Mn	Total Cations	X *1	Fe/Fe+Ti	R% *2	Remarks
AUL 1.1.2	69.5	51.2	13.4	3.1	2.2	1.5	1.4	72.8	0.63	0.79	16.9	In phenocrysts
AUL 2.1.5	99.1	51.8	13.0	3.2	2.2	0.8	1.7	72.7	0.61	0.80	16.1	In phenocrysts
AUL 8.1.2	170.1	50.3	16.0	2.7	1.9	0.5	0.7	72.1	0.75	0.75	15.2	In groundmass
AUL 19.2.6	235.5	53.6	15.0	2.0	1.9	0.0	0.0	72.5	0.71	0.78	14.9	In groundmass
AUL 142.1.6	940	52.1	12.1	3.2	2.4	0.3	0.6	70.7	0.57	0.81	14.3	In groundmass
AVERAGE		51.8±1.2	13.9±1.6	2.9±0.5	2.1±.2	0.6±0.6	0.9±0.7	72.2	0.7±0.1	0.79±.02	15.5±1.0	

*1 X is the molecular proportion of ulvöspinel in titanomagnetite X Fe_2TiO_4 (1-X)Fe_3O_4 without taking into consideration impurities other than Ti.

*2 R is the reflectivity percentage of titanomagnetite measured in air at wavelength 546 nm.

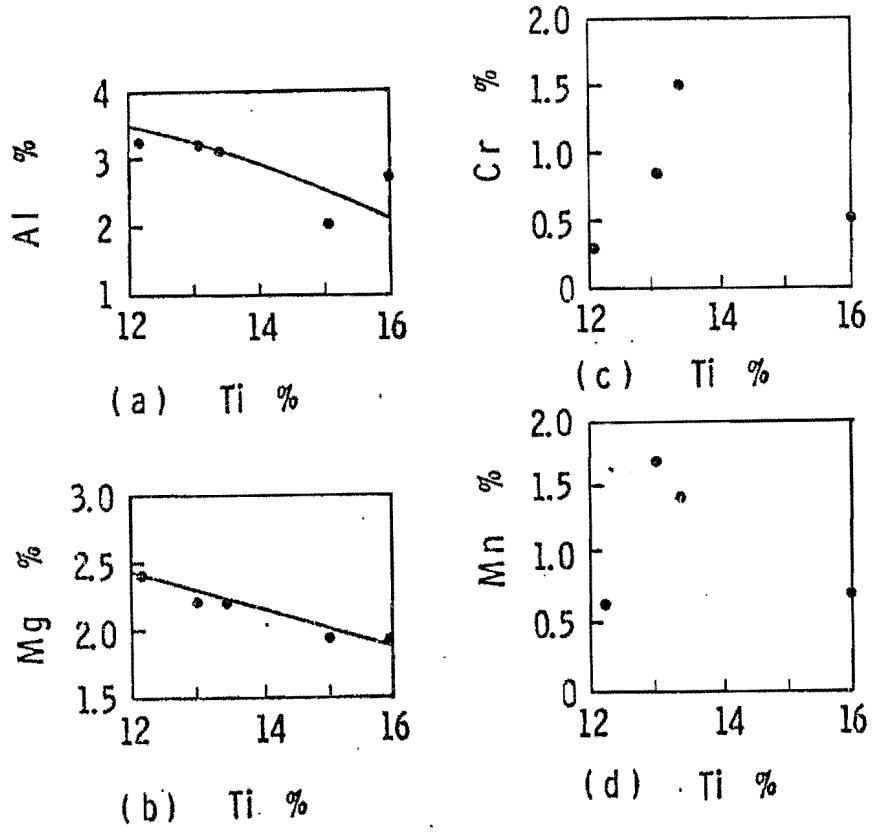

Figure 16. Plots of Ti content versus contents of other elements in titanomagnetite type (1).

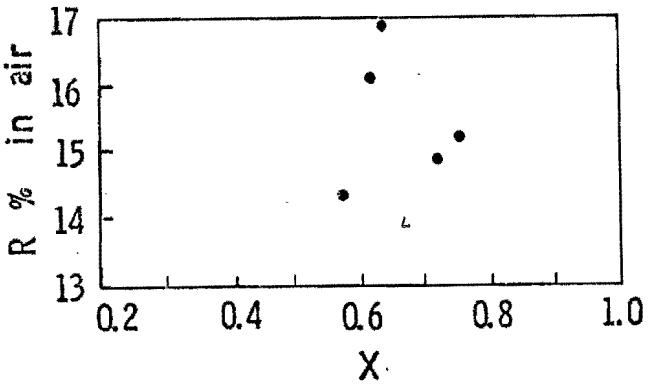

Figure 17. Relation between molecular proportion of ulvöspinel (X) in titanomagnetite type (1) and reflectivity (R) measured in air at wave length 546 nm.

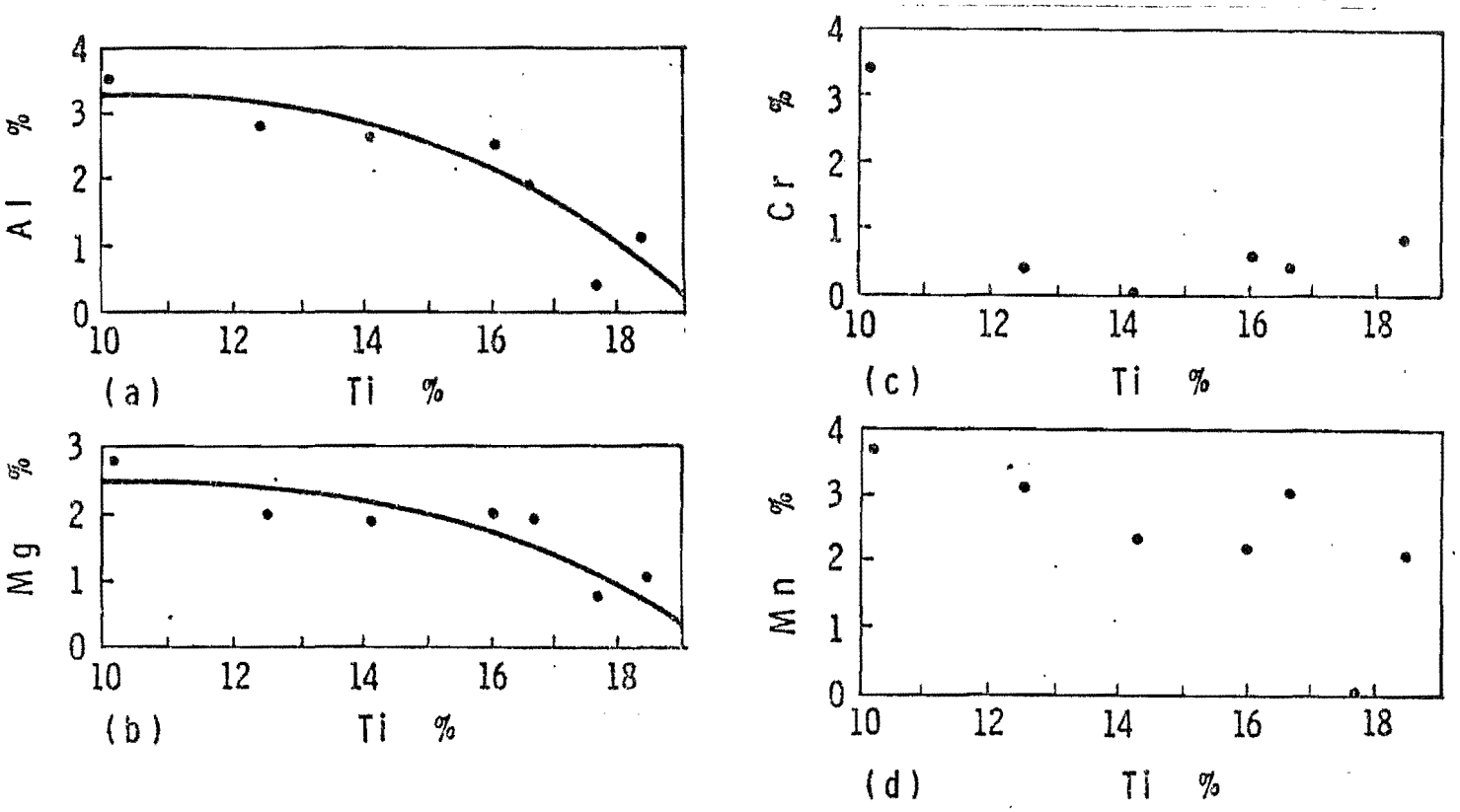

Figure 18. Plots of Ti content versus contents of other elements in titanomagnetite type (2).

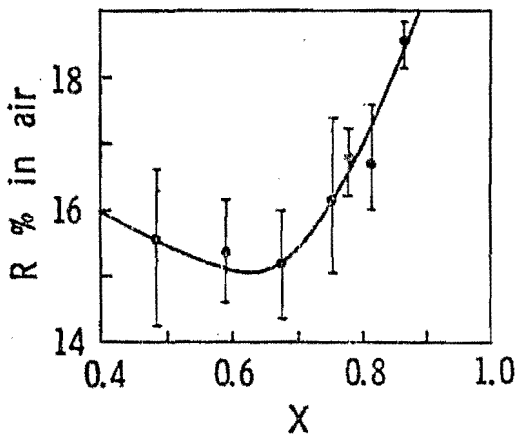

Figure 19. Relation between molecular proportion of ulvöspinel (X) in titanomagnetite type (2) and reflectivity (R) measured in air at wave length 546 nm.

contents decrease as Ti content increases, while such correlation does not exist with Cr and Mn, (iii) the ratio Fe/Fe+Ti is constant (0.8) for all the samples.

(2) Titanomagnetite type 2: This type always occurs as fine to medium euhedral grains. Grain size ranges from 5 to 20μ, plate 2(b). No apparent oxidation texture has been observed with or without etching. Fe/Fe+Ti ratios are slightly lower and reflectivity values are higher than those for type 1 titanomagnetite. Table 2 shows the microprobe data together with reflectivity measurements in air at wavelength 546 nm while figures 18 and 19 gives the relations between the various components of titanomagnetite type 2.

From the study of Table 2 and figures 18 and 19, the following are noted:

(i) reflectivity of titanomagnetite from the one agglomerate unit AUG 5.1 studied is higher than that of titanomagnetite from lava flow units.

(ii) as Ti content increases, Mg and Al contents generally decrease while Cr and Mn contents do not show regular distribution.

(iii) reflectivity decreases as the ulvöspinel content increases until it reaches a minimum value of 15% when the ulvöspinel content is equal to 0.65. After this value is reached, an increase in reflectivity follows increase in X, see figure 19.

(iv) it must be noted that sample AUL 24.1.1. has a (Si) content of 2.1 and (Ca) content of 2.4.

Table 2. Microprobe and reflectivity data of titanomagnetite type 2.

SAMPLE	Depth in m	Fe	Ti	Al	Mg	Cr	Mn	Total Cations	X	Fe/Fe+Ti	R%	Remarks
AUG 5.1.1	155	49.1	18.4	1.1	1.0	0.8	2.0	72.4	0.86	0.73	18.5	Agglomerate
AUL 6.1.7	165	49.6	16.6	1.9	1.9	0.4	3.0	73.4	0.78	0.75	16.8	
AUL 19.2.6	235.5	46.5	10.1	3.5	2.8	3.4	3.7	70.0	0.48	0.82	15.5	
AUL 24.1.1	257.4	44.3	17.6	0.4	0.8	0.0	0.0	63.1	0.82	0.72	16.7	
AUL 51.2.1	396.3	49.6	16.0	2.5	2.0	0.6	2.2	72.9	0.75	0.76	16.1	
AUL 69.7.3	490.7	50.6	14.2	2.6	1.9	0.0	2.3	71.6	0.67	0.78	15.1	
AUL 138.1.10	924.2	49.9	12.5	2.8	2.0	0.4	3.1	70.7	0.59	0.80	15.4	
AVERAGE		48.5±2.3	15.1±3.0	2.1±1.1	1.6±0.7	0.8±1.2	2.3±1.2	70.6	0.7±.1	0.77±0.04	16.3±1.2	

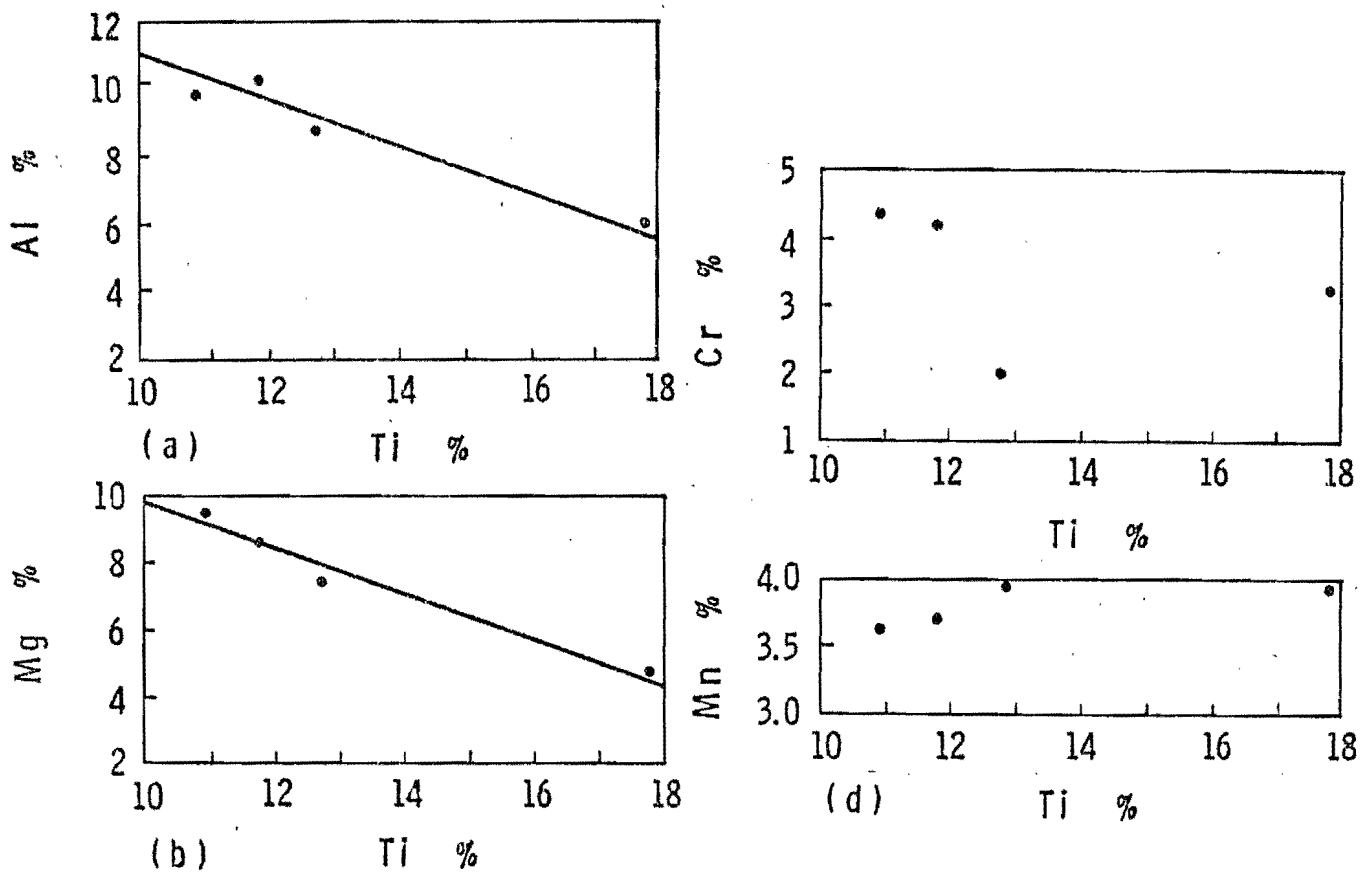

Figure 20. Plots of Ti content versus contents of other elements in spinel.

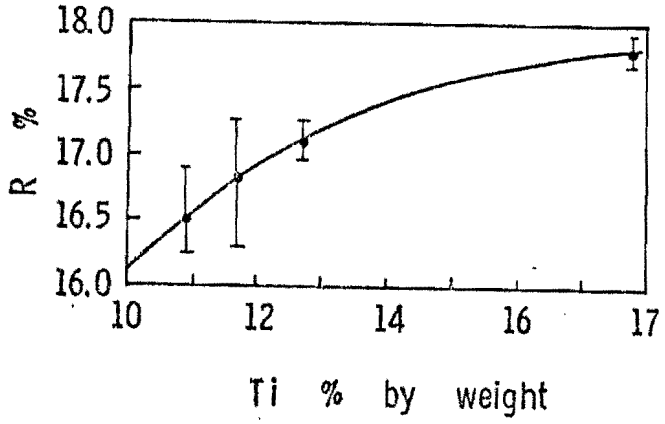

Figure 21. Relation between Ti content and reflectivity of spinels.

(3) Titanomagnetite type 3: Type 3 titanomagnetite is close to type 2 in chemical composition and reflectivity value (Table 3), but it is significantly different in structure and cooling history. This type occurs as skeletal form, plate 2(c), with grain size ranging from 15-18μ.

The differences and similarities between type 1 and type 2 titanomagnetite are as follows:

(i) type 1 is larger in grain size (> 50μ) than type 2 (5-20μ).

(ii) average reflectivity value for type 1 (15.5% ± 1.0) is not significantly different from the average value for type 2 (16.3% ± 1.2).

(iii) the Fe/Fe+Ti ratios of both type 1 and type 2 are not significantly different.

(iv) type 1 and type 2 are similar in crystallization trend, during which Al and Mg decrease with increasing Ti content and in the irregularity of relationships between Mn, Cr and Ti.

Type 3 is very similar to type 2, the only difference which occurred was in the cooling history where type 3 represented rapid cooling and hence the skeletal form of titanomagnetite was observed.

2.1.2. Ilmenite: Two types of ilmenite were observed; equidimensional type 1 and separate elongate single crystal type 2, plate 2 (e and f). Both types are similar in chemical composition (see Table 4) but type 1 is very strongly anisotropic, lower in reflectivity and darker in color than type 2.

Table 3. Microprobe and reflectivity data of titanomagnetite type 3.

SAMPLE	Depth in m	Fe	Ti	Al	Mg	Cr	Mn	Total Cations	X	Fe/Fe+Ti	R%	Remarks
AUL 122.3.2	813.2	49.3	16.0	2.1	1.8	0.3	2.0	71.5	0.75	0.75	16.4	
AUL 138.14	917.8	47.1	17.2	1.6	1.5	0.5	1.8	69.7	0.81	0.73	16.6	
AVERAGE		48.2±1.6	16.6±0.9	1.9±0.4	1.7±0.2	0.4±0.1	1.9±0.1	70.7	0.78±0.04	0.74±0.01	16.5±0.14	

Ilmenites of type 1 are fine-medium grained. Grain size ranges between 15-30μ. Grains of this type always occurred together with titanomagnetite, however, sometimes (but not often) with geikielite, plate 2(f). Geikielite is $MgTiO_3$, dark brown, very strongly anisotropic and has a bireflectance value of 11.9-14.6%. This mineral is found in sample AUL 20.3.2 which is stated by McGraw (1976) to be a basalt with plagioclase, olivine and augite as phenocryst phases. This sample is relatively high in MgO (6.5%) in the drill core. Microprobe data for geikielite is given in Table 4. Geikielite is not known to occur as an independent mineral in basaltic lavas, it occurs as the product of exsolution in many magnetite ores (Ramdohr 1969) and in kimberlites (Haggerty 1975).

Ilmenites of type 2 are fine to coarse grained. Grain size varies between fine 5-10μ and coarse > 40μ.

From Table 4, it is clear that the variations in the element contents in all analysed ilmenites are nearly constant. Fe/Fe+Ti ratios are equal to 0.6. The similarity in chemical composition between type 1 and 2 ilmenites may indicate a crystallization from the same source but the contrast in physical properties could reflect a change in the environment and cooling history of the magma.

2.1.3. Spinel s.l. (Sensu Lato): Primary spinel occurs either as xenocrystic crystals or as a groundmass phase throughout the drill core. Xenocrysts are coarse euhedral grains (> 50μ) often containing cracks and are greyish white in their color, while groundmass spinels are medium-coarse (20-40μ) with a grey color. Some of the grains show a primary

Table 4. Microprobe and reflectivity data of ilmenites

SAMPLE	Depth in m	Fe	Ti	Mg	Al	Cr	Mn	Total Cations	Fe/Fe+Ti	$R_1 - R_2$	Remarks
AUL 20.1.2	236.2	35.7	29.3	1.2	0.6	0.6	0.8	68.2	0.55	14.7-16.3	Type 1
AUL 20.3.2	241.9	36.0	29.2	1.1	0.6	0.6	0.6	68.1	0.55	14.4-16.8	Type 1
AUL 6.1.7	165	35.8	29.7	1.4	0.7	0.4	0.7	68.7	0.55	15.0-17.3	Type 2
AUL 19.2.6	235.5	35.7	29.7	1.1	0.6	0.6	0.7	68.4	0.55	15.1-17.0	Type 2
AVERAGE		35.8±0.1	29.5±0.3	1.2±0.1	0.6±0.1	0.6±0.1	0.7±0.1	68.4	0.55	14.8-16.9 ±0.3-±0.4	
AUL 20.3.2	241.9	1.1	38.7	19.0	0.4	0.0	0.0	59.2		11.9-14.6	Geikielite

zoning, plate 3(a) and others exhibit oscillatory zoning, plate 3(b). However, oxidation textures cannot be excluded. The chemical and textural criteria for distinction between primary and secondary phases is rather difficult. Table 5 shows microprobe and reflectivity data of spinels while figure 20 illustrates the relation between the various elements in spinel and figure 21 gives the relation between reflectivity of spinels and their titanium contents. From the study of Table 5 and figures 20 and 21, the following are noted:

(1) the range of chemical variation of spinels indicates enrichement in titanium and iron with crystallization.
(2) the increase in (Ti) content in spinels by crystallization is followed by a decrease in Al and Mg contents and a slight increase in Mn content, figure 20.
(3) the increase in (Ti) content in spinels is accompanied by an increase in reflectivity, figure 21.

The study of primary opaque oxide phases has shown the following interesting points:

(1) there are at least three different crystallization histories, for the primary phases; an early crystallization before eruption which can be seen in the formation of titanomagnetite phenocryst, some of them show a magmatic corrosion, and in the formation of spinel xenocryst which exhibits primary growth zoning with Fe and Ti enriched peripherally, plate 3(a). After eruption, two different lava cooling histories occurred; a slow cooling resulted in formation

Table 5. Microprobe and reflectivity data of spinels.

SAMPLE	Depth in m	Fe	Ti	Al	Mg	Cr	Mn	Total Cations	R%	Remarks
AUL 1.1.2	56.7	35.4	11.7	10.2	8.7	4.2	3.7	73.9	16.8	Xenocrysts
AUG 5.1.1	155	37.0	17.8	6.0	4.7	3.3	3.9	72.7	17.8	Xenocrysts agglomerate
AUL 6.1.7	165	38.7	12.7	8.8	7.3	2.0	3.9	73.4	17.1	Xenocrysts
AUL 8.1.2	170.1	29.2	2.2	21.1	10.0	1.2	0.0	63.0	16.0	Groundmass
AUL 77.4.6	534.1	34.6	10.9	9.9	9.6	4.4	3.6	73.0	16.5	Groundmass
AVERAGE *		36.4±1.8	13.3±3.1	8.7±1.9	7.6±2.1	3.5±1.1	3.8±0.2	73.3	17.1±0.6	

* average of spinels is taken excluding sample AUL 8.1.2 which is Al rich spinel

of subhedral-euhedral medium-coarse grains of opaque phases and a rapid cooling which formed skeletal and fine grains.

(2) in all oxide phases, generally as crystallization proceeds, Ti content increases, Al and Mg contents decrease.

(3) the increase in ulvöspinel contents is followed by an increase in reflectivity of titanomagnetite and spinel. However, when X is less than 0.7 no fixed relation can be constructed.

2.2. Primary sulphides: Few sulphides were detected in the drill core. Chalcopyrite was identified in sample Aul 11.2.7 at 195.5 m depth in sequence III and a few examples of pyrrhotite have been recognized in the subaqueeous section, plate 3(c).

The depletion of sulphides in the drill core is quite interesting. Generally sulphides are easily destroyed by oxidation and alteration. Possibly their rare occurrence in the core can be attributed to their alteration to oxide and hydroxide phases.

2.3. Secondary phases: These are the products of oxidation and alteration effects on the primary phases. They represent the majority of opaque phases in the drill core and they include various types of iron and titanium oxides. Their composition, distribution in the core, mineralogical properties and optical behavior will be dealt with in Chapter V, the Alteration Sequences.

3. Structure and Texture

The terms structure and texture have wide definitions which are applied differently by every school. Here I follow exactly the German definitions and classifications (Rehwald 1966) where structure describe mineral grain shape, its size and mutual surface boundaries, and the term texture is applied to space lattice, space arrangement and distribution of the various constituents. The American school use the term fabric to describe spatial relations of the components which is by no means the same as structure in the German sense. The classification of textures by Schneiderhöhn (1952) and Ramdohr (1969), although presenting a good approach, is rather confusing. There is a great overlap in their classifications. The work on texture by Schwartz (1951) which the American school follows uses rather descriptive terms of which some are difficult to understand.

3.1. Structure:

(i) Grain shape (form): Most of the grain shapes have been described before. Generally they are euhedral to subhedral crystals. Besides, skeletal, tabular and elongated grains, two other shapes have been recognized. First, is a radial growth shape, plate 3(d), which has been identified in lepidocrocite and in some hematite. Secondly, spheroidal grains occur, plate 3(e), which were recognized in crystallization of some pyrrhotites.

(ii) Grain size: Examination of opaque phases in the drill core rocks reveals that medium to coarse (20->50 μ) grain size is one of the characteristic features of the core. Mineral grain sizes can be influenced by different factors; the physico-chemical concepts of rate of nucleation and rate of crystallization and most commonly concentration. Most of the plates show the variation of grain size in the core. Phenocrysts are also detected in many sections. However, it must be noted that a "phenocryst" is not necessarily a product of early crystallization brought up from depth. They simple indicate that in this instance an idiomorphic mineral grain occurs in the midst of surrounding fine grains and that it is older than its surrounding minerals.

3.2 Texture:

(i) Zoning: Various types of zoning were recognized in the opaque phases of the drilled core, (Plate 3(f and g). They were detected by the differences in color and hardness between phases with or without etching with HCl concentration for a period between 10 second and 3 minutes. Zoning may originate from crystallizing magma as a result of changes in equilibrium conditions. Other possible cause of zoning may be an interruption of growth and deposition of successive bands with inclusions of foreign minerals.

In many cases original zoning was completely or partly destroyed by diffusion processes that accompanied the continued heating in hydrothermal solution as seen in many of the plates (next chapter).

(ii) Twinning: This feature is uncommon and was only detected in some ilmenite grains in sequence III of the subaerial part of the core.

(iii) Secondary or transform textures: These include all textures which show any evidence that primary opaque mineral content has been changed. The Azores drill core shows that the majority of opaque mineral textures are transform textures (see Appendix I). Transform textures recognized in the drill core are: Ex-solution, decomposition, replacement and oxidation textures. These textures will be discussed in detail in next chapter (Alteration Sequences).

The study of the texture and structure of various grains of different minerals in the Azores core yielded much information on the origin of the minerals, nature of the lava and the processes which affected the minerals after their formation. The following general points were derived from examination of structure and texture of opaque minerals (Appendix I):

1. The absence of hydrothermal alteration texture in some minerals does not mean that they necessarily have a magmatic origin, because certain high temperature replacements may take place without destroying the form of the unaltered minerals.
2. Minerals can be stable in contact with each other at high temperature but react with each other at lower temperature to form complex compounds.
3. The minerals in this core are capable of reacting in part in the solid state and, of course, readily in the presence of a hydrothermal solution.

4. It is difficult to explain why some mineral grains are oxidized and altered while others in the same section show no sign of oxidation and alteration. Also, why in one case the unmixing textures have been preserved while others in similar cases obliterated. A different rate of cooling within the temperature range in which the mobility is still very large may be one of the reasons but is certainly not the only one.

CHAPTER V

ALTERATION SEQUENCES OF THE OPAQUE MINERALS

This chapter deals with the secondary iron-titanium oxides, their composition, optical properties, structures, textures and paragenesis. The distribution of the secondary oxide minerals in the core is given. A new classification of titanomagnetite and ilmenite alteration in the hydrothermal environment is proposed.

1. Secondary phases

The products of oxidation and alteration of the opaque minerals in the drill core comprise various phases. Description of the phases in all 232 polished sections, as identified by their optical properties is given in Appendix I and a summary is given here.

1.1. Titanomaghemites: These form as the result of low hydrothermal alteration of titanomagnetite. Under the microscope, in oil at magnification of 1350 X, they occur as bluish grey patches and off-white thin irregular lines in titanomagnetite grains.

1.2. Titanohematites: These are the products of the high temperature oxidation of titanomagnetite and ilmenite. They also develop during medium-high hydrothermal alteration of titanomagnetite. Decomposition of pseudobrookite at low temperatures may result in the formation of

titanohematite. Titanohematite is a single phase mineral grain consisting of various molecular proportions of hematite and ilmenite, ($Fe_{2-y}\ Ti_y\ O_3$ $(0 < y < 1)$). The color is greyish white with green tint in oil and they have a strong bireflectance. No internal reflection has been noticed.

1.3. Hematites: These occur as the products of oxidation of magnetite, as well as crystallizing directly from hydrothermal solution. Hematite is distinctly anisotropic, especially in oil. Internal reflections are frequent and the deep-red reflection is one of the diagnostic features. The color in air is greyish-white and greyish white with bluish tint in oil.

1.4. Ilmenites: Lamellae of ilmenite are common in high temperature oxidation of titanomagnetite. The lamellae vary in thickness from 8 μ to less than 1 μ and most likely submicroscopic size. Their color ranges from light to dark brown. They are very strongly anisotropic but they have no internal reflection. Secondary ilmenite results also from decomposition of pseudobrookite at low temperatures.

1.5. Crichtonite: Hey et al., (1967) gave a chemical composition of crichtonite as ($Fe^{+2}_{16}\ Fe^{3+}_{14}\ Ti_{66}\ O_{169}$). It is relatively common as a product of oxidation at high temperatures of ilmenite and occurs as irregular thin light brown lamellae in the ilmenite. It is slightly anisotropic. Little is known of its thermodynamic properties.

1.6. Pseudobrookites (Fe_2TiO_5): These are the end products of titanomagnetite and ilmenite high temperature oxidation. The color is dark grey in oil. They are anisotropic with weak bireflectance.

1.7. Rutiles (TiO_2): Rutiles are the intermediate mineral assemblages between titanomagnetite and ilmenite and pseudobrookite in high temperature oxidation of titanomagnetite and ilmenite. They also form the decomposition of pseudobrookite at low temperatures. Hydrothermal alteration of ilmenite also produces secondary rutile.

1.8. Sphenes ($CaTiSiO_5$): Sphenes have a variety of colors. Yellow orange tinted color when Fe^{+3} replaces Ti and blue color if no iron is present. They occur as an end product of the alteration of ilmenite at low temperatures. They are also a product of the alteration of pseudobrookite and ilmenite networks replacing titanomagnetite.

1.9. Pseudorutiles: The composition of these phases are close to $Fe_2Ti_3O_9$. These are intermediate stage phases derived from the low temperature oxidation of ilmenite and have been named by Teufer and Temple (1966). The color ranges from light grey to yellowish white. Pseudorutile is slightly anisotropic and has a higher reflectivity than ilmenite but lower than that of rutile.

1.10. Spinels: The general chemical formula for spinel is $(M^{2+}M_2^{3+}O_4)$ where M^{2+} is mostly Mg and Fe and M^{3+} is Fe and Al. Secondary spinel occurs as a fine dark lamellae in {100} planes in high temperature.

oxidation of titanomagnetite. The fine size (less than 1 μ) prevents the analysis and the observation of the diagnostic properties.

1.11. Goethites (α $Fe_2O_3 \cdot H_2O$): Goethite is a replacement of magnetite and sometimes ilmenite in the hydrothermal environment. The color is grey with bluish tint. Anisotropy occurs but is masked by internal reflection which is a reddish brown color.

1.12. Lepidocrocites (γ $Fe_2O_3 \cdot H_2O$): Lepidocrocite is associated with the medium and high hydrothermal alteration of titanomagnetite and sometimes ilmenite. It has a green tinted greyish white color. Anisotropy is very high but the color is masked by brownish red high internal reflection.

2. Textures

Textures described in this section comprise all those that result from transformations from the primary state. They are: ex-solution, decomposition and replacement textures.

2.1. Ex-solution textures: Many of the opaque minerals, in the present study, are capable of solid solution. The stability of the solid solution depends on many factors such as ionic radii, lattice structure and bonding strength in the two components of a solid solution. With decreasing temperature and with large changes in the factors controlling solid solution, unmixing takes place giving rise to ex-solution

textures. At first the ex-solution bodies are extremely small but they grow to microscopic size by collection crystallization. Unmixing of a solid solution takes place by the diffusion of the solute ions through the lattice of the solvent substance. Edward (1960) listed five factors which influence the diffusion process. These are:

(i) low solubility of the solute.

(ii) large differences of melting point between solute and solvent.

(iii) large differences in atomic radii of solute and solvent.

(iv) increasing separation of solute and solvent in the periodic table.

(v) the diffusion rate increases with increasing concentration of the solute.

The mechanism of ex-solution is simple; if the crystal lattices are in general very similar, the original texture will be irregular. On the other hand, if only one plane of the lattices corresponds closely, strong directional preferences will appear, as an example ilmenite lamellae in {111} plane of magnetite and hematite in {0001} direction of ilmenite host. The oriented intergrowth of ilmenite in magnetite is attributed to the sharing of oxygen planes. Intergrowth of hematite in ilmenite reflects the presence in both crystal structures of pronounced oxygen planes parallel to their {0001} direction, in which the oxygen atoms have practically identical spacing.

Lamellae of ilmenite in titanomagnetite, plate 4(a), are common

in high temperature oxidation sections of the drill core, figure 22. Possibly this could be formed first as an exsolution of ulvöspinel, then it oxidized to ilmenite as no one has yet proven any existence of solid solution between magnetite and ilmenite (Lindsley 1962 and Buddington and Lindsley 1964). From a study of natural specimens and from the common occurrences of ilmenite lamellae in titanomagnetite of many volcanic and plutonic rocks, Ramdohr (1953 and 1969) emphasized the existence of solid solution between ilmenite and magnetite. Experimental work by Ramdohr (1926), Wilson (1953) and Roy (1954) also supported the existence of such solid solution. However, these workers did not demonstrate that the bulk composition of the heated sample rocks remained unchanged. Several authors have doubted the existence of solid solution between magnetite and ilmenite. Vincent et al. (1957) and Basta (1960) have found it experimentally impossible to homogenize ilmenite-magnetite intergrowths of mixtures if the bulk composition is maintained; instead, an exchange reaction took place with ilmenite gaining Fe_2O_3 and magnetite gaining Fe_2TiO_4. The oxidation hypothesis of ulvöspinel to ilmenite has been supported by phase equilibrium studies (Webster and Bright 1961, Taylor 1961, Verhoogen 1962 and Lindsley 1962).

The exsolution bodies which separate at relatively high temperature are themselves still solid solutions which, with further decrease in temperature, tend to exsolve the contained portions of the guest component. Plate 4(b), shows an example of this multistage exsolution with

exsolution bodies of spinel in magnetite which itself has separated from titanomagnetite. Plate 4(c), is an analogous rutile exsolution in titanohematite. The small size of these fine bodies of spinel and rutile hinder any sophisticated studies.

2.2. Decomposition textures: These textures were observed in the medium and high hydrothermal alteration sections of the drill core. Two types of decomposition were identified. Type 1, where the products of decomposition are crystallographically different from the original minerals but the chemical composition of the products still somewhat related to the original mineral. Example of this type is the decomposition of pseudobrookite to rutile and titanohematite. Plate 4(d) shows a second type of decomposition where olivine is chemically decomposed to a secondary magnetite as a result of chemical reaction with the hot solutions.

2.3. Replacement textures: Replacement textures were very common in all iron-titanium oxide minerals in the drill core and especially the medium-hydrothermal alteration section. This texture may result from the subsequent variations in the temperature of hydrothermal solution and possibly from a change in pH of the solutions. Plate 4(e), shows a replacement in spinel by a chloritic mineral (?).

3. Oxidation and alteration of iron-titanium oxides

Several types of oxidation and alteration of iron-titanium oxides

were identified in the Azores drill rocks. Each type is a function of a specific cooling history of the rocks to which they belong. A detailed study of each type follows.

3.1. High Temperature (deuteric) Oxidation:

(1) Titanomagnetite: Deuteric oxidation in basaltic rocks is a well known process. It has been investigated in the field from oxygen fugacity measurements in lava lake drill holes (Sato and Wright 1966) and by the methods of experimental petrology (Lindsley 1962, 1965 and Haggerty and Lindsley 1969). The changes in opaque mineralogy by this process were studied by Wilson and Haggerty (1966), Wilson and Watkins (1967), Ade-Hall et al. (1968a) and Gromme et al. (1969). The process takes place during initial cooling of lava in 900-600°C temperature range (Lindsley 1962, 1965, Sato and Wright 1966 and Haggerty and Lindsley 1969).

The classification of degree of high temperature oxidation in terms of titanomagnetite oxidation (Watkins and Haggerty 1967 and Ade-Hall et al. (1968a) depends on:

(i) the formation of a series of iron-titanium oxide assemblages in which ilmenite, rutile and titanohematite are intermediate forms

(ii) pseudobrookite solid solutions are the end products of high temperature oxidation.

According to Haggerty (1971), these assemblages vary with the degree of solubility that is possible in the pseudobrookite series and the degree of immiscibility that exists in the ilmenite-hematite solid solution series at temperatures between 600-900°C. As a result of this limited solid solubilities, rutile and hematite form a distinct oxidation assemblage as end products and do not necessarily result from the breakdown of pseudobrookite solid solution.

The chemical composition of high temperature oxidation titanomagnetite phases was determined by microprobe analysis. Reflectivity of each phases was measured in air at wavelength of 546 nm. Table 6 gives the reflectivity data together with the analyses for titanomagnetite of high temperature oxidation.

Deuteric oxidation of titanomagnetite occurs in various parts of the Azores drill core from sample AUL 8.1.1 at depth 170 m of sequence III in the drill core, figure 22 , and comprises all oxidation classes of Watkins and Haggerty (1967) and Ade-Hall et al. (1968a), Plate 5. Deuteric oxidation was observed also in two samples in the subaqueous section, with oxidation up to class 4 of Adel-Hall et al. (1968a) classification, Plate 5(f). The presence of deuteric oxidation in the subaqueous section is quite interesting because this oxidation is known to occur preferentially in slow cooling environments, such as subaerial environment (Grommé et al. 1969 and Ade-Hall et al. (1976a). Some other few examples of deuteric oxidation in submarine lavas have been reported (Irving et al. 1970, Ade-Hall 1974 and Ade-Hall et al.

Table 6. Reflectivity data and microprobe analyses for titanomagnetite of high temperature oxidation

SAMPLE	Depth	Class[1]	Fe	Ti	Al	Mg	Cr	Mn	Ca	Si	Total Cations	Fe/Fe+Ti[2]	Reflectivity % in air
AUL 8.1.1	170.1	1	52.3	11.2	3.5	2.4	0.2	0.4	0.5	0.7	71.2	0.82	16.0
AUL 20.3.4	241.9	1	55.2	13.1	2.7	1.6	0.0	0.2	0.0	0.1	72.9	0.81	16.0
AUL 82.1.8	563.8	1	54.2	10.6	3.6	2.7	0.2	0.3	0.3	0.3	72.2	0.84	16.0
AVERAGE CLASS 1		1	53.9±1.5	11.6±1.3	3.3±0.5	2.2±0.6	0.1±0.1	0.3±0.1	0.3±0.3	0.4±0.3	72.1	0.82±0.0	16.0±0.0
AUL 14.1.1	200.9	2 ilmenite lamellae	50.5	13.7	3.2	2.1	0.4	0.4	0.4	0.4	71.1	0.79	17.1
	(3)		35.6	30.8	0.7	1.2	0.4	0.9	0.2	0.0	69.8	0.54	R_1 R_2 14.3 - 15.8
AUL 89.1.7	611.0	2	50.6	14.2	3.1	2.0	0.3	0.6	0.4	0.2	71.4	0.78	16.9
AVERAGE CLASS 2		2	50.6±0.1	14.0±0.4	3.2±0.1	2.1±0.1	0.4±0.1	0.5±0.1	0.4±0.0	0.3±0.1	71.5	0.79±0.0	17.0±0.1
AUL 14.3.2	205.9	3	48.9	15.9	2.3	1.7	0.4	1.2	0.3	0.2	70.9	0.75	17.8
AUL 98.2.4	665.3	3	48.4	15.8	2.2	1.8	0.5	1.3	0.2	0.3	70.5	0.75	18.0
		ilmenite lamellae	34.0	32.7	0.7	1.3	0.4	1.4	0.2	0.0	70.7	0.51	15.2 - 17.0
AVERAGE CLASS 3		3	48.7±0.4	15.9±0.1	2.3±0.1	1.8±0.1	0.5±0.1	1.3±0.1	0.3±0.1	0.3±0.1	71.1	0.75±0.0	17.9±0.1
AUL 45.1.2	366.5	4	43.3	17.4	2.4	1.9	0.5	1.2	0.6	0.8	68.1	0.71	R_1 R_2 20.2 - 22.6
	(4)	Brown islands	46.9	16.8	2.6	1.5	0.3	0.5	0.4	0.4	69.4	0.74	19.5
AUL 52.4.5	402.7	4	44.2	17.6	2.5	1.8	0.5	1.4	0.3	0.5	68.8	0.72	20.1 - 22.5
AUL 96.1.3	651.1	4	44.9	16.5	2.6	1.8	0.5	1.3	0.3	0.5	68.4	0.73	20.5 - 22.8
AVERAGE CLASS 4		4	44.1±0.8	17.2±0.6	2.5±0.1	1.8±0.1	0.5±0.0	1.3±0.1	0.4±0.2	0.6±0.2	68.4	0.72±0.0	20.3 - 22.6 ±0.2 ±0.2
AUL 78.1.2	536.8	Brown isotropic	62.4	2.4	1.6	0.3	0.4	0.4	0.0	0.0	67.7	0.96	21.4
AUL 113.1.8	757.1	Brown isotropic	59.9	3.9	1.9	1.0	0.5	1.2	0.0	0.0	68.4	0.94	21.8
AUL 78.1.2	536.8	5 white	47.7	18.9	1.6	0.6	0.3	1.4	0.0	0.0	70.5	0.72	22.8 - 25.2
AUL 113.1.8	757.1	5	44.4	19.2	1.8	1.0	0.4	1.4	0.0	0.0	68.2	0.70	22.4 - 25.0
AUL 78.1.2	536.8	Brown anisotropic	7.1	49.8	0.5	0.8	0.5	1.3	0.0	0.4	60.4	0.12	18.2 - 19.4
AUL 113.1.8	757.1		5.1	52.1	0.6	0.8	0.6	1.7	0.0	0.4	61.3	0.09	18.8 - 20.1
AVERAGE CLASS 5	(5)	Brown isotropic	61.2±1.8	3.2±1.1	1.8±0.2	0.8±0.4	0.5±0.1	0.8±0.6	0.0	0.0	68.3	0.95±0.0	21.6±0.3
	(6)	White 5	46.1±2.3	19.1±0.2	1.7±0.1	0.8±0.3	0.4±0.1	1.4±0.0	0.0	0.0	69.5	0.71±0.0	22.6 - 25.1 ±0.3 ±0.1
	(7)	Brown anisotropic	6.1±1.4	51.0±1.6	0.6±0.1	0.8±0.0	0.6±0.1	1.5±0.3	0.0	0.4±0.0	61.0	0.11±0.0	18.5 - 19.8 ±0.4 ±0.5
AUL 8.5.2	171.9	Pseudo-brookite	39.8	20.8	1.3	1.7	0.4	2.1	0.9	0.9	67.9	0.66	15.1 - 16.3
AUL 46.2.7	370.8	"	41.5	24.2	0.8	0.7	0.2	1.0	0.0	0.0	68.4	0.63	15.2 - 16.0
AUL 8.5.2	171.9	white titano-hematite	53.2	14.5	1.0	0.7	0.3	0.3	0.0	0.0	70.0	0.79	21.2 - 23.2
AUL 46.2.7	370.8		53.2	13.8	0.8	0.9	0.4	0.3	0.0	0.0	69.4	0.79	21.2 - 23.0
AVERAGE CLASS 6		Pseudo-brookite	40.7±1.2	22.5±2.4	1.1±0.4	1.2±0.7	0.3±0.1	1.6±0.8	0.5±0.6	0.5±0.6	68.4	0.65±0.0	15.2 - 16.2 ±0.1 ±0.2
		titano-hematite	53.2±0.0	14.2±0.5	0.9±0.1	0.8±0.1	0.4±0.1	0.3±0.0	0.0	0.0	69.8	0.79±0.0	21.2 - 23.1 ±0.0 ±0.0

(1) deuteric oxidation classes of Ade-Hall et al., (1968)
(2) ratio is calculated without taking into account Al, Mg, Cr, Ca and Si impurities
(3) size of ilmenite lamellae is small (< 0µ) so that contamination in the probe analysis is possible and results in high total ilmenite value
(4) magnetite phase
(5) magnetite phase
(6) titanohematite phase
(7) rutile phase

1976a). One possible explanation is that these samples represent the interior of a flow since all of them are coarse grained basalts.

(2) Ilmenite: The high temperature oxidation of ilmenite has been categorized by Haggerty (1971) in six classes. The classification was based on the formation of iron-titanium phases from partitioning and redistribution of iron and titanium ions within the crystal lattice. This oxidation takes place above 600°C at high oxygen fugacity (Haggerty 1971).

Ilmenite at different stage of Haggerty's high temperature oxidation scale, where recognized in the Azores drill core, was studied by the microprobe analyzer and the microphotometer. The chemical composition and the intensity of reflectivity are shown in Table 7.

Several of Haggerty's classes of high temperature oxidation of ilmenite was observed in the Azores drill core and these are illustrated in Plate 6.

A summary of high temperature oxidation classifications of titanomagnetite and ilmenite is given in Table 8.

3.2. Hydrothermal Alteration: Several lines of evidence indicate that the rocks of the Azores drill core have undergone phase transformations caused by hydrothermal processes. This evidence comes from field observations, measurements of in-hole temperatures and from laboratory studies of the drill core, as detailed in Chapter III. Field measurements of in-hole geothermal gradient, figure 23, defined tem-

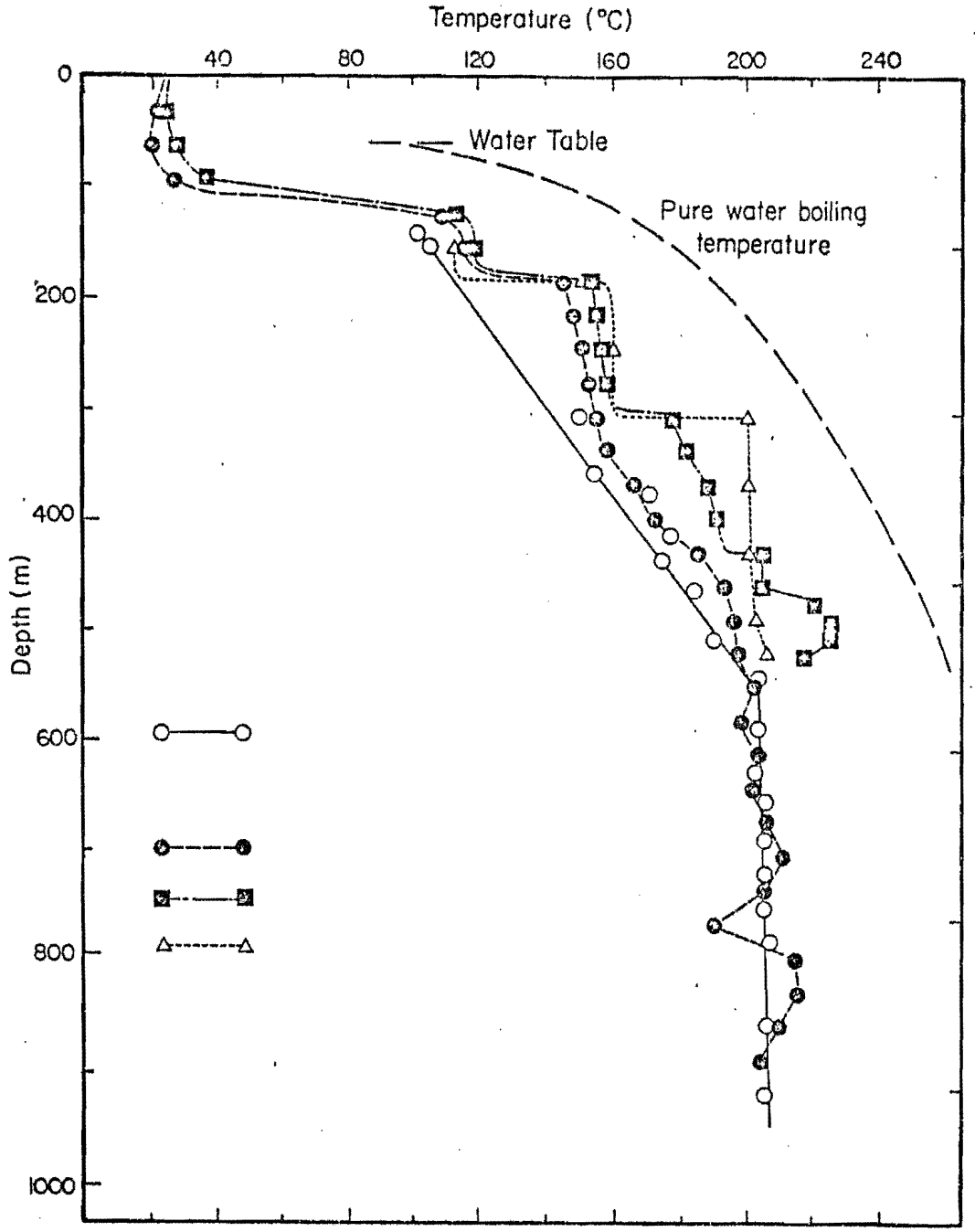

Figure 23. Temperature measurements with maximum thermometers (±2°C) to 9.4 m during drilling; to 885 m with thermocouple (±1°C) between 1 and 2 h and again 4 days after termination of water circulation. Two days after further circulation maximum thermometer measurements were made to 518 m. O: temperatures at the bottom of the hole; temperature logs: O: 26 August (1-3 h): : 2 September (4 d): Δ: 7 September (3 d). (After Muecke et al. 1974).

Table 7. Reflectivity and microprobe data for ilmenite and its high temperature oxidation products

SAMPLE	Depth in m	Class	Fe	Ti	Al	Mg	Cr	Mn	Ca	Si	Total Cations	Fe/Fe+Ti	Reflectivity % in air R_1 R_2
AVERAGE CLASS 1 (1)		1	35.8±0.1	29.5±0.3	0.6±0.1	1.2±0.1	0.6±0.1	0.7±0.1	0.0	0.0	68.4	0.55	14.8 - 16.9 ±0.3 ±0.4
AUL 8.5.2	171.9	Ferri-ilmenite	39.2	19.2	0.9	1.6	0.9	1.1	0.4	0.7	64.0	0.67	15.3 - 16.9
AUL 31.1.2	292.3	" (2)	37.9	21.0	0.7	1.5	1.0	1.3	0.0	0.8	64.2	0.64	15.3 - 16.9
AUL 8.5.2	171.9	Crichtonite	23.9	37.6	0.6	1.2	0.5	0.9	0.0	0.3	65.0	0.39	17.0 - 17.1
AUL 31.1.2	292.3	"	26.0	33.2	0.6	1.4	0.6	0.7	0.2	0.4	63.1	0.44	17.3 - 17.4
AVERAGE CLASS 2		Ferri-ilmenite	38.6±0.9	20.1±1.3	0.8±0.1	1.6±0.1	1.0±0.1	1.2±0.1	0.2±0.3	0.8±0.1	64.3	0.66±0.0	15.3 - 16.9 ±0.0 ±0.0
		Crichtonite	25.0±1.5	35.4±3.1	0.6±0.0	1.3±0.1	0.6±0.1	0.8±0.1	0.1±0.1	0.4±0.1	64.2	0.42±0.0	17.2 - 17.3 ±0.2 ±0.2
AUL 18.1.2	223.7	Crichtonite	23.2	37.1	0.4	1.3	0.4	0.7	0.5	0.4	64.0	0.38	17.2 - 17.6
AUL 31.1.2	292.3	"	22.9	37.5	0.6	1.0	0.6	0.6	0.5	0.5	64.2	0.38	17.3 - 17.7
AUL 18.1.2	223.7	Ferri-ilmenite	37.9	20.1	0.8	1.5	0.8	1.1	0.5	0.2	62.9	0.65	15.2 - 17.0
AUL 31.1.2	292.3	"	38.3	19.8	0.9	1.5	0.6	1.0	0.5	0.6	63.2	0.66	15.2 - 16.9
AUL 18.1.2	223.7	Titanohematite	49.8	16.2	0.6	0.9	0.4	0.6	0.0	0.0	68.5	0.75	21.2 - 25.4
AUL 31.1.2	292.3	"	52.4	16.0	0.4	0.6	0.3	0.3	0.0	0.0	70.0	0.77	21.5 - 25.6
AUL 18.1.2	223.7	Rutile	13.3	43.2	0.5	0.6	0.4	1.2	0.0	0.0	59.2	0.23	19.6 - 18.3
AUL 31.1.2	292.3	Rutile	12.9	43.1	0.3	0.5	0.4	1.0	0.0	0.0	58.2	0.23	20.3 - 18.9
AVERAGE CLASS 3		Crichtonite	23.1±0.2	37.3±0.3	0.5±0.1	1.2±0.2	0.5±0.1	0.7±0.1	0.5±0.0	0.5±0.1	64.3	0.38±0.0	17.3 - 17.7 ±0.1 ±0.1
		Ferri-ilmenite	38.1±0.3	20.0±0.2	0.9±0.1	1.5±0.0	0.7±0.1	1.1±0.1	0.5±0.0	0.4±0.3	63.2	0.66±0.0	15.2 - 17.0 ±0.0 ±0.1
		Titanohematite	51.1±1.8	15.1±0.1	0.5±0.1	0.8±0.2	0.4±0.1	0.5±0.2	0.0	0.0	69.4	0.76±0.0	21.4 - 25.5 ±0.2 ±0.1
		Rutile	13.1±0.3	43.2±0.1	0.4±0.1	0.6±0.1	0.4±0.0	1.1±0.1	0.0	0.0	58.4	0.23±0.0	20.0 - 18.6 ±0.5 ±0.4
AUL 8.5.2	171.9	Titanohematite	55.6	13.1	0.3	0.8	0.5	0.4	0.0	0.6	71.3	0.81	22.4 - 25.9
AUL 66.4.3	475.2	"	55.0	13.0	0.4	0.7	0.4	0.4	0.0	0.5	70.4	0.81	22.6 - 26.3
AUL 8.5.2	171.9	Rutile (3)	10.1	46.8	0.5	0.4	0.4	1.0	0.0	0.0	59.2	0.81	20.7 - 19.2
AUL 66.4.3	475.2	Rutile	11.2	46.7	0.5	0.5	0.3	0.9	0.0	0.0	60.1	0.19	19.8 - 18.5
AVERAGE CLASS 4		Titanohematite	55.3±0.4	13.1±0.1	0.4±0.1	0.8±0.1	0.5±0.1	0.4±0.0	0.0	0.6±0.1	71.1	0.81±0.0	22.5 - 26.1 ±0.1 ±0.3
		Rutile	10.7±0.8	46.8±0.1	0.5±0.0	0.5±0.1	0.4±0.1	1.0±0.1	0.0	0.0	59.9	0.18±0.0	20.3 - 18.9 ±0.6 ±0.5
AUL 31.1.6	296.2	Pseudobrookite	43.9	19.8	0.6	1.0	0.4	0.7	0.7	0.6	67.7	0.69	15.4 - 16.2
AUL 49.1.1	382.9	"	44.0	19.5	0.8	1.1	0.3	0.6	0.4	0.5	67.2	0.69	15.1 - 16.2
AUL 31.1.6	296.2	Titanohematite	53.4	21.2	0.5	0.5	0.3	0.3	0.0	0.0	76.2	0.72	22.0 - 25.6
AUL 49.1.1	382.9	Titanohematite	52.2	22.3	0.6	0.5	0.4	0.3	0.0	0.0	76.3	0.70	22.9 - 26.1
AUL 31.1.6	296.2	Rutile	10.3	48.2	0.4	0.4	0.4	0.9	0.0	0.0	60.6	0.18	19.7 - 18.2
AUL 49.1.1	382.9	Rutile	7.7	49.8	0.5	0.4	0.4	0.8	0.0	0.0	59.6	0.13	19.6 - 18.1
AVERAGE CLASS 5		Pseudobrookite	44.0±0.1	19.7±0.2	0.7±0.1	1.1±0.1	0.4±0.1	0.7±0.1	0.6±0.2	0.6±0.1	67.8	0.69±0.0	15.3 - 16.2 ±0.2 ±0.0
		Titanohematite	52.8±0.9	21.8±0.8	0.6±0.1	0.5±0.0	0.4±0.1	0.3±0.0	0.0	0.0	76.4	0.71±0.0	22.5 - 25.9 ±0.6 ±0.4
		Rutile	9.0±1.8	49.0±1.1	0.5±0.1	0.4±0.0	0.4±0.0	0.9±0.1	0.0	0.0	60.2	0.16±0.0	19.7 - 18.2 ±0.1 ±0.1
AUL 8.5.2	171.9	Pseudobrookite	41.3	20.3	0.8	0.9	0.5	0.7	0.6	0.0	65.1	0.67	15.0 - 15.4
AUL 31.1.6	296.2	"	43.5	19.6	0.7	0.9	0.6	0.7	0.4	0.0	66.4	0.69	15.3 - 16.1
AVERAGE CLASS 6		Pseudobrookite	42.4±1.6	20.0±0.5	0.8±0.1	0.9±0.0	0.6±0.1	0.7±0.0	0.5±0.1	0.0	65.9	0.68±0.0	15.2 - 15.8 ±0.2 ±0.5

(1) Average is taken from previous calculations, Table 4.
(2) Size of crichtonite lamellae is extremely small (less than 2µ) so that contamination with ferri-ilmenite has occurred and thus results in high total cations
(3) Rutile lamellae (less than 4µ)

Table 8. A summary of high temperature oxidation classification of titanomagnetite and ilmenite.

CLASS		MINERAL PHASE		MICROPROBE DATA																	REFLECTIVITY PERCENTAGE IN AIR AT 546 nm	
				Titanomagnetite									Ilmenite									
Titano-maghemite	Ilmenite	Titanomagnetite	Ilmenite	Fe	Ti	Al	Mg	Cr	Mn	Ca	Si	Fe/Fe+Ti	Fe	Ti	Al	Mg	Cr	Mn	Ca	Si	Fe/Fe+Ti	Titanomagnetite	Ilmenite R_1 R_2
1	1	Homogeneous titanomagnetite	Homogeneous ilmenite	53.9±1.5	11.6±1.3	3.3±0.5	3.2±0.6	0.1±0.1	0.3±0.1	0.3±0.3	0.4±0.3	0.82±0.0	35.8±0.1	29.5±0.3	0.6±0.1	1.2±0.1	0.6±0.1	0.7±0.1	0.0	0.0	0.55±0.0	16.0±0.0	14.8-16.9 ±0.3 ±0.4
2	2	Titanomagnetite with less than 50% of the grain area ilmenite	Ferrilmenite contains lamellae of crichtonite	Titanomagnetite									Ferrilmenite									17.0-17.1
				50.6±0.1	14.0±0.4	3.2±0.1	2.1±0.1	0.4±0.1	0.5±0.1	0.4±0.0	0.3±0.1	0.76±0.0	34.6±0.9	20.[illegible]±1.1	0.8±0.1	1.6±0.1	1.0±0.1	1.2±0.1	0.2±0.1	0.8±0.1	0.66±0.0	17.0±0.1	±0.0 ±0.0
				Ilmenite									Crichtonite									17.2-17.1
				35.6	30.6	0.7	1.2	0.1	0.9	0.2	0.0	0.54	25.0±1.5	35.4±1.1	0.6±0.0	1.3±0.1	0.6±0.1	0.8±0.1	0.1±0.1	0.4±0.1	0.42±0.0	14.3-15.8	±0.2 ±0.2
3	3	Titanomagnetite with more than 50% of the grain area ilmenite lamellae	Ferri ilmenite contains lamellae of crichtonite and titanohematite contains rutile lamellae	Titanomagnetite									Ferri-ilmenite									17.0-17.0
				48.7±0.4	15.9±0.1	2.3±0.1	1.8±0.1	0.5±0.1	1.3±0.1	0.3±0.1	0.3±0.1	0.75±0.0	38.1±0.3	20.0±0.2	0.9±0.1	1.5±0.0	0.7±0.1	1.1±0.1	0.5±0.0	0.4±0.1	0.66±0.0	17.9±0.1	±0.0 ±0.0
				Ilmenite									Crichtonite									17.3-17.7
				34.0	32.7	0.7	1.3	0.4	1.4	0.2	0.0	0.51	23.1±0.2	37.3±0.3	0.5±0.1	1.2±0.2	0.6±0.1	0.7±0.1	0.5±0.0	0.5±0.1	0.38±0.0	15.2-17.0	±0.1 ±0.1
													Titanohematite									21.4-23.5
													51.1±1.8	16.1±0.1	0.5±0.1	0.8±0.2	0.4±0.1	0.3±0.2	0.0	0.0	0.76±0.0	±0.2 ±0.1
													Rutile									20.0-18.6
													13.1±0.3	43.2±0.1	0.4±0.1	0.6±0.1	0.4±0.0	1.1±0.1	0.0	0.0	0.23±0.0	±0.5 ±0.4
4	4	Titanomagnetite forming titanohematite. Brown magnetite appear	Strongly anisotropic titanohematite contains lamellae of rutile	Titanohematite									Titanohematite									20.3-22.5
				44.1±0.4	17.2±0.6	2.5±0.1	1.8±0.1	0.4±0.0	1.3±0.1	0.4±0.2	0.4±0.2	0.72±0.0	55.3±0.4	13.1±0.1	0.4±0.1	0.8±0.1	0.5±0.1	0.4±0.0	0.0	0.6±0.1	0.81±0.0	±0.2 0.2	22.5-26.1 ±0.1 0.3
				Magnetite									Rutile									20.3 19.4
				46.9	16.8	2.6	1.5	0.3	0.5	0.4	0.4	0.74	10.7±0.3	46.8±0.1	0.5±0.0	0.5±0.1	0.4±0.1	1.0±0.1	0.0	0.0	0.18±0.0	19.5	±0.6 ±0.5
5	5	Here, titanohematite, rutile and some titanomagnetite are present	At this stage pseudobrookite rim forms on titanohematite and rutile	Titanohematite									Pseudobrookite									22.6-23.1
				46.1±2.3	19.1±0.2	1.7±0.1	0.8±0.3	0.4±0.1	1.4±0.0	0.0	0.0	0.71±0.0	44.0±0.1	19.7±0.2	0.7±0.1	1.1±0.1	0.4±0.1	0.7±0.1	0.6±0.2	0.6±0.1	0.69±0.0	±0.3 ±0.1	21.3±0.0
				Rutile									Titanomagnetite									18.5-19.8	22.5-25.9
				6.1±1.4	51.0±1.6	0.6±0.1	0.8±0.0	0.6±0.1	1.5±0.3	0.0	0.4±0.0	0.11±0.0	52.8±0.9	21.8±0.8	0.6±0.1	0.5±0.0	0.4±0.1	0.3±0.0	0.0	0.0	0.71±0.0	±0.4 ±0.5	19.6±0.4
				Titanomagnetite									Rutile									19.7-18.2
				61.2±1.8	3.2±1.1	1.8±0.2	0.8±0.4	0.5±0.1	0.8±0.6	0.0	0.6	0.95±0.0	9.0±1.8	49.0±1.1	0.5±0.1	0.4±0.0	0.4±0.0	0.9±0.1	0.0	0.0	0.16±0.0	21.6±0.3	±0.1 ±0.1
6	6	Pseudobrookite after ilmenite in titanohematite	Pseudobrookite is the end product of ilmenite high temp oxidation	Pseudobrookite									Pseudobrookite									15.2-16.2	15.2-15.8
				40.7±1.2	22.5±2.4	1.1±0.4	1.2±0.7	0.3±0.1	1.6±0.8	0.5±0.6	0.5±0.6	0.65±0.0	42.4±1.6	20.0±0.5	0.8±0.1	0.9±0.0	0.6±0.1	0.7±0.0	0.5±0.1	0.0	0.68±0.0	±0.1 ±0.2	±0.2 ±0.5
				Titanohematite																		21.2 23.1	
				53.2±0.8	14.2±0.5	0.9±0.1	0.8±0.1	0.4±0.1	0.3±0.0	0.0	0.0	0.79±0.0										±0.0 ±0.1	

peratures of between 20-25°C to a depth of 100 m. The temperature suddenly increased to over 100°C between 100 and 175 m. A uniform geothermal gradient of about 250°C/km was encountered between 175 and 550 m. From 550 m to the bottom of the hole, a very small temperature gradient of 10°C/km was measured.

Laboratory studies of the rocks have been conducted by McGraw (1976), Sarkar (unpublished report 1976), Lawrence and Maxwell (1977, in preparation), Mitchell et al. (1977), and by the present author. McGraw (1976) has studied the petrography and chemical variation of major and trace elements with depth. She divided the Azores basalts, on the basis of whole rock total alkalis and phenocryst microprobe analyses, into alkalic and tholeiitic types. She concluded that tholeiitic chemical affinities were the result of hydrothermal alteration and that the basalts were originally of alkali affinities. Although her examination of silicate minerals revealed small variations in chemical composition, some plagioclase phenocrysts were fractured and strongly corroded at different depths of the drill core. Ferromagnesium minerals showed a chloritic type of alteration in most of the core. Olivine of the altered samples usually showed fine irregular stringers of magnetite and hematite.

Sarkar (1976) has conducted an x-ray study of the secondary minerals found in vugs and fractures and in the groundmass of the basalts. Although he did not detect any zeolite minerals other secondary phases were abundant. The secondary phases which were

taken as indications of hydrothermal alteration, included; Ca-rich and Fe-rich montmorillonites, kaolinites, barite, anhydrite, fluorite, hematite, limonite and calcite. Limonite, chlorite and barite were found between 250-400 m and 550-750 m depths in the high temperature hydrothermal zone.

Lawrence and Maxwell (1977) have measured the oxygen and carbon isotopic ratios for some calcite vugs and veins in the drill core basalts. They used these ratios to calculate the temperatures of equilibration of calcites with water. The calculated temperatures agreed well with the observed temperatures in the region of 600-700 meter, figure 24, but were distinctly lower than the observed temperatures in all other depths. The scatter in the distribution of calculated temperatures was attributed to the incomplete equilibration with hot fluids.

Mitchell et al. (1977) used the fission track method to detect the uranium distribution in the Azores drill rocks. The average concentration of uranium was higher than that of oceanic basalts. Mitchell et al. suggested that the relatively high uranium concentration was a secondary enrichment caused by alteration in the presently active geothermal environment.

The microscopic examination of polished sections of core rocks (Appendix I) indicates that progressive textural and mineralogical variations in Fe-Ti oxide phases with hydrothermal conditions occur in the core. These variations presumably originate in the interaction of thermal fluids and rock masses. Presumably time of exposure, range of temperatures and extreme chemical conditions are important factors for the relatively

low temperature processes. Temperatures were both measured and calculated in the drill core, but unfortunately, Ph of the hot solutions was not measured. Pressure and oxygen fugacity probably have a small effect on the alteration of rocks in near surface area (Kerr 1955). The common occurrences of decomposition and replacement textures, reaction haloes, dissiminations, bleached zones and the nature of secondary minerals, were all consistent with other hydrothermal alteration criteria. The high Curie temperatures throughout the core were taken as an evidence to support the existence of hydrothermal alteration as the major feature of the drill core.

The mineralogical study of iron-titanium oxide phases in the Azores drill core together with other hydrothermal alteration criteria allow a unique classification of hydrothermally altered iron-titanium oxide minerals in active areas. Depending on the degree of hydrothermal alteration, three stages are proposed; low, medium and high hydrothermal alteration. Each stage is characterized by the presence of certain mineral phases and specific textures within a defined temperature range. The temperature range is taken from the average of both the in-hole observed and oxygen isotopic calculated temperatures. However, when the difference between the observed and maximum calculated temperatures exceeds 20°C, either the isotopic temperature or available stability field data of iron-titanium oxides (Verhoogen 1962) is used as a guide. All supposed temperatures of alteration are given in Appendix I and the location of the samples in the drill core with their various degrees of hydrothermal alteration is given in figure 25.

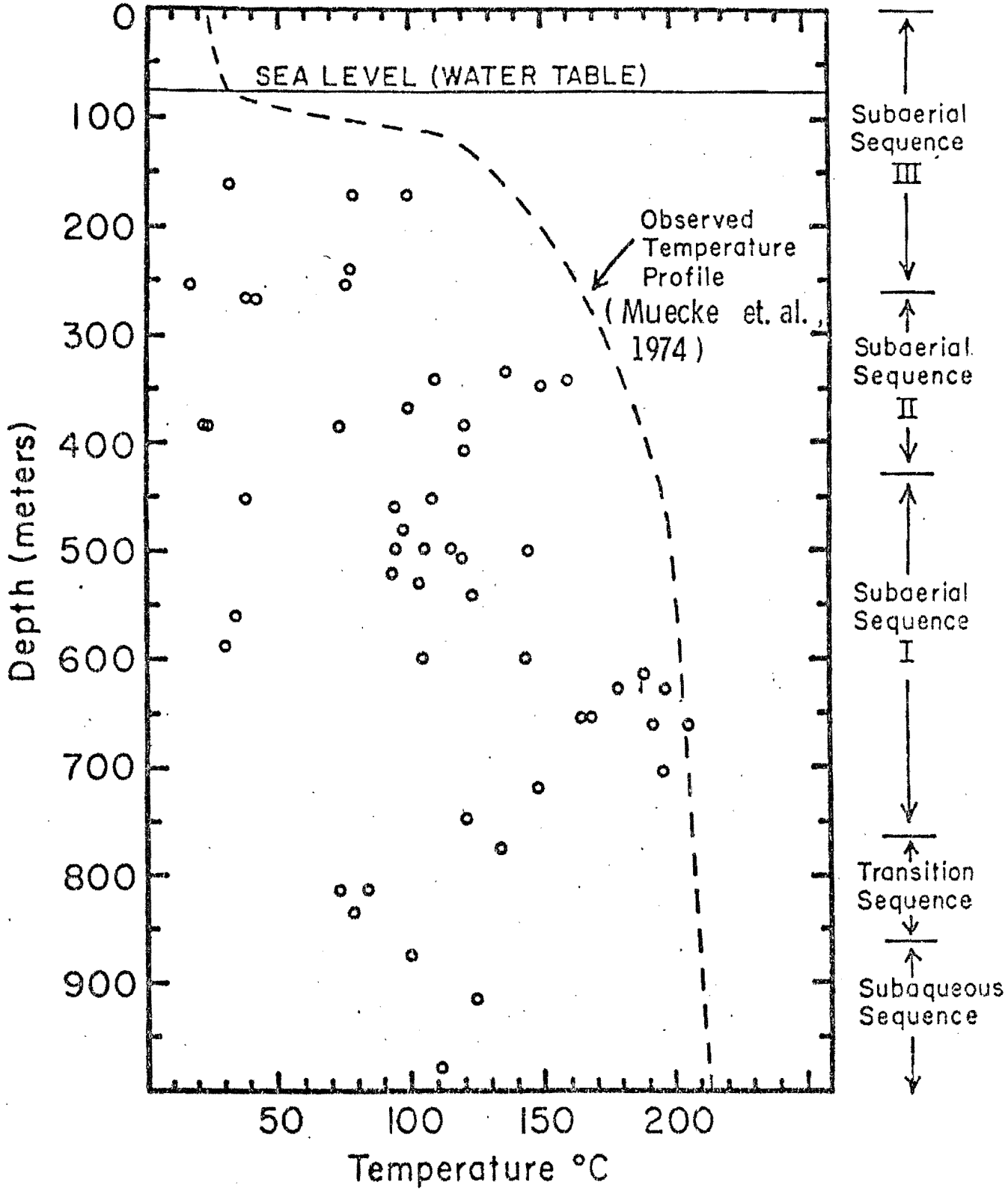

Figure 24. Correlation between the calculated temperatures and depth. (From Lawrence and Maxwell by permission).

(1) Hydrothermal alteration of titanomagnetite: The chemical composition of hydrothermally altered titanomagnetite, its reflectivity and temperatures of alteration, are all given in Table 9. The following are the proposed alteration classifications:

Stage 1: Low degree hydrothermal alteration: The temperature range for this stage is from 20°-80°C (taken from in-hole measured temperatures, oxygen isotope ratios and stability field of the mineral phases, see Appendix I). The classification of low degree hydrothermal alteration of titanomagnetite depends on (i) partial alteration of titanomagnetite to titanomaghemite as an intermediate stage and (ii) complete alteration to titanomaghemite as the end of the stage. Titanomagnetite is classified in this stage into four classes, Plate 7 (a,b,c, and d).

Class L_1: Homogeneous titanomagnetite, Plate 7(a).

Class L_2: Some Fe^{2+} oxidizes to Fe^{2+} which results in the formation of randomly distributed lines of an isotropic whitish blue phase identified as titanomaghemite. This is accompanied either by volume change cracks or microcracking which can only be seen at a very high magnification (2500 X in oil). Tianium diffuses through the lattice and the whitish blue areas always how an increase in Ti and decrease in Fe (see microprobe data, Table 6, Plate 7(b).

Table 9. Reflectivity and microprobe analyses of hydrothermally altered titanomagnetite

SAMPLE	Depth in m	Average Temp. °C	Fe	Ti	Al	Mg	Cr	Mn	Ca	Si	Total Cations	Fe/Fe+TO	R%
AVERAGE *1	L_1	19.5	49.5±2.0	15.2±1.4	2.3±0.5	1.9±0.2	0.6±0.2	1.7±0.7	0.0	0.0	71.2	0.77	16.0
AUL 11.2.7	195.5	34	50.3	16.5	2.2	1.1	0.2	0.8	0.0	0.0	71.1	0.75	16.8
AUL 22.1.2	249.1	46	48.5	17.1	2.6	1.3	0.3	1.3	0.0	0.0	71.1	0.74	16.7
AUL 25.5.7	266.1	42	47.3	16.7	2.6	2.0	0.4	1.3	0.3	0.3	70.9	0.74	16.7
AUL 52.2.7	455.8	32	48.9	16.2	2.7	1.3	0.5	1.3	0.0	0.0	70.9	0.75	17.2
AVERAGE	L_2	38.5±6.6	48.8±1.2	16.6±0.4	2.5±0.2	1.4±0.4	0.4±0.1	1.2±0.3	0.1±0.2	0.1±0.2	71.1	0.75±0.0	16.9±0.2
AUL 54.1.4	411.1	58	46.9	17.7	2.6	1.0	0.4	1.2	0.0	0.0	69.8	0.73	19.0
AUL 66.4.7	475.2	52	46.9	17.1	2.5	1.1	0.4	1.3	0.2	0.3	69.8	0.73	19.6
AVERAGE	L_3	55±4.2	46.9±0.0	17.4±0.4	2.6±0.1	1.1±0.0	0.4±0.0	1.3±0.1	0.1±0.1	0.2±0.2	69.8	0.73±0.0	19.3±0.4
AUG 5.1.1 *2	155	75	43.8	19.2	0.8	1.0	3.8	0.9	0.0	0.0	69.5	0.70	19.2
AUL 62.2.3	453.9	68	44.5	18.6	2.9	1.0	0.4	1.4	0.0	0.0	68.8	0.70	22.2
AUL 75.4.7	521.3	72	44.3	19.0	2.6	0.8	0.5	1.6	0.0	0.0	68.8	0.70	21.9
AUL 116.1.7	776.4	74	45.5	18.2	2.7	0.7	0.3	1.4	0.0	0.0	69.8	0.71	22.6
AUL 131.1.1	867.3	72	46.5	18.7	2.5	0.7	0.4	1.1	0.0	0.0	69.9	0.71	22.0
AVERAGE	L_4	77.2±2.3	45.2±1.0	18.6±0.3	2.7±0.2	0.8±0.1	0.4±0.1	1.4±0.2	0.0	0.0	69.1	0.71±0.0	22.2±0.3
AUL 49.3.1	385.6	85	45.5	20.4	2.4	0.6	0.4	1.2	0.0	0.0	70.5	0.69	22.9
AUL 63.1.3	481.8	80	44.8	20.8	2.3	0.6	0.2	1.2	0.0	0.0	69.9	0.68	22.7
AVERAGE	M_1	82.5±3.5	45.2±0.5	20.6±0.3	2.4±0.1	0.6±0	0.3±0.1	1.2±0	0.0	0.0	70.3	0.69±0.0	22.8±0.1
AUL 19.2.2	231.6	125	41.6	20.3	2.9	0.9	0.5	2.1	0.4	0.0	68.7	0.67	23.6-27.8
AUL 92.1.2	626.9	115	41.0	20.6	2.7	0.9	0.4	2.1	0.5	0.3	68.5	0.67	23.6-27.7
AUL 96.1.6	655.5	120	42.3	20.8	3.1	0.6	0.3	1.8	0.3	0.3	69.5	0.67	23.3-27.2
AUL 101.2.4	692.2	125	42.8	22.0	2.2	0.6	0.3	1.1	0.0	0.2	69.2	0.66	23.0-27.1
AVERAGE	M_2	121.3±4.8	41.9±0.8	20.9±0.8	2.7±0.4	0.8±0.2	0.4±0.1	1.8±0.5	0.3±0.2	0.2±0.1	69.0	0.67±0.0	23.4-27.5 ±0.3±0.4
AUL 39.2.7	334.3	145	28.5	33.5	3.0	0.5	0.3	0.9	1.3	0.8	68.8	0.46	22.2
AUL 144.1.8	956.7	158	31.4	32.1	2.4	0.6	0.3	0.8	1.1	0.7	69.4	0.49	22.0
AVERAGE	M_3	151.5±9.2	30.0±2.1	32.8±1.0	2.7±0.4	0.6±0.1	0.3±0	0.9±0.1	1.2±0.1	0.8±0.1	69.3	0.48±0.0	22.1±0.1
AUL 45...7	367.1	158	26.4	36.9	2.1	0.8	0.3	0.6	2.1	0.7	69.9	0.42	20.7
AUL 89...5	607.6	168	19.6	40.7	1.7	1.0	0.4	0.8	3.1	0.8	68.1	0.32	20.1
AVERAGE	M_4	163.0±7.1	23.0±4.8	38.8±2.7	1.9±0.3	0.9±0.1	0.4±0.1	0.7±0.1	2.6±0.7	0.8±0.1	69.1	0.37±0.1	20.4±0.4

*1 average taken from previous calculations of unaltered samples, Table 1, 2 & 3
*2 different flow (not included in averagings)

N.B. no titanomagnetite remains at higher stage of alteration.

Class L_3: Fe^{2+} continues to oxidize and migrate and Ti continues to diffuse. Titanomaghemite lines now become small patches in titanomagnetite grain. The total area of patches is less than 50% of the grain area, Plate 7(c).

Class L_4: In this division more than 50% of the grain area contains patches of titanomaghemite and in some cases the grain is completely changed to titanomaghemite, Plate 7(d).

Stage 2: Medium degree hydrothermal alteration: The temperatures for this stage range from 80° to 160°C. The criteria for classification of titanomagnetite in this stage is (i) the formation of a high reflectivity phase, a titanohematite, (ii) the formation of granular Ti rich phases. The classification of titanomagnetite alteration in this stage includes four classes, Plate 8(a,b,c and d).

Class M_1: This class involves all the patchy titanomagnetite as well as the totally transformed titanomaghemite. This is also the same as L_4 class of low degree hydrothermal alteration titanomagnetite, Plate 8(a).

Class M_2: Here, titanomaghemite is altered to an anisotropic white color, highly reflecting titanohematite. Titanohematite occurs as

a dissiminated phase (spots) replacing titanomaghemite and/or as small areas in the original titanomagnetite depending on where titanomaghemite is present. In this class almost all Fe^{2+} is oxidized to Fe^{3+} and Ti continues to diffuse. Some of Fe^{3+} migrates from the lattice and reacts with OH^- in the hot solutions to form a red-orange colored phase, limonite, in adjacent silicates, which can be seen in the polished section, Plate 8(b).

Class M_3: Titanohematite becomes unstable in the presence of hot solution and transforms to granules phase rich in TiO_2, anatase (Plasse, 1977 pers. comm.). Iron leaves the lattice and reacts with the hot solutions to form iron hydroxides. The granules have variety of colors in oil (blue, orange, yellow and red) possibly as a result of internal reflection. This alteration and the increase in migration of Fe^{3+} ions (see microprobe results) cause an increase in the width of the cracks, which are already present from the various stages, and a dark brown to black colored phase (sphene) is formed.

The granulated areas occupy less than half the area of the original titanomagnetite, Plate 8(c).

Class M_4: The granulated areas now include whole grains and the dark brown-black sphene spreads throughout grains, Plate 8(d).

Stage 3: High degree hydrothermal alteration: The temperature range for this stage is from 160° to 210°C. This stage represents the maximum hydrothermal alteration of titanomagnetite, where the original titanomagnetite becomes as ghost. Limonite and sphene are the dominant phases in this stage. The alteration of titanomagnetite is classified into three classes, Plate 9(a,b, and c).

Class H_1: Totally granulated grains of titanomagnetite. This is the same as M_4 class of medium degree hydrothermal alteration, Plate 9(a).

Class H_2: The original titanomagnetite is completely replaced with a sphene in the cracks. Some titanohematite remains, Plate 9(b).

Class H_3: In this class the original titanomagnetite grain can be detected from the presence of red limonite areas and the presence of sphene. No titanohematite is left, Plate 9(c).

N.B. In the above classification, the maximum alteration class in every stage is equivalent to the minimum alteration class for the next stage. The former indicates a lower temperature range while the latter represents a higher temperature range for the overall state of alteration.

(2) Hydrothermal alteration of ilmenite: The alteration of ilmenite involves oxidation of ferrous iron to ferric and the progressive removal of iron by leaching, resulting in the production of rutile and sphene in the high hydrothermal alteration conditions. The various phases in the hydrothermal alteration of ilmenite were identified microscopically (Appendix I) and the chemical composition was determined by the microprobe analyzer. The intensity of reflectivity was used in identifying the phases and in determining the degree of hydrothermal alteration of ilmenite. The microprobe and reflectivity data are given in Table 10. Hydrothermal alteration of ilmenite is abundant in the Azores drill core, figure 25. A new classification of hydrothermal alteration of ilmenite is proposed. The classification is a temperature dependent and based on the textural variations and phase changes in ilmenite as a result of hydrothermal solution. No alteration of ilmenite was detected in the temperature range 20° to 80°C.

Stage 1: Low degree hydrothermal alteration: The temperature range for this stage is from 80°-100°C. Four classes are proposed and they are shown in Plate 10(a,b,c and d).

Class S_1: Homogeneous ilmenite with no alteration, Plate 10(a).

Table 10. Reflectivity and microprobe data for ilmenite and its hydrothermal alteration products

SAMPLE	Depth in m	Average Temp °C	Fe	Ti	Al	Mg	Cr	Mn	Ca	Si	Total Cations	Fe/Fe+Ti	R%
AVERAGE*	S_1	42	35.8±0.1	29.5±0.3	0.6±0.1	1.2±0.1	0.6±0.1	0.7±0.1	0.0	0.0	64.8	0.55	14.8-16.9 ±0.3 ±0.4
AUL 6.1.3	159.4	80	33.9	32.4	0.8	0.8	0.4	0.8	0.0	0.0	69.1	0.51	16.8-17.1
AUL 8.1.9	170.2	78	33.2	33.2	32.0	0.5	1.0	0.4	1.0	0.0	68.1	0.51	17.0-17.2
AUL 49.3.1	385.6	85	31.5	30.3	0.7	1.1	0.6	0.9	0.0	0.0	65.1	0.51	16.1-16.8
AUL 51.2.8	397.9	78	33.8	32.2	0.7	0.9	0.5	0.7	0.0	0.0	68.8	0.51	17.2-17.3
AUL 68.1.3	481.8	80	33.1	31.9	0.5	1.0	0.5	0.8	0.0	0.0	67.8	0.51	16.9-17.1
AUL 120.1.6	802.1	80	31.5	30.3	0.8	1.0	0.6	0.9	0.0	0.0	65.1	0.51	17.0-17.3
AUL 124.1.8	825.8	82	33.3	32.0	0.5	0.8	0.5	0.6	0.0	0.0	67.7	0.51	17.0-17.2
AVERAGE	S_2	80.4±2.4	32.9±1.0	31.6±0.9	0.6±0.1	0.9±0.1	0.5±0.1	0.8±0.1	0.0	0.0	67.3	0.51±0	16.8-17.1 ±0.4-±0.2
AUL 41.1.7	342.1	92	32.2	33.3	0.5	0.5	0.4	0.6	0.0	0.0	67.5	0.49	17.9-18.1
AUL 71.3.2	501.0	98	32.3	33.4	0.4	0.6	0.5	0.6	0.0	0.0	67.8	0.49	17.8-18.0
AUL 73.2.8	511.6	92	32.5	32.0	0.5	0.4	0.4	0.5	0.0	0.0	66.3	0.50	18.1-18.3
AUL 78.1.5	541.2	95	31.4	32.1	0.4	0.5	0.4	0.4	0.0	0.0	65.2	0.49	18.1-18.3
AUL 83.2.4	569.9	98	31.4	33.0	0.5	0.4	0.3	0.4	0.0	0.0	66.0	0.49	18.0-18.2
AUL 83.2.7	574.8	92	32.3	33.7	0.5	0.4	0.4	0.4	0.0	0.0	67.7	0.49	17.8-18.1
AUL 129.2.1	856.8	95	32.2	33.5	0.6	0.4	0.3	0.4	0.0	0.0	67.4	0.49	18.1-18.4
AUL 129.2.2	858.6	92	33.2	34.8	0.3	0.3	0.2	0.3	0.0	0.0	69.1	0.49	18.1-18.3
AUL 135.1.3	894.1	90	32.6	33.1	0.4	0.4	0.3	0.4	0.0	0.0	67.2	0.49	18.0-18.2
AVERAGE	S_3	93.8±2.9	32.2±0.6	33.2±0.8	0.5±0.1	0.4±0.1	0.4±0.1	0.4±0.1	0.0	0.0	67.1	0.49±0	18.0-18.2 ±0.1 ±0.1
AUL 46.2.8	372.1	105	29.8	34.0	0.4	0.4	0.3	0.5	0.3	0.5		0.47	18.7-18.9
AUL 69.7.6	491.2	102	28.6	33.9	0.6	0.5	0.4	0.6	0.5	0.6		0.46	18.6-18.8
AUL 137.1.3	907.4	105	29.8	36.1	0.4	0.4	0.5	0.3	0.0	0.0		0.45	18.9-19.2
AUL 137.1.5	911.5	100	30.1	36.6	0.4	0.3	0.5	0.3	0.3	0.3		0.45	19.1-19.4
AVERAGE	S_4 T_1	102±2.5	29.6±0.7	35.2±1.4	0.5±0.1	0.4±0.1	0.4±0.1	0.4±0.2	0.3±0.2	0.4±0.3		0.46±0.0	18.8-19.1 ±0.1 ±0.3
AUL 103.2.7	698.8	115	5.4	46.2	0.6	0.6	0.3	0.3	1.3	0.9	55.6	0.10	20.0-18.7
AUL 103.2.7		115	43.5	3.4	0.6	0.4	0.5	0.3	2.8	3.7	55.2	0.93	23.0-24.6
AUL 103.2.7		115	18.1	31.9	0.6	0.5	0.4	0.3	1.8	1.9	55.5	0.36	21.0-20.7
AUL 105.3.6	700.7	110	6.2	49.8	0.4	0.5	0.5	0.4	1.5	1.2	60.5	0.11	20.0-18.6
AUL 105.3.6		110	41.6	3.7	0.4	0.6	0.5	0.5	2.2	4.0	53.5	0.92	23.4-25.3
AUL 105.3.6		110	18.0	34.5	0.4	0.5	0.5	0.5	1.7	2.0	58.1	0.34	21.1-20.9
AVERAGE	T_2	112.5 3.5	5.8 0.6 42.6 1.3 18.1 0.1	48.0 2.6 3.6 0.2 33.2 1.8	0.5 0.1 0.5 0.1 0.5 0.1	0.6 0.1 0.5 0.1 0.5 0.0	0.4 0.1 0.5 0.0 0.5 0.1	0.4 0.1 0.4 0.1 0.4 0.1	1.4 0.1 2.5 0.4 1.8 0.1	1.1 0.2 3.9 0.2 2.0 0.1	58.2 54.5 57.0	0.11 0.0 0.93 0.0 0.35 0.0	20.0-18.7 ±0 ±0.1 23.2-25.0 ±0.3 ±0.5 21.1-20.8 ±0.1 ±0.1
AUL 39.2.7	334.3	145	4.1	51.5	0.4	0.3	0.3	0.3	1.7	1.3	59.9	0.07	20.3-18.9
AUL 39.2.7		145	34.2	6.1	0.6	0.6	0.4	0.4	3.9	4.1	50.3	0.85	22.1-23.8
AUL 39.2.7		145	14.1	36.4	0.5	0.4	0.3	0.3	2.5	2.2	56.7	0.28	20.9-20.6
AUL 144.1.8	956.7	158	4.9	52.1	0.3	0.4	0.3	0.4	1.8	1.3	61.5	0.09	21.2-19.0
AUL 144.1.8		158	36.7	7.0	0.6	0.5	0.4	0.5	4.6	4.7	55.0	0.84	22.6-24.1
AUL 144.1.8		158	15.5	37.1	0.4	0.4	0.3	0.4	2.7	2.5	59.3	0.29	21.7-20.7
AVERAGE	T_3 V_1	151.5 9.2	4.5 0.6 35.5 1.8 14.8 1.0	51.8 0.4 6.6 0.6 36.8 0.5	0.4 0.1 0.6 0.0 0.5 0.1	0.4 0.1 0.6 0.1 0.4 0.0	0.3 0.0 0.4 0.0 0.3 0.0	0.4 0.1 0.5 0.1 0.4 0.1	1.8 0.1 4.3 0.5 2.6 0.1	1.3 0.0 4.4 0.4 2.4 0.2	60.9 52.9 58.2	0.08 0.0 0.85 0.0 0.29 0.0	20.8-19.6 ±0.6 ±0.1 22.4-24.0 ±0.4 ±0.2 21.3-20.7 ±0.6 ±0.1
AUL 89.1.5	607.6	168	11.2	38.7	0.6	0.7	0.5	0.4	4.9	6.1	63.1	0.22	19.3
AUL 90.1.4	618.3	175	12.6	40.1	0.4	0.4	0.6	0.4	4.8	5.8	65.1	0.24	20.0
AUL 941.3	641.0	175	10.7	37.5	0.4	0.7	0.5	0.4	5.1	6.1	61.4	0.22	20.2
AUL 98.2.6	665.3	178	13.9	40.1	0.6	0.5	0.4	0.4	5.1	5.9	66.8	0.26	19.2
AUL 99.1.6	668.1	172	12.0	38.9	0.3	0.3	0.6	0.3	4.8	5.8	63.0	0.24	20.7
AVERAGE	V_2	173.6±3.8	12.1±1.3	39.1±1.1	0.5±0.1	0.5±0.2	0.5±0.1	0.4±0.1	4.9±0.2	5.9±0.2	63.9	0.24±0.0	19.9±0.6

* Average taken from previous calculations, Table 4.

N.B. No ilmenite remains at higher stages of alteration.

Class S_2: The first appearance of ilmenite alteration is the change in color from pinkish to greyish tint and the progressive decrease in anisotropy. Reflectivity increases slightly but is still less than that of rutile. At this stage, iron diffuses through the lattice and oxidation starts by transformation from Fe^{2+} to Fe^{3+}, Plate 10(b).

Class S_3: This class is characterized by the appearance of rims, patches and irregular lamellae of a light grey phase, Plate 10(c). In this stage, oxidation occurs and iron is removed from the ilmenite structure according to the equation (Grey and Reid 1975):

$$3FeO \cdot TiO_2 \rightarrow Fe_2O_3 \cdot 3TiO_2 + Fe$$

This results in the formation of the mineral pseudorutile (Teufer and Temple 1966) which is a light grey in contrast to the grey color of the rest of the ilmenite grain. The orientation of pseudorutile crystallites is governed by the original ilmenite lattice.

Class S_4: The altered areas become enlarged and merge into one another, Plate 10(d). In this division, iron continues to migrate and alteration is facilitated by the introduction of hot solution into the cracks which result from volume change by oxidation. The mineral pseudorutile is slightly anisotropic and has a reflectivity

value of (18.8 ± 0.2) higher than ilmenite (16.8 ± 0.4) but still lower than rutile (20.8 ± 0.6). It has no internal reflection. The composition can change due to metal diffusion and oxidation up to the point of conversion of all Fe^{2+} and Fe^{3+} where a final composition of pseudorutile ($Fe_2 Ti_3 O_9$) is reached. The mineral at this stage is stable and relatively resistant to further alteration at these temperatures.

Stage 2: Medium degree hydrothermal alteration: The temperatures for this stage ranges from 100° to 150°C. Ilmenite is classified into three classes, Plate 11(a,b and c):

Class T_1: Ilmenite contains pseudorutile. This is the same class as S_4, Plate 11(a).

Class T_2: Here pseudorutile is replaced by a grey color rutile and whitish yellow hematite. The change from pseudorutile to rutile is a function of iron content according to the equation (Grey and Reid 1975):

$$Fe_2O_3 \cdot 3TiO_2 \rightarrow 3TiO_2 + \underbrace{2Fe^{3+} + 3O^{-2}}_{Fe_2O_3}$$

This reaction involves a disruption of the lattice as both iron and oxygen are removed and cracks appear in the grain, Plate 11(b).

Class T_3: In this class all the pseudorutile is converted to rutile and hematite and cracks due to the oxidation and

leaching of iron spread through the grain, Plate 11(c). Some red to orange colored phase appears around the cracks and in the surrounds of the grain. This phase is an iron hydroxide and results from the reaction between leached iron and water. At this stage reflectivity increases and reaches that of rutile.

Stage 3: High degree hydrothermal alteration: This is the final stage of hydrothermal alteration of ilmenite. The temperatures for this stage range from 150° to 210°C. Ilmenite in this stage is classified into three classes, Plate 12(a,b and c).

Class V_1: In this class, the original ilmenite is totally replaced by rutile and hematite. This is the same class as T_3, Plate 12(a).

Class V_2: In this class, a white mineral with a yellow tint and high internal reflection is developed and it is assumed to be leucoxene. The composition is primarily TiO_2. The mineral is associated with a transparent orange tinted yellow color mineral which is believed to be a sphene (see probe data, Table 7). The cracks become wider and the red stained phase is frequently present. The grains as a whole become luminous under crossed nicols due to the increase in the strength of internal reflections (Plate 12(b)). The color of the internal reflection range from brown to white.

Class V_3: This is the ultimate in ilmenite hydrothermal alteration. The ilmenite grains disappear and dark brown to black colored pseudomorphs after ilmenite occur, Plate 12(c).

A summary of classification of hydrothermally altered titanomagnetite and ilmenite is given in Table 11.

3.3. Oxidation at intermediate temperatures: This type of oxidation, which took place between 600°-300°C consisted of a mixture of high and low temperature oxidation phases. It occurs during the initial cooling of lava and before burial by younger flows. The change in equilibrium due to the continued cooling of the rock and the effect of volatiles and gases led to a transformation in some minerals into phases stable under this condition. Several opaque phases of this stage were recognized in the Azores drill core. Pseudobrookite is broken down to rutile and hematite. Titanomagnetite is marginally altered to titanomaghemite.

3.4. Low Temperature Oxidation: Oxidation of this type includes all that has taken place between 300° to 0°C and particularly at sea water temperature of 4°C. Oxidation features of Fe-Ti oxides of this type are: irregular lightening of the grains, volume change cracking and the transformation from ferrous to ferric state. Most of the opaque phases in the Azores drill core shows these features.

3.5. The combined action of hydrothermal alteration and other oxidation types: The hydrothermal solutions in the Azores drill core affect all

Table 11. A summary of hydrothermal alteration classes of titanomagnetite and ilmenite.

TEMP. °C	CLASS		MINERAL PHASE		Titanomagnetite									Ilmenite								REFLECTIVITY PERCENTAGE IN AIR AT WAVELENGTH 546 nm		STAGE OF ALTERATION	
	Titano-magnetite	Ilmenite	Titanomagnetite	Ilmenite	Fe	Ti	Al	Mg	Cr	Mn	Ca	Si	Fe/Fe+Ti	Fe	Ti	Al	Mg	Cr	Mn	Ca	Si	Fe/Fe+Ti	Titanomagnetite	Ilmenite R_1 R_2	Titano-magnetite	Ilmenite
20	L_1	S_1	titanomagnetite	ilmenite	49.5±2.0	15.2±1.4	2.1±0.5	1.9±0.2	0.6±0.2	1.7±0.7	0.0	0.0	0.77	35.8±0.1	29.5±0.1	0.6±0.1	1.2±0.1	0.6±0.1	0.7±0.1	0.0	0.0	0.55±0.0	16.0±0.2	14.8–16.9 ±0.3 ±0.4	LOW	LOW
40	L_2	S_1	first appearance of titanomaghemite	ilmenite	49.8±1.2	16.6±0.4	2.5±0.2	1.4±0.4	0.4±0.1	1.2±0.3	0.1±0.2	0.1±0.2	0.75±0.0	(as for S_1)									16.9±0.2	as for S_1		
55	L_3	S_1	titanomaghemite less than 50%	ilmenite	46.9±0.0	17.4±0.4	2.6±0.1	1.1±0.0	0.4±0.0	1.3±0.1	0.1±0.1	0.2±0.2	0.73±0.0	(as for S_1)									19.3±0.4	as for S_1		
70	L_4	S_1	titanomaghemite more than 50%	ilmenite	45.2±1.0	18.6±0.3	2.7±0.2	0.6±0.1	0.4±0.1	1.4±0.2	0.0	0.0	0.71±0.0	(as for S_1)									22.2±0.3	as for S_1		
80	M_1	S_2	titanomaghemite more than 50%	ilmenite type 2	43.2±0.5	20.6±0.3	2.4±0.1	0.6±0.0	0.3±0.1	1.2±0.0	0.0	0.0	0.69±0.0	32.9±1.0	31.6±0.9	0.6±0.1	0.9±0.1	0.5±0.1	0.8±0.1	0.0	0.0	0.51±0.0	22.8±0.1	16.8–17.1 ±0.4 ±0.2	MEDIUM	LOW
90	M_1	S_3	titanomaghemite more than 50%	first appearance of pseudorutile	(as for M_1)									32.2±0.6	33.2±0.8	0.5±0.1	0.4±0.1	0.4±0.1	0.4±0.1	0.0	0.0	0.49±0.0	as for M_1	16.0–18.2 ±0.1 ±0.1		
100	M_1	S_4	titanomaghemite more than 50%	pseudorutile	(as for M_1)									29.6±0.7	35.2±1.4	0.5±0.1	0.4±0.1	0.4±0.1	0.4±0.2	0.3±0.2	0.4±0.3	0.46±0.0	as for M_1	18.8–19.1 ±0.2 ±0.3		
100	M_1	T_1	titanomaghemite more than 50%	pseudorutile	(as for M_1)									(as for S_4)									as for M_1	as for S_4		MEDIUM
110	M_1	T_2	titanomaghemite more than 50%	first appearance of rutile and hematite	(as for M_1)									18.1±0.1	33.2±1.6	0.5±0.1	0.5±0.0	0.5±0.1	0.4±0.1	1.6±0.1	2.0±0.1	0.35±0.0	as for M_1	21.1–20.8 ±0.1 ±0.1	MEDIUM	
120	M_2	T_2	first appearance of titanohematite	rutile and titanohematite	41.9±0.5	20.9±0.8	2.7±0.4	0.8±0.2	0.4±0.1	1.8±0.5	0.3±0.2	0.2±0.1	0.67±0.0	(as for T_2)									R_1 – R_2 21.4 – 27.5 ±0.3 ±0.4 (see text)	as for T_2		
150	M_3	T_3	first appearance of granulation texture/ghost	first appearance of granulation	30.0±2.1	32.8±1.0	2.7±0.4	0.6±0.1	0.3±0.0	0.9±0.1	1.2±0.1	0.8±0.1	0.48±0.0	14.8±1.0	36.8±0.5	0.5±0.1	0.4±0.0	0.3±0.0	0.4±0.1	2.6±0.1	2.4±0.2	0.29±0.0	22.1±0.1	21.3–20.7 ±0.6 ±0.1		
160	M_4	V_1	granulation more than 50%	granulation	23.0±4.8	38.6±2.7	1.9±0.3	0.5±0.1	0.4±0.1	0.7±0.1	2.6±0.7	0.8±0.1	0.3± 0.1	(as for T_3)									20.4±0.4	as for T_3		
160	M_1	V_1	granulation more than 50%	granulation	(as for M_1)									(as for T_3)									as for M_4	as for T_3	HIGH	HIGH
170	M_1	V_2	granulation more than 50%	appearance of leucoxene	(as for M_1)									12.1±1.3	39.1±1.1	0.5±0.1	0.5±0.2	0.5±0.1	0.4±0.1	4.9±0.2	5.5±0.2	0.24±0.0	as for M_4	19.9±0.6		
190	M_2	V_2	original titanomagnetite is replaced by titania	leucoxene	No magnetite remaining									(as for V_2)										as for V_2		
200	M_3	V_3	dark brown to black sphene & red limonite	dark brown to black sphene	No magnetite remaining									No ilmenite remains												

the mineral phases of low, intermediate and high temperature oxidation types and thus result in complicated textures of the opaque phases. Several examples of this combined action in the Azores drill core are given in Plate 13.

Ade-Hall et al. (1971) have studied the variation in opaque mineral phases due to the combined action of hydrothermal alteration and high temperature oxidation and have described how this affects the magnetic properties of basalts. A major concern was the mineralogical changes in titanomagnetite of deuteric oxidation (classes 1-6) due to the overprint of hydrothermal alteration. However, some objections to the scheme of Ade-Hall et al. (1971) arose during the present work on the Azores drill core. Some of the phases identified by them are considered unstable in the hydrothermal environment in the present study.

4. Opaque mineralogical aspects of the drill core

From the opaque mineralogy study, the following characteristic features of the Azores drill core have been noted:

4.1. General features of the drill core:

(1) The Azores drill rocks were subjected to hydrothermal alteration throughout the core. The degree of alteration varies according to the temperature and the content of hydrothermal solution.

(2) High temperature oxidation of titanomagnetite and ilmenite were found in subaerial and transition sequences but were never found in the subaqueous sequence below 947 m.

(3) Overprinting and complex textures due to the effect of combined action of hydrothermal alteration, high, intermediate, and low temperature oxidation were the most characteristic features of the opaque phases.

(4) The grain size of the opaque phases varied from medium to coarse and sometimes very coarse even in the subaqueous sequence.

4.2. Features of subaerial sequence III: 0-268.4 m:

(1) With the exception of flow unit AUL 1.1.2, titanomagnetite contents in the lava flows were quite high (more than 90% of the opaque phases), while ilmenite contents were rather low (less than 5%). Flow unit AUL 6.1.1, however, contains a high amount of ilmenite as well as titanomagnetite.

(2) Agglomerate units AUG 3.1.1 and 5.1.1 contained very small amounts of titanomagnetite and they were almost devoid of ilmenite.

(3) In flow unit AUL 14.3 almost all titanomagnetite grains contained large amounts of cracks accompanied by alteration. The drill log indicated a rise in temperature of 3-5°C above the ambient temperature at the time of extraction of the core.

(4) The first appearance of high temperature oxidation in titanomagnetite and ilmenite was encountered in flow unit AUL 8.1.

4.3. Features of subaerial sequence II: 268.4-428.6 m:

(1) Flow units AUL 30.4, 31.1 and 36.1 were characterized by small contents of titanomagnetite and ilmenite which contained both high temperature oxidation and hydrothermal alteration textures. These units were trachyte.

(2) Generally most of titanomagnetite and ilmenite grains in the flow units of this sequence showed medium to high hydrothermal alteration.

4.4. Features of subaerial sequence I: 428.6-762.8 m:

(1) The flow units in this sequence showed the highest degree of hydrothermal alteration of titanomagnetite and ilmenite in the core.

(2) High temperature oxidation of titanomagnetite and ilmenite were present.

(3) Textures of titanomagnetite and ilmenite were the most complex textures in the core.

(4) Intrusives AUS 98.5, 110.1 and 111.2 contained small amounts of titanomagnetite and ilmenite in a low hydrothermal alteration state.

4.5. Features of transition sequence: 762.8-913.2 m:

(1) In this sequence, both skeletal and euhedral titanomagnetite grains were present.

(2) The thickness of this sequence should extend to 913.2 m instead of 856.8 m as in Muecke et al. (1974), because of the presence of the subaerial type of titanomagnetite in all flows down to flow 138.1.

(3) One of the characteristic features in this sequence was the low abundance of high temperature oxidation textures in titanomagnetite and ilmenite.

(4) The hydrothermal alteration of titanomagnetite and ilmenite were of medium to low-medium degree.

4.6. Features of subaqueous sequence: 913.2-980.5 m:

(1) Skeletal and fine to medium grains of titanomagnetite were present.

(2) Sulfides were common in this sequence.

(3) There were two examples of high temperature oxidation in this sequence.

(4) The hydrothermal alteration was of medium degree (i.e.) a lower scale than in several shallower sections.

5. Discussion of the results

5.1. Microprobe and reflectivity data for titanomagnetite of high temperature oxidation: From the study of Tables 6 and 8 the following

are noted:

(1) When oxidation starts, iron (Fe_T) in titanomagnetite decreases while titanium (Ti_T) increases. This is followed by an increase in reflectivity until it reaches a maximum value of 22.6 ± 0.3 in class 5 where titanohematite forms. The relation between reflectivity of titanomagnetite of high temperature oxidation and oxidation classes is shown in figure 26.

(2) Ilmenite lamellae start to oxidize in class 3. Oxidation is accompanied by an increase in reflectivity from R_1 14.3-15.8% R_2 to R_1 15.2-17.0% R_2.

(3) The presence of an isotropic magnetite phase in class 5 is in agreement with the observations of Wilson and Haggerty (1966), Watkins and Haggerty (1967) and Ade-Hall et al. (1968a). The results also agree with Gidskehaug and Davison's (in press) analysis but they are in complete disagreement with Smith's claim (1968) that a titanomagnetite phase is not present in class 5.

5.2. Microprobe and reflectivity data for ilmenite of high temperature oxidation: The study of Tables 7 and 8 reveals the following:

(1) The oxidation of ilmenite results in an increase in reflectivity until it reaches a maximum value of 22.5 ± 0.1 when titanohematite is formed in class 4. Figure 27 shows the relation between reflectivity and the oxidation class of high temperature oxidation ilmenite.

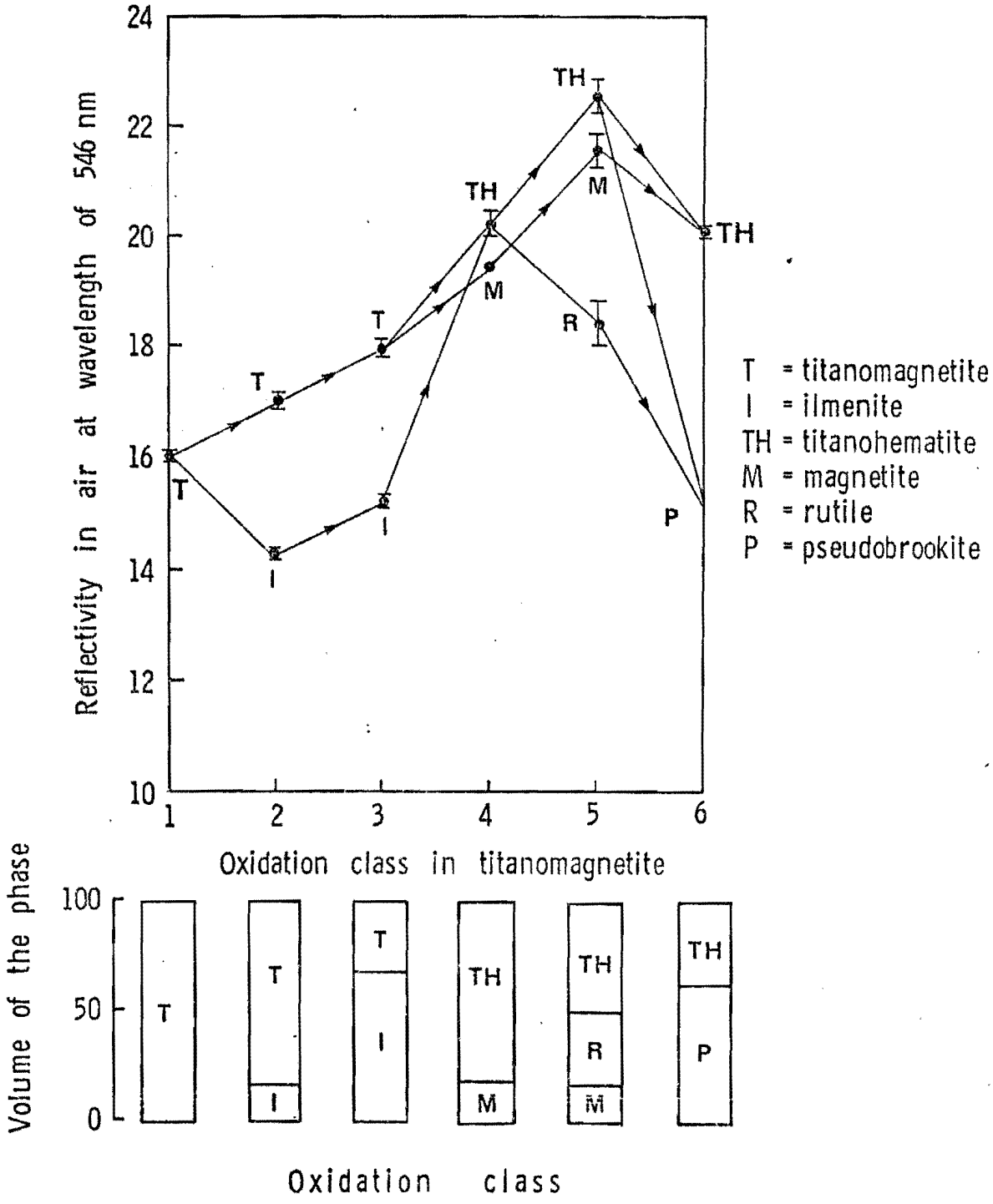

Figure 26. Relation between oxidation classes and reflectivity in air for titanomagnetite of high temperature oxidation.

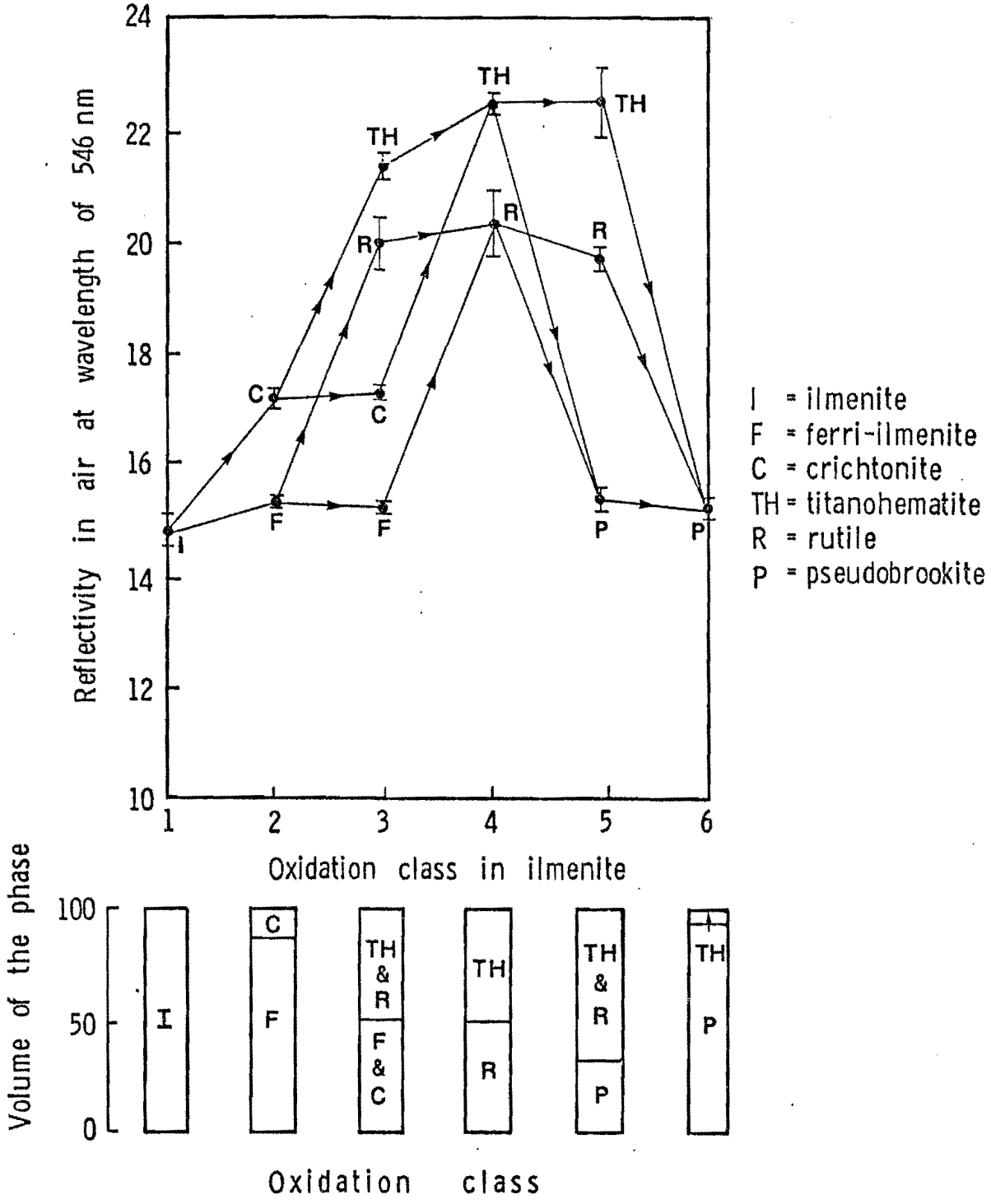

Figure 27. Relation between oxidation classes and reflectivity in air for ilmenite of high temperature oxidation.

(2) The ratio Fe/Fe+Ti changes from one phase to another but the overall ratio for each mineral aggregate remains nearly the same regardless of oxidation state. As an example, in class 2 ferri-ilmenite and crichtonite have Fe/Fe+Ti ratios of 0.66 and 0.42 respectively. When these ratios add together, relative to their volume in the grain ($0.66 \times \frac{2}{3} + 0.42 \times \frac{1}{3}$) an overall ratio of 0.56 is the result, which is almost equal to the ratio for ilmenite of class 1. This indicates that high temperature oxidation of ilmenite involves redistribution of iron and titanium within the grain rather than exchange with the silicate matrix, until sphene forms.

5.3. Characteristic features of the hydrothermal alteration of Fe-Ti oxides: From microprobe analyses and reflectivity measurements of titanomagnetite and ilmenite, the following characteristic features are recognized.

(1) Iron/Titanium ratio, reflectivity and oxidation stages: Figures 28 and 29 show the correlation between reflectivity and iron/titanium ratio of titanomagnetite and ilmentite respectively. In titanomagnetite, Fe/Fe+Ti decreases with increasing oxidation (arrows on curve). The decrease in Fe/Fe+Ti ratio is accompanied by an increase in reflectivity until it reaches a maximum value of 23.5% when the Fe/Fe+Ti ratio is equal to 0.64. Reflectivity then decreases as the Fe/Fe+Ti ratio decreases.

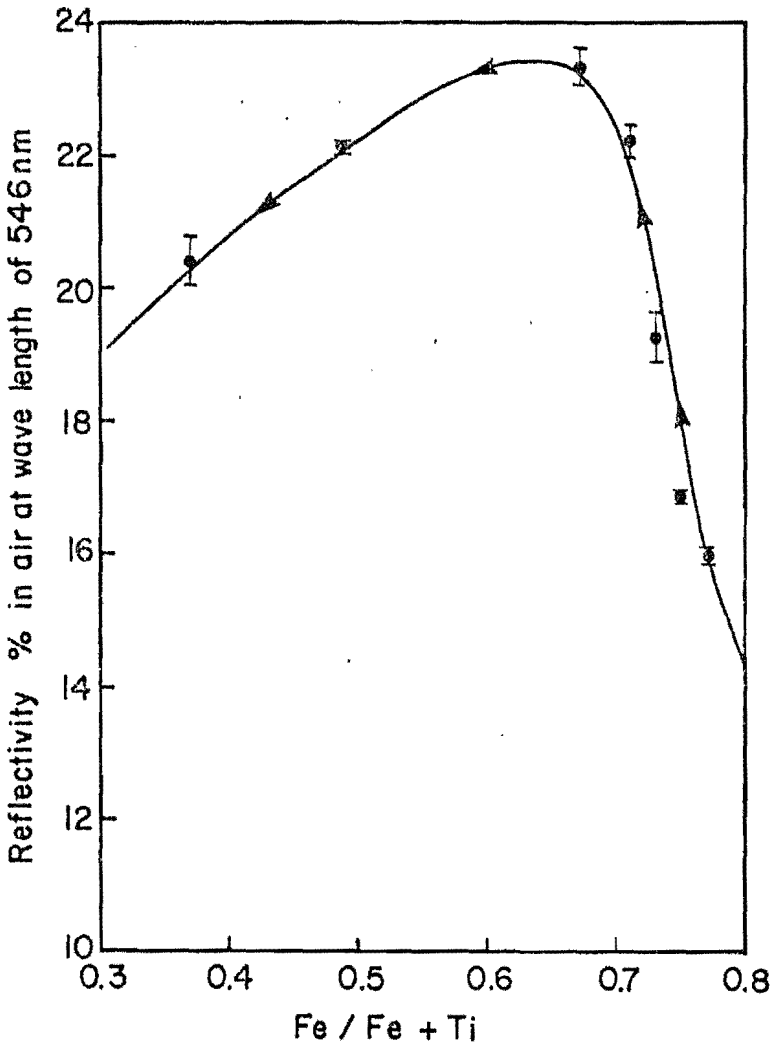

Figure 28. Correlation between reflectivity and iron/titanium ratio in titanomagnetite and its hydrothermal alteration products.

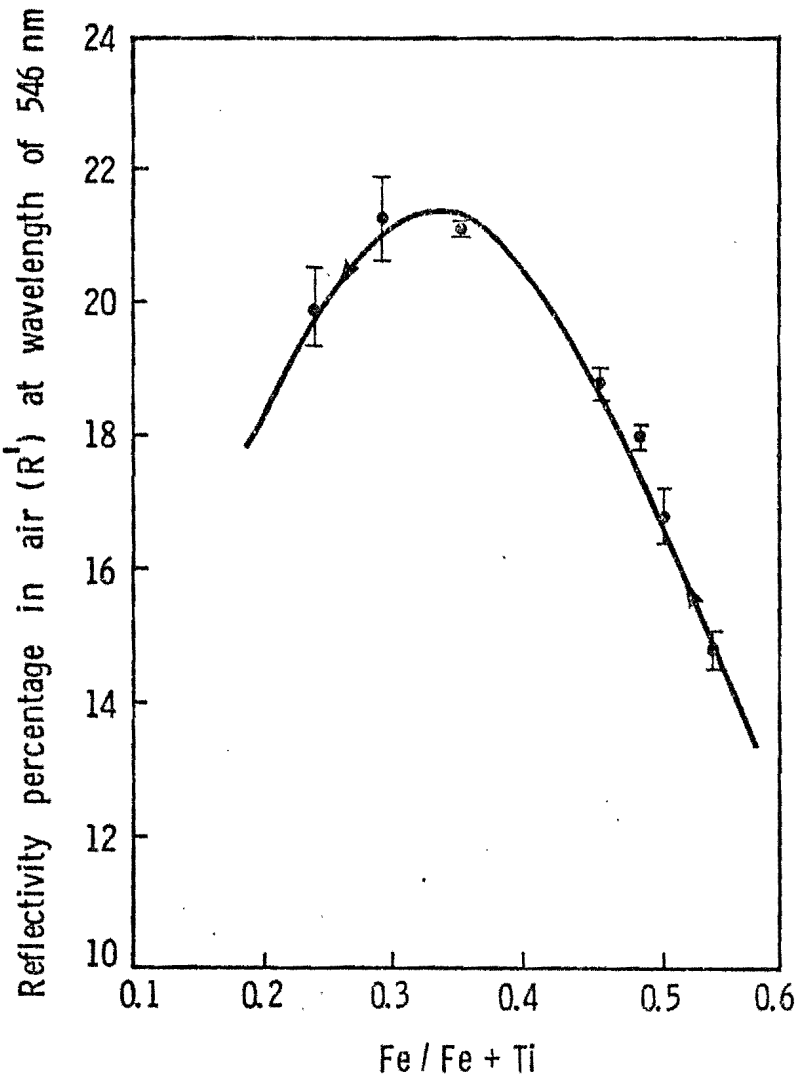

Figure 29. Correlation between reflectivity and iron/titanium ratio in ilmenite and its alteration products.

Ilmenite follows the same trend. The maximum reflectivity value (21.4%) is reached when the ratio Fe/Fe+Ti in ilmenite drops to 0.35. However, the steepness of the ilmenite curve is noticeable and can be attributed to the vigorous migration of iron from the rhombohedral structure of ilmenite (Grey and Reid 1975).

(2) Elemental behaviour of Fe and Ti: The behaviour of elements Fe and Ti in titanomagnetite and ilmenite during the hydrothermal alteration is shown in figures 30 and 31 respectively. Iron in titanomagnetite decreases slowly with increasing alteration until class M_2 of medium degree hydrothermal alteration; then the curve registers a sharp decrease as the alteration proceeds. In ilmenite, the sharp decrease of iron starts earlier in class S_4 of low degree hydrothermal alteration, otherwise the two curves look similar.

Titanium in titanomagnetite shows inverse relationship with iron, while in the case of ilmenite, there is a steady increase in titanium with increasing the degree of hydrothermal alteration.

(3) Behaviour of Al and Cr: The relations between aluminum and chromium contents in titanomagnetite, and ilmenite and the degree of hydrothermal alteration, are shown in figures 32 and 33 respectively. In titanomagnetite aluminium, figure 32a shows slight increases until class M_2, then slightly decreases with increasing degrees of hydrothermal alteration. However, it is not clear whether this variation results from hydrothermal alteration or a variation in the original titanomagnetite before alteration. Figures 32b, 33a, b, show a slight

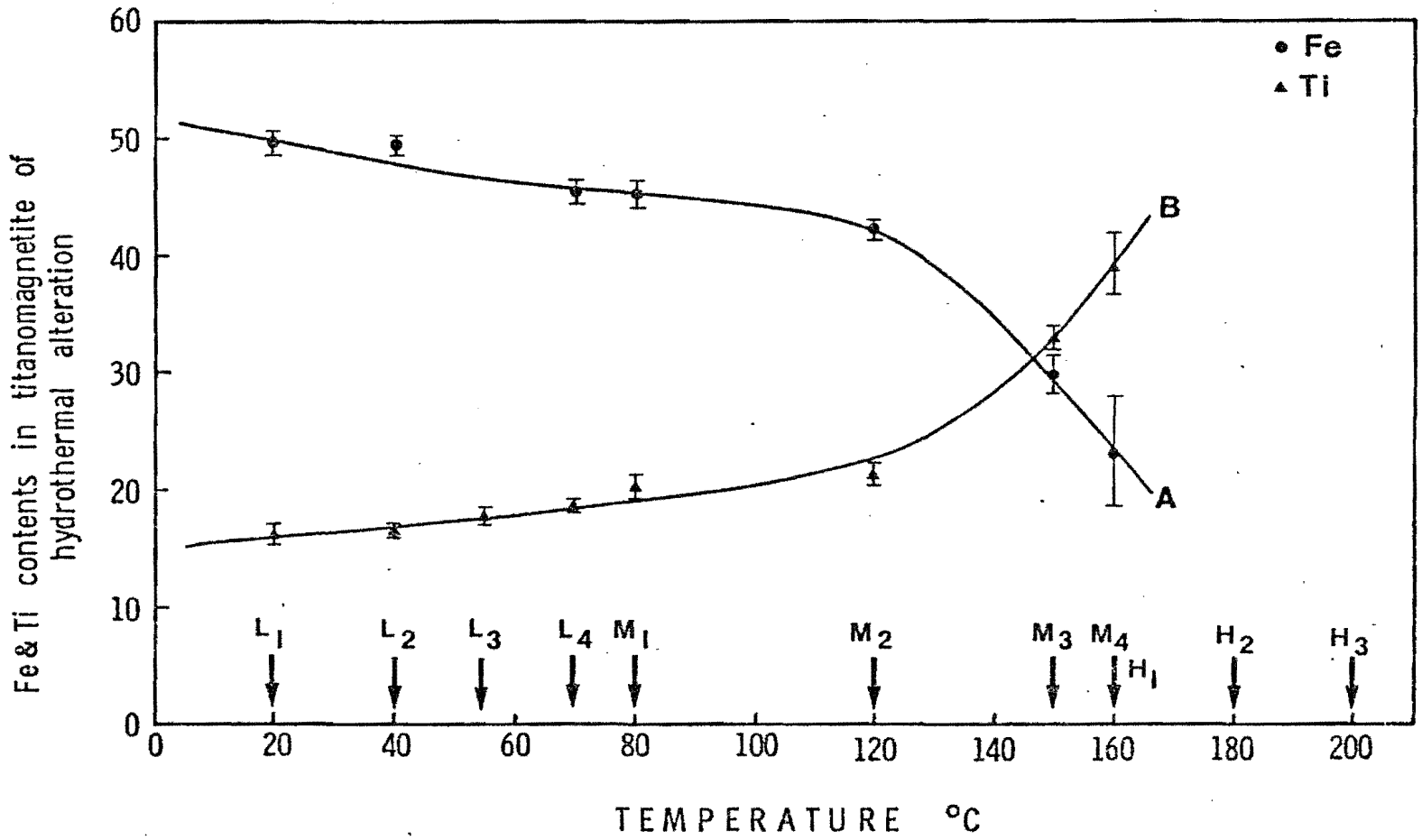

Figure 30. Correlation between temperatures and Fe and Ti contents by weight percent in titanomagnetite and its hydrothermal alteration products. Minimum and maximum Fe and Ti contents in unaltered titanomagnetite are 44.3-53.6 and 10.1-17.6 percent respectively. (See Tables 1, 2 and 3).

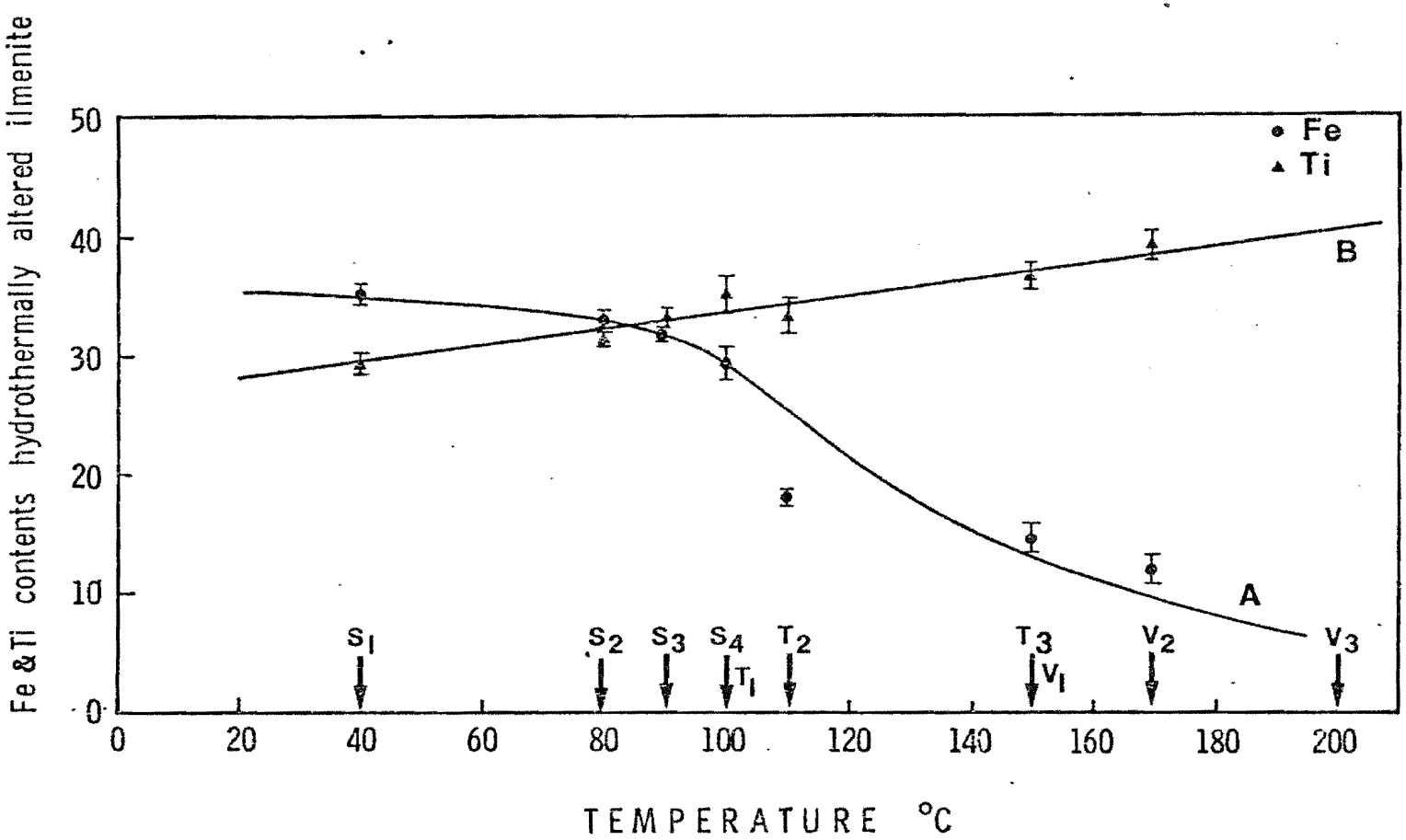

Figure 31. Correlation between temperatures and Fe and Ti contents by weight percent in ilmenite and its hydrothermal alteration products. Minimum and maximum Fe and Ti contents in unaltered ilmenite are 35.7-36.0 and 29.2-29.7 percent respectively. (See Table 4).

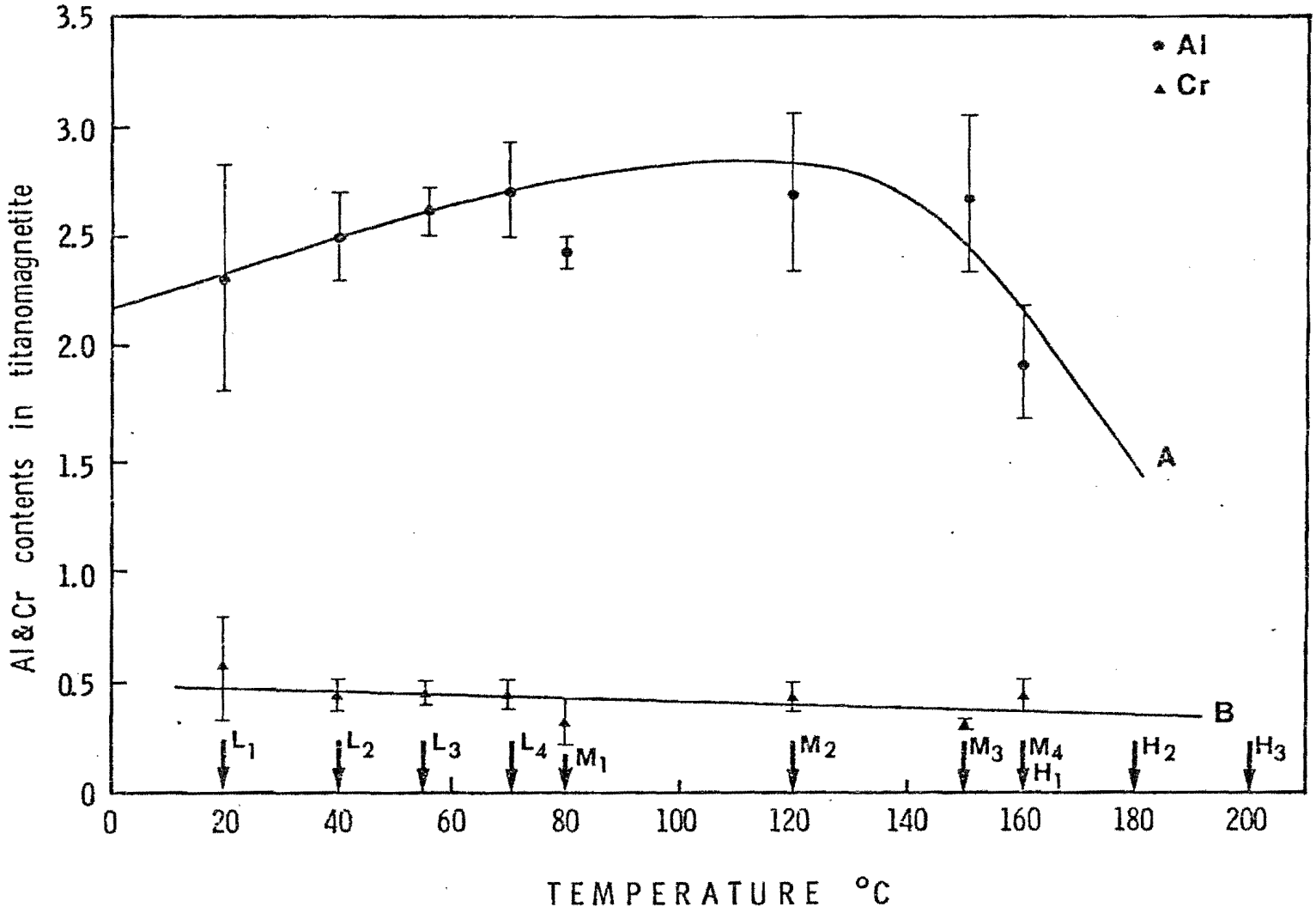

Figure 32. Correlation between temperatures and Al and Cr contents by weight percent in titanomagnetite and its hydrothermal alteration products. Minimum and maximum Al and Cr contents in unaltered titanomagnetite are 0.3-3.5 and 0.0-3.4 percent respectively. (See Tables 1, 2 and 3).

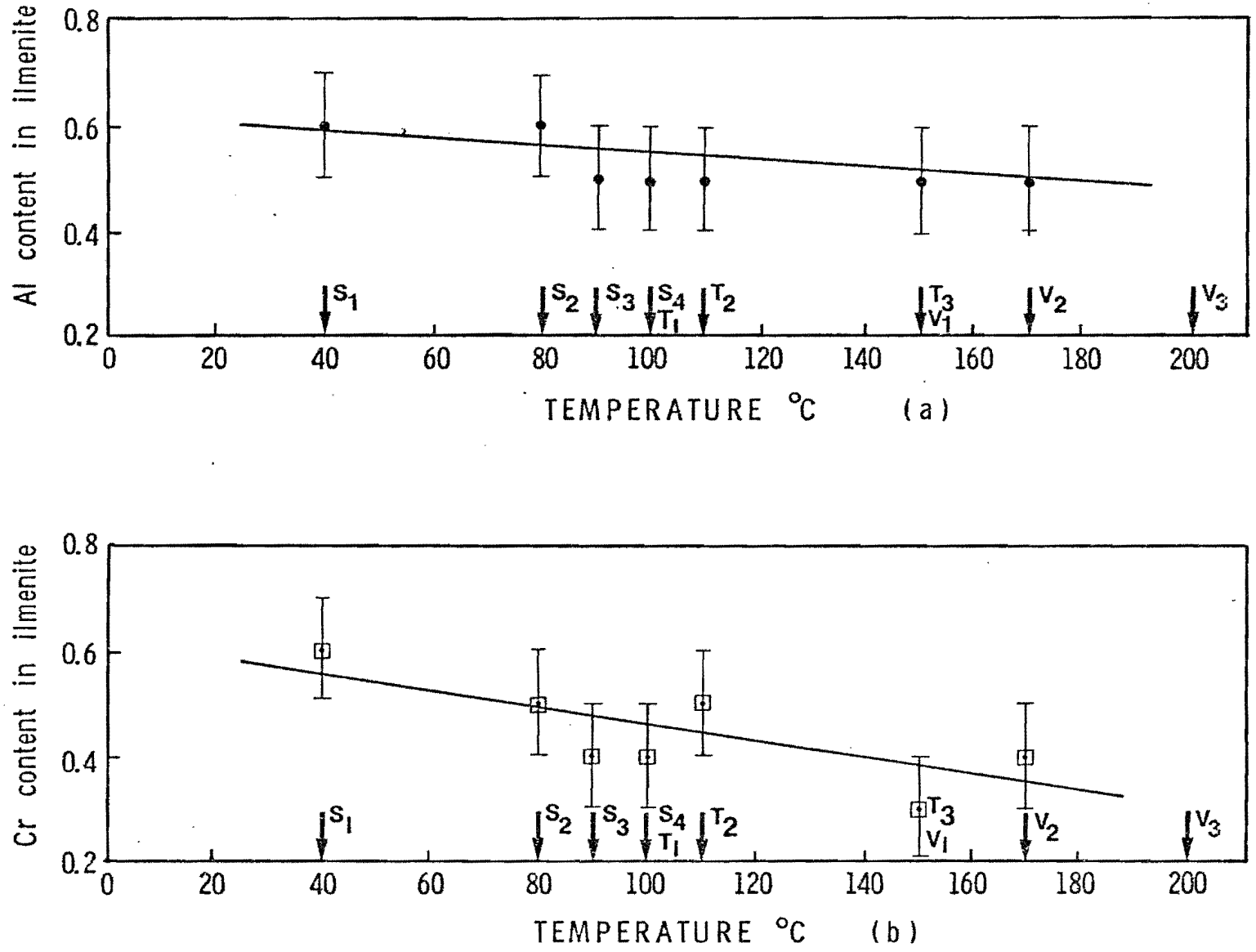

Figure 33. Correlation between temperatures and Al and Cr contents by weight percent in ilmenite and its hydrothermal alteration products. Minimum and maximum Al and Cr contents in unaltered ilmenite are 0.6-0.7 and 0.4-0.6 percent respectively. (See Table 4).

decrease in Al and Cr contents. This indicates that Cr in titanomagnetite and Al and Cr in ilmenite are held tightly in the structure regardless of the degree of hydrothermal alteration.

(4) Behaviour of Mg and Mn: Figures 34, 35, 36a and 36b show the correlation between magnesium and manganese contents and the degree of hydrothermal alteration in titanomagnetite and ilmenite respectively. Magnesium in titanomagnetite and ilmenite decreases with increasing the degree of hydrothermal alteration up to 90°C (medium degree of alteration), however, titanomagnetite curve shows a sharper decrease than ilmenite. Both curves then show a slight increase by increasing the degree of hydrothermal alteration.

The correlation between manganese content in titanomagnetite and ilmenite and the degree of hydrothermal alteration is unique in this set of relationships because of the difference in behaviour of Mn in titanomagnetite and ilmenite. Mn in ilmenite shows a sharp decrease with the increase in degree of hydrothermal alteration between class S_2 and T_1. However, the curve (figure 3b6) indicates that Mn is tightly held in the structure lattice at higher stages of alteration. In titanomagnetite, however, Mn shows irregular content and it is difficult to detect if such irregularity results from the effect of hydrothermal alteration or it is an original irregularity in the unaltered titanomagnetite.

(5) Behaviour of Ca and Si: The relations between Ca and Si contents in titanomagnetite and ilmenite and the degree of hydrothermal alter-

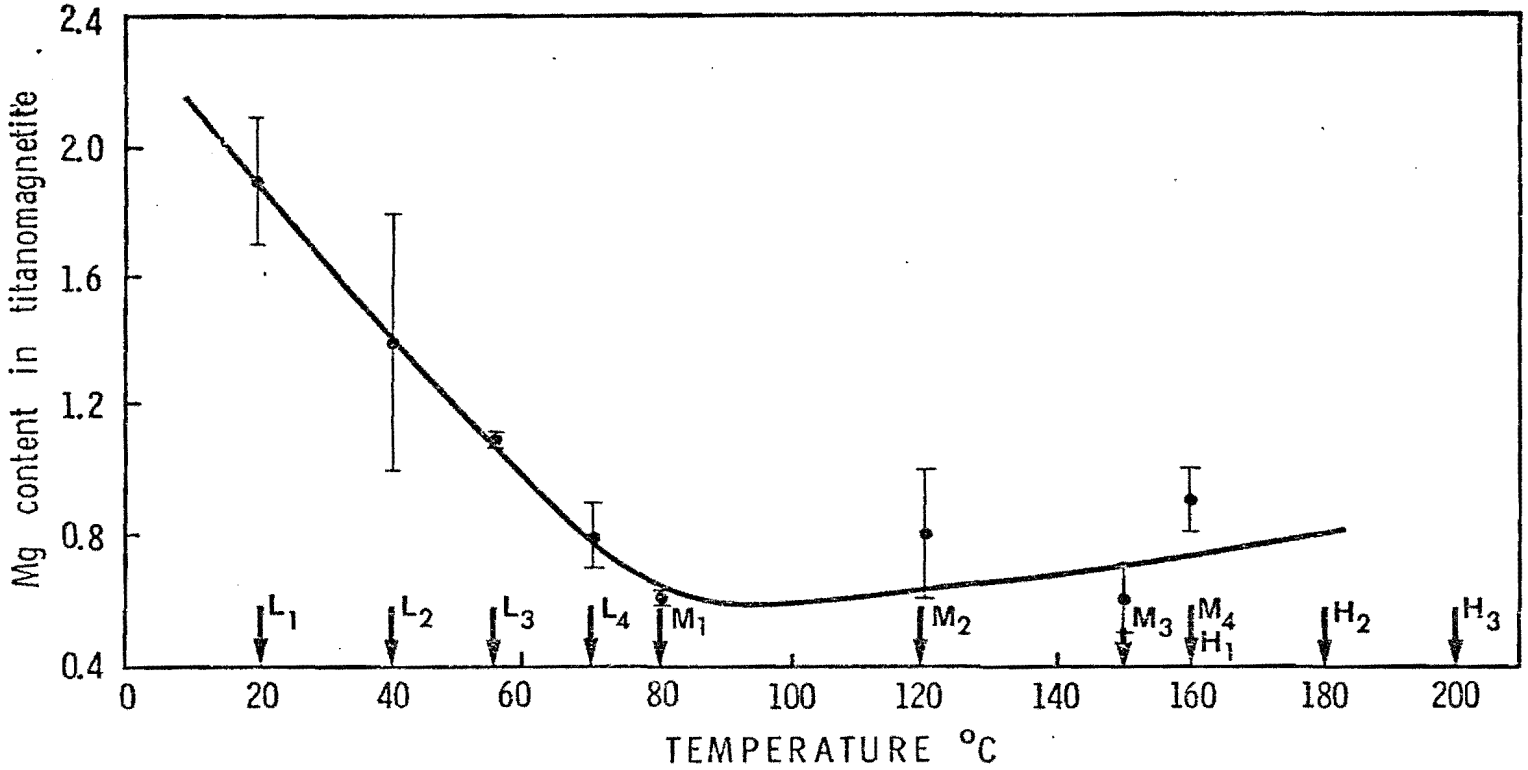

Figure 34. Correlation between temperatures and Mg content by weight percent in titanomagnetite and its hydrothermal alteration products. Minimum and maximum Mg content in unaltered titanomagnetite are 0.8-2.8 respectively. (See Tables 1, 2 and 3).

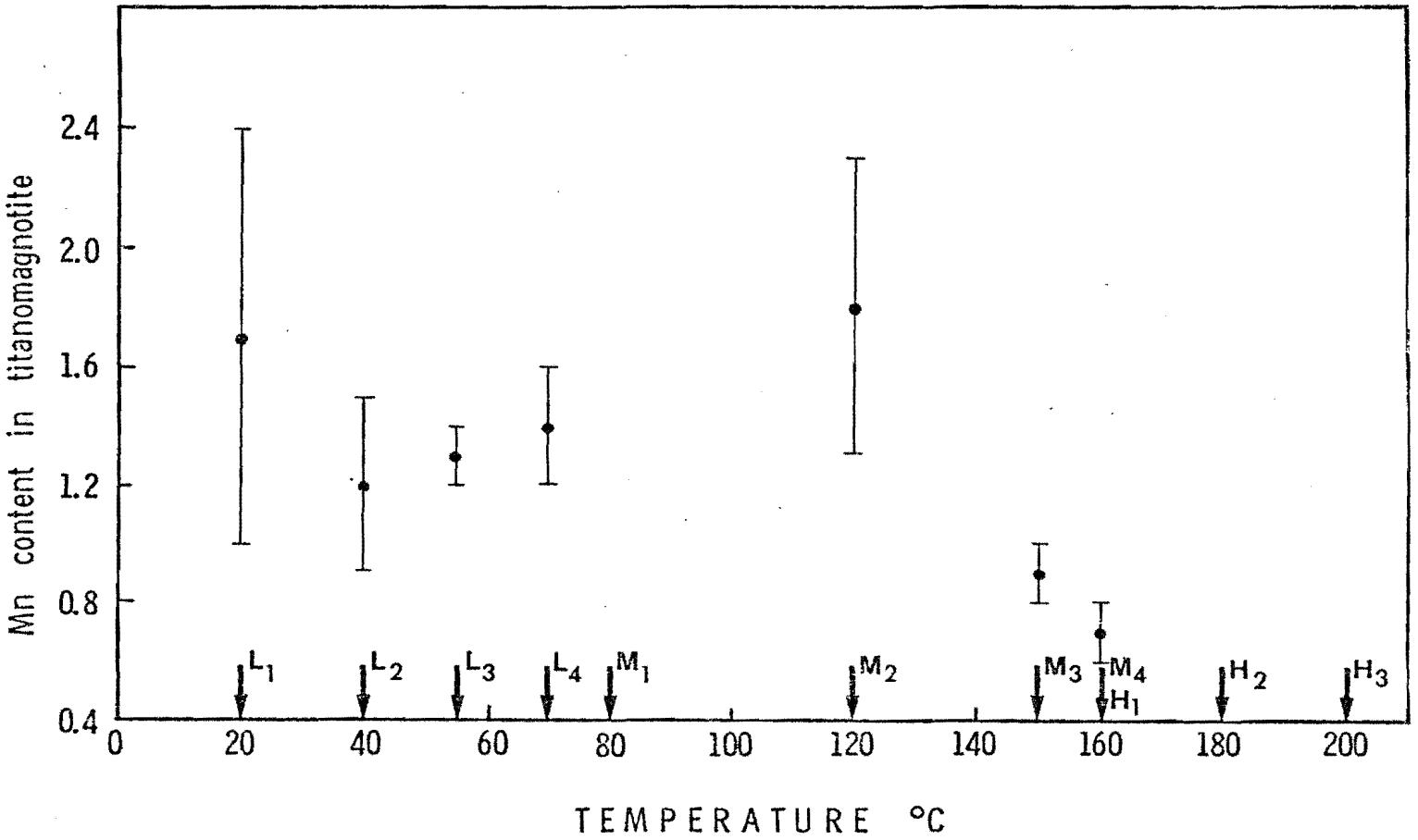

Figure 35. Correlation between temperatures and Mn content by weight percent in titanomagnetite and its hydrothermal alteration products. Minimum and maximum Mn content in unaltered titanomagnetite are 0.0-3.7 percent respectively, (See Tables 1, 2 and 3).

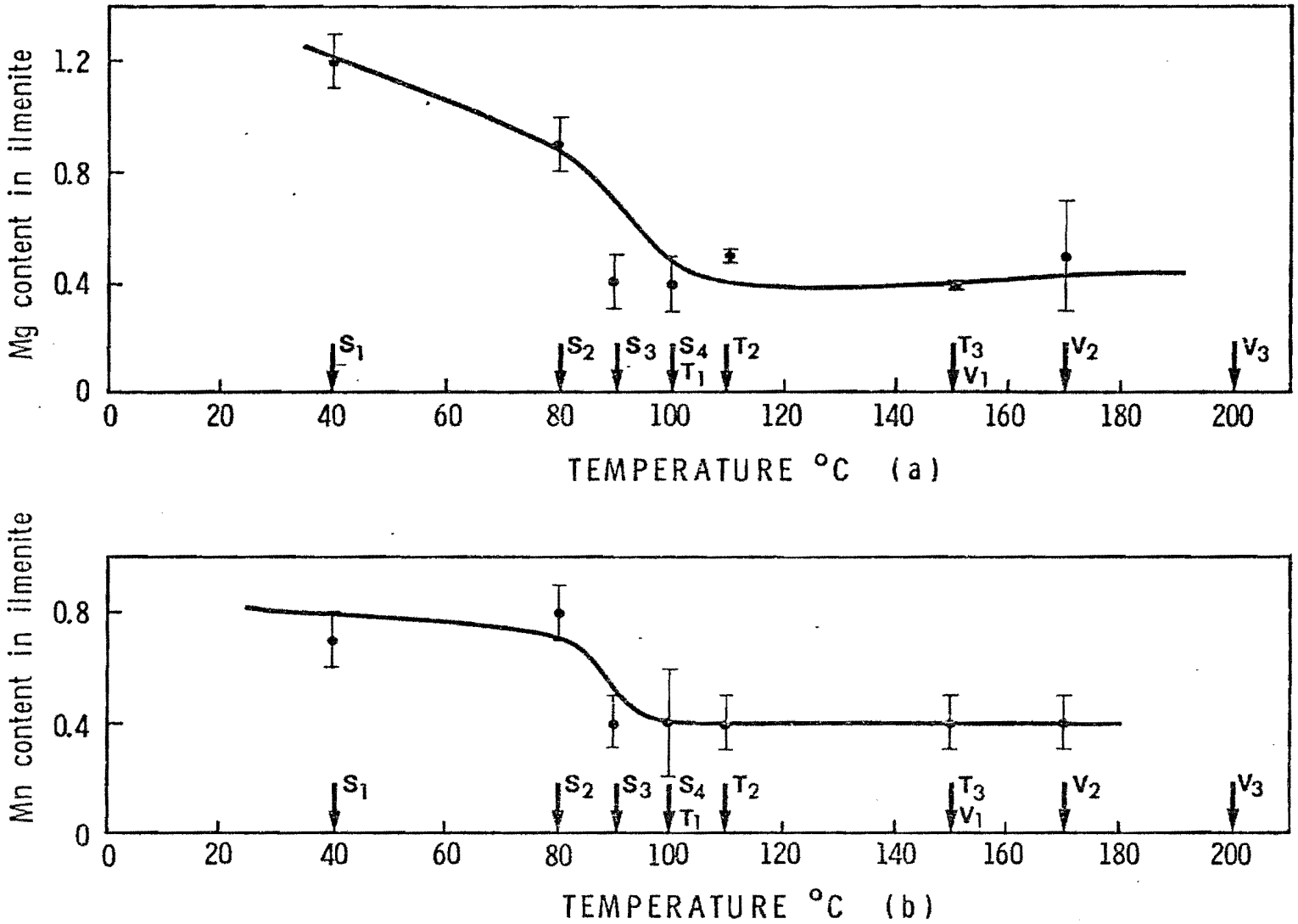

Figure 36. Correlation between temperatures and Mg and Mn contents by weight percent in ilmenite and its hydrothermal alteration products. Minimum and maximum Mg and Mn contents in unaltered ilmenite are 1.1-1.4 and 0.6-0.8 respectively. (See Table 4).

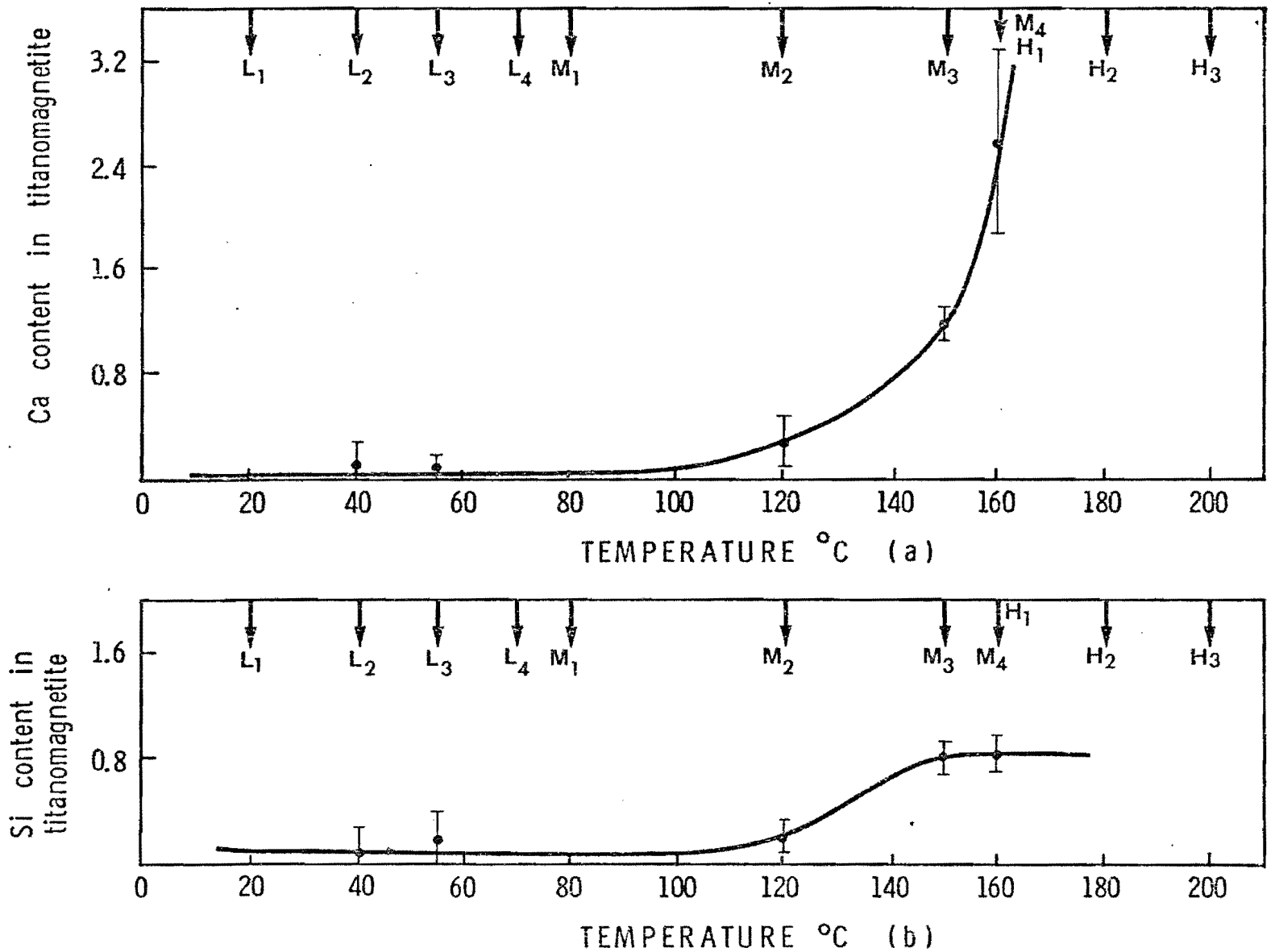

Figure 37. Correlation between temperatures and Ca and Si contents by weight percent in titanomagnetite and its hydrothermal alteration products. No detectable Ca or Si in the unaltered titanomagnetite.

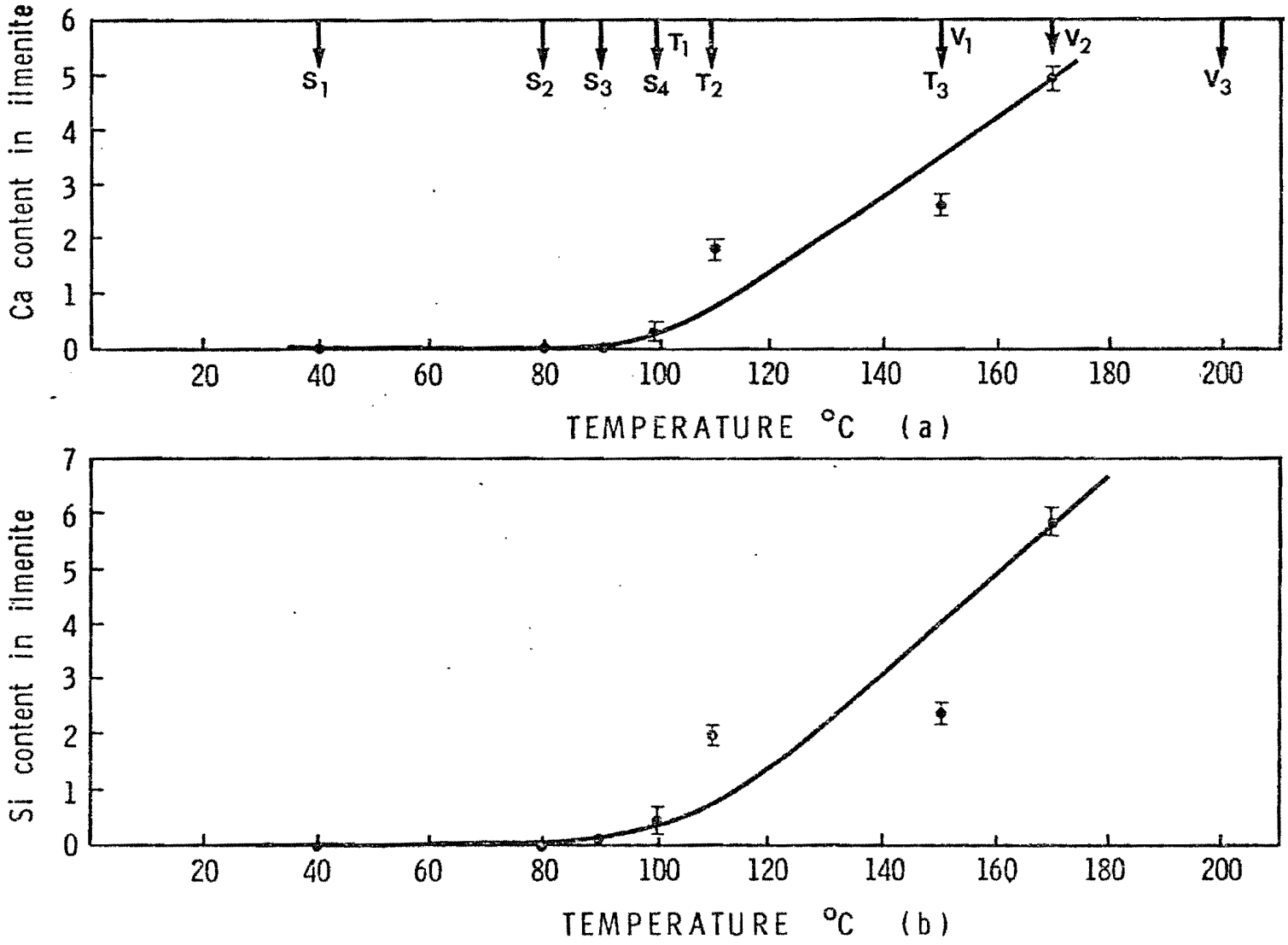

Figure 38. Correlation between temperatures and Ca and Si contents by weight percent in ilmenite and its hydrothermal alteration products. No detectable Ca or Si in the unaltered ilmenite.

ation are shown in figures 37 and 38, respectively. The relations indicate a gain in Ca and Si contents in both titanomagnetite and ilmenite by increasing the degree of hydrothermal alteration beyond class M_2 (titanomagnetite) and class T_2 (ilmenite). This gain can be attributed to the addition of new phases in titanomagnetite and ilmenite granulation. However, contamination with the altered silicates at this stage is very likely.

CHAPTER VI

ROCK MAGNETISM AND PALEOMAGNETISM

The magnetic properties of the Azores drill core, which are dominated by the iron-titanium oxides, are discussed in this chapter. The discussion involves, in one hand, the rock magnetic properties: Curie temperature (T_C), saturation magnetization (J_S), initial susceptibility (K) and hardness of the remanence (S). On the other hand, paleomagnetic measurements include NRM intensity, inclination (I) and Konigsberger ratio (Q). Correlations between magnetic properties, depth and oxidation state are given.

1. Thermomagnetic properties

Curie temperatures and saturation magnetizations of the Azores drill core rocks were measured using a Cahn electro-balance (Chapter III). The strong field thermomagnetic curves (J_S - T_C) were examined and the Curie temperatures and saturation magnetization calculated (Appendix II).

The thermomagnetic curves are classified into five groups which are listed below.

1.1. Unaltered samples: Curie temperatures for these samples are in the range of 200-250°C corresponding to an average x value of 0.61. Microscopic examination and microprobe analyses indicate that the magnetic minerals are homogeneous titanomagnetite with no apparent oxida-

tion. A typical sample, AUL 2.1.5, is shown in figure 39a, has a Curie temperature of 232°C and has an x value of 0.61.

1.2. Hydrothermal alteration without previous deuteric oxidation samples:

(1) Samples with low hydrothermal alteration (L): The range of Curie temperatures for these samples is between 500-550°C as shown in figure 40a. The average Curie temperature is 528 ± 14(3)°C. A typical sample, AUL 142.1.6, is shown in figure 39b. Samples of this group were found to contain titanomaghemite as the magnetic mineral. Thus increasing the degree of hydrothermal alteration from class L_1 to class L_4 tends to increase Curie temperature from 232°C to 528°C.

(2) Samples with medium hydrothermal alteration (M): Samples of this group have a Curie temperature range of 550 to 580°C, figure 40b, with an average value of 562 ± 9(2)°C. Figure 39c shows a typical sample of this group. Microscopic examination and microprobe analysis of samples in this region showed that titanomagnetite in these samples was altered to titanohematite and granules phase rich in TiO_2. In both phases the Fe/Fe+Ti ratio (0.67, 0.48 respectively) is less than that of the unaltered titanomagnetite (0.77). If iron decreases by alteration how can we account for the increase in Curie temperatures? One possible answer is that the iron migrated from the structural lattice of titanomagnetite has reacted with hot solutions and formed magnetic phases with high

Figure 39

Example of Curie temperatures in the Azores drill core

1. Horizontal scale in m.v.
2. Vertical scale represents the variation in weight of the sample.
3. Curie temperature is calculated by using a modified calibration chart.

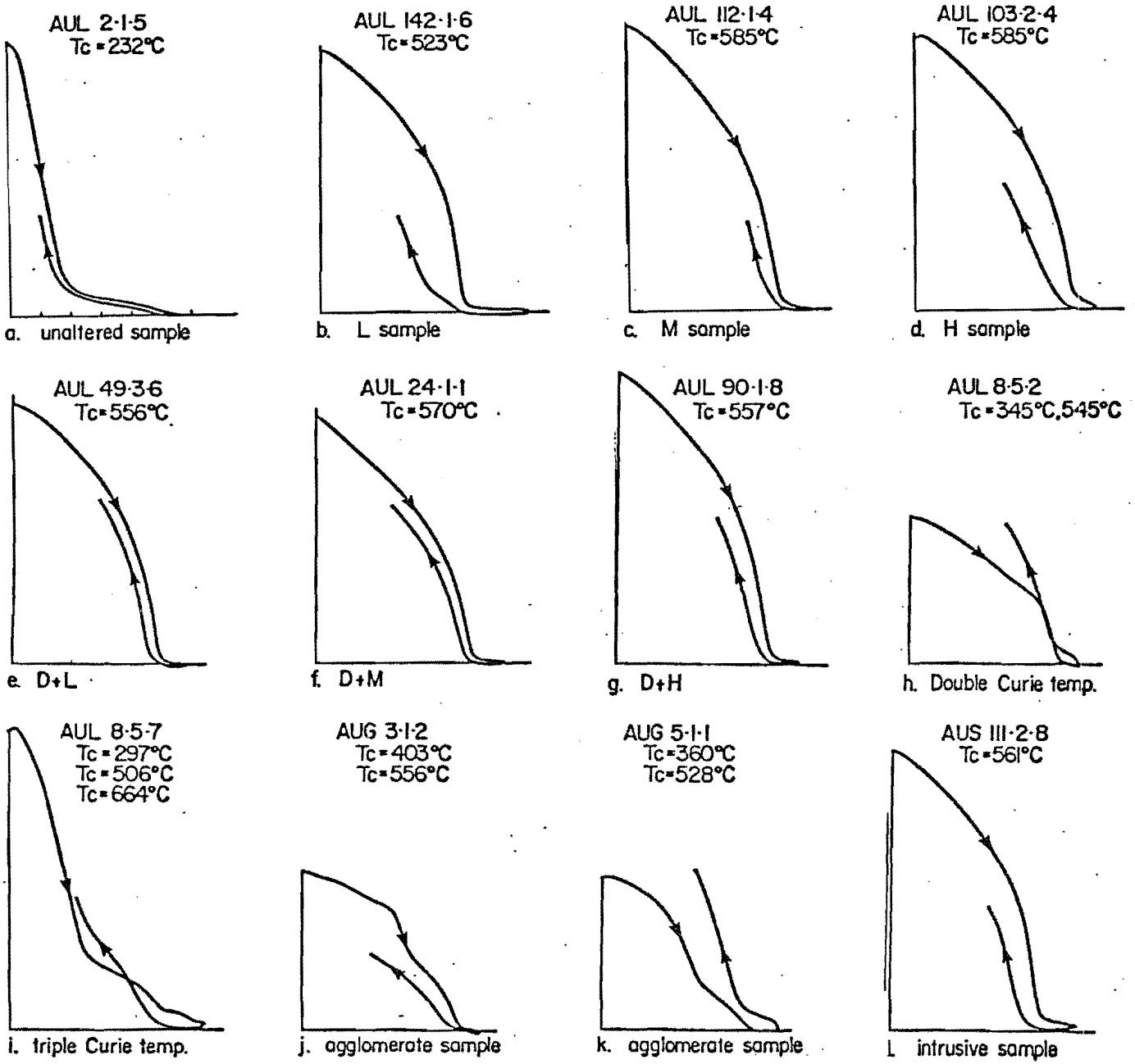
AUL 2-1-5
Tc = 232°C
a. unaltered sample
AUL 142-1-6
Tc = 523°C
b. L sample
AUL 112-1-4
Tc = 585°C
c. M sample
AUL 103-2-4
Tc = 585°C
d. H sample
AUL 49-3-6
Tc = 556°C
e. D+L
AUL 24-1-1
Tc = 570°C
f. D+M
AUL 90-1-8
Tc = 557°C
g. D+H
AUL 8-5-2
Tc = 345°C, 545°C
h. Double Curie temp.
AUL 8-5-7
Tc = 297°C
Tc = 506°C
Tc = 664°C
i. triple Curie temp.
AUG 3-1-2
Tc = 403°C
Tc = 556°C
j. agglomerate sample
AUG 5-1-1
Tc = 360°C
Tc = 528°C
k. agglomerate sample
AUS 111-2-8
Tc = 561°C
L intrusive sample

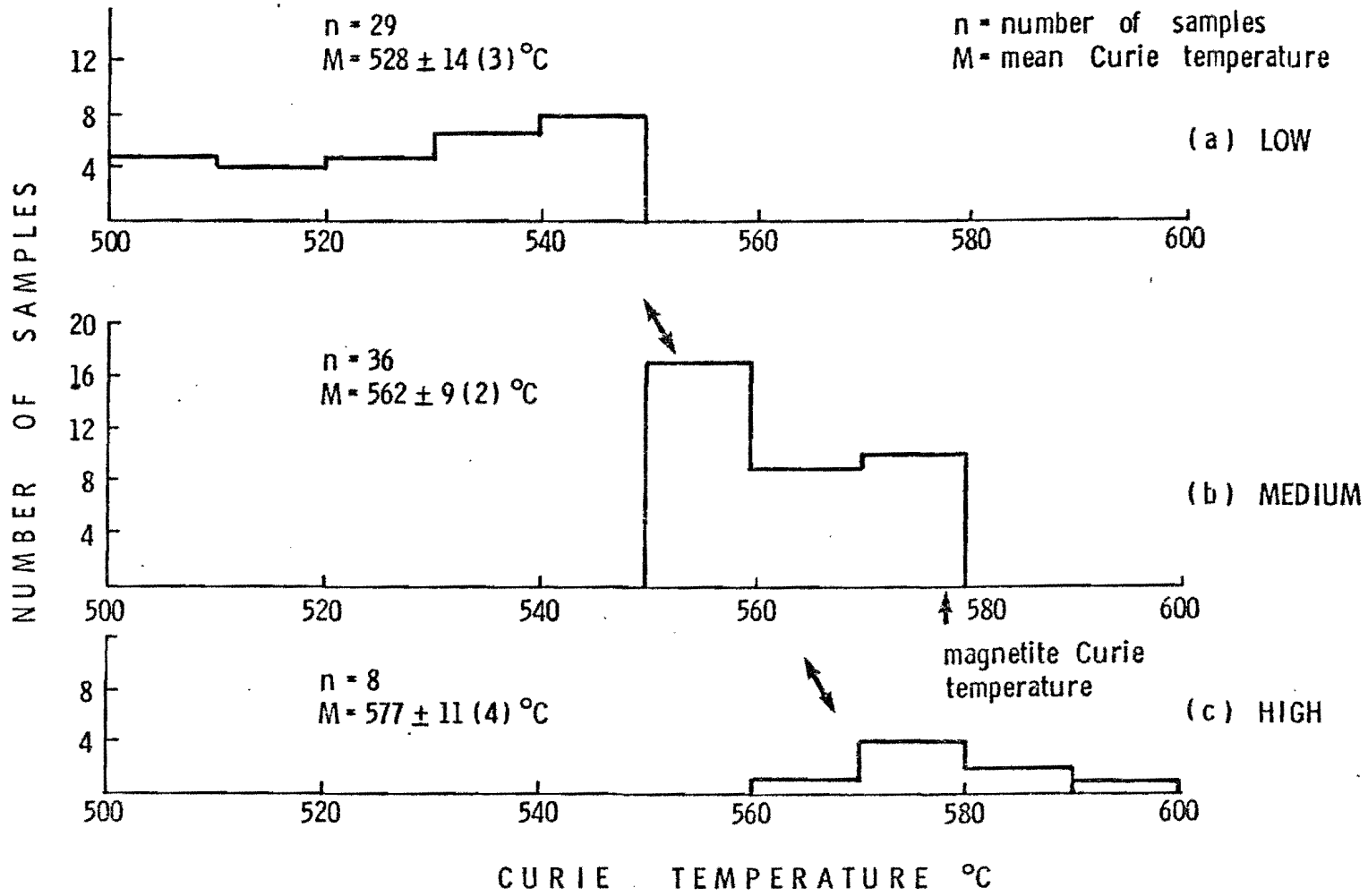

Figure 40. Histogram of Curie temperatures of hydrothermally altered samples showing the increase in Curie temperature with increasing the degree of hydrothermal alteration.

Curie temperatures (Curie temperatures for ferric hydroxides are not known yet). Consistent with this a red stain is always been found surrounding titanomagnetite in most of the altered samples. In addition, McGraw (1976) has found no major variation in total iron content between unaltered and altered samples of the Azores drill rocks.

(3) Samples with high hydrothermal alteration (H): Curie temperatures of this group show an increase in the range between 560-600°C with an average value of 577 ± 11(4), figure 40c. A typical sample, AUL 103.2.4 is shown in figure 39d. Although microscopic examination indicated that titanomagnetite and ilmenite in these samples are almost completely decomposed and replaced by silicate phases, nevertheless Curie temperatures indicate that ferrimagnetic phases are still present.

1.3. Deuteric oxidation with hydrothermal alteration samples: These samples are subdivided, according to the degree of hydrothermal alteration, into three groups.

(1) Deuterically oxidized samples with no or low hydrothermal alteration (D+L): Curie temperatures for this group fall between 540-570°C, figure 41a, with an average of 557 ± 6(2)°C, which is significantly lower than pure magnetite (578°C, McElhinny 1973). Curie temperature curves for this group have a characteristically smooth geniculate form, figure 39e. Consistent with this, microscopic examination of samples in this group indicated that most of titanomagnetite grains were oxidized to a high state of deuteric oxidation.

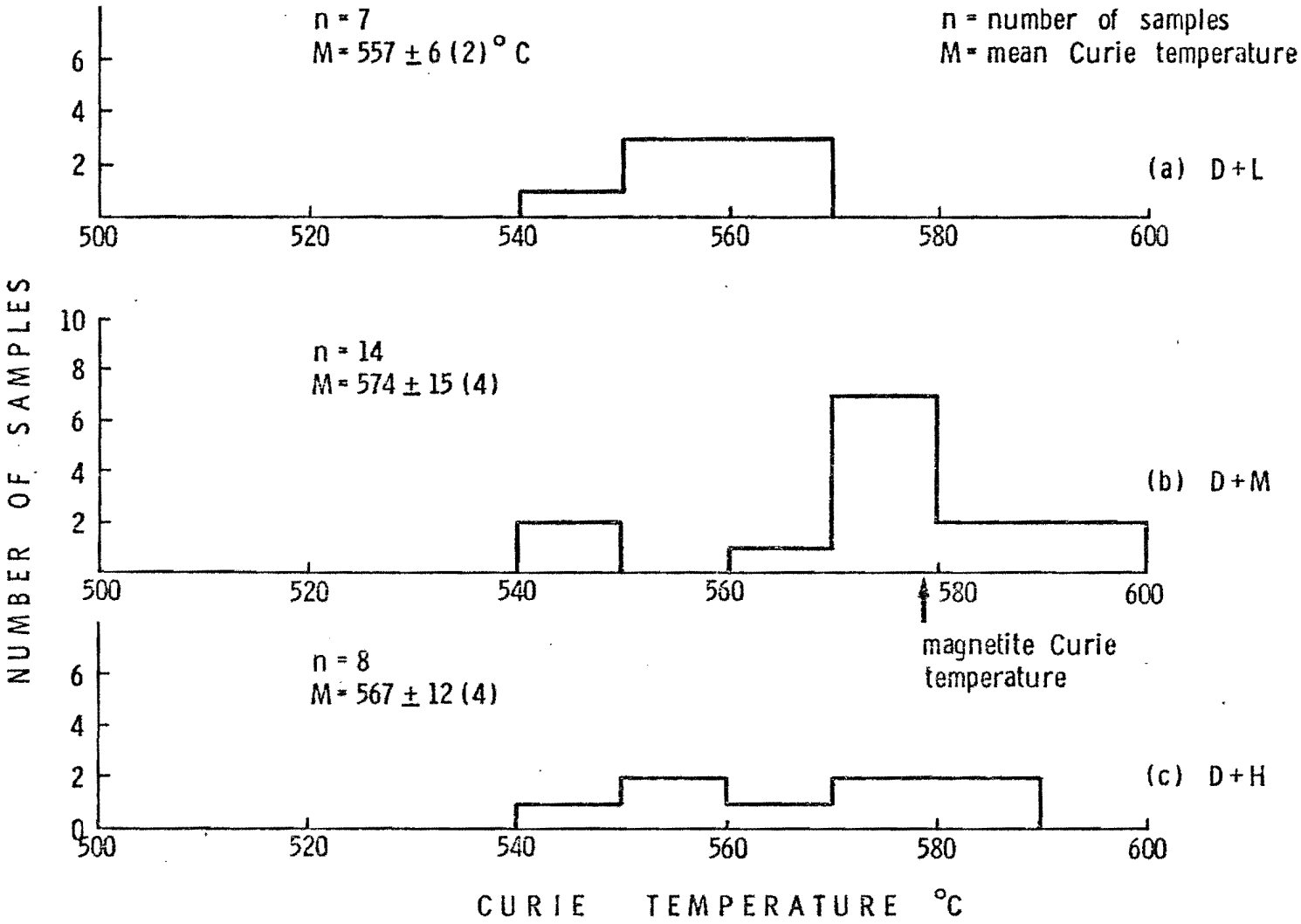

Figure 41. Histogram of Curie temperatures of deuterically oxidized and hydrothermally altered samples.

(2) Deuterically oxidized samples with medium hydrothermal alteration (D+M): This group has a high range of Curie temperatures (540-600°C), figure 41b, with an average of 574 ± 15(4)°C, close to that of pure magnetite. Sample AUL 24.1.1. represents this group, figure 39f.

Although the increase in the degree of hydrothermal alteration results in an increase in Curie temperature, the overall Fe: Ti ratio (as indicated before from microprobe analyses) shows a decrease from the ratio for the unaltered samples. The increase in Curie temperature from 557 to 573°C may be attributed to the formation of a slightly Ti bearing cation deficient magnetite (Readman and O'Reilly 1972).

(3) Deuterically oxidized samples with high hydrothermal alteration (D+H): The range of Curie temperatures for this group is between 540 and 600°C as in (2) D+M, and the average value 567 ± 12(4)°C, figure 41c is not significantly different from that of D+M value. Ade-Hall et al. (1971) noted that a kink features and "e" type Curie point curves were accompanied the increase in deuteric oxidation and hydrothermal alteration. Although microscopic examination of polished sections of this group indicated that both titanomagnetite and ilmenite were in the high state of deuteric oxidation and hydrothermal alteration, neither the kink feature nor the "e" type Curie point were observed, figure 39g.

1.4. Samples with more than one Curie temperature: Two samples from flow unit AUL 8.5 show a double and a triple Curie temperatures, respectively, figures 39h, i. Under the microscope, titanomagnetite

grains, both in low and higher state of deuteric oxidation, were found. Some of these grains showed a medium degree of hydrothermal alteration. The grains without deuteric oxidation must be responsible for the low Curie temperature while those with medium degree of hydrothermal alteration and a higher deutric oxidation state will be responsible for the high Curie temperatures.

1.5. Agglomerate and Intrusive samples: Two agglomerate samples AUG 3.1.2 and AUG 5.1.1 have thermomagnetic curves which are different from those for flow units. Both samples have a double Curie point, figures 39j, k, one of them, AUG 3.1.2 shows the kink feature and the "e" type of Curie point of Ade-Hall et al. (1971). Opaque mineralogy study indicated that both samples were of low degree hydrothermal alteration stage. Sample AUG 3.1.2 contained a cation deficient relatively Ti free maghemite, while AUG 5.1.1. had a titanomaghemite phase in it.

Intrusive samples (AUS 98.5.1, AUS 110.1.2 and AUS 111.2.8) have the same thermomagnetic curves as those for the flow units. A typical sample, AUS 111.2.8, is shown in figure 39l. Although these intrusives were located in the section of highest degree of hydrothermal alteration of the drill core, only a low degree of alteration of titanomagnetite was observed. A possible explanation is that the intrusion might be later than some part of the hydrothermal alteration process.

From the above study of thermomagnetic curves, it seems clear that hydrothermal alteration has a considerable effect on the Curie temperatures. With increasing the degree of hydrothermal alteration, a re-

lative increase in Curie temperature occurs, figures 40 and 41. The correlation between Curie temperatures, depth and zones of alteration is given in figure 42a.

2. Initial Susceptibility (K)

Susceptibilities for the Azores flow-unit samples were measured and are given in Appendix II. Variation in susceptibilities with depth is plotted in figure 42b. Generally, the plot does not show any correlation with depth. A histogram of the measurements is given in figure 43 with arithmetic mean value for $K = 10.7 \pm 5.6\ (0.6) \times 10^{-4}$ emu $oe^{-1}.g^{-1}$. When we correlate K with each zone of hydrothermal alteration in the core, the study becomes much easier. Table 12 shows the arithmetic mean for K in each zone and figure 44 is the modified correlation between K and depth. From this relation we notice the following:

(1) Generally, susceptibility increases with increasing degree of hydrothermal alteration until it reaches a maximum value (13.7) in the medium-high hydrothermal zone, then it decreases as the degree of alteration increases, figure 45.

(2) The recovery of drill core was poor in the first 148 m, so the information from the upper zone of subaerial sequence III is rather low.

(3) In alteration zone (c), K has its lowest value (1.6). Only four samples were available for study of this zone and all but one represent a trachytic flow. Under the microscope, the trachyte samples were all in the highest state of deuteric

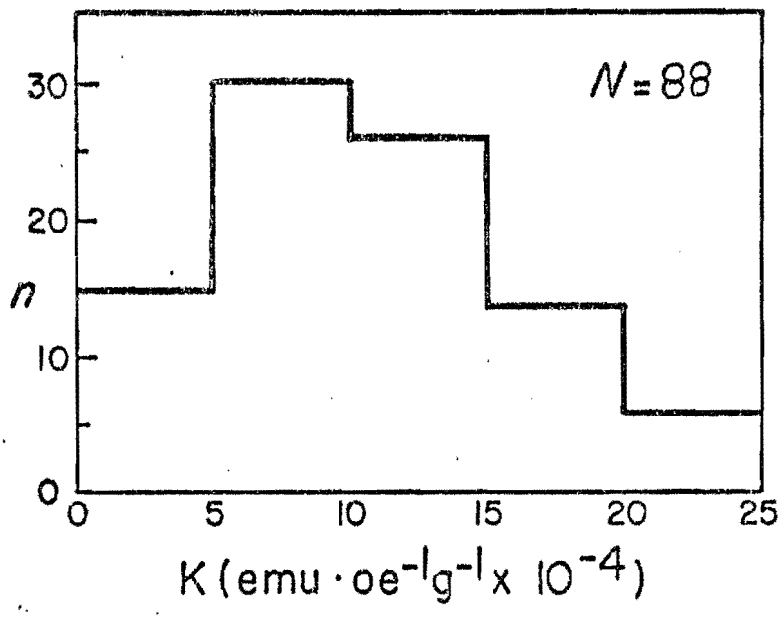

Figure 43. Susceptibilities of Azores basalts. N is the total number of samples measured, and n the number in each class.

Table 12. Mean K, NRM, Q and zones of hydrothermal alteration in the Azores drill core rocks

NUMBER OF SAMPLES	DEPTH IN m	DEGREE OF ALTERATION	ALTERATION ZONES	MEAN K x 10^{-4} emu.oe^{-1} g^{-1}	MEAN NRM x 10^{-4} emu g^{-1}	MEAN Q
2	88	L	a		26.9±1.8 (1)*	
19	205	M	b	11.8±2.9 (0.8) N = 13	16.2±5.7 (1)	2.7±1 (0.3) N = 13
4	287	L	c	1.6±2.8 (1)	3.2±5.7 (3)	6.1±4.1 (2)
9	352	M-H	d	13.7±6.2 (2)	16.9±11.2 (4)	3.6±3.6 (1)
12	438	M-L	e	12.3±7.0 (2)	14.2±8.1 (2)	5.0±7.0 (2)
12	550	M	f	12.9±4.0 (1)	8.4±4.1 (1)	1.7±1.2 (0.3)
16	650	H	g	9.9±5.2 (1)	14.3±11.8 (3)	4.1±4.1 (1)
8	750	M	h	11.8±6.9 (2)	13.1±7.1 (3)	4.0±3.8 (1)
4	838	M-L	i	9.1±4.0 (2)	15.7±4.2 (2)	4.5±2.9 (1)
10	923	M	j	6.3±2.0 (0.6)	19.2±11.9 (4)	6.6±3.0 (1)

* Errors are one standard deviation, values in brackets are standard deviations of the mean

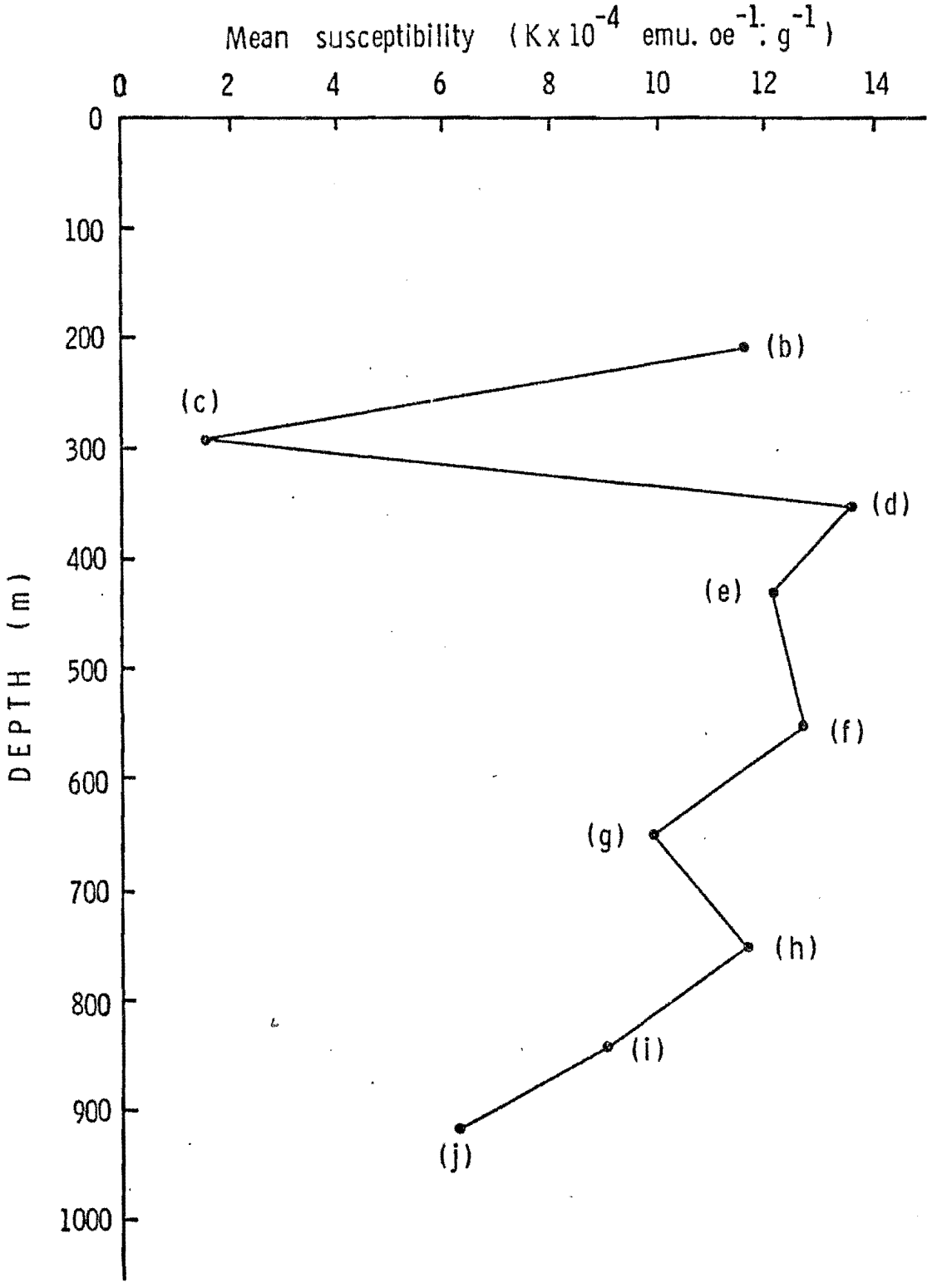

Figure 44. Relation between mean susceptibility in each hydrothermal alteration zone and depth. (For explanation of letters see Table 12).

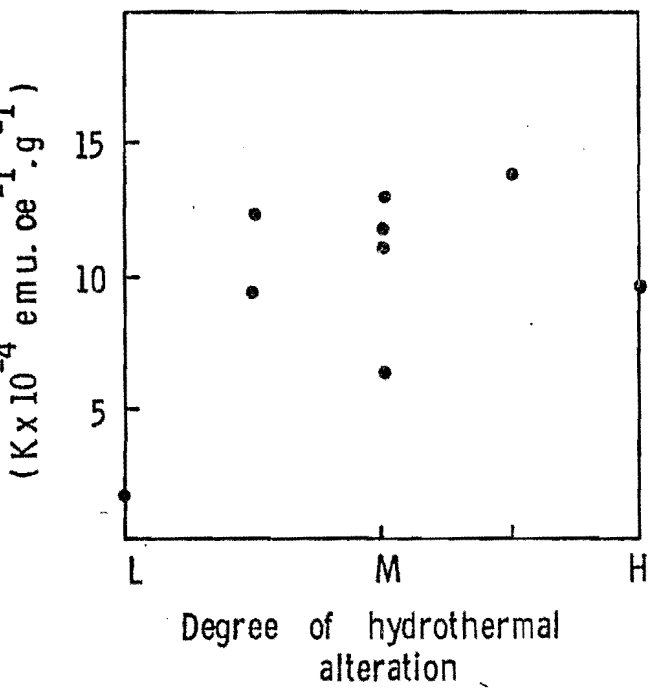

Figure 45. Correlation between the mean susceptibility in each zone and the degree of hydrothermal alteration.

oxidation and have small opaque grain size and with low volume contents. The relation between these factors and susceptibility has been discussed by Nagata (1961), Ade-Hall et al. (1976) and Smith and Prévot (1977). The author believes that these factors could be responsible for the low susceptibility value of zone (c) in the drill core.

(4) Susceptibility has a wide range in the subaerial and transition sequences and a relatively low value (6.3) in the subaqueous section. As mentioned before this can be explained by the variations in alteration and oxidation states, volume contents and grains size. In zones (b, d, e, f and h), the opaque minerals in the rocks were mostly titanohematite and magnetite, while in zone (g) high hydrothermal alteration products are granulation phases and sphene. In zone (i), the magnetic grains were a mixture of skeletal and anhedral form with medium-coarse grain size. The grains were mostly titanomaghemite. Zone (j) was characterized by the occurrence of skeletal titanomagnetite which was altered to titanomaghemite and in some cases titanohematite and granulation texture. Some of the samples shows deuteric oxidation.

3. Natural Remanent Magnetization (NRM)

NRM intensity values are a measure of the magnetic state and the history of rocks. All NRM intensities for the drill core were measured

(Appendix II) and plotted versus depth, figure 42c. The intensity values are classified according to the degree of hydrothermal alteration and the mean intensity for each zone is given in Table 12 and plotted in figure 46. The NRM values of deuterically oxidized samples have been separated. Table 13 and figure 47 shows NRM intensity values of only hydrothermally altered samples (i.e. class 1) versus zones of alteration.

The average NRM intensity of the drill core is 14.4 ± 9.2 (0.9) x 10^{-4} emu.g^{-1}.

Examination of figures 42c, 46 and 47 reveals the following:

(1) NRM values of higher than 30 x 10^{-4} are always associated with high deuteric oxidation samples.

(2) Low NRM values < 2 are also associated with high deuteric oxidation samples. However, all these samples are trachytic and as mentioned before, the oxide abundance in trachytes was relatively low, with sizes ranging from 5-15μ. This could be the reason for these low NRM values.

(3) Generally, figures 42c and 46 do not show any trend with depth. Locally, the intensity varies rapidly on small scale of centimeters to a large scale of meters. Such changes could result from the local effect of oxidation and alteration, however, the difference in initial magnetization field between units (Smith 1967, Ryall et al. 1977) must be included. Figure 48a shows the relation between NRM intensity of all samples and the degree of hydrothermal alteration. In

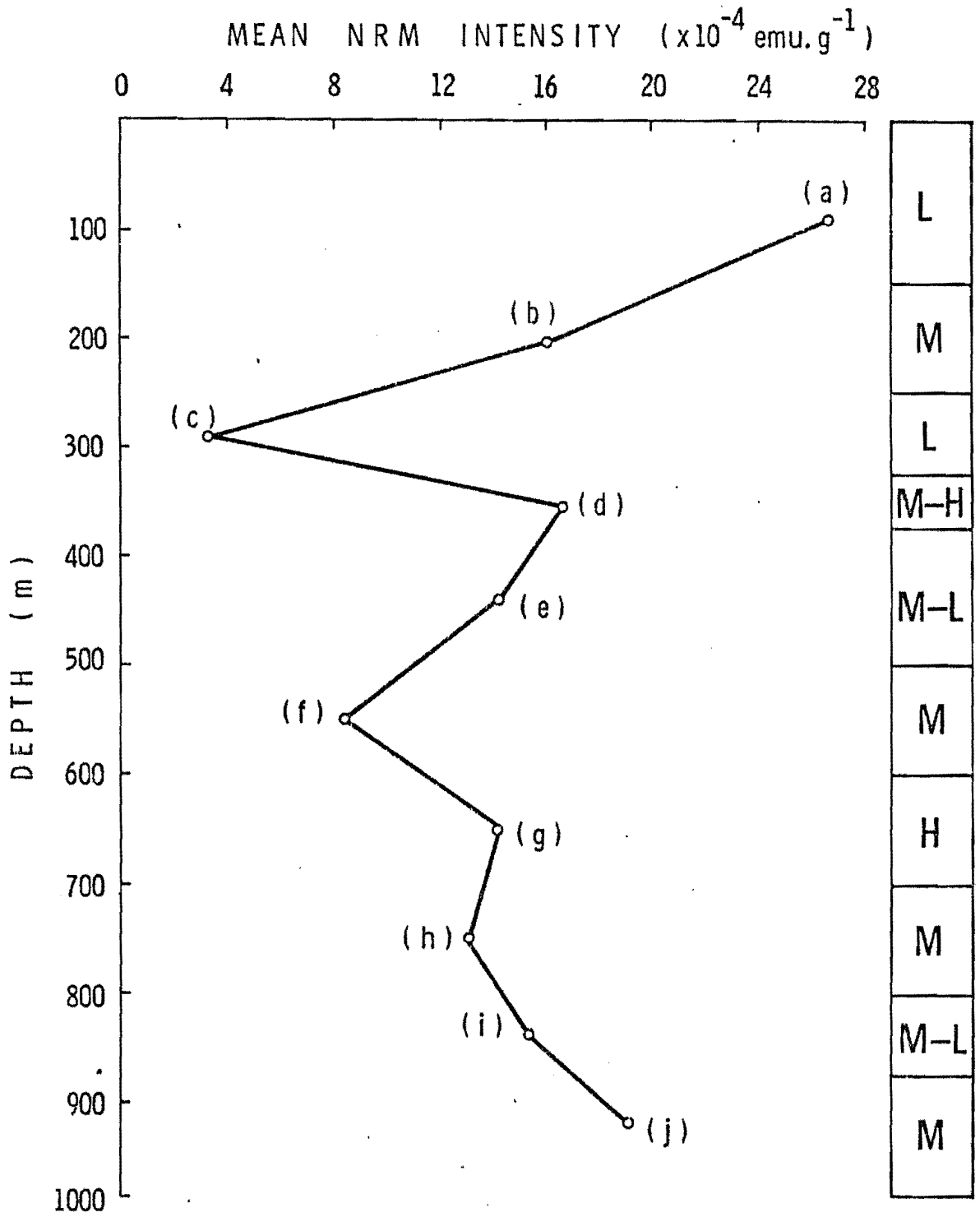

Figure 46. Relation between NRM intensities of all samples in each hydrothermal alteration zone and depth.

Table 13. Mean NRM intensity values of only hydrothermally altered samples

NUMBER OF SAMPLES	DEPTH IN METERS	DEGREE OF ALTERATION	ALTERATION ZONES	MEAN NRM x 10^{-1}emu.g^{-1}
2	88	L	a	26.9±1.8 (1)
15	205	M	b	16.4±5.8 (2)
1	287	L	c	11.7±0 (0)
1	352	M-H	d	5.8±0 (0)
7	438	M-L	e	13.0±8.3 (3)
6	550	M	f	7.3±3.5 (2)
9	650	H	g	12.2±8.3 (3)
7	750	M	h	11.7±6.5 (2)
4	838	M-L	i	15.7±4.2 (2)
9	923	M	j	16.1±7.5 (3)

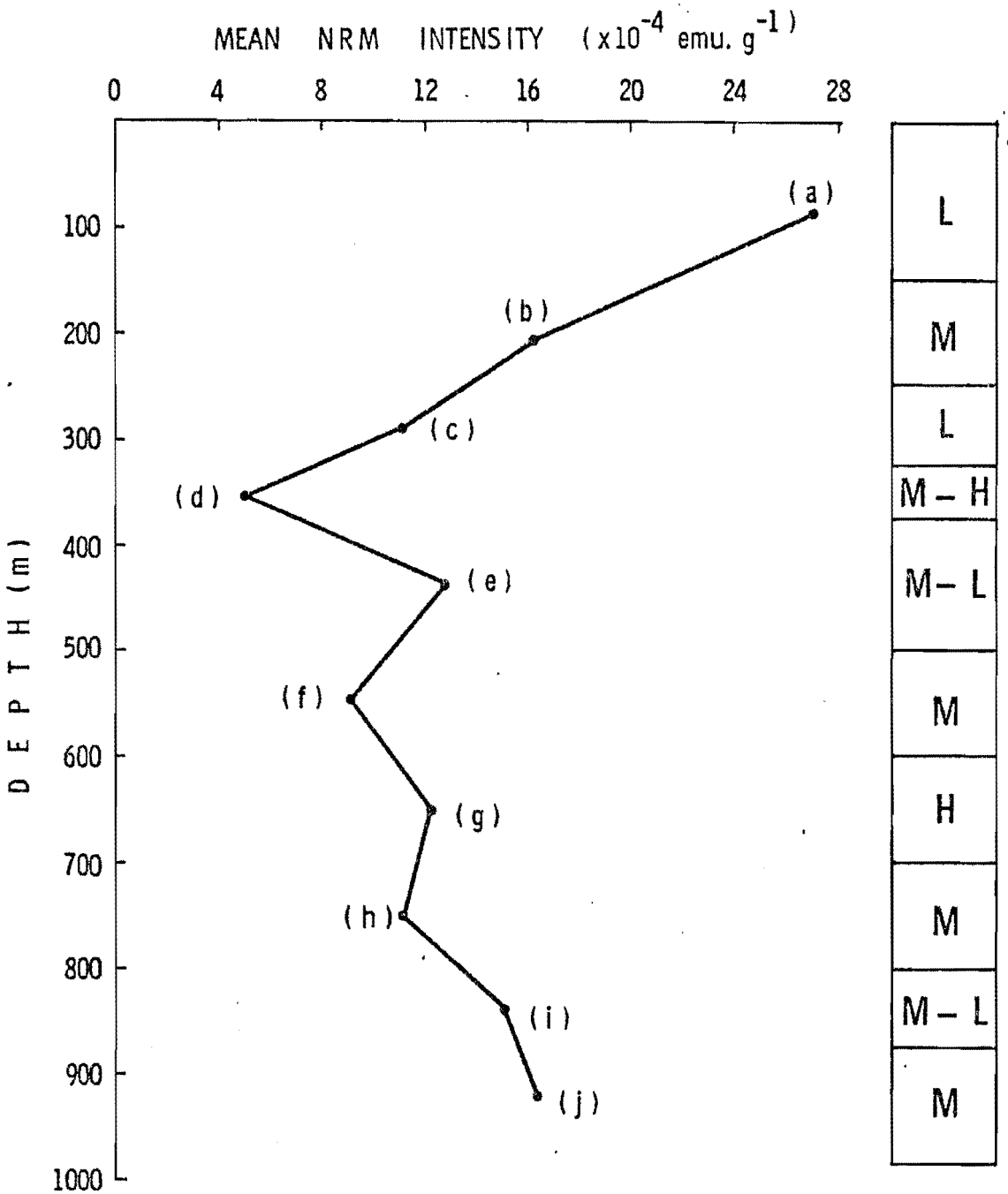

Figure 47. NRM intensities of only hydrothermally altered samples versus zones of alteration.

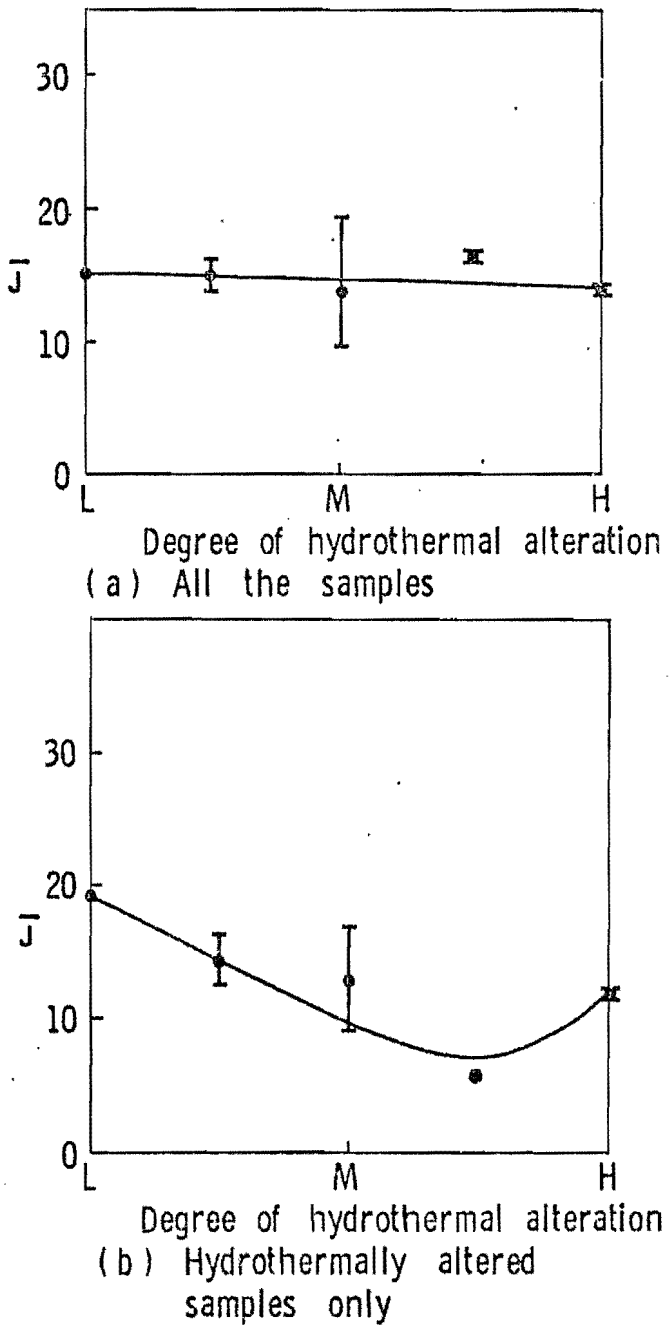

Figure 48. Plot between average intensity ($\bar{J}$) and the degree of hydrothermal alteration (a) for all samples, (b) for hydrothermally altered samples (class 1) only. $\bar{J}$ is in (x 10^{-4}emu.g^{-1}) unit.

order to study the effect of hydrothermal alteration on the NRM intensities, samples which show only hydrothermal alteration have been separated and plotted against the degree of hydrothermal alteration, figure 48b. Although figure 48a does not indicate any changes in NRM intensity with increasing the degree of hydrothermal alteration, figure 48b shows indeed an interesting relation. The NRM intensity decreases as the degree of hydrothermal alteration increases until it reaches a minimum value (5) half way between medium and high degree of alteration. The curve then shows slight increase as the degree of alteration increases.

The relation between NRM intensity and oxidation has been studied by various people but is not very well established. Marshall and Cox (1971a) have shown that the oxidation of titanomagnetite near 200°C actually increases the intensity of NRM. But later (1971b), they demonstrated empirically that the intensity of the oxidized rim of a submarine pillow was substantially lower than that of the fresh interior. This might suggest a different oxidation mechanism for the naturally occurring samples. Johnson and Merrill (1972, 1973 and 1975) found experimentally that at low temperatures (50°C or less) the intensity of titanomagnetite was reduced by oxidation and increased by oxidation at 150°C or so. Indeed the present study, figure 48b, of the natural samples agrees very well with their results.

4. Konigsberger Q ratio

Konigsberger (Q) ratios for all the Azores rocks are given in Appendix II. Q is taken as the ratio between remanent to induced magnetization

$$Q = \frac{J}{KF}$$

where J = remanent magnetization $emu.g^{-1}$

K = susceptibility $emu.g^{-1}oe^{-1}$

F = ambient field, taken as 0.45 oe for the Azores area.

The mean Q ratio for the drill core is 4.0 ± 3.9 (0.4). This indicates that the remanence is the dominant form of magnetization in the drill core, with induced magnetization on average accounting for only one fifth of the total in-situ magnetization.

When Q was plotted versus depth in each hydrothermal zone, figure 49, the following were noted:

(1) The lowest value (1.7) occurred in zone (f) (medium hydrothermal alteration). In this zone the induced magnetization was clearly high and NRM is lower than other medium alteration areas.

(2) The average Q value in the submarine basalts zone (j) was the highest for the drill core, but is still somewhat lower than Q values for other submarine basalts sample from DSDP sites (11.7) (Lowrie 1977).

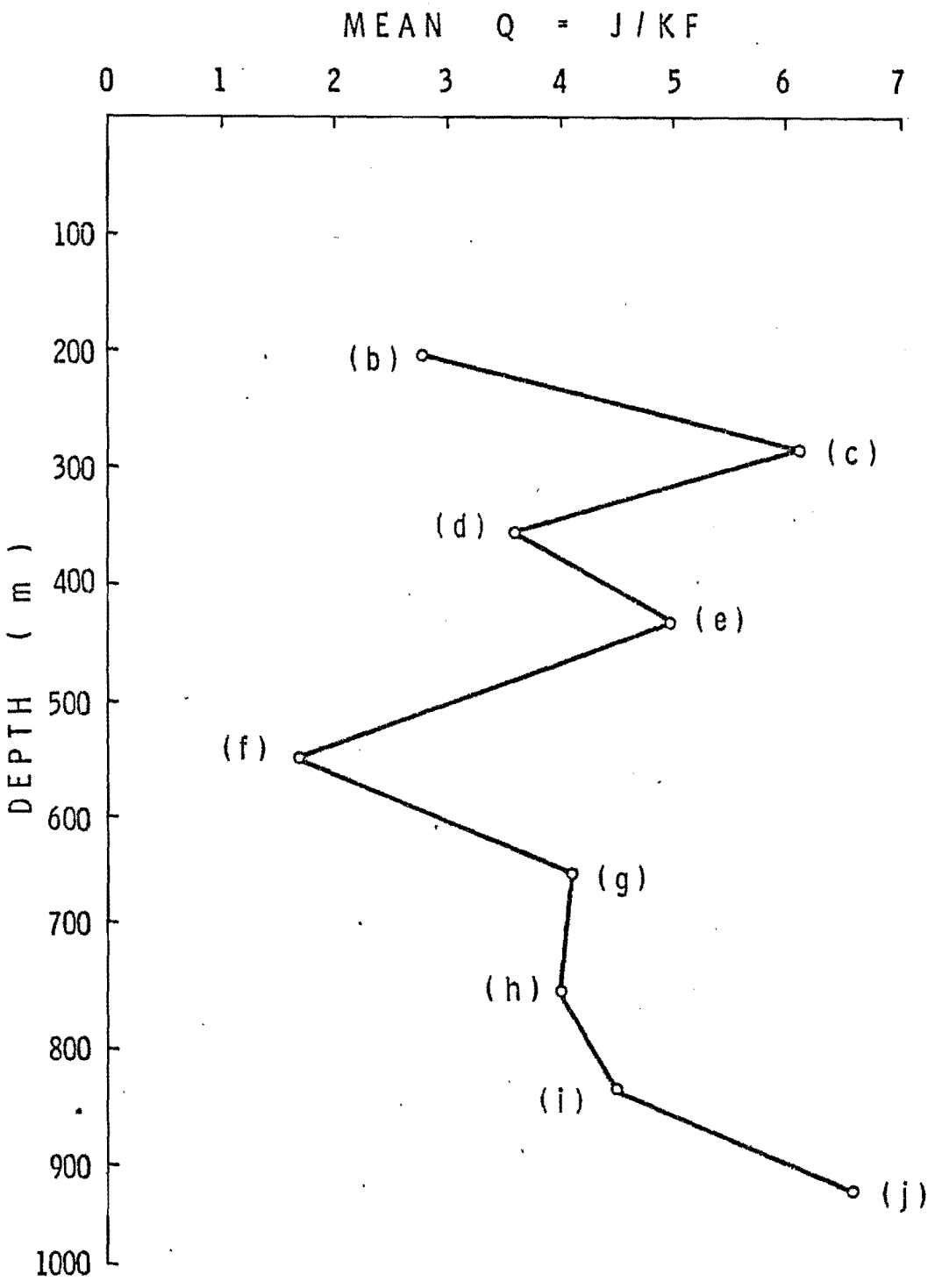

Figure 49. Relation between Konigsberger ratio (Q) in each hydrothermal zone and depth.

(3) The absence of correlation between NRM and K, figure 50, suggests that NRM and K depend largely on different physical parameters.

Generally Q values in the drill core were relatively low and this lead to the conclusion that in the Azores drill core the induced magnetization must constitute a substantial fraction of the total magnetization.

5. Hardness of the Remanence (S)

The ratio R_{200}/J_0 is taken as a measure of the hardness of remanence in the drill core. All S values are given in Appendix II. Hardness of deuterically oxidized and hydrothermally altered samples in each hydrothermal alteration zone are calculated in Table 14 and plotted separately in figure 51.

From figure 51, the following are noted:

(1) High hardness values are always associated with high deuteric oxidation state.

(2) The trachytic flow samples in zone (c) have the highest hardness value (0.8).

(3) In hydrothermal zones (C and D) and deuteric zones (h and j) only one sample is present, so hardness values in these zones must not be interpreted as a deviation from the general trend.

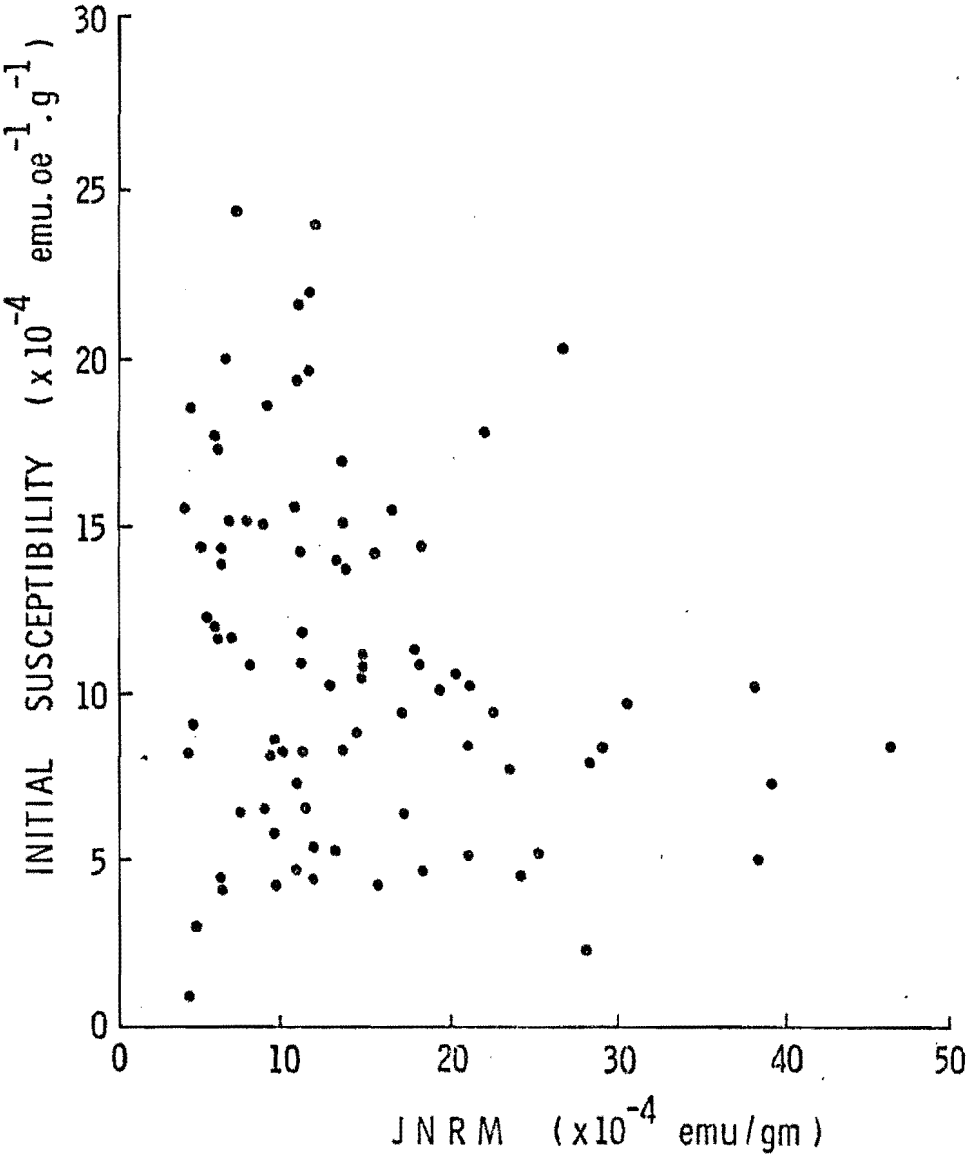

Figure 50. Relation between initial susceptibility and JNRM.

Table 14. Mean hardness values of hydrothermally altered and deuterically oxidized samples

Hydrothermally altered samples		ALTERATION ZONES	Deuterically oxidized samples	
Number of samples	Mean S		Number of samples	Mean S
2	0.09 0.0 (0)	a	--	--
15	0.18 0.2 (.1)	b	4	0.37±.2 (0.1)
1	0.06 0 (0)	c	3	0.79±0.3 (0.2)
1	0.66 0 (0)	d	8	0.31±0.2 (0.1)
7	0.31 0.2 (0.1)	e	5	0.34±0.2 (0.1)
6	0.34 0.3 (0.1)	f	6	0.37±0.1 (0.1)
9	0.27 0.2 (0.1)	g	7	0.48±0.2 (0.1)
7	0.20 0.2 (0.1)	h	1	0.41±0 (0)
4	0.16 0.1 (0.1)	i	--	--
9	0.11 0.1 (0.0)	j	1	0.14±0 (0)

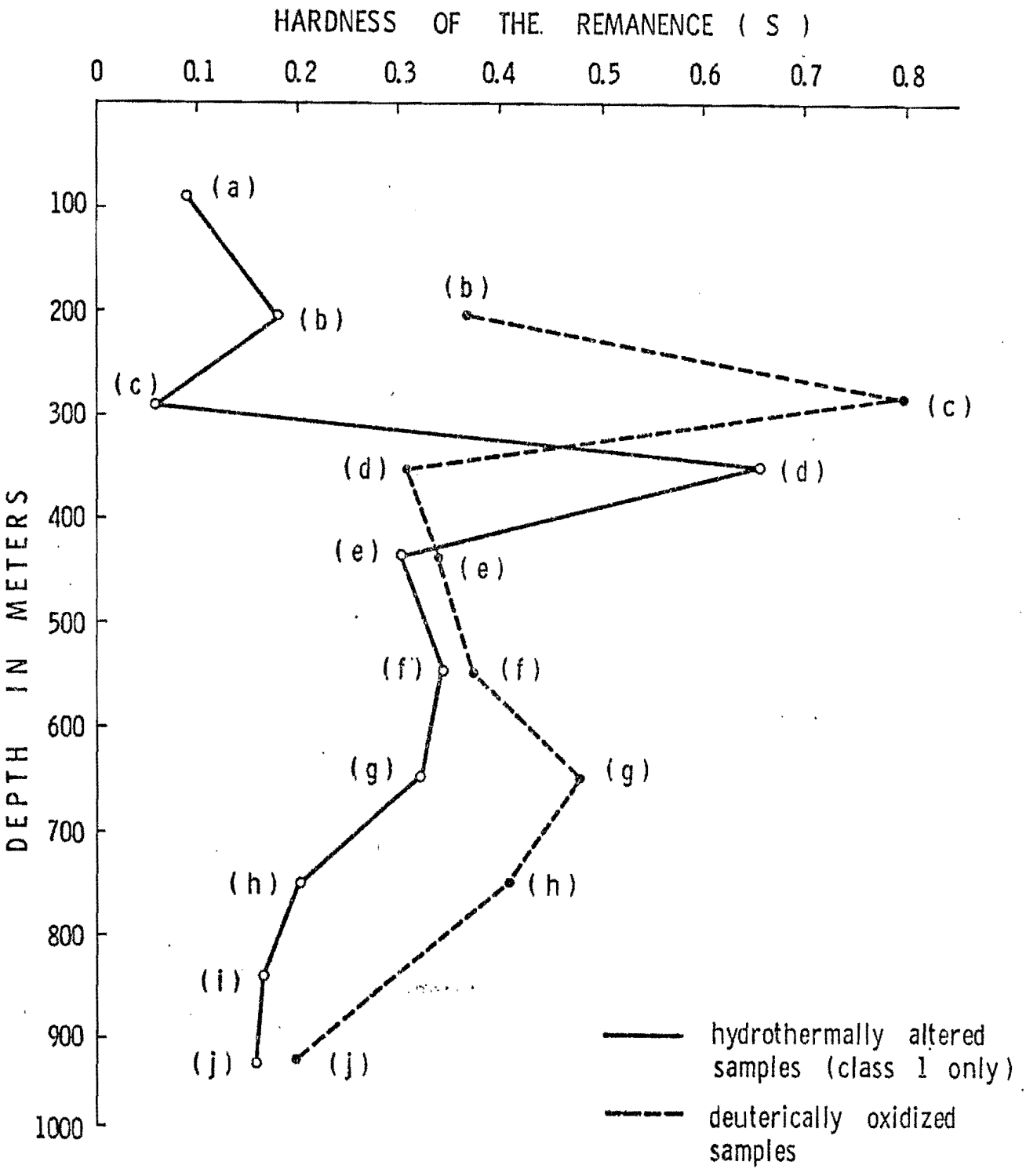

Figure 51. Correlation between hardness of the remanence and the alteration zones.

(4) There is no clear relationship between hardness and the degree of hydrothermal alteration. As indicated by Merrill (1975) hardness depends on several other factors such as grain size, grain shape, abundance of magnetic phases and saturation magnetization.

6. NRM Inclination and Polarity

NRM inclinations could be the resultant of two components; the in situ magnetization and the viscous remanent magnetization (VRM) induced during drilling or acquired during subsequent transport and storage. Ade-Hall and Johnson (1976b) have discussed the drilling induced remanence in Leg 34 samples. The drilling induced remanence was associated with unoxidized and coarse grain (> 20 μ) titanomagnetite. However, it is unlikely that significant drilling induced remanence is present in most of the Azores NRM's as most of the samples, although coarse grained, are highly oxidized and consequently subdivided into small grain size phases.

Stable inclination can be obtained by alternating field partial demagnetization. From stable inclination, the direction of magnetization of the earth's field when the lavas were erupted can be deduced. However, the chemical overprinting of the phases must be considered.

In situ NRM inclination and stable inclination for the Azores rocks were measured and are given in Appendix II. Their distribution

with depth in the drill core is given in figures 42d and 42e. The similarity between the two figures, suggests that VRM did not contribute much to NRM direction inclinations and the uncleaned NRM inclinations can be considered the in situ NRM inclinations for most of the drill core rocks.

At 37°48'N, the dipole inclination is ± 57° and the present inclination is close to 56°. From figures (42d and 42e), it is clear that NRM and stable inclinations both closely approximate the normal polarity dipole inclination. However, there is a group of shallow inclinations in zone b which deviates from the general pattern of stable inclinations in the drill core. This area is hydrothermally altered with medium degree of alteration. Although the deviation of inclination in zone (b) could simply be related to the normal secular variation of the field, oxidation and chemical changes could also have some effect. Merrill (1975), argued that a sudden change in environment of the rock long after it has formed could result in a chemical remanent magnetization (CRM) acquired over a short period and thus a change in magnetic direction which would affect the original inclination. Grommé and Mankinen (1976) agreed with Merrill. However, there is no evidence to suggest that the acquired CRM has caused any change in magnetic direction in the Azores drill core.

All the magnetic inclination measurements are normal and this indicates magnetization during the Brunhes polarity epoch. The possibility that the Azores rocks have acquired self reversal is discussed here.

Self-reversals (both reproducible and nonreproducible) are rare in subaerially erupted basalts (Merrill 1975). Uyeda (1958) and Hoffman (1975) have discussed the possibility of self reversal in titanohematite solid solutions. The mechanism for this self-reversal is very complicated and involves an ordering of Ti in the lattice and probably exsolution as well. In any case, Merrill (1975) stated that such self-reversal is rare in basalts. Self-reversal may also occur on low temperature oxidation of some titanomagnetites (Verhoogen 1956, 1962; O'Reilly and Banerjee 1966). As low-temperature oxidation of titanomagnetite occurs, vacancies are introduced into sites previously occupied by cations. The magnetic moment will change significantly depending on which cation sites (octahedral or tetrahedral) the vacancies eventually occupy and on the initial distribution of the Fe^{2+}, Fe^{3+} and Ti^{4+} ions in the titanomagnetite. Self-reversal is believed to occur on oxidation, providing that the dominant magnetic moment switches from the octahdral to the tetrahedral sites. The two models by Verhoogen (1962) and O'Reilly and Banerjee (1966) have given conflicting titanomagnetite compositions that could self-reverse on oxidation. Experimental work by Ozima and Ozima (1974, quoted in Merrill (1975)) supports neither model. Peterson and Bleil (1973) and Ryall and Ade-Hall (1975) have suggested that there is some mechanism related to unmixing of titanomagnetite and not to maghematization that produces self-reversal of titanomagnetite. However, the Curie temperatures of the Azores rocks as well as the microscopic investigation do not show any evidence of the phase splitting which according to Ryall and Ade-Hall (1975) could cause self-reversal in basalts.

In conclusion, from the study of all self-reversal models and with the abundance of different types of oxidation and alteration in the Azores drill core, it is unlikely that self-reversal has occurred in the Azores rocks.

7. Summary and Conclusion

The magnetic study of the Azores rocks revealed the following:

(1) Curie temperatures for most of the Azores rocks ranges between 500 and 600°C. This indicates that hydrothermal alteration in different intensity, but generally high, sometimes coupled with deuteric oxidation were the major processes that affected the opaque minerals.

(2) The increase in the degree of hydrothermal alteration is always accompanied by an increase in the Curie temperatures.

(3) Initial susceptibility of basaltic rocks varies in the drill core with a mean value of 10.7×10^{-4} emu.oe^{-1}.g^{-1}. Generally susceptibility increases initially with increasing the degree of hydrothermal alteration until it reaches a maximum value in the medium-high hydrothermal zone, then it decreases as the degree of alteration increases.

(4) The average NRM intensity in the drill core is 14.4×10^{-4} emu.g^{-1}. NRM varies with depth with high values, mostly associated with deuteric oxidation. Oxidation, difference in initial magnetizing field between units and induced mag-

netization in the rocks are listed as possible factors that affect the NRM intensity values. When the effect of deuteric oxidation is removed, NRM shows decrease in intensity with increase in the degree of hydrothermal alteration until it reaches a minimum value half-way between medium and high degree hydrothermal alteration. NRM intensity then increases as the degree of alteration increases. This agrees with the experimental work of Johnson and Merrill (1972, 1973 and 1975).

(5) The average Konigsberger ratio (Q) is 4.0 which indicates that although the remanence was the dominant form of magnetization in the drill core, induced magnetization has added substantial contribution to total magnetization.

(6) The hardness of the remanence varies in the drill core but high hardness is always associated with high deuteric oxidation state. There is no clear correlation between hardness and the degree of hydrothermal alteration.

(7) The NRM inclinations in the drill core represent the in situ NRM inclination. Stable inclinations are close to the dipole inclination at 37°48'N, except for zone (b), and they can be considered as the ambient field inclination during eruption. The shallow inclination in zone (b) could be explained as the result of secular variation in the area.

(8) All the magnetic inclination measurements are normal. This indicates magnetization during the Brunhes polarity epoch

with an upper age limit of 0.69 Myr, if no self-reversal has occurred. The concept of self-reversal in the drill core rocks is rejected on the ground of its rare occurrence in subaerial basalts and the presence of different types of alteration without difference in polarity.

CHAPTER VII

SUMMARY, CONCLUSIONS AND DISCUSSION

In this chapter, a summary of the present work as well as some conclusions drawn from this study are given. The meaning of the results and a general history of the crystallization and alteration of the iron-titanium oxides in the drill core are also discussed.

1. Introduction and general view:

(1) The volcano Agua de Pau is presently considered an active volcano (Machado 1967 and Muecke et al. 1974). The volcanic activity is probably generated in an elongated magma chamber at a mean depth of 5 km beneath the island of Saõ Miguel on which the volcano Agua de Pau is located (Machado 1972 and 1974).

(2) The opaque mineralogy and the magnetic studies were carried out on a 981 m drill core from the lower northern flank of this volcano. The rocks from the drill core were divided into five major lithological divisions, subaerial sequences III, II, I, a transition sequence and a subaqueous sequence (Muecke et al. 1974). These divisions consisted of subaerial and submarine lavas of alkali affinities (McGraw 1976) and pyroclastics.

(3) The bottom hole temperatures were measured during and after drilling and indicated that much of the lavas are presently

experiencing temperatures of about 200°C. The oxygen and carbon isotope results (Lawrence and Maxwell, in preparation) suggested that the zone of greatest penetration of hot waters is the 600-700 m depth interval. The calculated temperatures from the stable isotope results in this interval are all very close to the observed temperatures. The lower calculated temperatures at all other depths indicate that incomplete equilibrium with hot fluids were certainly present. This is supported by microscope examination of the polished sections. However, convection following drilling was probably responsible for some of the high observed temperatures.

2. Opaque mineralogy:

Muecke et al. (1974) have reported that 140 extrusive flow units occur in the Azores drill core. A temperature-time sketch for an Azorean lava is given in figure 52, assuming, from the paleomagnetic data, that the average time for each eruptive event is at the most 5000 yrs. The temperature-time sketch shows 6 time-temperature zones; a (α and β solid solution zone), b (deuteric oxidation, high temperature zone), c (intermediate temperature zone), d (low temperature zone), e (hydrothermal alteration zone) and f (weathering and erosion or continuing volcanic activity and burial of flow by younger flow zone).

The path by which the iron-titanium oxide phase reach their final form is variable and complex. The number of degrees of freedom in such a system is large. My attempt, in this chapter, is only to give a

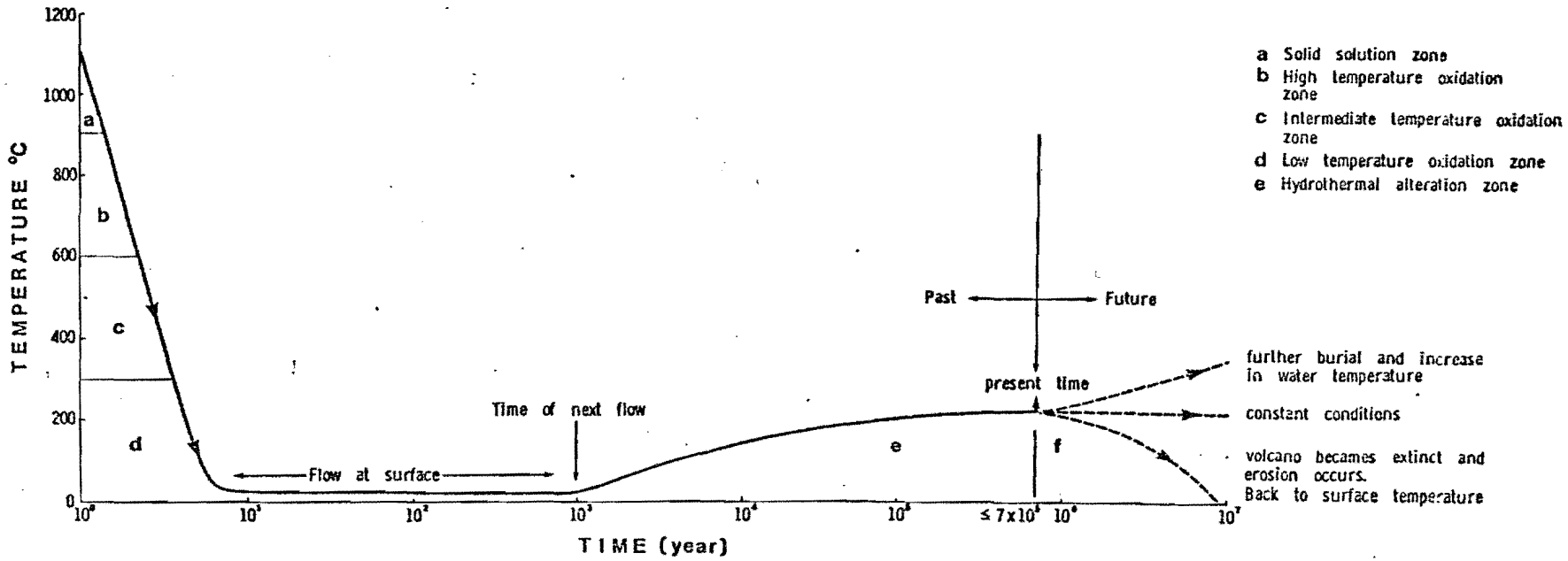

Figure 52. Temperature-time sketch for an Azorean lava. (See text for explanation).

general discussion and average history of the iron-titanium oxide phases from the point of initial crystallization to their final present state in the rocks.

Two hundred and thirty-two polished sections representing ninety-four flow units, three agglomerates and three intrusions were prepared by standard grinding and polishing methods for opaque mineralogy study and seventy-eight of them were selected for microprobe analysis of oxide minerals. The opaque minerals were found to be titanomagnetite, ilmenite and their alteration products. Some spinels (s.l.) were detected and few sulfides were present in the lower part of the subaqueous section. Certain characteristic features of the Azores drill core were recognized during this study and they are summarized and discussed as follows.

(1) The crystallization trend of the unaltered Fe-Ti oxides: The stage of crystallization of iron-titanium phases depends on; the composition of the magma, the oxygen partial pressure (fO_2) and the Fe^{2+}/Fe^{3+} ratio in the magma (Carmichael and Nicholls 1967). The composition of the magma seems to be a primary factor in determining the first iron-titanium oxides to appear during crystallization. McGraw (1976) concluded that the Azores drill core rocks were crystallized from an alkali basalt magma. The order of crystallization of Fe-Ti oxides in such a magma is not clear from the microscope study of the Azores drill rocks.

The effects of oxygen fugacity and the Fe^{2+}/Fe^{3+} ratio are in conflict. Osborn (1959) demonstrated two fundamentally different courses

of crystallization depending on whether the total composition of the mixture or the oxygen partial pressure remain constant during crystallization. He considered the actual ratio Fe^{2+}/Fe^{3+} of secondary importance. In contrast, Carmichael and Nicholls (1967) stated that the precipitation of iron-titanium oxides in natural liquids is necessarily involved with oxygen fugacity and the ferric ion component in the liquid. They pointed out that the residual liquid seems in general to become progressively more oxidized as fractionation proceeds. Examination of Tables 1, 2 and 3 of the unaltered titanomagnetite in the Azores drill core indicates that contrary to Carmichael and Nicholls claim, zoned titanomagnetite has higher ulvöspinel contents near the outer margin of the crystals. In addition, the highest ulvöspinel contents occur in the groundmass which surely does not indicate increased oxidation. It seems that several factors can affect the ulvöspinel content in titanomagnetite other than oxygen fugacity and ferric ion content of the liquid such as alkali content, temperature and the crystallized silicates. Carmichael and Nicholls apparently have not considered all the factors that influencing the composition of titanomagnetite solid solution. In addition, they developed their model for the ilmenite free condition which is different than the present work observation as we have ilmenite joining the crystallization with titanomagnetite.

(2) The trend of minor elements in unaltered titanomagnetite: The minor element trends in titanomagnetite, ilmenite and spinel, Tables 1-5 and

figures 16-21 is as follows; as crystallization proceeded, generally titanium increase and aluminum and magnesium decrease. Manganese and chromium show erratic variation. The decrease in Al and Mg contents agrees well with the few other results in the literature (Carmichael and Nicholls 1967 and Prévot and Mergoil 1973). Cr content of spinels in general decrease with fractionation (Cameron and Glover 1973). Dasgupta (1967, 1969) and Prévot and Mergoil (1973) observed an increase in Mn content as Ti content increases. It is not clear why Mn of the present study shows a different type of behaviour.

The minor element trends can be attributed to the decrease in oxygen fugacity with advance in crystallization which in turn results in an increase in Ti content of Fe-Ti oxides. The decrease in oxygen fugacity may be caused, as suggested by Anderson and Wright (1972), by the effervescence and loss of gas (water and SO_2) during magma ascent.

Another explanation of the minor element trends is taken from the study of thermodynamic considerations of the partition of an element between phases in equilibrium (Kretz 1961, Dasgupta 1967). The substitution of Fe^{3+} by Ti^{4+} in magnetite would cause greater polarization (relative to that in Ti-free magnetite) of the oxygen ions and thereby presumably weaken the structure. In the presence of Ti, in order that the structure of titanomagnetite be rendered stable, there is a necessity for incorporation of "weak" cations into the mineral such as Mn^{2+} in place of Fe^{2+} as an example and for concomitant explusion of Al^{3+} from the structure.

(3) The texture of ilmenite: All the ilmenite intergrowths in titanomagnetite, as identified by Buddington and Lindsley (1964), were recognized in the Azores drill core, plate 14 a-d. Three textural forms were identified (i) trellis type, (ii) composite type and (iii) sandwich type. The trellis type are concentrated along cracks and titanomagnetite grain boundaries. From the textural and crystallographic features as explained before, it represents oxidation followed by phase separation and not exsolution in the strict sense. The composite type occur as internal and external inclusions in titanomagnetite, plate 14 b and c. Three suggestions for the formation of this type are listed and discussed in the literature. Vincent et al. (1954) and Wright (1961) believed that this type formed as a result of diffusion at high temperatures. On the other hand, Buddington and Lindsley (1964) stated that the composite type represents an increase in the degree of oxidation and diffusion. Thirdly, Vincent (1960) and Haggerty (1976) presented evidence and observations which strongly suggest that the composite ilmenite-titanomagnetite intergrowths in basalts are the result of a primary precipitation. The author tends, unless independent evidence indicates that oxidation exsolution has taken place in those grains, to agree with Vincent and Haggerty that this intergrowths are primary precipitation. The third ilmenite type present in the Azores drill core is the sandwich type. These sandwich types may be primary inclusions or may result by oxidation of titanomagnetite. Their origin is not clearly defined.

3. Oxidation of titanomagnetite and ilmenite

It is now widely accepted that the composition of the primary Fe-Ti

oxides in basalts at solidus temperatures (∿ 1100°C), (a, figure 52) is restricted to a certain compositional range of the two solid solution series of magnetite-ulvöspinel and hematite and ilmenite. The rate of cooling and the change in environment during cooling play an important role on the final assemblage. Some of the Azorean lavas were erupted and rapidly cooled and a homogeneous phase with a texture indicating rapid cooling appeared. This comprised fine skeletal phases, which are found in the subaqueous and transition sequences of the drill core. Slow cooling of other lava units, on the other hand produced six titanomagnetite oxidation classes of two distinct textural assemblage of Fe-Ti oxides; (1) oxidation lamellae of ilmenite along {111} planes in titanomagnetite and (2) the pseudomorphic oxidation products rutile, titanohematite and pseudobrookite. The oxidation during the initial cooling of an ideal Azorean lava is represented by zone b (figure 52) and took place between 900°-600°C (Haggerty 1976). Oxygen fugacity is an important factor in determining the oxidation products with high value $10^{-8.1}$ atm. at 800°C for the pseudomorphic assemblage and lower value $10^{-15.4}$ atm. at the same temperature for the oxidation lamellae assemblage (Verhoogen 1962). Most of titanomagnetite deuteric oxidation in the Azores drill core is of the highest degree (class 4, 5 and 6) giving an indication of high oxygen fugacity during the initial cooling of lava.

Deuteric oxidation of ilmenite in the Azores core produced six oxidation classes with pseudobrookite is the end class. However, pseudobrookite which were formed directly from ilmenite and thus by-passing other intermediate stages were observed in many sections,

plate 14e. These pseudobrookites are optically and texturally different than those resulting from progressive oxidation of ilmenite. The factors which control the development of either of these sequences are largely temperature dependent (Haggerty 1976) and, by implication, fO_2 dependent. The latter develops at correspondingly higher temperatures (> 800°C) while the former at lower temperatures ≃ 600°C (Haggerty 1971).

Grommé et al. (1969) and Haggerty (1976) have pointed out that the deuteric oxidation process is rarely an equilibrium process. Individual grains in many cases do approach equilibrium, but there are clearly wide variations in the microenvironmental conditions which affect reaction rates and the degree to which cationic exchange process will respond to rapidly changing physical and chemical parameters. Therefore a definite estimate of temperatures or oxygen fugacity (Buddington and Lindsley 1964) for the whole rock is not possible. However, the high oxidation state of titanomagnetite and ilmenite (class 4, 5 and 6) and the presence of pseudobrookite forming directly from oxidation of ilmenite leads the author to suggest that most of the deuteric oxidation in the Azores lavas has taken place at high oxygen fugacity $10^{-8.1}$ atm. and at high temperature ≃ 800°C.

Haggerty (1971, 1976) noticed that in deuteric oxidation of ilmenite and titanomagnetite, the decomposition of each of these minerals kept the Fe: Ti ratio constant. The present work analysis do not agree well with Haggerty, at least in the titanomagnetite analysis, where the Fe/Ti ratio decreases with advancing oxidation. The author believes that the reason for this disagreement is the loss of iron in the Azores lavas

through later hydrothermal alteration and that the iron is less mobile in ilmenite structure than titanomagnetite.

During the initial cooling of the Azores lavas and between approximately 600°-300°C (zone c, in figure 52) titanomagnetite and ilmenite may develop a mixture of high temperature as well as low temperature oxidation phases. This has been observed in some samples in the low hydrothermal alteration sections which show titanomaghemite, and hematite as well as high temperature oxidation textures.

Between 300°-0°C and after the rocks have cooled (zone d, in figure 52), all the Fe-Ti oxide phases except hematite and rutile (Verhoogen 1962) will oxidize to another stable phase under ambient (atmospheric) temperature and normal pressure. The products of oxidation here are cation deficient spinels, titanomaghemite and pseudorutile. This process started in titanomagnetite by the formation of curved cracks which are considered by Ade-Hall et al. (1976) to develop as a result of the volume change from titanomagnetite to titanomaghemite. They also may represent the consequence of octahedral cationic deficiences in titanomagnetite (Haggerty 1976). Water seems to be an important factor in determining the end stable phase of oxidation at this stage with titanomaghemite forms under wet conditions and titanohematite in dry conditions at low temperatures (≃ 300°C) (Elder 1965 and Sakamoto et al. 1968). In ilmenite, the presence of water leads to the formation of pseudorutile and in dry conditions hematite and rutile are the stable phases at low temperatures (Grey and Reid 1975).

4. Hydrothermal alteration of titanomagnetite and ilmenite:

The consequent eruption and burial of younger lava flows results in reheating of the rocks and further oxidation subsequently occurs in the Azores rocks (zone e, figure 52). Microscope observations showed that hydrothermal alteration was the major alteration process in the drill core. Field observations, measurements of in-hole temperatures, calculated temperatures from oxygen and carbon isotope results and the study of secondary minerals by Sarkar (unpublished report) were all taken as a guide in identifying the conditions of hydrothermal alteration in Fe-Ti oxides in the Azores drill core.

The degree of hydrothermal alteration generally depends on and is controlled by porosity and permeability of the rocks and composition and temperature of the fluid. Although the exact relation between porosity and permeability is not known, it is known qualitatively (Yoder 1955) that permeability decreases as porosity decreases. From this assumption and from the geothermal gradient in the drill core, Muecke et al. (1974) suggested a hot water region (205°C) flowing parallel to the bedding at about 550 m and water at 100°C flowing at 110-120 m depth. However, the microscope observations, in this study, as well as the oxygen and carbon isotope data suggest that the principal region of hot water is probably between 600-700 m. The permeability of the drilled rocks has not been measured. The pH of the fluid, which is controlled by the fluid composition has not been also measured, although from paragenesis of the

secondary minerals Sarkar predicted at least three time changes in the fluid composition. The pressure is believed to be much less effective, particularly under near-surface conditions (Kerr 1955).

The degree of hydrothermal alteration of titanomagnetite and ilmenite in the Azores drill core is taken as the basis for a new classification of basalts alteration in hydrothermal areas. The abundance of the phases, their stability and location in the drill core were correlated with both the observed and calculated temperatures. Three stages of titanomagnetite and ilmenite alteration were adopted:

(1) Titanomagnetite

(a) Low degree hydrothermal alteration (20-80°C): The alteration is progressively increased from class L_1 to class L_4, with the formation of a curve cracking cation deficient spinel phase and titanomaghemite (all iron are ferric). Only the structure of the phases remains constant in this stage. This alteration resembles the low temperature oxidation in zone d, figure .

(b) Medium degree hydrothermal alteration (80-160°C): In this stage (M_1-M_4), both the composition and the structure of the original titanomagnetite are changed. A granular, microcrystalline and porous phase rich in TiO_2 with the addition of Ca and Si in the highest class (M_4) was formed. Iron which is presumably transfered to the ferric state migrated from the present lattice and formed a red stain of iron hydroxides,

while other elements Ti, Al, Mg, Mn and Cr remain unchanged or showed a slight decrease.

(c) High degree hydrothermal alteration (160-210°C): The composition and structures of the phases in this stage (H_1-H_3) are completely changed from the original titanomagnetite and a silicate phase (?) surrounded with a remanent of titanomagnetite and iron hydroxides is formed.

(2) Ilmenite

(a) Low degree hydrothermal alteration (80-100°C): Ilmenite in this stage (S_1-S_4) is characterised by the formation of pseudorutile, which is a cation vacant hexagonal phase (Grey and Reid 1975). Some of Fe^{2+} transfers to Fe^{3+} and some migrates from the ilmenite lattice.

(b) Medium degree hydrothermal alteration (100-150°C): In this stage (T_1-T_3) the phases include coarse granules of rutile and titanohematite and cracks as a result of volume reduction from ilmenite → pseudorutile to rutile (Grey and Reid (1975)).

(c) High degree hydrothermal alteration (150-210°C): This final stage (V_1-V_3) shows a compositional and structural change from that of the original ilmenite. Dark brown to black colored pseudomorphs after ilmenite were formed. Low degree of hydrothermal alteration, low temperature oxidation and weathering are texturally and mineralogically identical. However, the time involved in low temperature oxidation is much less than

that in low hydrothermal alteration. The presence of the thermal fluids as an exchange medium account for the removal of iron from Fe-Ti oxides and thus the textural and mineralogical changes in medium and high degree hydrothermal alteration.

5. The absence of sulfides in the Azores drill core:

Very few sulfide minerals were observed in the subaqueous section of the drill core. The occurrence of sulfides in the subaqueous sections agrees well so far with the data in the literature (for example Moore and Fabbi 1971, Anderson 1974). Two interpretations can be suggested in the present study. First, it is possible that hydrothermal solutions in the drill core have destroyed the sulfide minerals in the subaerial section. A great part of this section has been subjected to extreme hydrothermal alteration, which probably results in the alteration of sulfides to more stable oxide and hydroxide phases. However, it is unlikely that this is the only cause of the rare occurrence of sulfides in the subaerial section. Another and most likely interpretation comes from the studies of the basaltic gaseous system by Gerlach and Nordlie (1975) and from the compositions of volcanic gases by Anderson (1975). Gerlach and Nordlie, suggested that the composition of the basaltic gas phases falls within the system C-O-H-S and thereby the basaltic gases are restricted to H_2O, SO_2, CO_2 and H_2. Anderson (1974 and 1975) indicated that the gas phase released during degassing is sulfur rich, while the gas accumulated after degassing is more advanced is relatively

sulfur deficient. From these studies and from the occurrence of sulfides in the submarine basalts in the present study and elsewhere, the author is inclined to believe that basaltic magma may be saturated in sulfur at depth, i.e. higher temperature and pressure. As surface conditions are approached, decreasing sulfur and increasing H_2O in the gas phase may ultimately cause a condensed sulfide phase to become unstable unless rapid quenching is possible.

6. Magnetic study:

One hundred and eleven samples representing seventy flow units, two agglomerates and three intrusions were used for rock magnetic studies and ninety-six samples representing fifty flow units were selected for paleomagnetic study. A summary of the results are followed:

(1) The Curie temperatures for all the samples, with rare exceptions for near surface flows, were in the range of 500° to 600°C, indicating a high degree of overall oxidation and alteration.

(2) The average initial susceptibility was 10.7×10^{-4} emu. $oe^{-1}.g^{-1}$. Susceptibility initially increased with increasing degree of hydrothermal alteration until it reached a maximum value in the medium-high hydrothermal zone, susceptibility then decreased as the degree of alteration increased.

(3) The average NRM intensity was 14.4×10^{-4} emu.g^{-1}. High NRM values were mostly associated with deuteric oxidation. In titanomagnetite with no deuteric oxidation (class 1) samples, NRM decreased with increase in the degree of hydrothermal alteration up

to a point between the medium and high hydrothermal alteration alteration degrees. NRM then increased as the degree of hydrothermal alteration increased.

(4) The average Konigsberger ratio (Q) was 4.0 indicating that induced magnetization contributes significantly to but does not dominate the total magnetization.

(5) The hardness of the remanence varied in the drill core but high hardness was always found to be associated with high deuteric oxidation state.

(6) The stable inclinations were close to the dipole inclination at 37°48'N and were considered to be the ambient field inclination during eruption.

(7) All the magnetic inclination measurements were normal. This indicates a magnetization during the Brunhes polarity epoch with an upper age limit of 0.69 myr, if no self reversal has occurred. The possibility of the self-reversal in the drill core was discussed and rejected.

7. Future work:

The study of opaque mineralogy and magnetic properties of basalts in active geothermal areas is far from complete. Although the magnetic variations in the drill core were related to the effect of hydrothermal alteration on the magnetic minerals, still more work is needed to confine these relationships. The nature of magnetic minerals and the extent to which granulation may affect the magnetic properties of the rocks

is yet to be explained. However, one positive aspect of the present study is that granulation has been found to be related to medium hydrothermal environment. The variation in mineralogy and magnetic properties of the rocks have been studied in vertical section. A lateral study of the rock properties is indeed needed. More drilling is suggested and is in fact being carried out.

REFERENCES

Abdel-Aal, O. Y. (1973), Reflectivity measurements of some ore minerals and synthetic compounds: M.Sc. thesis, Cairo University, Egypt, 124 p.

Abdel-Aal, O. Y., Hall, J. M. and H. P. Johnson (1976), Opaque mineralogy of basalts from the Mid-Atlantic Ridge at 37°N (FAMOUS project): GAC/MAC meeting, Edmonton, p. 59.

Abdel-Monem, A., Fernandez, L. A. and G. A. Boone (1968), Pliocene-Pleistocene minimum K-Ar ages of the older eruptive centers, eastern Azores: Am. Geophys. Union, Trans., 49, 363.

Ade-Hall, J. M. (1964), Electron probe microanalyser analyses of basaltic titanomagnetites and their significance to rock magnetism: Geophys. J. R. Astr. Soc., 8, 301-312.

Ade-Hall, J. M. (1969), Opaque petrology and the stability of natural remanent magnetism in basaltic rocks: Geophys. J. R. Astr. Soc., 18, 93-107.

Ade-Hall, J. M. (1974), The opaque mineralogy of basalts from DSDP Leg 26: In, T. A. Davies and B. P. Luyendyk, Eds., Initial Reports of the Deep Sea Drilling Project, 26, 533-539, U.S. Government Printing Office, Washington, D.C.

Ade-Hall, J. M. and H. P. Johnson (1976b), Review of magnetic properties of basalts and sediments, Leg 34: In, S. R. Hart and R. S. Yeats, Eds., Initial Reports of the Deep Sea Drilling Project, 34, 769-777, U.S. Government Printing Office, Washington, D.C.

Ade-Hall, J. M. and N. D. Watkins (1970), Absence of correlations between opaque petrology and natural remanence polarity in Canary Island lavas: Geophys. J. R. Astr. Soc., 19, 351-360.

Ade-Hall, J. M. and R. L. Wilson (1969), Opaque petrology and natural remanence polarity in Mull (Scotland) dykes: Geophys. J. R. Astr. Soc., 18, 333-352.

Ade-Hall, J. M., Fink, L. K. and H. P. Johnson (1976a), Petrography of opaque minerals, Leg 34: In, S. R. Hart and R. S. Yeats, Eds., Initial Reports of the Deep Sea Drilling Project, 34, 349-362, U.S. Government Printing Office, Washington, D. C.

Ade-Hall, J. M., H. P. Johnson, and R. J. C. Ryall (1976b), Rock magnetism of basalts, Leg 34: In, S. R. Hart and R. S. Yeats, Eds., Initial Reports of the Deep Sea Drilling Project, 34, 459-468, U.S. Government Printing Office, Washington, D.C.

Ade-Hall, J. M., M. A. Khan, P. Dagley and R. L. Wilson (1968), A detailed opaque petrological and magnetic investigation of a single tertiary lava from Skye, Scotland - I. Iron-titanium oxide petrology: Geophys. J. R. Astr. Soc., 16, 375-388.

Ade-Hall, J. M., M. A. Khan, P. Dagley, and R. L. Wilson (1968), A detailed opaque petrological and magnetic investigation of a single Tertiary lava flow from Skye, Scotland - II. Spatial variations of magnetic properties and selected relationships between magnetic and opaque petrological properties: Geophys. J. R. Astr. Soc., 16, 389-399.

Ade-Hall, J. M., H. C. Palmer, and T. P. Hubbard (1971), The magnetic and opaque petrological response of basalts to regional hydrothermal alteration: Geophys. J. R. Astr. Soc., 24, 137-174.

Ade-Hall, J. M., R. L. Wilson, and P. J. Smith (1965), The petrology, Curie points and natural magnetizations of basic lavas: Geophys. J. R. Astr. Soc., 9, 323-335.

Akimota, S., Katsura, T. and M. Yoshida (1957a), Magnetic properties of $TiFe_2O_4$-Fe_3O_4 system and their change with oxidation: J. Geomag. Geolectricity, 9, 165-178.

Akimoto, S., Nagata, T. and T. Katsura (1957b), The $TiFe_2O_5$-Ti_2FeO_5 solid solution series: Nature, 179, 37-38.

Anderson, A. J., Jr. (1966), Mineralogy of the labrieville anorthosite, Quebec: Am. Mineral., 51, 1671-1711.

Anderson, A. T., Jr. (1968a), The oxygen fugacity of alkaline basalt and related magmas, Tristan da Cunha: Am. J. Sci., 266, 704-727.

Anderson, A. T., Jr. (1968b), Oxidation of the LaBlache Lake titaniferous magnetite deposit, Quebec: J. Geol. 76, 528-547.

Anderson, A. T., Jr. (1974), Chlorine, sulfur and water in magmas and oceans: Bull. Geol. Soc. Am., 85, 1485-1495.

Anderson, A. T., Jr. (1975), Some basaltic and andesitic gases: Rev. Geophys. Space Phys., 13, 37.

Anderson, A. T., Jr. and T. L. Wright (1972), Phenocrysts and glass inclusions and their bearing on oxidation and mixing of basaltic magmas, Kilauea Volcano, Hawaii: Am. Mineral., 57, 188-216.

Assunção, Torre de, C. F. and M. H. Canilho (1970), Notas sobra petrografia comparada das ilhas Atlanticas: Lisboa Univ. Fac. Cienc. Mus. e Lab. Mineral. e Geol. Bol., 11, 305-342.

Bailey, S. E., Cameron, E. N., Spedden, H. R. and R. J. Weege (1956), The alteration of ilmenite in beach sands: Econ. Geol., 51, 263-279.

Banerjee, S. K., O'Reilly, W., Gibb, T. C. and N. N. Greenwood (1967), The behaviour of ferrous ions in iron-titanium spinels: J. Phys. Chem. Solids, 28, 1323-

Banghar, A. R. and L. R. Sykes (1969), Focal Mechanisms of earthquakes in the Indian ocean and adjacent regions: J. Geophys. Res., 74, 632-649.

Basta, E. Z. (1959), Some mineralogical relationships in the system Fe_2O_3-Fe_3O_4 and the composition of titanomaghemite: Econ. Geol., 54, 698-719.

Basta, E. Z. (1960), Natural and synthetic titanomagnetites (the system Fe_3O_4-Fe_2TiO_4-$FeTiO_3$): Neues Jahrb. Mineral. Abh., 94, Festband Famdohr, 1017-1048.

Bhimasankaram, V. L. S. (1964), Partial magnetic self-reversal of pyrrhotite: Nature, 202, 478-480.

Bleil, U. (1971), Cation distribution in titanomagnetites: Z. Geophys., 37, 305-319.

Boone, G. M. and L. A. Fernandez (1971), Phenocrystic olivines from the eastern Azores: Min. Mag., 38, 165-178.

Bowles, J. F. (1977), A method of tracing the temperature and oxygen-fugacity histories of complex magnetite-ilmenite grains: Mineral. Mag., 41, 103-109.

Buddington, A. F. and D. H. Lindsley (1964), Iron-titanium oxide minerals and synthetic equivalents: J. Petrol., 5, 310-357.

Cameron, E. N. (1961), Ore Microscopy: John Wiley & Sons, Inc.,

Cameron, E. N. and E. D. Glover (1973), Unusual titanian-chromian spinels from the eastern Bushveld Complex: Am. Mineral., 58, 172.

Carmichael, C. M. (1960), The magnetic properties of ilmenite-hematite crystals: Proc. Roy. Soc., Ser. A, 263, 508-550.

Carmichael, C. M. (1970), The Mid-Atlantic-Ridge near 45°N. VII. Magnetic properties and opaque mineralogy of dredged samples: Can. J. Earth Sci., 7, 239-256.

Carmichael, I. S. E. (1967), The iron-titanium oxides of salic volcanic rocks and their associated ferromagnesian silicates: Contr. Mineral. Petrology, 14, 36-64.

Carmichael, I. S. E. and J. Nicholls (1967), Iron-titanium oxides and Oxygen fugacities in volcanic rocks: J. Geophys. Res., 72, 4665-4687.

Cloos, H. (1939), Zur tektonik der Azoreh: Abh. preuss. Akad. Wiss. Phys. - Math. Kl., 5, 59-64.

Colombo, U., Fagherazzi, G., Gazzarrini, F., Lanzavecchia and G. Sironi (1968), Mechanism of low temperature oxidation of magnetite: Nature, 219, 1036-1037.

Czamanske, G. K. and P. Mihalik (1972), Oxidation during magmatic differentiation, Finnmarka complex, Oslo area, Norway, Part 1, The opaque oxides: J. Geology, 13, 493-509.

Creer, K. M. and J. D. Ibbetson (1970), Electron microprobe analyses and magnetic properties of non-stoichiometric titanomagnetites in basaltic rocks: Geophys. J. R. Astr. Soc., 21, 485-

Dachille, F., Simons, P. Y. and R. Roy (1968), Pressure-temperature studies of anatase, brookite, rutile, and TiO_2-II: Am. Mineral., 53, 1929-1939.

Dasgupta, H. C. (1967), Intracrystalline element correlation in magnetite: Econ. Geol., 62, 487-493.

Dasgupta, H. C. (1969), Distribution of magnesium and manganese between co-existing titaniferous magnetite and ilmenite: Their geothermometric implications: J. Geochem. Soc. India,

Dasgupta, H. C. (1970), Influence of temperature and oxygen fugacity on the fractionation of manganese between coexisting titaniferous magnetite and ilmenite: J. Geol., 78, 243-249.

David, I. and A. J. E. Welch (1956), The oxidation of magnetite and related spinels constitution of gamma ferric oxide: Trans. Faraday Soc., 52, 1642-1650.

Davis, B. L., Rapp, Jr., G. and M. J. Walawender (1968), Fabric and structural characteristics of the martitization process: Am. J. Sci., 266, 482-496.

Desborough, G. A. (1963), Mobilization of iron by alteration of magnetite-ulvöspinel in basic rocks in Missouri: Econ. Geol., 58, 332-

Desborough, G. A., Anderson, T. A. and T. L. Wright (1968), Mineralogy of sulfides from certain Hawaiian basalts: Econ. Geol., 63, 636-644.

Dewey, J. F. and J. M. Bird (1970), Mountain belts and the new global tectonics: J. Geophys. Res., 75, 2625-2647.

Edwards, A. B. (1960), Textures of ore minerals and their significance: The Australasian Institute of Mining and Metallurgy,

Elder, T. (1965), Particle size effect in oxidation of natural magnetite: J. Apply. Phys., 36, 1012-

Elsdon, R. (1972), Iron-titanium oxide minerals in the upper layered series, Kap Edvard Holm, east Greenland: Min. Mag., 38, 946-956.

Elsdon, R. (1975), Iron-titanium oxide minerals in igneous and metamorphic rocks: Mineral. Sci. Engng., 7, 48-70.

Fernandez, L. A. (1973), Petrology of the Nordeste volcanic complex, São Miguel Island, Azores: Geol. Soc. Amer. (abstract), p. 618.

Flinter, B. H. (1959), The alteration of Malayan ilmenite grains and the question of "Arizonite": Econ. Geol., 54, 720-729.

Freund, H. (1966), Applied Ore Microscopy: Theory and Techniques: The MacMillan Company, 607 p.

Geith, M. A. (1952), Differential thermal analysis of certain iron oxides and oxide hydrates: Am. J. Sci., 250, 677-695.

Gerlach, T. M. and B. E. Nordlie (1975), The C-O-H-S gaseous system, Part I: Composition limits and trends in basaltic gases: Am. J. Sci., 275, 353-376.

Gerlach, T. M. and B. E. Nordlie (1975), The C-O-H-S gaseous system, Part II: Temperature, atomic composition and molecular equilibria in volcanic gases: Am. J. Sci., 275, 377-394.

Gerlach, T. M. and B. E. Nordlie (1975), The C-O-H-S gaseous system, part III: Magmatic gases compatible with oxides and sulfides in basaltic magmas: Am. J. Sci., 275, 395-410.

Gidskehaug, A. (1975), Method to determine the degree of non-stoichiometry of iron-titanium oxides: Geophys. J. R. Astr. Soc., 41, 255-269.

Gidskehauge, A. and W. T. Davison (in press), Electronprobe microanalyses of opaque mineralogy in Mesozoic lavas form south-west Africa: Phys. Earth Planet. Int.

Graham, J. W. (1953), Changes in ferromagnetic minerals and their bearing on magnetic properties of rocks: J. Geophys., 58, 243.

Grey, I. E. and A. F. Reid (1975), The structure of pseudorutile and its role in the natural alteration of ilmenite: Am. Mineral., 60, 898-906.

Grommé, S. and E. A. Mankinen (1976), Natural remanent magnetization, magnetic properties, and oxidation of titanomagnetite in basaltic rocks from DSDP Leg 34: In, S. R. Hart and R. S. Yeats, Eds., Initial Reports of the Deep Sea Drilling Project, 34, 485-494, U.S. Government Printing Office, Washington, D. C.

Grommé, S., Wright, T. L. and D. L. Peck (1969), Magnetic properties and oxidation of iron-titanium oxide minerals in Alae and Makaopuhi lava lakes, Hawaii: J. Geophys. Res., 74, 5277-5294.

Hagg, G. (1935), The crystal structure of magnetic ferric oxides γ-Fe_2O : Z. Physik. Chem., Abt. B, 29, 95-103.

Haggerty, S. E. (1971), High-temperature oxidation of ilmenite in basalts: Ann. Rep. Dir. Geophys. Lab. Year Book 70, 165-176.

Haggerty, S. E. (1973), Spinels of unique composition associated with ilmenite reactions in the Ligobong Kimberlite pipe, Lesotho: In Lesotho Kimberlites. P. H. Nixon, Ed., 149-158, Lesotho National Development Corp. Maseru.

Haggerty, S. E. (1973b), Armalcolite and genetically associated opaque minerals in the Lunar samples: Proceeding of the fourth Lunar Science Conference: Supplement 4, Geochim. Cosmochim. Acta, 1, 777-797.

Haggerty, S. E. (1975), The chemistry and genesis of opaque minerals in Kimberlites: Phys. Chem. Earth, 9, 295-307.

Haggerty, S. E. (1976a), Oxidation of opaque mineral oxides in basalts: In, Oxide Minerals, Short Course Notes, Mineralogical Society of America, D. Rumble, III, Ed., 3.

Haggerty, S. E. (1976b), Opaque mineral oxides in terrestrial igneous rocks: In, Oxide Minerals, Short Course Notes, Mineralogical Society of America, D. Rumble, III, Ed., 3.

Haggerty, S. E. and D. H. Lindsley (1969), Stability of the pseudobrookite (Fe_2TiO_5)-ferropseudobrookite ($FeTi_2O_5$) series: Carnegie Inst. Washington, Year Book, 68, 247-249.

Halfen, B. (1976), Difference in spectral reflectivity between grains of homogeneous and exsolved titanomagnetite: Min. Mag., 40, 843-851.

Hall, J. M. and J. F. Fischer (1977), Opaque mineralogy of basement rocks, Leg 37: In, F. Aumento and W. G. Melson, et al., Initial Reports of the Deep Sea Drilling Project, 37, 857-873, U.S. Government Printing Office, Washington, D. C.

Hargraves, R. B. and J. M. Ade-Hall, (1975), Magnetic properties of separated mineral phases in unoxidized and oxidized Icelandic basalts: Am. Mineral., 60, 29-34.

Harrison, C. G. A. and M. N. A. Peterson (1965), A magnetic mineral from the Indian Ocean: Am. Mineral., 50, 704-712.

Hart, R. A. (1973), A model for chemical exchange in the basalt-seawater system of oceanic layer II: Can. J. Earth Sci., 10, 799-816.

Hauptman, Z. (1974), High-temperature oxidation, range of non-stoichiometry and Curie point variation of cation deficient titano-magnetite $Fe_{2.4}Ti_{0.6}O_{4+\gamma}$: Geophys. J. R. Astr. Soc., 38, 29-47.

Heald, E. F. and C. W. Weiss (1972), Kinetics and mechanism of the anatase/rutile transformation, as catalyzed by ferric oxide and reducing conditions: Am. Mineral., 57, 10-23.

Hey, M. H., Embrey, P. G. and E. E. Fejer (1967), Crichtonite, a distinct species: Min. Mag., 37, 349-356.

Hoblitt, R. P. and E. E. Larson (1975), New combination of techniques for determination of the ultrafine structure of magnetic minerals: Geology, 3, 723-726.

Hoffman, K. A. (1975), Cation diffusion processes and self-reversal of thermoremanent magnetization in the ilmenite-hematite solid solution series: Geophys. J. R. Astr. Soc., 41, 65-80.

Iida, Y. and S. Ozaki (1961), Grain growth and phase transformation of titanium oxide during calcination: J. Am. Ceram. Soc., 44, 120-127.

Irving, E., Park, J. K., Haggerty, S. E., Aumento, F., and B. Loncarevic (1970), Magnetism and opaque mineralogy of basalts from the Mid-Atlantic Ridge at 45°N: Nature, 228, 974-976.

Jacobs, I. S., Bayerlein, R. A., Foner, S. and J. P. Remeika (1971), Field induced magnetic phase transitions in anti-ferromagnetic hematite (α-Fe_2O_3): Int. J. Magn., 1, 193-208.

Jensen, S. D. and P. N. Shive (1973), Cation distribution in sintered titanomagnetites: J. Geophys. Res., 78, 8474-8480.

Johnson, H. P. (in press), Opaque mineralogy of the igneous rock samples from hole 395A-DSDP Leg 45: Initial Reports of the Deep Sea Drilling Project, 45, U.S. Government Printing Office, Washington, D.C.

Johnson, H. P. and R. T. Merrill (1972), Magnetic and mineralogical changes associated with low-temperature oxidation of magnetite: J. Geophys. Res., 77, 334-341.

Johnson, H. P. and R. T. Merrill (1973), Low temperature oxidation of titanomagnetite and the implications for paleomagnetism: J. Geophys. Res., 78, 4938-4949.

Johnson, H. P. and R. T. Merrill (1975), Low temperature oxidation of single-domain magnetite: J. Geophys. Res., 79, 5533-

Johnson, H. P. and T. M. Atwater (1977), A magnetic study of basalts from the Mid-Atlantic Ridge at 37°N: Bull. Geol. Soc. Am., 88, 637-647.

Karkhanavala, M. D., Momin, A. C. and S. G. Rege (1959), An X-ray of leucoxene from Quilon India: Econ. Geol., 54, 913-918.

Katsura, T. and I. Kushiro (1961), Titanomaghemite in igneous rocks: Am. Mineral., 46, 134-145.

Kennedy, G. C. (1955), Some aspects of the role of water in rock melts: Geol. Soc. America, special paper, 62, 489-504.

Kerr, P. E. (1955), Hydrothermal alteration and weathering: Geol. Soc. America, special paper, 62, 525-544.

Krause, D. C. and N. D. Watkins (1970), North Atlantic crustal genesis in the vicinity of the Azores: Geophys. J. R. Astr. Soc., 19, 261-283.

Kretz, R. (1961), Some applications of thermodynamics to coexisting minerals of variable composition; example orthopyroxene-clinopyroxene and orthopyroxene-garnet: J. Geol., 69, 361-387.

Larson, E. E. and D. W. Strangway (1966), Magnetic polarity and igneous petrology: Nature, 212, 756-

Larson, E. E., Ozima, M., Nagata, T. and D. W. Strangway (1966), Studies concerning the stability of remanent magnetization of a variety of rocks: Trans. AGU, 47, 69.

Lawley, E. A. and J. M. Ade-Hall (1971), A detailed magnetic and opaque petrological study of thick palaeogene tholeiite lava flow from northern Ireland: Earth Planet. Sci. Lett., 11, 113-120.

Lawrence, J. R. and S. Maxwell (in preparation), Geothermal exploration in the Azores: O^{18}/O^{16} in calutes from volcanics.

Lepichon, X. (1968), Sea-floor spreading and continental drift: J. Geophys. Res., 73, 3661-3697.

Lepp, H. (1957), Stages in the oxidation of magnetite: Am. Mineral., 42, 679-681.

Lerz, H. (1968), Hydrothermal paragenesis of anatase, brookite and rutile of Dorfer Keesfleck, prägraten, eastern Tirol: Neues Jahrb. Mineral. Mh., 414-420.

Lind, M. D. and R. M. Housley (1972), Crystallization studies of Lunar igneous rocks: crystal structures of synthetic armalcolite: Science 175, 521-523.

Lindh, A. (1972), A hydrothermal investigation of the system $FeO-Fe_2O_3$, TiO_2: Lithos, 5, 325-343.

Lindsley, D. H. (1962), Investigations in the system $FeO-Fe_2O_3-TiO_2$: Carnegie Inst. of Washington, Year Book, 61, 100-106.

Lindsley, D. H. (1965), Iron-titanium oxides: Carnegie Inst. Washington, Year Book, 64, 144-148.

Lindsley, D. H. (1973), Delimitation of the hematite-ilmenite miscibility gab: Geol. Soc. Am. Bull., 84, 657-661.

Lindsley, D. H. and A. Lindh (1974), A hydrothermal investigation of the system $FeO-Fe_2O_3$, TiO_2: a discussion with new data: Lithos, 7, 65-68.

Lowrie, W. (1977), Intensity and direction of magnetization in oceanic basalts: J. Geol. Soc., 133, 61-82.

Lynd, L. E., Sigurdson, H., North, C. H. and W. W. Anderson (1954), Characteristics of titaniferous concentrates: Mining Eng., 6, 817-824.

Machado, F. (1959), Submarine pits of the Azores plateau: Bull. Volcano., 2e sér., tome 21, 109-116.

Machado, F. (1967), Active volcanoes of the Azores: catalogue of the active volcanoes of the world, part 21, 7-52, Int. Ass. Volcano., Rome.

Machado, F. (1969), Sobre a tectónica do Atlântico Norte a oeste de Portugal: Rev. Fac. Ciên. Lisbon, 2a Sér. C, 16, 1-14.

Machado, F. (1972), Acid volcanoes of São Miguel, Azores: Bull. Volcano., 36, 319-327.

Machado, F. (1974), The search for magmatic reservoirs: In, L. Civetta, Gasparina, P., Luongo, G. and A. Rapolla, eds., Physical volcanology. Elsevier, Amsterdam, 255-273.

Machado, F., Quintino, J. and J. H. Monteiro (1972), Geology of the Azores and the mid-Atlantic rift: Proc. 24th Int. Geol. Congr. Montreal, 3, 134-142.

Maclean, W. H. (1977), Sulfides in the core from Leg 37 drill holes: In, F. Aumento and W. G. Melson, et al., Initial Reports of the Deep Sea Drilling Project, 37, 875-881, U.S. Government Printing Office, Washington, D. C.

Marshall, M. and A. Cox (1971a), Effect of oxidation on the natural remanent magnetization of titanomagnetite in suboceanic basalt: Nature, 230, 28-

Marshall, M. and A. Cox (1971b), Magnetism of pillow basalts and their petrology: Geol. Soc. Am. Bull., 82, 537-

McElhinny, M. W. (1973), Paleomagnetism and Plate Tectonics: Cambridge University Press, New York,

McGraw, P. A. (1976), A petrological/geochemical study of rocks from the São Miguel drill hole, São Miguel, Azores: M.Sc. thesis, Dalhousie University, Halifax, Canada.

McKenzie, D. (1972), Active tectonics of the Mediterranean region: Geophys. J. R. Astr. Soc., 30, 109-186.

Merrill, R. T. (1975), Magnetic effects associated with chemical changes in igneous rocks: Geophys. Surv., 2, 277-311.

Mitchell, R. H. and D. B. Clarke (1976), Oxide and sulphide mineralogy of the Peuyuk Kimberlite, Somerset Island, N.W.T., Canada: Contrib. Mineral. Petrol., 56, 157-172.

Mitchell, W. S., Zentilli, M. and K. A. Taylor (1977). Distribution of uranium in an active geothermal area in the Azores: Geol. Surv. Canada (in press).

Moore, J. G. and B. P. Fabbi (1971), An estimate of the juvenile sulfur content of basalt: Contr. Min. Petr., 33, 118-127.

Morgan, W. J. (1971), Correction plumes in the lower mantle: Nature, 230, 42-43.

Morgan, W. J. (1972), Deep mantle convection plumes and plate motions: Bull. Am. Assoc. Pet. Geol., 56, 203-

Muecke, G. K., Ade-Hall, J. M., Aumento, F., MacDonald, A., Reynolds, P. H., Hyndman, R. D., Quintino, J., Opdyke, N. and W. Lowrie (1974), Deep drilling in an active geothermal area in the Azores: Nature, 252, 281-285.

Nagata, T. (1961), Rock Magnetism, revised ed.: Maruzen Co., Ltd., Tokyo, 350 p.

Nicholls, G. D. (1955), The mineralogy of rock magnetism: Adv. phys., 4, 113-190.

O'Donovan, J. B. and W. O'Reilly (1977a), Range of non-stoichiometry and characteristic properties of the products of laboratory maghemitization: Earth Planet. Sci. Lett., 34, 291-299.

O'Reilly, W. (1976), Magnetic minerals in the crust of the Earth: Rep. prog. phys., 39, 857-908.

O'Reilly, W. and S. K. Banerjee (1966), Oxidation of titanomagnetites and self-reversal: Nature (London), 211, 26-28.

Osborn, E. F. (1959), Role of oxygen pressure in the crystallization and differentiation of basaltic magma: Am. J. Sci., 257, 609-647.

Oshima, O. (1971). Compositional variation of magnetite during the eruption and its bearing on the stage of crystallization of magma of Futatsu-Dake, Haruna Volcano: Mineral. J., 6, 249-263.

Otteman, J. and G. Frenzel (1965), Der Chemismus der pseudobrookite van Vulkaniten (Eine Untersuchung mit der Elektronen-Mikrosonde): Schweiz. Mineral. pet. Mitt., 45, 819-836.

Ozima, M. and E. E. Larson (1968), Study of self-reversals of TRM in some submarine basalts: J. Geomag. Geoelectr., 20, 337-351.

Ozima, M. and N. Sakamoto (1971), Magnetic properties of synthesized titanomaghemite: J. Geophys. Res., 76, 7035-7046.

Ozima, M., Joshima, M. and H. Kinoshita (1974), Magnetic properties of submarine basalts and the implication on the structure of the oceanic crust: J. Geomag. Geoelectr., 26, 335-354.

Peck, D. L., Wright, T. L. and J. G. Moore (1966), Crystallization of tholeiitic basalt, Alae lava lake, Hawaii: Bull. Volcan., 29, 629-656.

Peterson, N. and O. Bleil (1973), Self-reversal of remanent magnetization in synthetic titanomagnetite: Z. Geophys., 39, 965-

Pillar, H. (1972), Performance of reflectance standards: Min. Materials News Bull. for Quant. Micr. Methods, 4.

Prévot, M. and J. Mergoil (1973), Crystallization trend of titanomagnetites in an alkali basalt from Saint-Clement (Massif Central, France): Mineral. Mag., 39, 474-481.

Prévot, M., Rémond, G. and R. Caye (1968), Étude de la transformation d'une titanomagnétite en titanomaghémite dans une roche volcanique: Bull. Soc. Franc. Mineral. Cristallogr., 91, 65-74.

Quintino, J. (1962a), Levantamento geomagnético da ilha de S. Miguel (Açores): RT 638, GEO 19, Serv. Meteor. Nac., Lisbon.

Quintino, J. and F. Machado (1977), Heat flow and the Mid-Atlantic rift volcanism of São Miguel Island, Azores: Tectonophysics, 41, 173-179.

Ramdohr, P. (1926), Beobachtungen an magnetit, ilmenit, eisenglanz und überlegungen über das system FeO-Fe_2O_3-TiO_2: Neues Jahrb. Beil. Bd. 54, 320-379.

Ramdohr, P. (1953), Ulvöspinel and its importance in titanium-rich magmatic iron deposits: Econ. Geol., 48, 677-688.

Ramdohr, P. (1969), The ore minerals and their intergrowths: Permagon Press, Oxford, 1174 pp.

Readman, P. W. and W. O'Reilly (1970), The synthesis and inversion of non-stoichiometric titanomagnetites: Phys. Earth Planet. Inter., 4, 121-128.

Readman, P. W. and W. O'Reilly (1972), Magnetic properties of oxidized (cation deficient) titanomagnetite $(Fe,Ti,\square)_3O_4$: J. Geomag. Geoelect., 24, 69-90.

Rehwald, G. (1966). The application of ore-microscopy in benefication of ores of the precious metals and of the non-ferrous metals: In, Applied Ore Microscopy, H. Freund, 441-537, MacMillan Company.

Ridley, W. I., Watkins, N. D. and D. J. MacFarlane (1974), The oceanic islands: Azores: In, The Ocean Basins and Margins, Vol. 1: The North Atlantic:, Narin, A.E.M. and F. G. Stehli, Eds., Plenum Press, N.Y., 445-483.

Roy, S. (1954), Ore microscopic studies of the Vanadium-bearing titaniferous iron ores of Mayurbhanj with a detailed note on their texture: Nat. Inst. Sci. India, Proc. 20, 691-702.

Rucklidge, J. C. (1967), A computer program for processing microprobe data: J. Geol., 75, 126.

Rumble, D., III (1971), Thermodynamic analysis of phase equilibria in the system Fe_2TiO_4-Fe_3O_4-TiO_2: Carnegie Inst. Washington, Year Book 69, 198-207.

Rumble, D., III (1972), Fe-Ti oxide minerals and the behaviour of oxygen during metamorphism: Carnegie Inst. Washington, Year Book, 157-165.

Ryall, P. J. C. (1974), A comparison between natural and laboratory oxidation of titanomagnetite in pillow lavas: Ph.D. thesis, Dalhousie University, Halifax, Canada.

Ryall, P. J. C. and J. M. Ade-Hall (1975), Laboratory-induced self reversal of thermoremanent magnetizatio in pillow basalts: Nature, 257, 117-118.

Ryall, P. J. C., Hall, J. M., Clark, J. and T. Milligan (1977), Magnetization of oceanic crustal layer 2--results and thoughts after DSDP Leg 37: Can. J. Earth Sci., 14, 684-706.

Sakamoto, N., Ince, P. I. and W. O'Reilly (1968), Effect of wet grinding on oxidation of titanomagnetites: Geophys. J. R. Astr. Soc., 15, 509-515.

Sarkar, P. K. (1976), Report on project secondary minerals in the drill core, in the active geothermal area, Ribeira Grande, São Miguel, Azores: Dept. of Geology, Dalhousie University, Halifax, Canada.

Sato, M. and T. L. Wright (1966), Oxygen fugacities directly measured in magnetic gases: Science, 153, 1103-1105.

Schilling, J. G. (1975), Azores mantle blob: Rare-earth evidence: Earth Planet. Sci. Lett., 25, 103-115.

Schmidt, E. R. and F. H. S. Vermaas (1955), Differential thermal analysis and cell dimensions of some natural magnetites: Am. Mineral., 40, 422-431.

Schmincke, H. U. (1973), Magmatic evolution and tectonic regime in the Canary, Madeira and Azores Island groups: Bull. Geol. Soc. Am., 84, 633-648.

Schmincke, H. U. and M. Weibel (1972), Chemical study of rocks from Madeira, Porto Santo, São Miguel and Terceira: Neues Jahrb. Mineral. Abh., 117, 253-281.

Schneiderhöhn, H. (1952), Erzmikroskopisches praktikum: Stuttgart, 274 p.

Schröder, A. (1928), X-ray investigation of the structure of brookite and the physical properties of the three titanium dioxides: Kristallogr., 66, 493-494.

Schwartz, E. J. and D. J. Vaughan (1972), Magnetic phase relations of pyrrhotite: J. Geomag. Geoelectr., 24, 441-458.

Schwartz, G. M. (1951), Classification and definitions of textures and mineral structures in ores: Econ. Geol., 46, 578-591.

Scientific Party (1973), Core Log for the Azores drillhole: Dalhousie University, Halifax, Canada.

Shannon, R. D. (1964), Phase transformation studies in TiO_2 supporting different defect mechanisms in vacuum-reduced and hydrogen-reduced rutile: J. Appl. Phys., 35, 3414-3416.

Shannon, R. D. and J. A. Pask (1964), Topotaxy in the anatase-rutile transformation: Am. Mineral., 49, 1707-1717.

Skinner, B. J. and D. L. Peck (1969), An immiscible sulfide melt from Hawaii: In, magmatic ore deposits, a symposium, Ed. H. D. B. Wilson: Econ. Geol., 4, 310-322.

Smith, B. M. and M. Prévot (1977), Variation of the magnetic properties in a basaltic dyke with concentric cooling zones: Phy. Earth Plan. Interiors, 14, 120-136.

Smith, P. J. (1967), The intensity of Tertiary geomagnetic field: Geophys. J. R. Astr. Soc., 12, 239-258.

Smith, P. J. (1968), Paleomagnetism and the composition of highly oxidized iron-titanium oxides in basalts: Phys. Earth. Planet. Int., 1, 88-92.

Stacey, F. D. and S. K. Banerjee (1974), The physical properties of Rock Magnetism: Elsevier, Amsterdam, vi + 195 p.

Stephenson, A. (1969), The temperature dependent cation distribution in titanomagnetites: Geophys. J. R. Astr. Soc., 18, 199-210.

Strangway, D. W., Honea, R. M., McMahon, B. E. and E. E. Larson (1968a), The magnetic properties of naturally occurring geothite: Geophys. J. R. Astr. Soc., 5, 345-359.

Strangway, D. W., Larson, E. E. and M. Goldstein (1968b), A possible cause of high magnetic stability in volcanic rocks: J. Geophys. Res., 73, 3787-3796.

Tarling, D. H. (1971), Principles and Applications of Palaeomagnetism: Chapman and Hall Ltd., London, 164 p.

Taylor, R. W. (1961), An experimental study of the system $FeO-Fe_2O_3-TiO_2$ and its bearing on mineralogical problems: Ph.D. thesis, Pennsylvania State University.

Taylor, R. W. (1963), Liquidus temperatures in the system $FeO-Fe_2O_3-TiO_2$, J. Am. Ceram. Soc., 46, 276-279.

Taylor, R. W. (1964), Phase equilibria in the system $FeO-Fe_2O_3-TiO_2$ at 1300°C: Am. Mineral. 49, 1016-1030.

Temple, A. K. (1966), Alteration of ilmenite: Econ. Geol., 61, 695-714.

Teufer, G. and A. K. Temple (1966), Pseudorutile--a new mineral intermediate between ilmenite and rutile in the natural alteration of ilmenite: Nature, 211, 179-181.

Thompson, R. N. (1976), Chemistry of ilmenites crystallized within the anhydrous melting range of a tholeiitic andesite at pressures between 5 and 26 kb: Min. Mag., 40, 857-862.

Uyeda, S. (1958), Thermoremanent magnetism as a medium of palaeomagnetism with special reference to reverse thermoremanent magnetism: Jap. J. Geophys., 2, 1-23.

Verhoogen, J. (1956), Ionic ordering and self-reversal in impure magnetite: J. Geophys. Res., 64, 2441-

Verhoogen, J. (1962), Distribution of titanium between silicates and oxides in igneous rocks: Am. J. Sci., 260, 211-220.

Verhoogen, J. (1962), Oxidation of iron-titanium oxides in igneous rocks: J. Geol., 70, 168-181.

Verwey, E. J. W. (1935), The crystal structure of γ- Fe_2O_3 and γ-Al_2O_3: Z. Kristallogr., 91, 65-69.

Vincent, E. A. (1960), Ulvöspinel in the Skaergaard intrusion, Greenland: Neues Jahrb. Mineral., Abh., 94, 993-1016.

Vincent, E. A. and R. Phillips (1954), Iron-titanium oxide minerals in layered gabbros of the Skaergaard intrusion, East Greenland, Part 1. Chemistry and ore-microscopy: Geochim. Cosmochim. Acta 6, 1-26.

Vincent, E. A., Wright, J. B., Chevallier, R. and A. Mathieu (1957), Heating experiments on some natural titaniferous magnetites: Mineral. Mag., London, 31, 624-655.

Walenta, K. (1960), Natürliches Eisen (II)--oxyd (Wüstit) aus der Vulkanischen tuffbreccie von Scharnhausen bei stuttgart: Neues Jahrb. Mineral. Mh., 151-159.

Watkins, N. D. and S. E. Haggerty (1965), Some magnetic properties and the possible petrogenic significance of oxidized zones in an Icelandic olivine basalt: Nature, 206, 797-800.

Watkins, N. D. and S. E. Haggerty (1967), Primary oxidation variation and petrogenesis in a single lava: Contrib. Mineral. Petrol., 15, 251-271.

Watkins, N. D. and S. E. Haggerty (1968), Oxidation and magnetic polarity in single Icelandic lavas and dykes: Geophys. J. R. Astr. Soc., 15, 305-

Webster, A. H. and N. F. H. Bright (1961), The system iron-titanium-oxygen at 1200°C and oxygen partial pressures between 1 atm and 2×10^{-14} atm: J. Am. Ceram. Soc., 44, 110-116.

Wilson, H. D. B. (1953), Geology and Geochemistry of base metal deposits: Econ. Geol., 48, 370-407.

Wilson, R. L. (1966), Further correlations between the petrology and the natural magnetic polarity of basalts: Geophys. J. R. Astr. Soc., 10, 413-

Wilson, R. L. and S. E. Haggerty (1966), Reversals of the earth's magnetic field: Endeavor, 25, 104-109.

Wilson, R. L. and N. D. Watkins (1967), Correlation of petrology and natural magnetic polarity in Columbia plateau basalts: Geophys. J. R. Astr. Soc., 12, 405-

Wilson, R. L., Haggerty, S. E. and N. D. Watkins (1968), Variation of paleomagnetic stability and other parameters in a vertical traverse of a single Icelandic lava: Geophys. J. R. Astr. Soc., 16, 79-96.

Wood, D. A., Gibson, I. L. and R. N. Thompson (1976), Elemental mobility during zeolite facies metamorphism of the Tertiary basalts of eastern Iceland: Contrib. Mineral. Petrol., 55, 241-254.

Wright, J. B. (1961), Solid-solution relationships in some titaniferous iron oxide ores of basic igneous rocks: Mineral. Mag., 36, 778-789.

Wright, J. B. (1967), The iron-titanium oxides of some Dunedin (New Zealand) lavas, in relation to their palaeomagnetic and thermomagnetic character (with an appendix on associated chromiferous spinel): Mineral. Mag., 36, 425.

Wright, J. B. and J. F. Lovering (1965), Electron probe microanalysis of the iron-titanium oxides in some New Zealand iron sands: Min. Mag., 35, 604-621.

Wright, T. L. and P. W. Weiblen (1967), Mineral composition and paragenesis in tholeiitic basalt from Makaopuhi lava lake, Hawaii: Abs. Geol. Soc. Am. Ann. Meeting, New Orleans, 242-243.

Yoder, H. S., Jr. (1955), Role of water in metamorphism: Geol. Soc. America, special paper, 62, 505-524.

Plate 1

Figure a: Reichert Zetopan reflected light microscope with micro-photometer

Figure b: Ultraphot II Carl Zeiss microscope

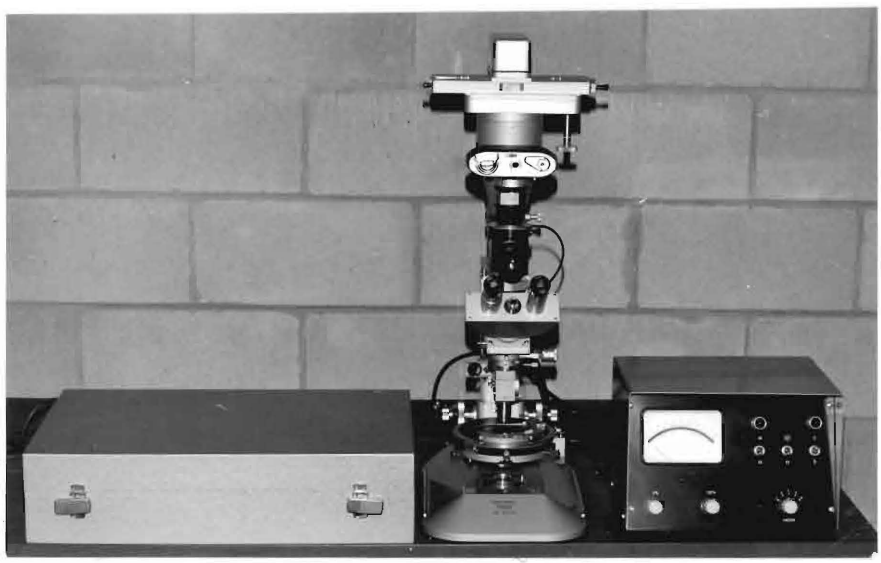

a

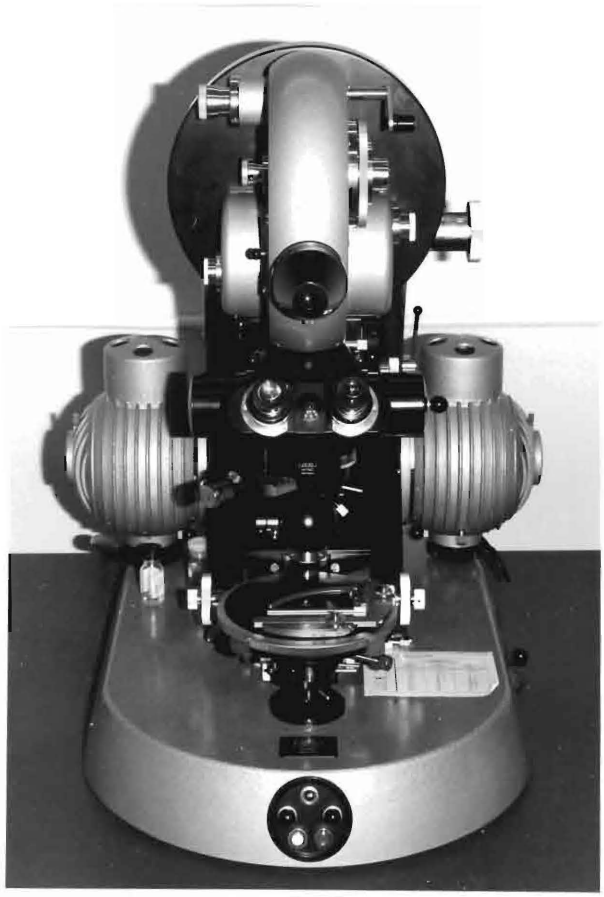

b

Plate 2

Typical forms of Fe-Ti oxides. Scale bars for photos on all plates are 20 μ except for photos with focus ring (microphotometer) where scale bar is 25 μ

Figure a: Coarse-subhedral titanomagnetite type 1

Figure b: Fine and medium subhedral to anhedral grains of titanomagnetite type 2

Figure c: Skeletal titanomagnetite type 3

Figure d: Coarse grained titanomagnetite showing peripheral corrosion. Showing also the aperture diaphragm of the microphotometer

Figure e: Equidimensional type 1 ilmenite (light grey) and Geikelite (dark grey)

Figure f: Elongated grain of type 2 ilmenite.

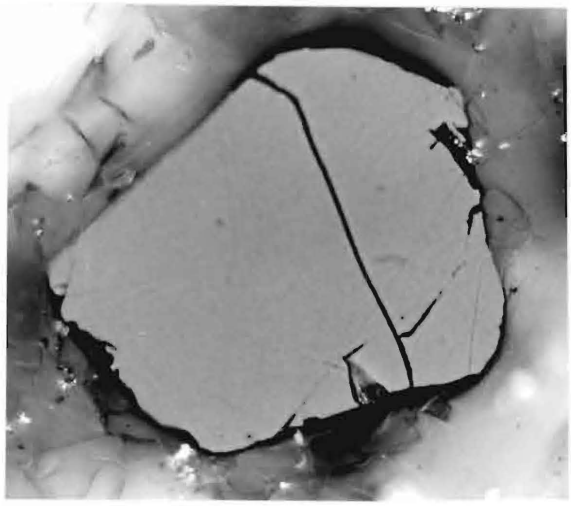

a

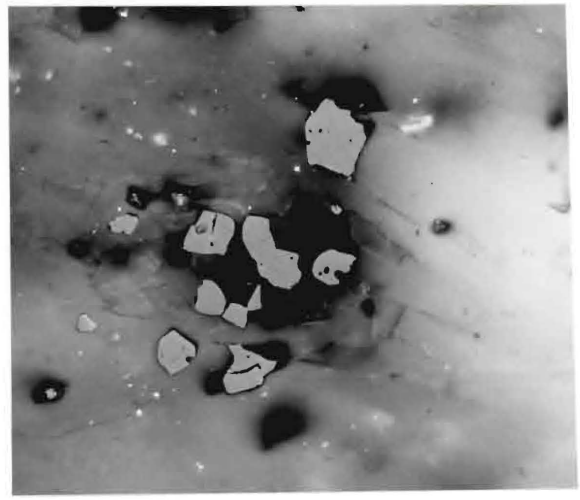

b

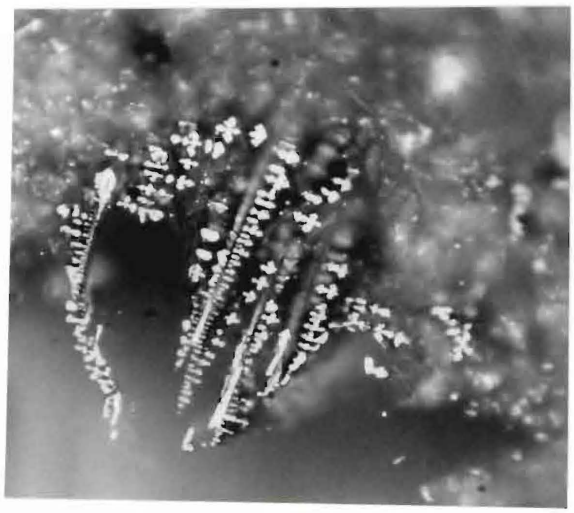

c

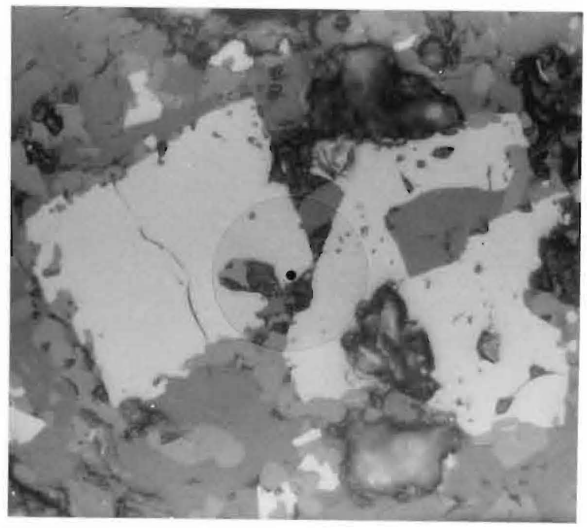

d

25 μ

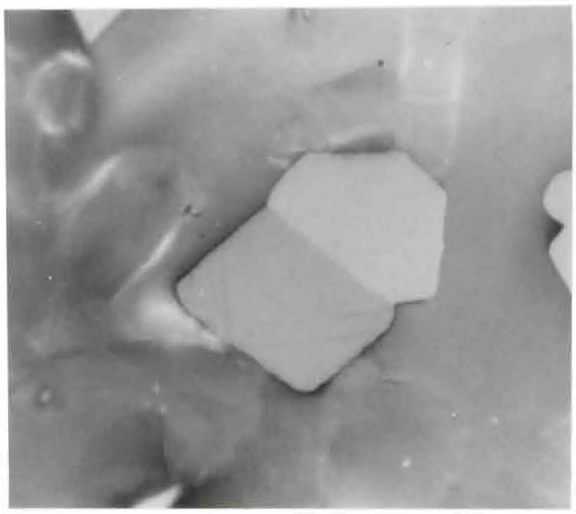

e

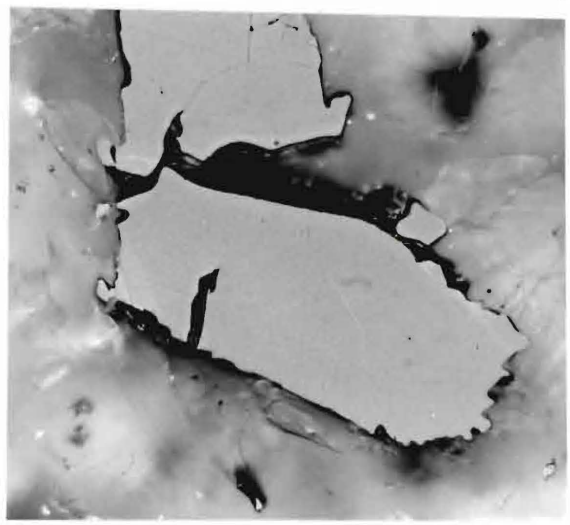

f

20 μ

Plate 3

Structure and texture of Fe-Ti oxides and sulfides

Figure a: Spinel with primary zoning. The lighter grey outer mantle is enriched in Fe^{3+} and Ti.

Figure b: Oscillatory zoning in spinel.

Figure c: Pyrrhotite (white) and titanomagnetite (dark grey).

Figure d: Radial growth grain of lepidocrocite

Figure e: Spheroidal grain of pyrrhotite (white) in coarse grain titanomagnetite (grey).

Figure f: Zoning in spinel. The central zone is enriched in Fe^{3+} and Ti.

Figure g: Epitaxial overgrowth in spinel. The dark central zone is enriched in Fe^{2+}, Cr and Al; the lighter grey outer mantle is enriched in Fe^{3+} and Ti.

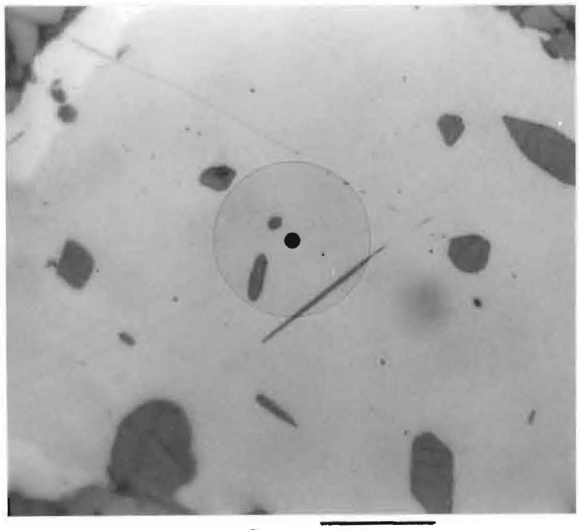

a 25 μ

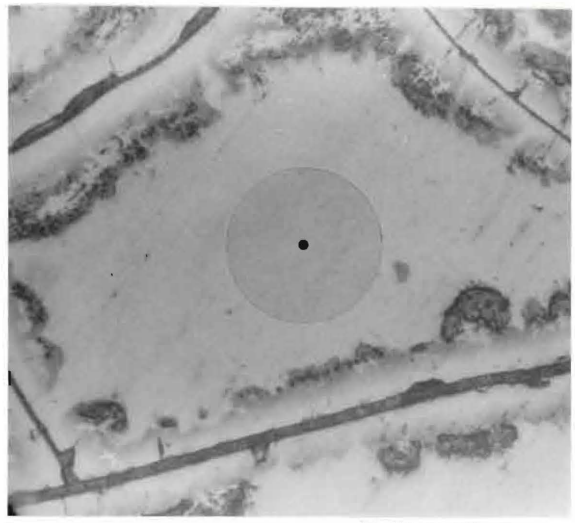

b 25 μ

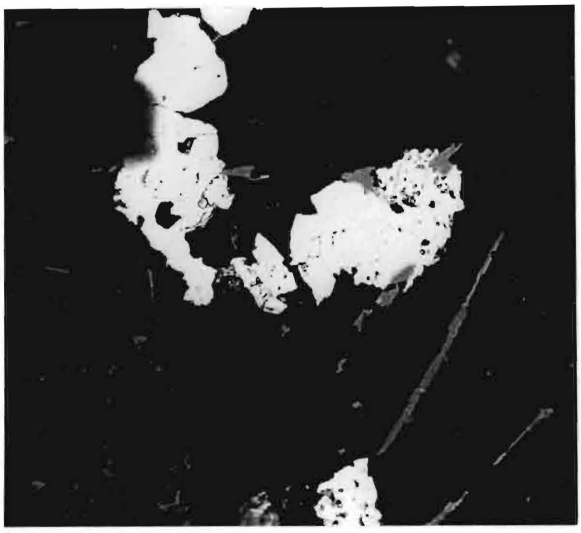

c

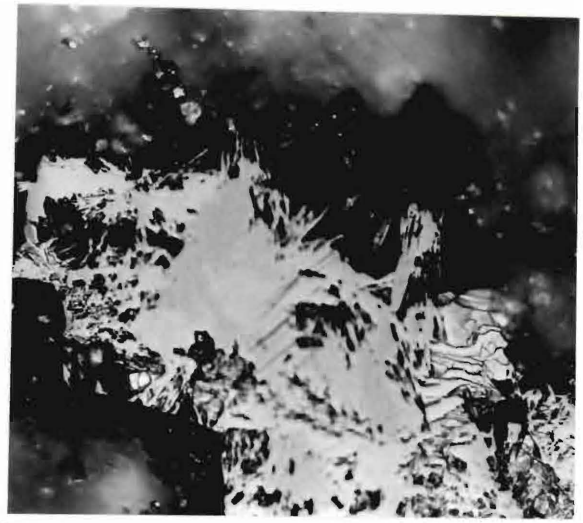

d

20 μ

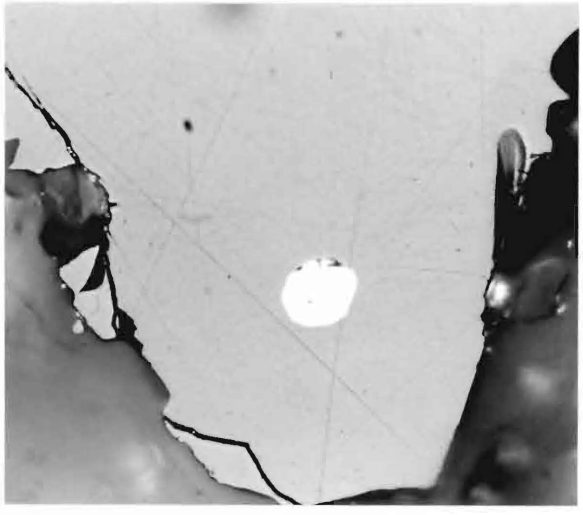

e

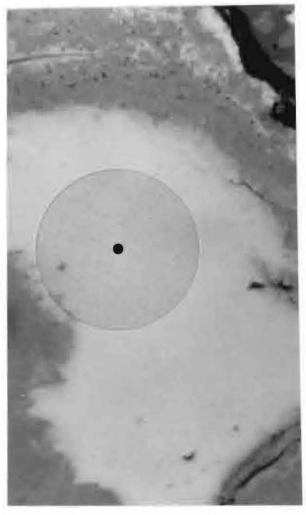

25 μ f

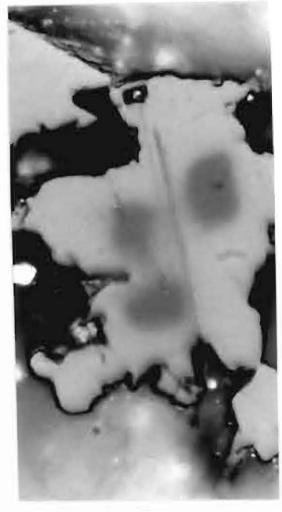

g

Plate 4

Texture of Fe-Ti oxides

Figure a: Fine lamellae of ilmenite in titanomagnetite

Figure b: Black rods (spinel) in magnetite (grey). The light grey is titanomagnetite.

Figure c: Complex texture of titanomagnetite. Grey are rutile lamellae in titanohematite (light grey). The dark grey is magnetite containing spinel rods.

Figure d: Decomposition of olivine. White is magnetite.

Figure e: Replacement in spinel by a chloritic mineral.

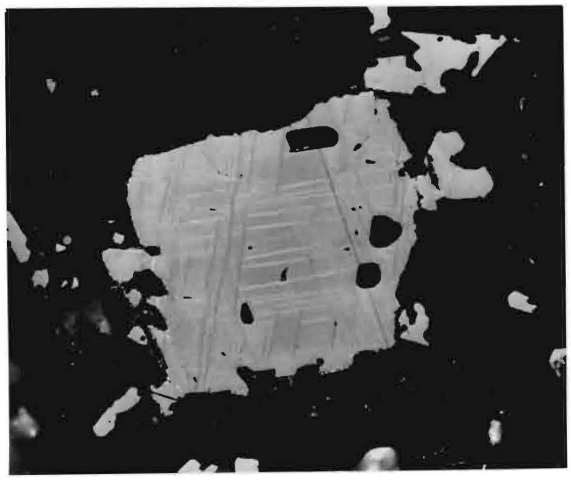

a

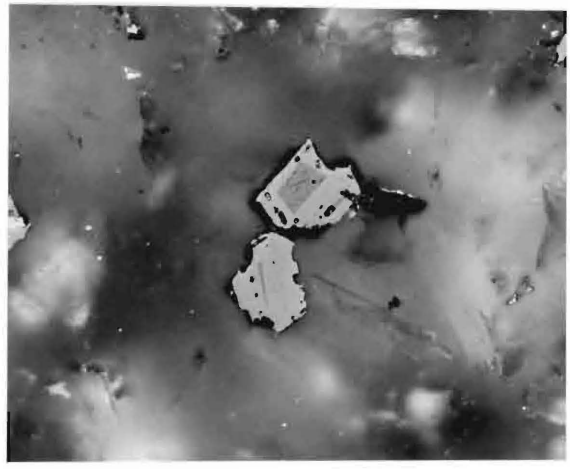

b

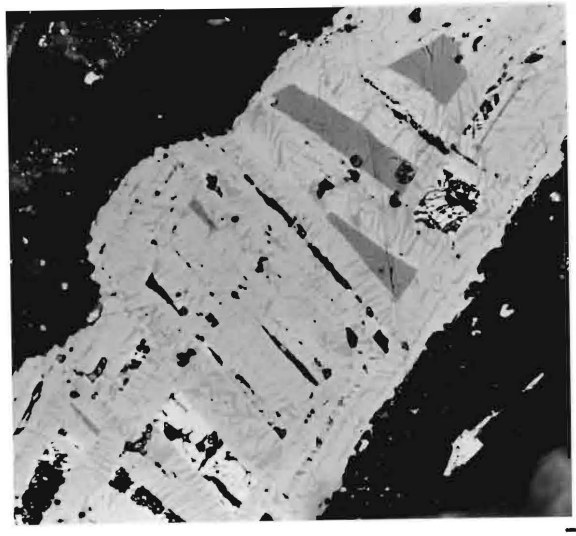

c

20 μ

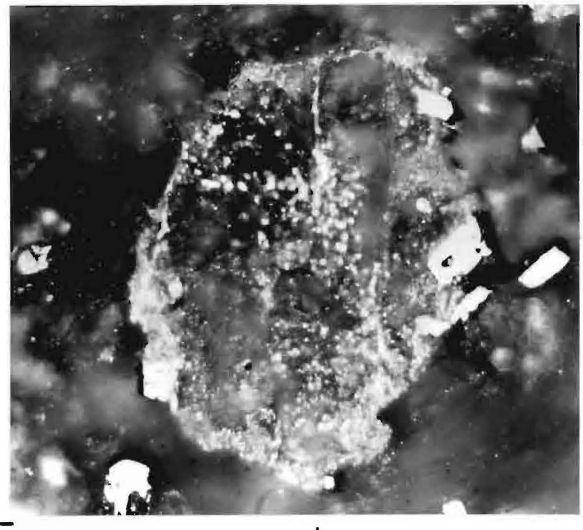

d

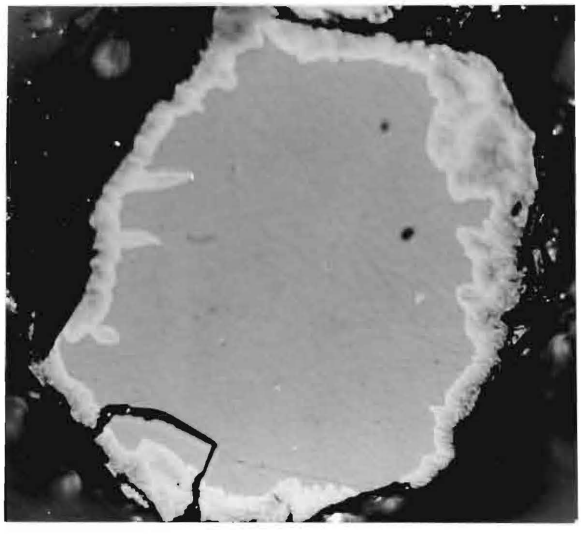

e

Plate 5

High temperature oxidation (deuteric) of titanomagnetite

Figure a: Class 2 titanomagnetite. Ilmenite lamellae (grey) in titanomagnetite (light grey).

Figure b: Class 3 titanomagnetite. Ilmenite lamellae (light grey) are more than 50% of titanomagnetite area.

Figure c: Class 4 titanomagnetite. Ilmenite lamellae are mottled and fine rutiles are developed in titanohematite. The host magnetite (dark grey) contains abundant spinel lamellae.

Figure d: Class 5 titanomagnetite. Lenses of rutile (dark grey) in titanohematite (light grey).

Figure e: Class 6 titanomagnetite: Pseudobrookite (dark grey) in titanohematite (off white).

Figure f: Class 4 in skeletal titanomagnetite.

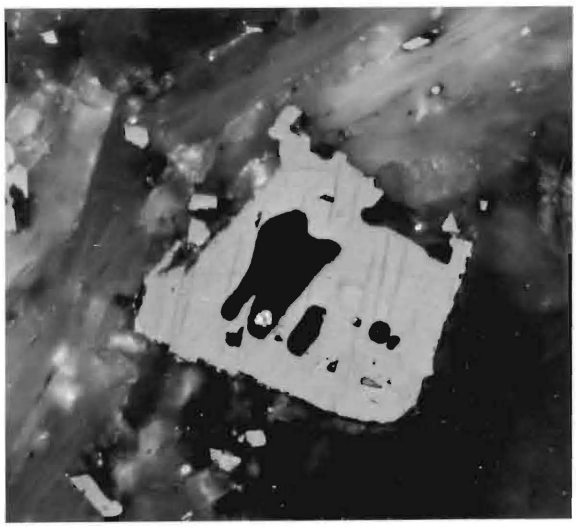

a

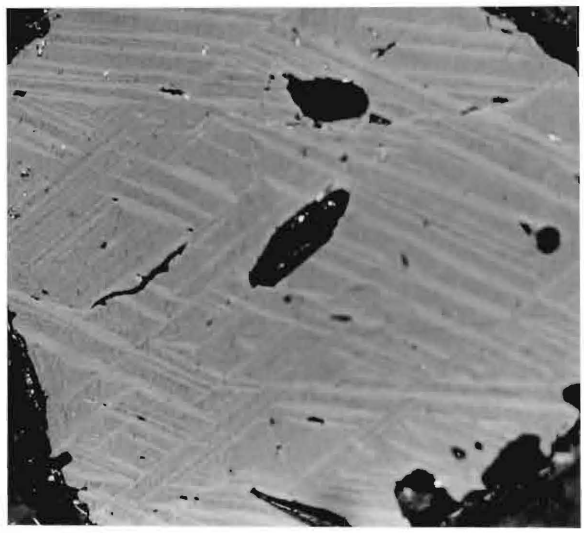

b

c

20 μ

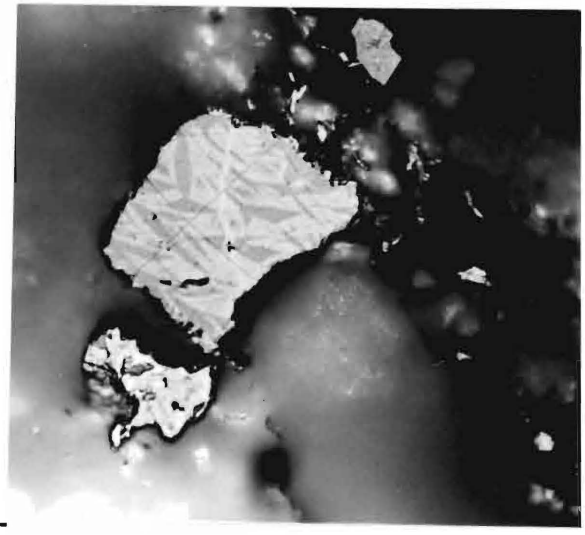

d

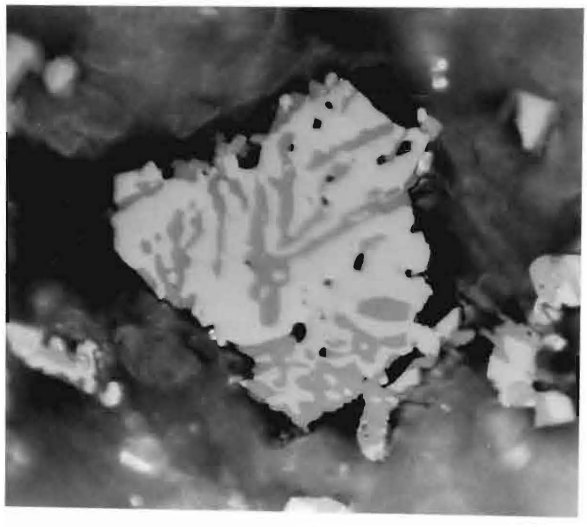

e

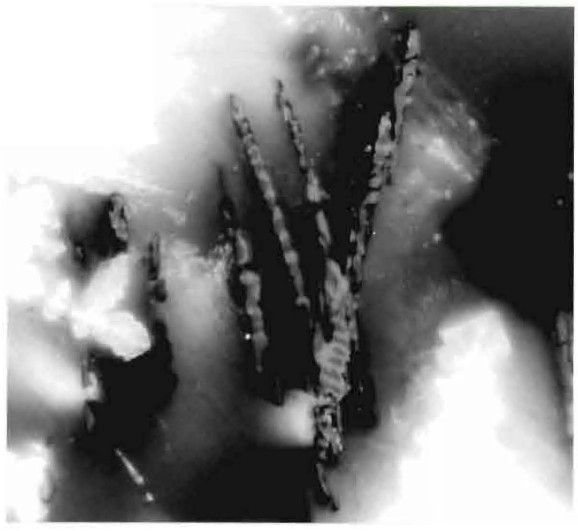

f

Plate 6

High temperature (deuteric) oxidation of ilmenite

Figure a: Class 1 ilmenite

Figure b: Class 2 ilmenite. Crichtonite (white) in ferri-ilmenite.

Figure c: Class 3 ilmenite. Crichtonite + ferri-ilmenite (white) in titanohematite + rutile (grey).

Figure d: Class 4 ilmenite. Rutile lamellae in titanohematite.

Figure e: Class 5 ilmenite. Pseudobrookite (dark grey) in titanohematite + rutile (off white).

Figure f: Class 6 ilmenite. Pseudobrookite (dark grey). Some titanohematite remains (off white).

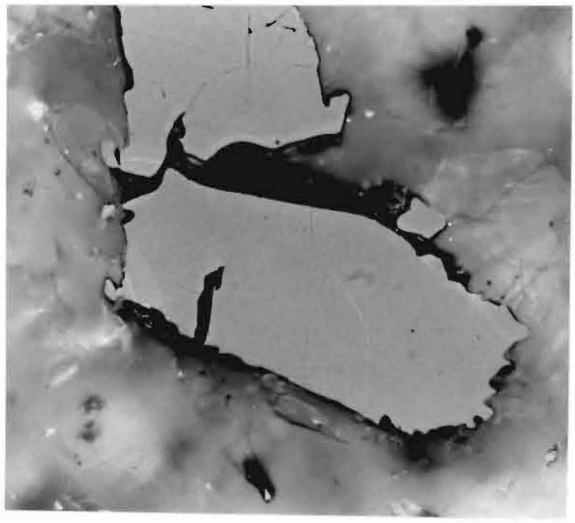

a

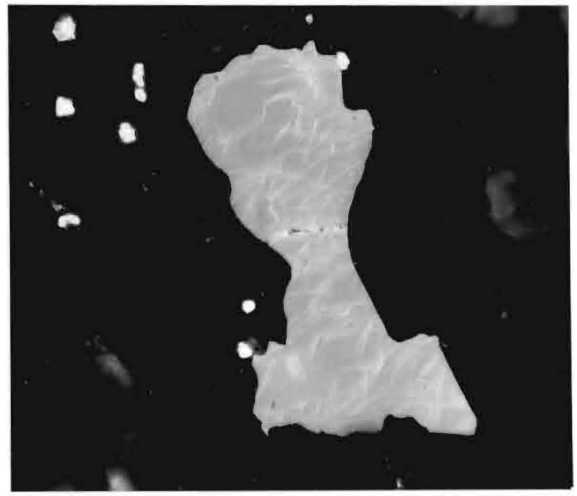

b

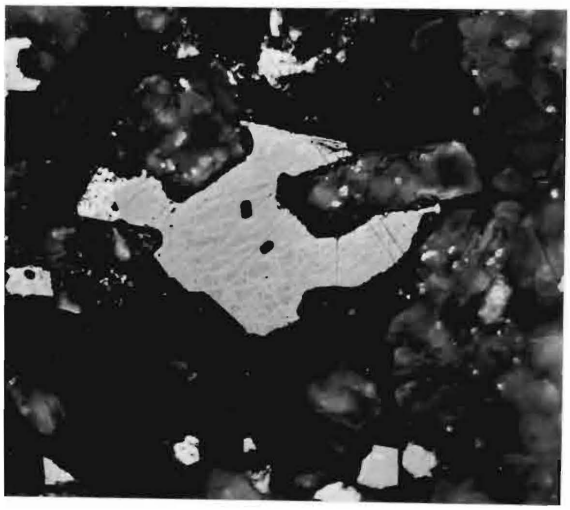

c

20 μ

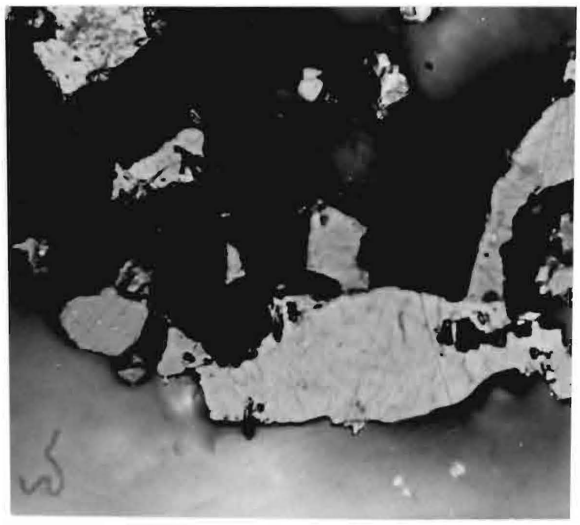

d

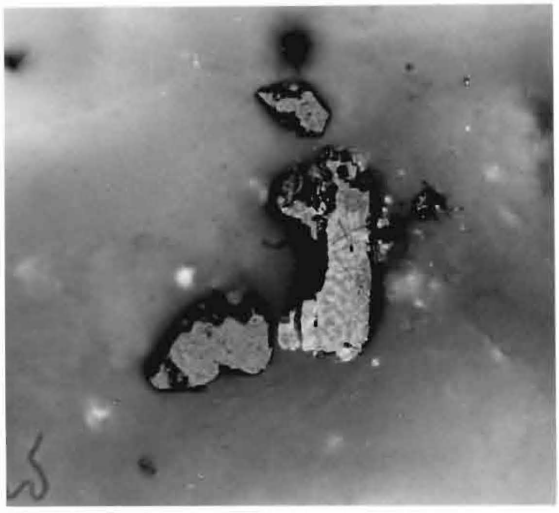

e

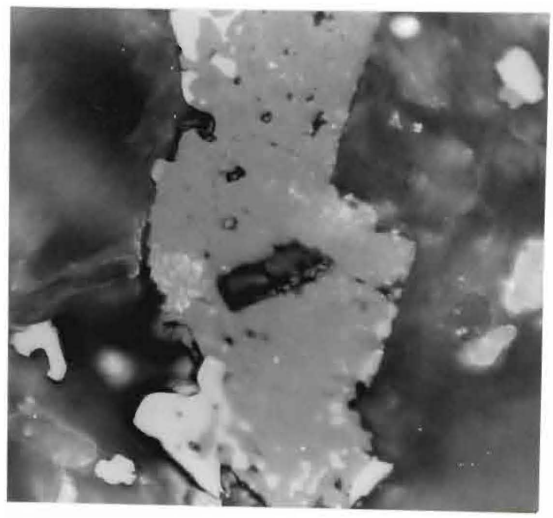

f

Plate 7

Low degree hydrothermal alteration of titanomagnetite

Figure a: Class L_1 titanomagnetite. Homogeneous titanomagnetite.

Figure b: Class L_2 titanomagnetite. Lines of titanomaghemite (off white) in titanomagnetite (grey).

Figure c: Class L_3 titanomagnetite. Patches of titanomaghemite (off white) in titanomagnetite (grey).

Figure d: Class L_4 titanomagnetite. Titanomaghemite (off white) occupys more than 50% of titanomagnetite (grey) area.

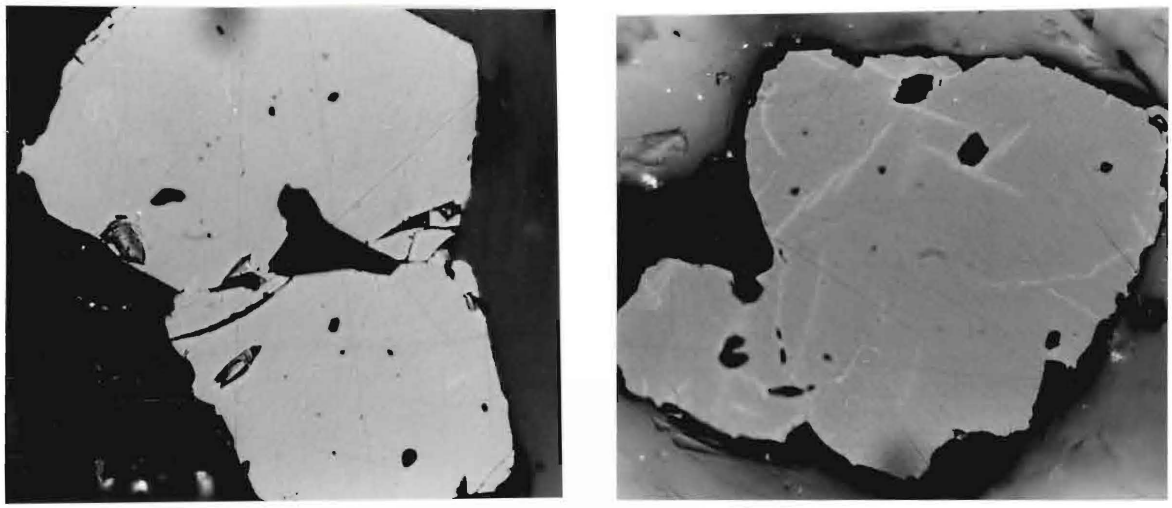

a

20 μ

b

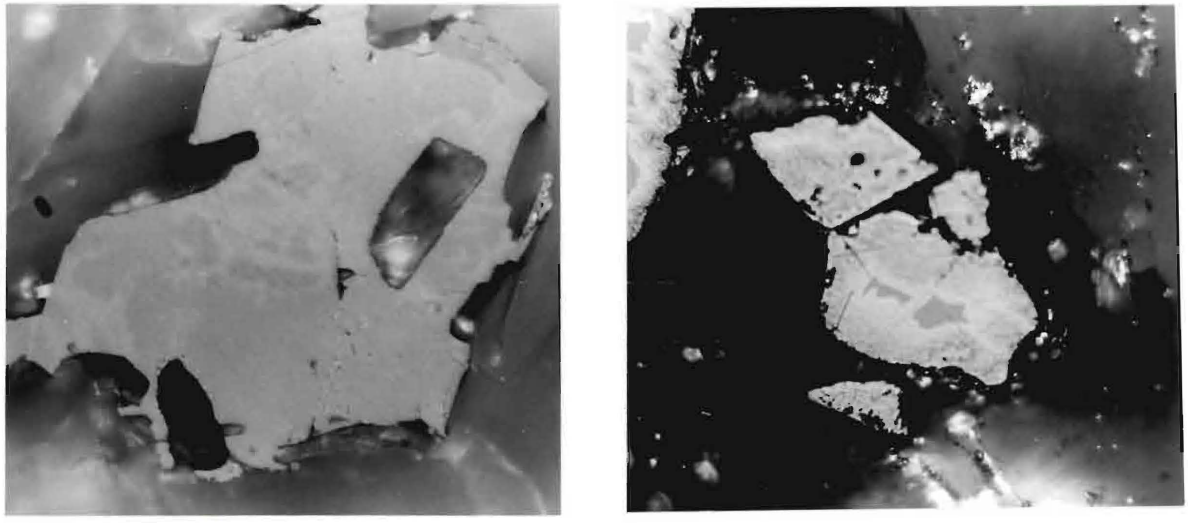

c

d

Plate 8

Medium degree hydrothermal alteration of titanomagnetite

Figure a: Class M_1 titanomagnetite. This is the same class as L_4.

Figure b: Class M_2 titanomagnetite. Dissiminated titanohematite (white spots) replacing titanomaghemite.

Figure c: Class M_3 titanomagnetite. Granule phase replacing titanohematite.

Figure d: Class M_4 titanomagnetite. Total granulation of original titanomagnetite.

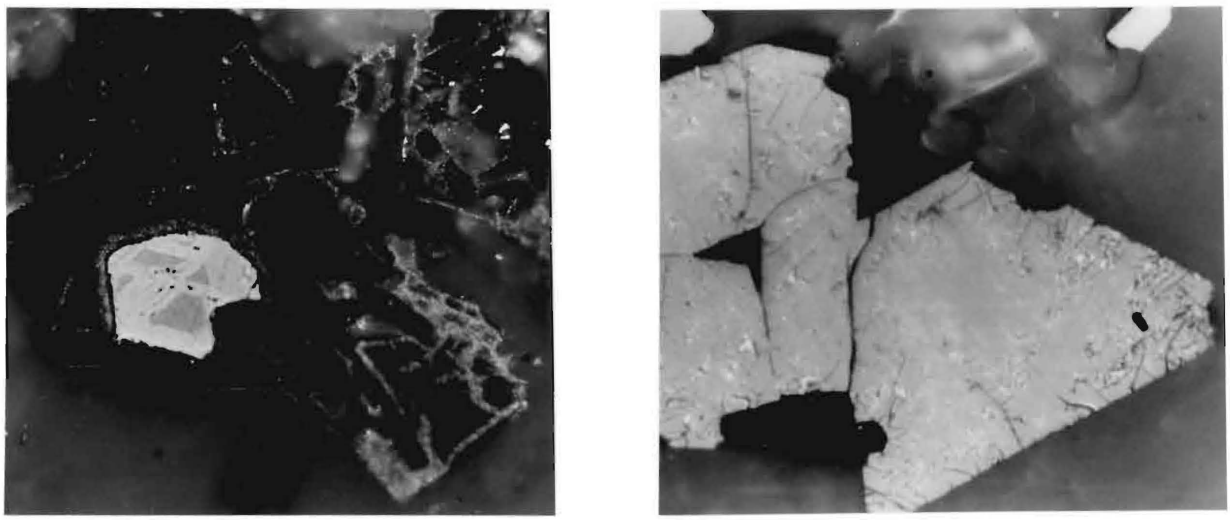

a

20 μ

b

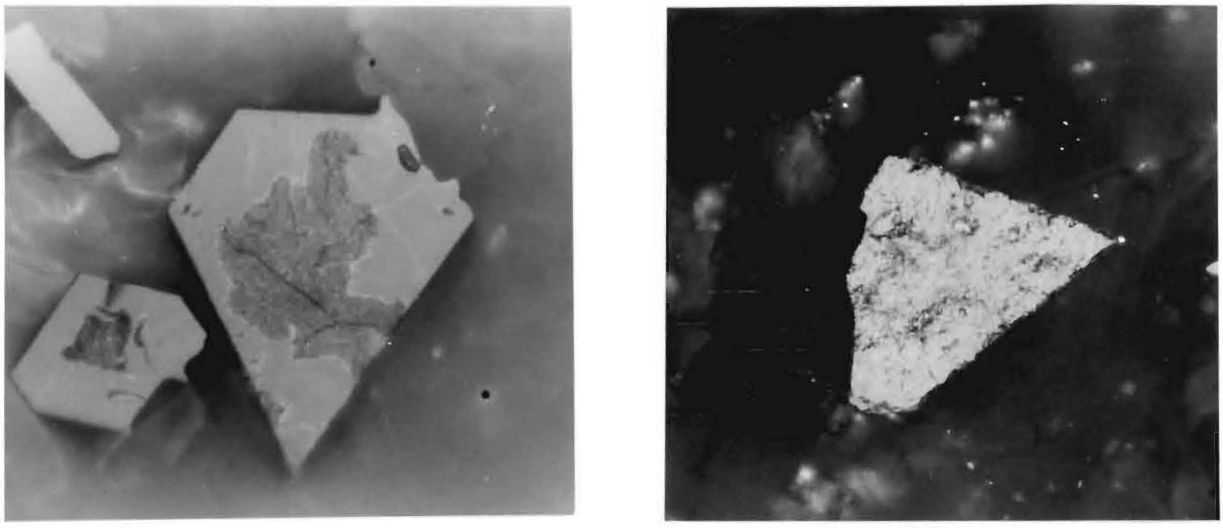

c

d

Plate 9

High degree hydrothermal alteration of titanomagnetite

Figure a: Class H_1 titanomagnetite. Totally granulated grain of titanomagnetite.

Figure b: Class H_2 titanomagnetite. Sphene (black) replacing granulated titanomagnetite. Some titanomagnetite remains unaltered (grey).

Figure c: Class H_3 titanomagnetite. Titanomagnetite is completely altered.

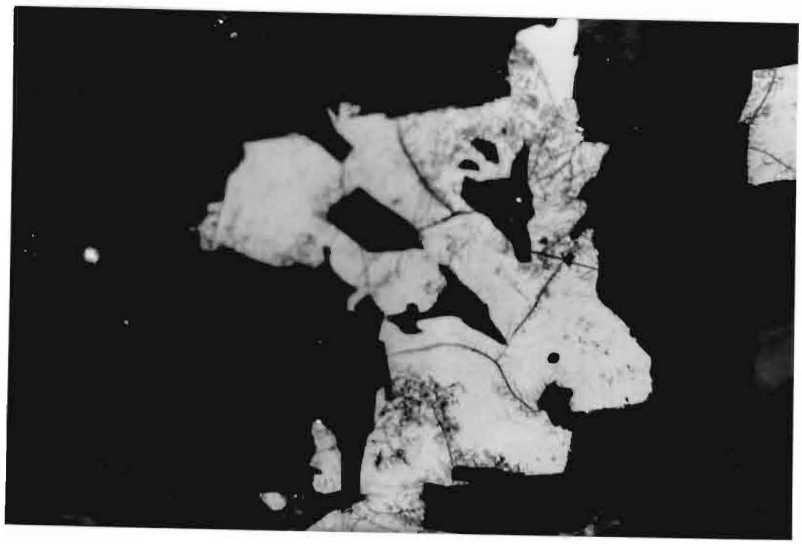

a

20 μ b

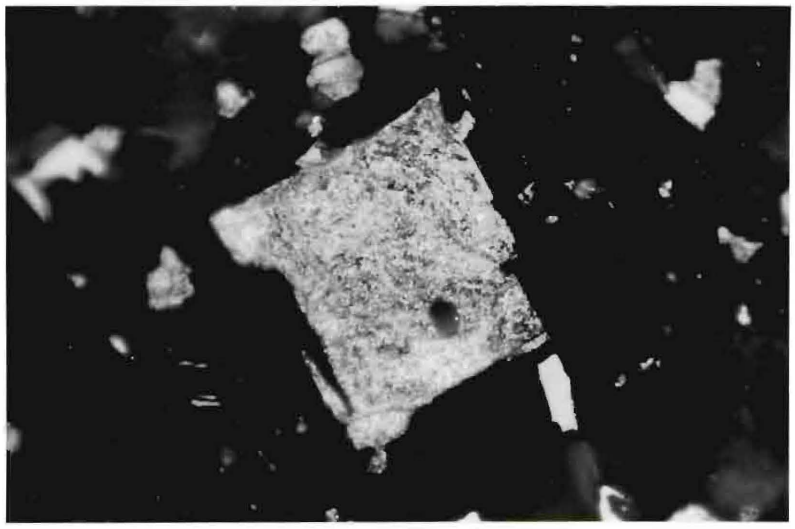

c

Plate 10

Low degree hydrothermal alteration of ilmenite

Figure a: Class S_1 ilmenite. Homogeneous ilmenite.

Figure b: Class S_2 ilmenite. Grey ilmenite.

Figure c: Class S_3 ilmenite lamellae and patches of light grey pseudo-rutile in (grey) ilmenite.

Figure d: Class S_4 ilmenite. Patches of pseudorutile (light grey) in ilmenite (grey).

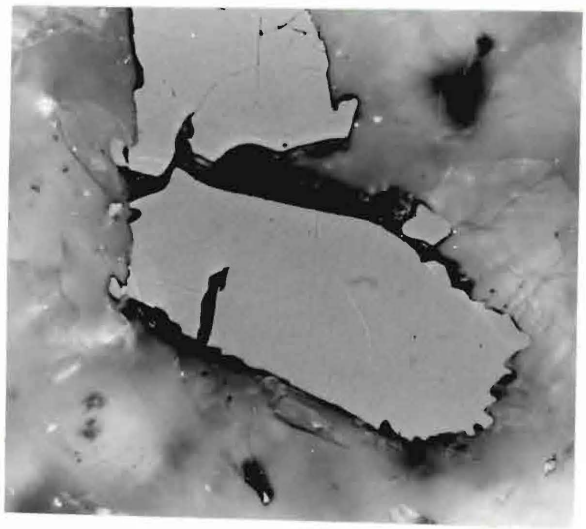

a

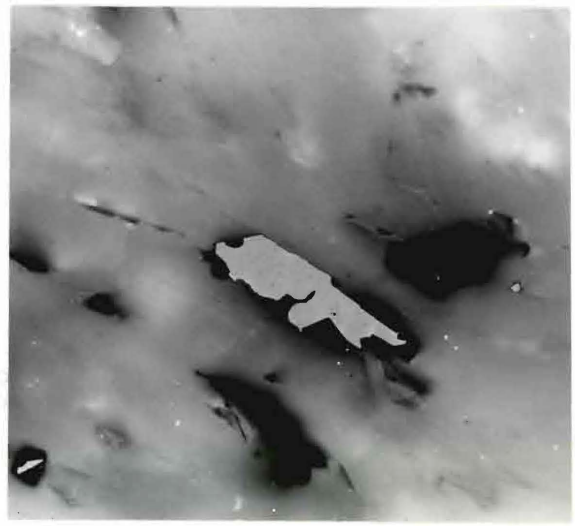

b

20 μ

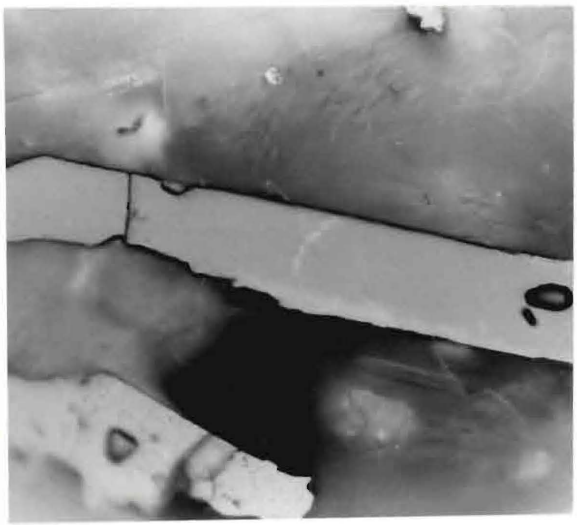

c

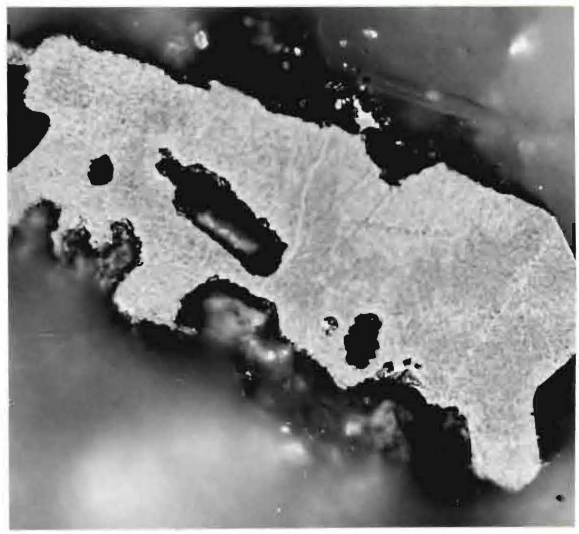

d

Plate 11

Medium degere hydrothermal alteration of ilmenite

Figure a: Class T_1 ilmenite. Ilmenite (grey) contains pseudorutile (light grey).

Figure b: Class T_2 ilmenite. Pseudorutile is replaced by (grey) color and (off white) hematite. Some ilmenite (dark grey) remains altered.

Figure c: Class T_3 ilmenite. All pseudorutile is converted to rutile (grey) and hematite (off white). The grain shows a volume change cracks. Some areas remain unaltered.

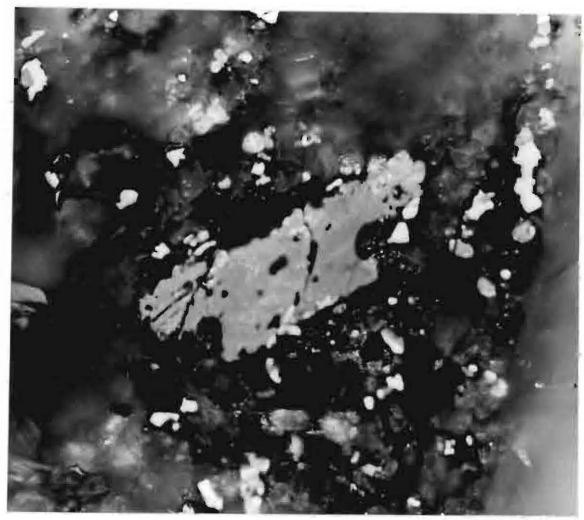

a

b 20 μ

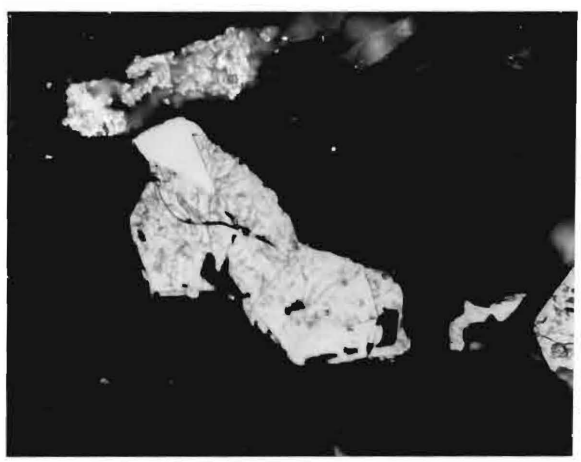

c

Plate 12

High degree hydrothermal alteration of ilmenite

Figure a: Class V_1 ilmenite. Rutile (grey) and hematite (off white).

Figure b: Class V_2 ilmenite. Leucoxene (off white) and sphene (black).

Figure c: Class V_3 ilmenite. Black sphene with some leucoxene (grey).

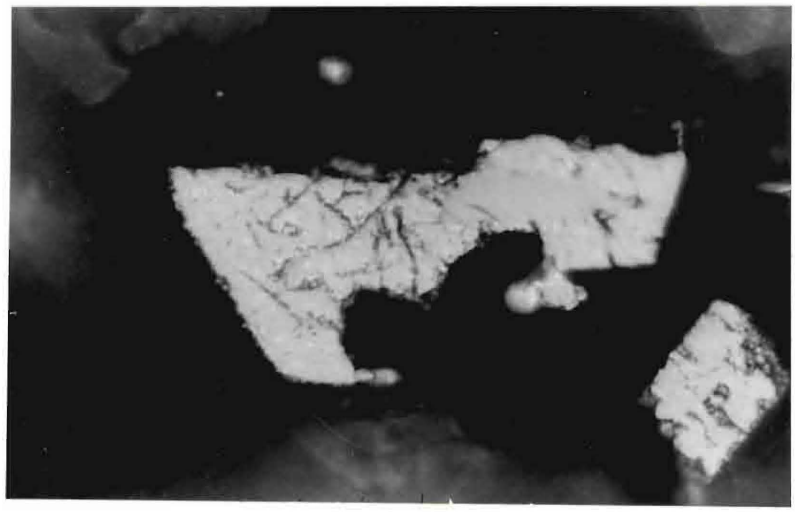

a

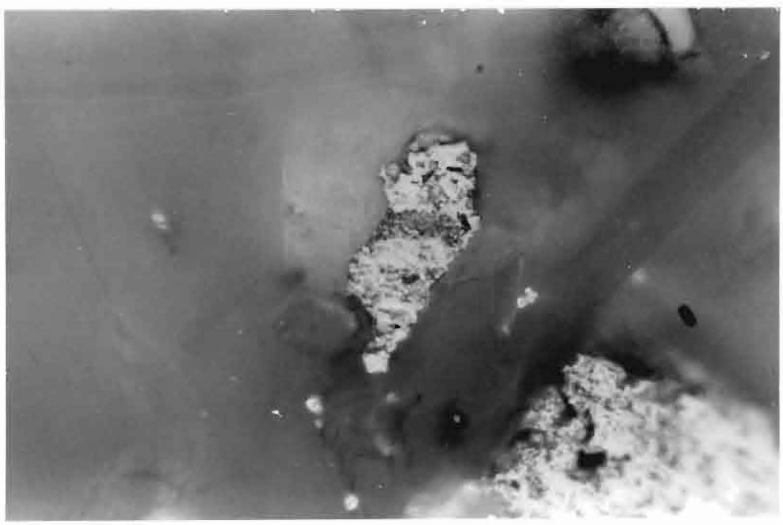

b 20 μ

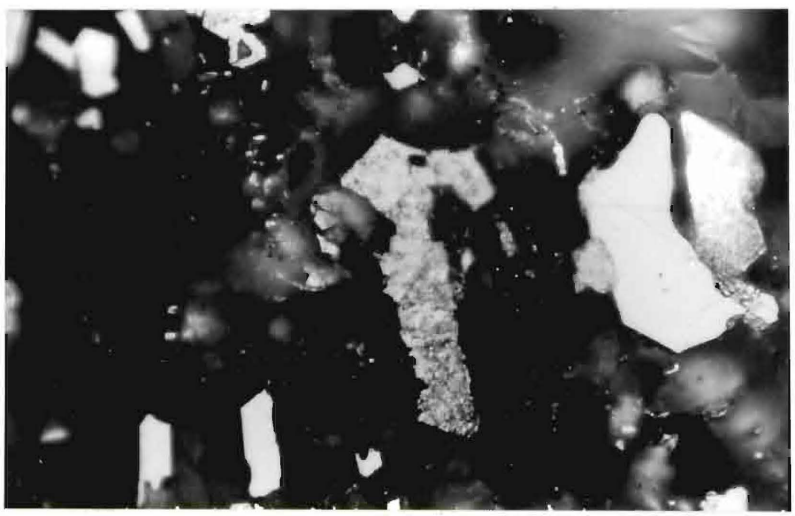

c

Plate 13

Combination of deuteric oxidation and hydrothermal alteration in titanomagnetite and ilmenite

Figure a: Hydrothermal alteration in class 2 titanomagnetite. Ilmenite lamellae are replaced by titanohematite (off white) and rutile (grey). Titanomagnetite is (light grey).

Figure b: Hydrothermal alteration in class 3 titanomagnetite. Ilmenite lamellae altered to hematite (white) and sphene (black). Titanomagnetite altered to (black) sphene. Some remanent of unaltered titanomagnetite (grey).

Figure c: Hydrothermal alteration in class 6 titanomagnetite. Titanohematite (white), rutile (grey) and pseudobrookite (dark grey). The grain is surrounded by red stain (black) in the polished section.

Figure d: Hydrothermal alteration in class 6 titanomagnetite. Hematite (white) altered to limonite (black in the photograph but red in the polished section). Some sphene (black) is present.

Figure e: Hydrothermal alteration in class 5 ilmenite. Pseudobrookite (light grey) in titanohematite (off white) and rutile (grey). The grain is surrounded by red stain (black) in the polished section.

Figure f: Hydrothermal alteration in class 6 ilmenite. Titanohematite (off white) in pseudobrookite (light grey).

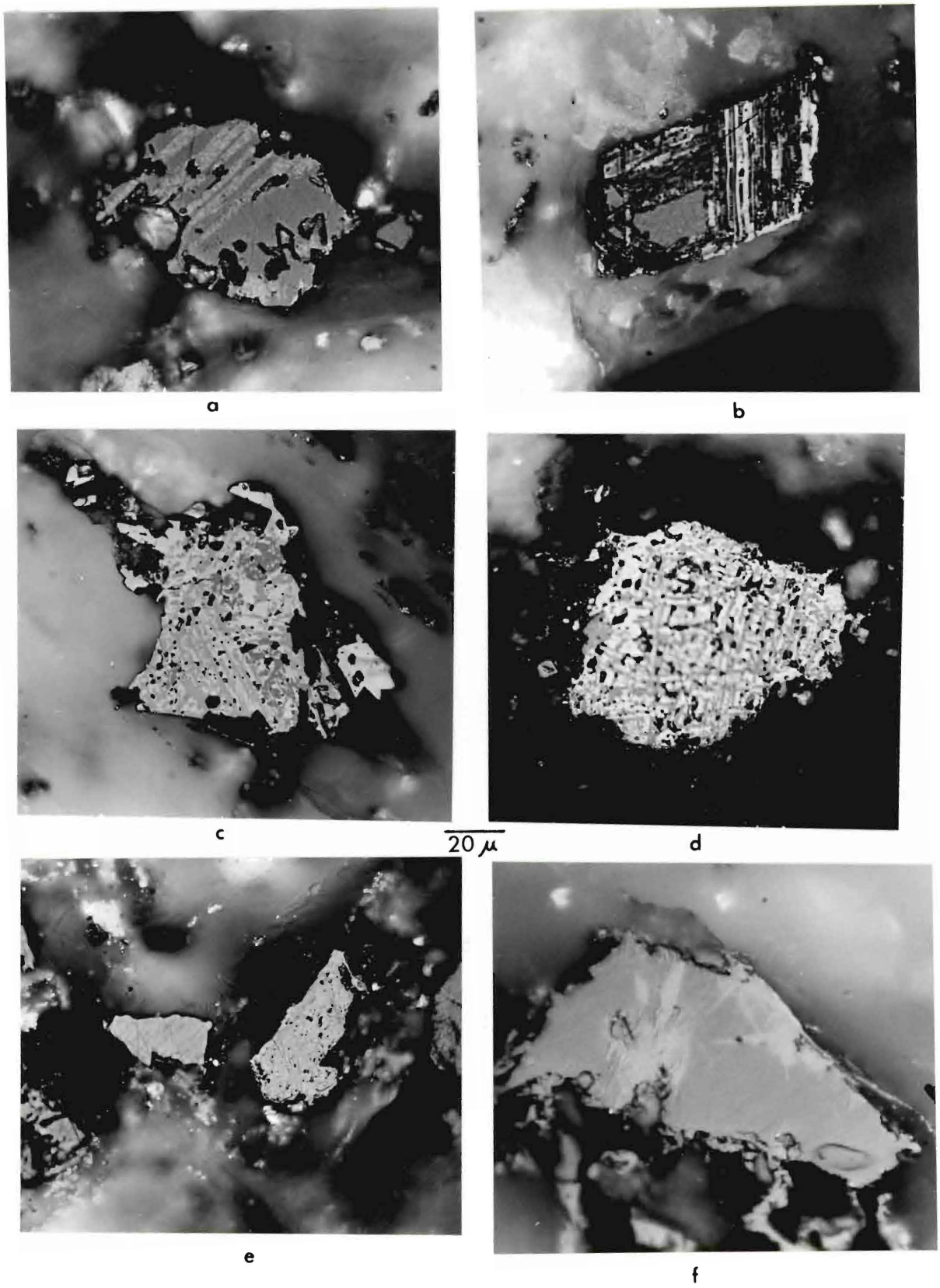
a
b
c
d
20 μ
e
f

Plate 14

Texture of ilmenite

Figure a: Trellis type ilmenite

Figure b: Internal inclusion, composite type ilmenite

Figure c: External inclusion, composite type ilmenite

Figure d: Sandwich type ilmenite

Figure e: Pseudobrookite

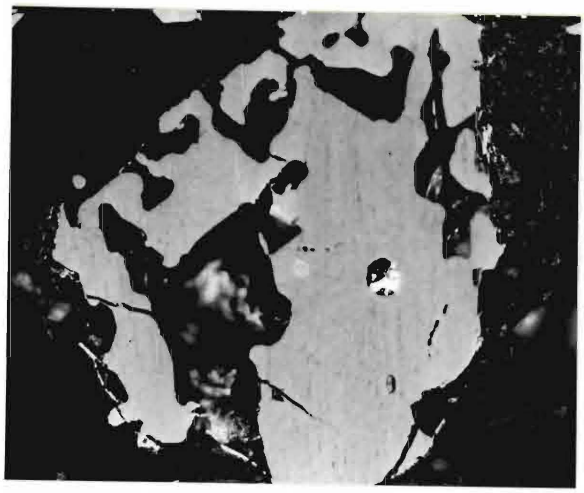

a

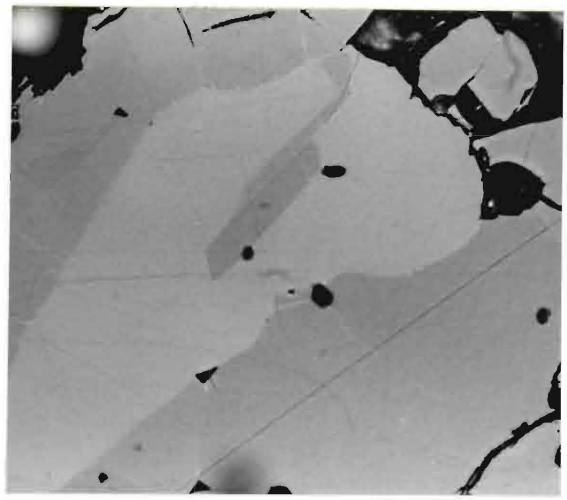

b

c

20 μ

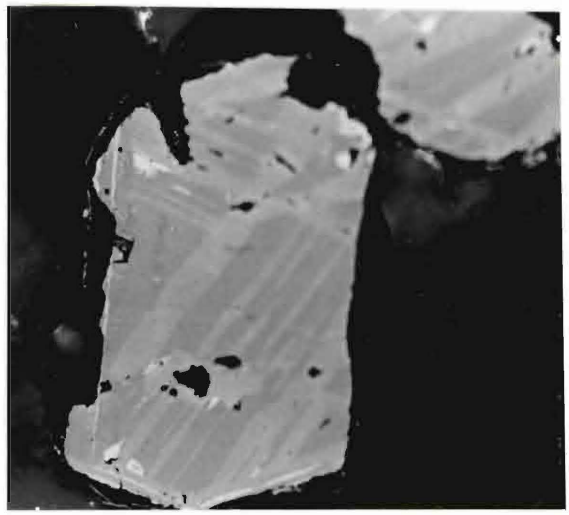

d

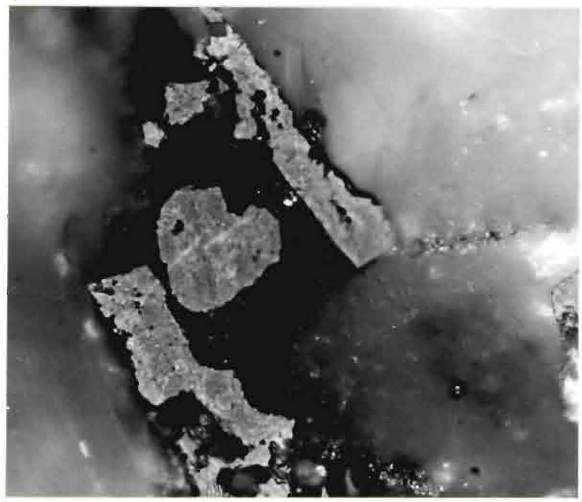

e

APPENDIX I

Opaque Mineralogy

AUL 1.1.2: 59.5 m

Greyish brown anhedral to subhedral titanomagnetite in 10-30 μ range. Low hydrothermal alteration. Phenocrysts, light brown euhedral to subhedral titanomagnetite in 40-90 μ range. Occasional spinel with primary growth zoning, the inner parts are enriched in Fe^{2+}, Cr, Al and Mg, while the secondary spinel mantles are rich in Fe^{3+} and Ti. Reflectivity in air is 16.9% for titanomagnetite and 16.8% for spinel. Temperature is 25°C (H).

AUL 2.1.5: 99.1 m

Greyish brown subhedral groundmass titanomagnetite of 10-30 μ dimension. Low hydrothermal alteration. Phenocrysts, light brown euhedral to subhedral titanomagnetite up to 90 μ dimension. Reflectivity in air is 16.1% for phenocrysts titanomagnetite and 16.5% for the medium grains. Temperatures is 25°C (H).

AUL 2.2.a: 109.4 m

Greyish brown subhedral small to medium (10-30 μ dimension) groundmass titanomagnetite. Low hydrothermal alteration. Occasional phenocrysts of titanomagnetite. Reflectivity is 16.2% for the phenocrysts and 16.4% for the groundmass titanomagnetite. Temperature is 25°C (H).

AUL 2.3.a: 114.9 m — Greyish brown subhedral to anhedral, small to medium (10-30 μ dimension) titanomagnetite. Low hydrothermal alteration. Phenocrysts, light brown subhedral titanomagnetite in 50-100 range. Occasional large (60-100 μ) subhedral spinel. Reflectivity for phenocrysts is 15.8%, for spinels 16.8% and for the groundmass 16.2%. Temperature is 25°C. (H)

AUL 2.3.b: 119.5 m — Occasional large (> 100 μ) subhedral titanomagnetite. Few large spinel. Low hydrothermal alteration. Reflectivity of the phenocrysts is 16.5%, for spinel 17.1% and for titanomagnetite groundmass 14.8%. Temperature is 25°C. (H)

AUL 2.4.b: 119.5 m — Few small (10-15 μ) greyish brown subhedral to anhedral titanomagnetite. Low hydrothermal alteration. Reflectivity is 15.9%. Temperature is 25°C. (H)

AUL 2.4.T: 119.5 m — Few large (> 80 μ dimension) subhedral spinel. Reflectivity is 17.1%. Temperature is 25°C. (H)

AUG 3.1.1: 148.4 m — Greyish brown subhedral to anhedral titanomagnetite in 60-100 μ range. Most of the grains are cracked and oxidized to whitish blue titanomaghemite. Low hydrothermal alteration. Occasional spinel with primary growth zoning. Few goethite and some minor ilmenite. Reflectivity of titanomaghemite is 16.9% for spinel 16.5% and temperature is 34 °C. (H)

AUG 3.1.2: 148.9 m — Greyish brown small to medium (10-30 μ dimension) titanomagnetite. Occasional large grains (60-80 μ range) titanomagnetite. Low hydrothermal alteration. Some of the grains are oxidized to titanomaghemite. Reflectivity of titanomaghemite is 17.1% and 16.2% for the large grains titanomagnetite, 14.9% for the groundmass small grains titanomagnetite. Temperature is 34°C (I).

AUG 3.2.a: 149.2 m — Small to medium (10- 30 μ dimension) greyish brown titanomagnetite with some occasional oxidation to whitish blue titanomaghemite. Low hydrothermal alteration. Reflectivity is 16.8% for titanomaghemite and 15.8% for titanomagnetite. Temperature is 34°C (I).

AUG 3.2.b: 149.2 m — Greyish brown, medium to large (30-60 μ dimension) titanomagnetite. Some grains are oxidized to titanomaghemite. Low hydrothermal alteration. Reflectivity is 16.7% for titanomaghemite and 15.9% for titanomagnetite. Temperature is 34°C (I).

AUG 3.4: 149.8 m — Fine to medium (5-20 μ) anhedral to subhedral, greyish brown titanomagnetite. Low hydrothermal alteration. Reflectivity of titanomagnetite is 15.7%. Temperature is 34°C (I).

AUG 3.4.T: 149.8 m — Occasional small grains (5-10 μ dimension) titanomagnetite. Low hydrothermal alteration. Reflectivity of titanomagnetite is 16.1%. Temperature is 34°C (I).

AUG.4: 150.4 m — Greyish brown, small-medium (10-30 μ dimension) titanomagnetite. Occasional large grains (in the 50-100 μ range) titanomagnetite. Much of the grains are oxidized to titanomaghemite. Low hydrothermal alteration. Reflectivity of titanomagnetite is 16.1%, for phenocrysts 15.8% and 17.2% for titanomaghemite. Temperature is 34°C (I).

AUG.4.a: 150.4 m — Small - medium (10-30 μ dimension) titanomagnetite. Few large grains (> 60 μ) subhedral titanomagnetite. Most of the grains show oxidation to titanomaghemite. Low hydrothermal alteration. Reflectivity of titanomagnetite is 16.2%, 15.4% for the phenocrysts and 17.1% for titanomaghemite. Temperature is 34°C (I).

AUG 4.1.2: 150.8 m — Two size generations of subhedral to anhedral titanomagnetite. The larger up to 80 μ, the smaller ranges in size from 5-15 μ. Low hydrothermal alteration. Reflectivity of titanomagnetite is 15.9% (large grains), 16.3% (small grains) and 16.8% for titanomaghemite. Temperature is 34°C (I).

AUG 4.1.b: 150.8 m — Titanomagnetite, greyish brown, size in the 5-15 μ range, anhedral form. Low hydrothermal alteration. Few grains. Reflectivity of titanomagnetite is 15.9%. Temperature is 34°C (I).

AUG 4.2.a: 150.9 m — Two size generations of titanomagnetite. Large subhedral ranges in size from 60 to 100 μ and anhedral small grain in 5-15 μ range. Low hydrothermal alteration. Reflectivity of titanomagnetite is 15.5% (small grains), 16.1% (large grains and 16.8% for titanomaghemite. Temperature is 34°C (I).

AUG 4.2.b: 150.9 m — Medium to large grains titanomagnetite in the 20-80 μ range. Occasional phenocrysts of spinel. Small minor pyrrhotite. Low hydrothermal alteration. Reflectivity of titanomagnetite is 14.9% and 16.7% for spinels. 17.8% for titanomaghemite. Temperature is 34°C (I).

AUG 4.2.T: 150.9 m — Medium subhedral to anhedral titanomagnetite in the size range of 15-30 μ. Few phenocrysts of spinel. Low hydrothermal alteration. Reflectivity of titanomagnetite is 16.2% and 16.7% for spinels. Temperature is 34°C (I).

AUG 4.3.a: 151.3 m — Anhedral, small size titanomagnetite in 5-15 μ range. Greyish brown color. Low hydrothermal alteration. Reflectivity of titanomagnetite is 15.8%. Temperature is 34°C (I).

AUG 4.3.b: 151.3 m — Small subhedral to anhedral grains of titanomagnetite in the size range of 5-15 μ. Low hydrothermal alteration. Reflectivity of titanomagnetite is 15.9%. Temperature is 34°C (I).

AUG 4.3.c: 151.3 m — Small to medium titanomagnetite grains in the size range of 5-20 μ. Occasional large phenocrysts (> 80 μ). Low hydrothermal alteration. Reflectivity of titanomagnetite is 15.7%, 15.2% for the phenocrysts and 19.2% for titanomaghemite. Temperature is 34°C (I).

AUG.5: 153.2 m — Anhedral to subhedral brown meduum titanomagnetite (15-30 μ dimension). Some phenocrysts of greyish brown titanomagnetite. Few phenocrysts of spinel. Low hydrothermal alteration. Reflectivity of titanomagnetite is 15.9%, phenocrysts 15.2% and 18.4%, for titanomaghemite. Temperature is 34°C (I).

AUG 5.1.1: 155 m — Greyish brown small (5-15 μ) groundmass titanomagnetite. Few phenocrysts greyish brown (> 60 μ). Spinel with primary growth zoning in the 50-80 μ size range. Low hydrothermal alteration. Reflectivity of titanomagnetite 18.5%, 15.3% for spinel and 17.8% for the oxidized spinel. Temperature is 34°C (I).

AUG 5.1.a: 155 m — Small greyish brown (5-10 μ) groundmass titanomagnetite. Few phenocrysts, spinel and titanomagnetite (60-80 μ). Low hydrothermal alteration. Reflectivity of titanomagnetite is 15.9%, 17.2% for spinel and 18.2% for titanomaghemite. Temperature is 34°C (I).

AUG 5.1.T: 155 m — Small to medium euhedral to subhedral grains of titanomagnetite in the size range of 10-20 μ. Few large grains (> 80 μ). Some phenocrysts of spinel.

Low hydrothermal alteration. Reflectivity of titanomagnetite is 15.9%, 16.5% for spinel and 18.9% for titanomaghemite. Temperature is 34°C (I).

AUG 5.2.a: 157.3 m — Medium greyish brown in the range of 15-30 μ. Subhedral to anhedral grains. Low hydrothermal alteration. Reflectivity is 16.1% for titanomagnetite and 18.7% for titanohematite. Temperature is 34°C (I).

AUG 5.2.b: 157.3 m — Small grains brown titanomagnetite in the size range of 5-15 μ. Internal inclusion of ilmenite inside titanomagnetite. Low hydrothermal alteration. Reflectivity is 15.9%. Ilmenite 14.3% - 17.2%. Temperature is 34°C (I).

AUG 5.4.a: 157.6 m — Small grains brown subhedral to anhedral titanomagnetite. Fairly abundant dark grey Cr spinel. Low hydrothermal alteration. Reflectivity is 16.3% for titanomagnetite and 13.7% for Cr spinel. Temperature is 34°C (I).

AUG 5.4.b: 157.6 m — Small brown subhedral to anhedral titanomagnetite. Few large grains (> 60 μ) titanomagnetite with oxidation to whitish blue titanomagnemite. Low hydrothermal alteration. Reflectivity of titanomagnetite is 15.9% and 15.5% (large grains), 19.2% for titanomaghemite. Temperature is 34°C (I).

AUL 6.1.a: 159.4 m

Small to medium greyish brown titanomagnetite, in the size range of 5-25 μ. Low hydrothermal alteration. Reflectivity of titanomagnetite is 17.2%. Reflectivity of titanomaghemite is 18.9%. For spinel is 15.8%. Temperature is 67°C (I).

AUL 6.1.T: 159.4 m

Small to medium, anhedral to subhedral brown titanomagnetite (10-30 μ dimension). Low hydrothermal alteration. Reflectivity of titanomagnetite is 16.8%, for titanomaghemite 18.9%. Temperature is 67°C (I).

AUL 6.1.3: 159.4 m

Small to medium, greyish brown, euhedral to subhedral grains titanomagnetite in the size range of 5-20 μ. Low hydrothermal alteration. Titanomaghemite with whitish blue color. Ilmenite as elongated anhedral grain in the 10-30 μ size range. Low hydrothermal alteration. Occasional phenocrysts of spinel 67°C (I). (> 60 μ). Reflectivity of titanomagnetite is 17.1%, 21.8% for titanomaghemite, 16.8-17.1% for ilmenite. Temperature is 67°C (I).

AUL 6.1.7: 165 m

Small to medium greyish brown titanomagnetite in the size range of 10-25 μ. Euhedral to subhedral forms. Low hydrothermal alteration. Ilmenite, small to medium brown with pinkish tint color. Elongated and equigranular grains. Low hydrothermal alteration. Occasional spinel, phenocrysts (> 80 μ). Reflectivity of titanomagnetite is 16.8%, 14.3-16.5% for ilmenite and 13.9% for spinel. Temperature is 67°C (I).

AUL 6.2.a: 169.5 m — Small to medium greyish brown titanomagnetite (10-20 μ dimension). Low hydrothermal alteration. Ilmenite, small to medium elongated grains. Low hydrothermal alteration. Reflectivity of titanomagnetite is 16.3% and 15.1-17.2% for ilmenite. Temperature is 67°C (I).

AUL 6.2.b: 169.5 m — Small-medium anhedral to subhedral grains in the range of 5-15 μ dimension. Few ilmenite. Low hydrothermal alteration. Reflectivity of titanomagnetite is 16.5% and 14.6-16.2% for ilmenite. Temperature is 67°C (I).

AUL 6.4.a: 169.8 m — Large grains greyish brown titanomagnetite in the range of 50-80 μ dimension. Some of the grains altered to whitish blue titanomaghemite. Low hydrothermal alteration. Reflectivity of titanomagnetite is 16.1% and 16.9% for titanomaghemite. Temperature is 67°C (I).

AUL 6.4.b: 169.8 m — Medium to large grains of titanomagnetite (30-60 μ dimension). Occasional phenocrysts of spinel. Low hydrothermal alteration. Reflectivity of titanomagnetite is 16.3% and 17.2% for titanomaghemite. Temperature is 67°C (I).

AUL 8.1.1: 170 m — Two generations of titanomagnetite, the smaller size (5-10 μ) is altered to titanomaghemite and titanohematite and the larger size (30-60 μ) is deuterically oxidized to class 2 and 4 as well as

low hydrothermal alteration. Ilmenite, small to medium elongated grains (10-25 μ) hydrothermally altered to light brown ilmenite type (2) and also deuterically oxidized. Low hydrothermal alteration. Reflectivity of titanomagnetite is 16.0%. Class 2, 17.1 (titanomagnetite), 14.3-15.2% (ilmenite), class 4, 19.1% (magnetite), 20.1-22.3% (titanohematite and meta-ilmenite). Ilmenite, 14.5-15.9% and 16.3-16.8% for ilmenite type (2). Temperature is 78°C (I).

AUL 8.1.2: 170.1 m

Two generations of titanomagnetite, small to medium size generation (10-25 μ) and large size generation (60-80 μ). The grains are altered to whitish blue titanomaghemite as well as some titanohematite. Occasional phenocrysts of spinel. Low to medium hydrothermal alteration. Elongated brown ilmenite in (10-30 μ) size range. Low hydrothermal alteration. Reflectivity of titanomagnetite is 16.3%, 21.8% for titanomaghemite, 23.4-27.1% for titanohematite and 16.5-17.0% for ilmenite. Temperature is 78°C (I).

AUL 8.1.3: 170.1 m

Small to medium grains brown titanomagnetite in the range of 10-30 μ. The grains are altered to titanomaghemite. Low hydrothermal alteration. Occasional phenocrysts of spinel with zoning. Elongated grains

of ilmenite in the range of 10-25 μ, brown color. Low hydrothermal alteration. Reflectivity is 15.9% for titanomagnetite, 21.8% for titanomaghemite, 14.9% for spinel and 15.0-17.2% for ilmenite. Temperature is 78°C (I).

AUL 8.1.9: 170.2 m — Light brown titanomagnetite, small to medium grains in the range of 10-30 μ. Most of the grains are anhedral with alteration to titanomaghemite. Low hydrothermal alteration. Ilmenite, anhedral elongated grains, dark brown in color, in the size range of 10-30 μ. Low hydrothermal alteration. Reflectivity is 16.2% for titanomagnetite, 19.8% for titanomaghemite and 14.7-16.8% for ilmenite. Temperature is 78°C (I).

AUL 8.1.a: 170.2 m — Medium to large subhedral greyish brown titanomagnetite in the range of (25-60 μ). Low hydrothermal alteration. Ilmenite, elongated grains dark brown (15-50 μ). Low hydrothermal alteration. Reflectivity is 16.0% for titanomagnetite, 19.9% for titanomaghemite and 14.6-16.6% for ilmenite. Temperature is 78°C (I).

AUL 8.1.b: 170.2 m — Medium-large grains greyish brown titanomagnetite (20-50 μ). Low hydrothermal alteration. Elongated brown ilmenite (15-40 μ). Low hydrothermal alteration. Reflectivity is 15.9% for titanomagnetite, 21.5% for titanomaghemite and 16.7-17.2% for ilmenite (2). Temperature is 78°C (I).

AUL 8.1.T: 170.2 m — Medium greyish brown titanomagnetite (15-25 μ). Low hydrothermal alteration. Ilmenite, elongated grains brown color. Low hydrothermal alteration. Reflectivity is 16.3% for titanomagnetite, 22.0% for titanomaghemite, 14.6-16.8% for ilmenite and 16.5-17.0% for ilmenite type (2). Temperature is 78°C (I).

AUL 8.2.a: 171.1 m — Medium subhedral grains of titanomagnetite in the range of 15-25 μ. Low hydrothermal alteration. Few elongated grains of ilmenite brown colored up to 25 μ. Low hydrothermal alteration. Reflectivity is 16.4% for titanomagnetite, 16.8% for titanomaghemite and 15.2-17.3% for ilmenite. Temperature is 78°C (I).

AUL 8.2.b: 171.1 m — Medium greyish brown titanomagnetite (15-30 μ). Low hydrothermal alteration. Occasional, small to medium elongated brown ilmenite (10-20 μ). Low hydrothermal alteration. Reflectivity is 16.2% for titanomagnetite, 17.0% for titanomaghemite and 14.8-16.8% for ilmenite. Temperature is 78°C (I).

AUL 8.2.T: 171.1 m — Anhedral to subhedral greyish brown titanomagnetite in the size range of (5-20 μ). Low hydrothermal alteration. Reflectivity is 15.8% for titanomagnetite, 16.6% for titanomaghemite. Temperature is 78°C (I).

AUL 8.4.a: 171.6 m — Medium anhedral to subhedral titanomagnetite. Deuteric oxidation class 4 and 5. Ilmenite, elongated and anhedral grains, class 4 and 5. Reflec-

tivity is 18.9% (brown magnetite), 20.1-22.3% (metailmenite and titanohematite), 21.2% (isotropic brown), 22.3-25.4 (titanohematite) and 18.8-20.1% (rutile). For ilmenite high temperature oxidation, reflectivity is 22.4-25.8% (titanohematite, 20.2-18.3% (rutile) and 15.4-16.3% (pseudobrookite). Temperature is 80°C (I).

AUL 8.4.b: 171.6 m — Anhedral grains of titanomagnetite (15-30 μ dimension). Low hydrothermal alteration with some medium alteration in few grains. Reflectivity is 22.3% (titanomaghemite). Temperature is 80°C.

AUL 8.4.c: 171.6 m — Deuteric oxidation class 5 and 6 titanomagnetite. The grains are anhedral to subhedral (15-35 μ dimension). Reflectivity is 21.3% (magnetite), 15.1-16.2% (pseudobrookite) and 21.3-23.6% (titanohematite). Temperature is 80°C (I).

AUL 8.5.a: 171.9 m — Small-medium titanomagnetite class 4, 5 and 6 deuteric oxidation. Ilmenite elongated to anhedral grains class 3, 5 and 6 deuteric oxidation. Medium-high hydrothermal alteration. Temperature is 158°C (A).

AUL 8.5.b: 171.9 m — Medium to large grains titanomagnetite in the deuteric oxidation state. Class 4, 5 and 6. Ilmenite medium to large grains (20-50 μ), class 4 and 5. High hydrothermal alteration. Temperature is 158°C (A).

AUL 8.5.c: 171.9 m — Medium anhedral to subhedral grains titanomagnetite in class 5 and 6 deuteric oxidation. Ilmenite, medium grains class 5 and 6. Medium-high hydrothermal alteration. Temperature is 158°C (A).

AUL 8.5.2: 171.9 m — Medium groundmass class 6 deuteric oxidation titanomagnetite. Ilmenite also in high state of deuteric oxidation (class 6). Both titanomagnetite and ilmenite are very high hydrothermally altered. Temperature is 158°C (A).

AUL 8.5.7: 171.9 m — Small to medium greyish brown titanomagnetite in the range of 15-30 μ. Occasional phenocrysts (> 60 μ). Separate ilmenite and inclusion with titanomagnetite. Low hydrothermal alteration. Reflectivity of titanomagnetite is 16.1% and 16.8% titanomaghemite. Ilmenite, reflectivity is 14.9%-16.8%. Temperature is 34°C (I).

AUL 9.3.a: 174.7 m — Anhedral small to medium greyish brown titanomagnetite. Low hydrothermal alteration. Few elongated separate ilmenite. Temperature is 34°C (I).

AUL 9.3.b: 174.7 m — Small medium greyish brown titanomagnetite in the size range of 10-30 μ. Few separate ilmenite. Low hydrothermal alteration. Temperature is 34°C (I).

AUL 9.3.c: 174.7 m — Titanomagnetite, small-medium grains (15-30 μ). Anhedral-subhedral form. Occasional ilmenite brown in color up to 35 μ. Low hydrothermal alteration. Temperature is 34°C (I).

AUL 10.1: 179.8 m

Medium to large titanomagnetite (35-80 μ) class 3, 4 and 5. Ilmenite separate elongated grains in deuteric alteration state, class 3, 4, 6. Low to medium hydrothermal alteration. Reflectivity for titanomagnetite is 17.8% (titanomagnetite), 14.4-15.6% (ilmenite lamellae), 21.5% (magnetite) and 23.4-25.0 % (titanohematite). For ilmenite 17.3-17.7%, 15.2-17.0%, 21.4-25.5%, 20.0-18.6% and 15.1-16.2% for pseudobrookite. Temperature is 80°C (I).

AUL 10.1.b: 179.8 m

Deuteric oxidation class 2, 3, and 4 titanomagnetite. Few ilmenite in class 2 and 4. Medium hydrothermal alteration. Temperature is 80°C (I).

AUL 11.2.2: 186.1 m

Small greyish brown groundmass titanomagnetite (5-15 μ). Occasional phenocrysts of titanomagnetite (> 60 μ). Separate ilmenite, elongated grain. Low hydrothermal alteration. Reflectivity of tipano-magnetite phenocrysts is 15.6% and 14.6-17.2% for ilmenite. Temperature is 34°C (I).

AUL 11.2.7: 195.5 m

Groundmass greyish brown titanomagnetite (10-35 dimension). Few large grains of titanomagnetite (up to 60 μ). Separate and intergrowth of ilmenite in the size range of 15-25 μ. Most of titanomagne-tite grains are altered to whitish blue titanomag-hemite. Low hydrothermal alteration. Reflectivity of titanomagnetite (phenocrysts) is 15.9%, ground-mass 16.2%, titanomaghemite 18.9% and 14.5-17.3% for ilmenite. Temperature is 34°C (I).

AUL 13.4.3: 199.8 m — Small-medium grains of titanomagnetite with cation deficiency. Medium hydrothermal alteration. Separate ilmenite hydrothermal altered. Reflectivity of titanomagnetite granulation is 22.8% and 23.4-27.5%. Ilmenite alteration is 18.0% and 18.8%. Temperature is 105°C (I).

AUL 14.1.1: 200.9 m — Medium-large anhedral titanomagnetite class 2 and 3 deuteric oxidation. Ilmenite separate and in class 2 and 3 deuteric oxidation. Low hydrothermal alteration. Reflectivity is 17.1% (for titanomagnetite class 2), 14.3-15.8% (for ilmenite lamellae) and 17.8% for class 3), 15.1-17.1% (for ilmenite lamellae). For ilmenite class 2 (15.3-16.9%) and 17.3%. For ilmenite class 3 (17.3-17.7%, (15.2-17.0%), (21.4-25.5%) and 20.0-18.6%). Temperature is 34°C (I).

AUL 14.1.5: 201.2 m — Titanomagnetite and ilmenite both in high state of hydrothermal alteration. The grains are small to medium in the size range of 15-35 μ. Temperature is 165°C (H).

AUL 14.1.8: 203.7 m — Small to medium grains titanomagnetite with cation deficiency cracks. Medium hydrothermal alteration. Ilmenite in low hydrothermal alteration state. Inclusion of ilmenite in titanomagnetite. Reflectivity is 23.2-27.1% for titanohematite. For ilmenite alteration reflectivity is 18.3% and 18.8%. Temperature is 115°C (I).

AUL 14.3.2: 205.9 m

Medium-large euhedral to subhedral grains of titanomagnetite, oxidized to titanomaghemite. The grains are deuterically oxidized and they are in class 2 and 3. Ilmenite deuterically oxidized and they are in class 2 and 3. Low hydrothermal alteration. Reflectivity for titanomagnetite class 2 is 16.8%, titanomaghemite 19.2%, ilmenite 14.6-15.9%. Reflectivity for ilmenite is 15.3-16.9%, 17.4%. Temperature is 80°C (I).

AUL 14.3.7: 217 m

Large euhedral to subhedral grains deuterically oxidized, class 2 and class 3. The grains are replaced by titanohematite (whitish color). Large grains of ilmenite also in the deuteric oxidation and hydrothermal alteration states. Some granulation occur. Medium hydrothermal alteration. Reflectivity of granulation is 20.2%. Temperature is 165°C (A).

AUL 18.1.2: 223.7 m

Small-medium anhedral grains of titanomagnetite deuterically altered to class 5 and 6. The grains contain red stain areas in silicates. Ilmenite grains are medium and in class 6 which are hydrothermally altered to yellow sphene. Medium-high hydrothermal alteration. Reflectivity of titanomagnetite alteration is 22.6% for titanohematite and 16.5% for sphene. For ilmenite, reflectivity is

17.2-17.6%, 15.2-17.0%, 21.2-25.4%, 19.6%-18.3%. Temperature is 165°C (A).

AUL 19.1.2: 229.6 m — Deuteric oxidation in titanomagnetite class 3 and 4. Separate elongated grains of ilmenite in deuteric oxidation state, class 2 and 3. Medium hydrothermal alteration. Temperature is 165°C (A).

AUL 19.1.6: 230.7 m — Class 5 and 6 deuteric oxidation in titanomagnetite and ilmenite. Both titanomagnetite and ilmenite are hydrothermally altered to granulation and sphene. Medium-high hydrothermal alteration. Reflectivity of titanomagnetite alteration is 20.4% and for ilmenite alteration is 20.8-19.0%, 22.4-24.0%, and 21.3-20.7%. Temperature is 155°C (A).

AUL 19.2.2: 231.6 m — Anhedral medium titanomagnetite grains altered to granulation texture with yellow, blue and orange colors. Ilmenite grains are elongated and altered to granulation texture. Medium hydrothermal alteration. Temperature is 160 °C (A).

AUL 19.2.6: 235.5 m — Medium titanomagnetite grains altered to whitish blue titanomaghemite and some titanohematite. Some of the grains contain granulation. Ilmenite with pseudo rutile are fairly present. However, some granulation after titanohematite is also present in ilmenite. Medium hydrothermal alteration. Reflectivity of titanomagnetite alteration is 22.4%, titanohematite 23.3-27.1%, granulation 20.6%. For ilmenite, 18.2%,

23.2-25.0% and 20.8-19.0%. Temperature is 160°C (A). Some unaltered grains.

AUL 20.1.1: 235.9 m — Very highly altered titanomagnetite and ilmenite. Black sphene after titanomagnetite and yellow sphene after ilmenite are present. High hydrothermal alteration. Some ilmenite grains remain unaltered. Temperature is 168°C (H).

AUL 20.1.2: 236.2 m — Subhedral medium grains of titanomagnetite. Very highly altered to granulation texture. Ilmenite also altered to granulation texture and some of the ilmenite are unaltered. Medium-high hydrothermal alteration. Temperature is 168°C (H).

AUL 20.3.4: 241.9 m — Deuteric oxidation of titanomagnetite, class 2. The grains are medium to large. Separate ilmenite in class 2. Both titanomagnetite and ilmenite are hydrothermally altered. Low hydrothermal alteration. Temperature is 76°C (I).

AUL 20.3.8: 247.8 m — Medium anhedral grains of titanomagnetite oxidized to whitish blue titanomaghemite. Separate elongated unaltered ilmenite. Low hydrothermal alteration. Temperature is 42°C (I).

AUL 22.1.2: 249.1 m — Medium subhedral to anhedral titanomagnetite oxidized to titanomaghemite. Ilmenite contains, ilmenite type (2) and pseudorutile. Low hydrothermal alteration. Reflectivity is 16.7% for titanomagnetite and 14.9-16.7% for ilmenite. Temperature is 42°C (I).

AUL 22.1.7: 251.1 m — Small grains of titanomagnetite altered to titanohematite and granulation texture. Overgrowth of hematite. Occasional ilmenite. Medium hydrothermal alteration. Temperature is 160°C (H).

AUL 22.2.2: 251.3 m — Medium to large (25-60 μ) subhedral grains of titanomagnetite. Elongated and equigranular ilmenite. Low hydrothermal alteration. Temperature is 18°C (I).

AUL 22.2.7: 256.3 m — Medium to large grains light brown color of titanomagnetite altered to titanomaghemite. Elongated separate ilmenite. Low hydrothermal alteration. Temperature is 18°C (I).

AUL 24.1.1: 257.4 m — Deuteric oxidation in titanomagnetite class 4, 5 and 6. Ilmenite in class 3 and 4 deuteric oxidation. Medium hydrothermal alteration. Some of the grains are in class 1 unaltered. Reflectivity of the unaltered grains is 16.7%. Temperature is 155°C.

AUL 24.1.9: 261.1 m — Deuteric oxidation in titanomagnetite and ilmenite. Class 3, 4 and 5. Medium hydrothermal alteration. Temperature is 160°C (H).

AUL 25.5.4: 263.4 m — Deuteric oxidation in titanomagnetite, class 4. Ilmenite class 5 and 6 deuteric oxidation. Both titanomagnetite and ilmenite are in high hydrothermal alteration state, forming sphene and granulation texture. Temperature is 162°C (H).

AUL 25.5.6: 265.9 m — Medium titanomagnetite grains (20-40 μ). Very high hydrothermally altered. Ilmenite altered to sphene. High hydrothermal alteration. Temperature is 170°C (H).

AUL 25.6.7: 266.1 m — Medium to large titanomagnetite grains. Cation deficient texture with cracks. Ilmenite altered to pseudorutile. Low-medium hydrothermal alteration. Reflectivity of titanomagnetite is 16.7% and 16.8-17.2% for ilmenite. Temperature is 42°C (I).

AUL 26.6.3: 270.9 m — Few medium titanomagnetite grains. Granulation texture with orange, yellow and red color. Medium-high hydrothermal alteration. Temperature is 170°C.

AUL 30.4.2: 291.1 m — Few large grains titanomagnetite in high deuteric oxidation state (class 5 and 6). Occasional ilmenite class 6. Both titanomagnetite and ilmenite are hydrothermally altered to sphene. Temperature is 175°C (H).

AUL 30.4.6: 291.1 m — Few grains of titanomagnetite in class 6 deuteric oxidation starts to form sphene. Medium-high hydrothermal alteration. Few pyrrhotite. Temperature is 175°C (H).

AUL 31.1.2: 292.3 m — Small grains of titanomagnetite class 6 deuteric oxidation. Ilmenite in class 6 deuteric oxidation. Both titanomagnetite and ilmenite are in high hydrothermal alteration state. Reflectivity of titanomagnetite alteration is 15.4-16.3% and 21.4-

23.5% for titanohematite. For ilmenite, reflectivity is 15.3-16.9%, 17.3-17.4%, 17.3-17.7%, 15.2-17.0%, 21.5-25.6%, 20.3-18.9%. Temperature is 175°C (H).

AUL 31.1.6: 296.2 m — Few grains of titanomagnetite (10-20 μ dimension). All in class 6 deuteric oxidation. Medium-high hydrothermal alteration. Reflectivity of ilmenite alteration, 15.4-16.2%, 22.0-25.6% and 19.7-18.2%. Temperature is 175°C (H).

AUL 31.1.11: 316.5 m — High hydrothermal alteration. Dark brown to black sphene. Temperature is 185°C (H).

AUL 31.1.16: 316.7 m — Few grains, small and in class 5 and 6 titanomagnetite deuteric oxidation. Very high hydrothermal alteration. Temperature is 185°C (H).

AUL 36.1.8: 317.4 m — Few large titanomagnetite grains in class 4 deuteric oxidation. Medium-high hydrothermal alteration. Temperature is 160°C (A).

AUL 38.3.7: 332.1 m — Medium grains titanomagnetite, class 4 and 6 deuteric oxidation. Elongated separate class 4 and 5 ilmenite. Medium-high hydrothermal alteration. Temperature is 165°C (A).

AUL 39.2.2: 332.8 m — Small grains of titanomagnetite in deuteric oxidation state (class 4 and 6). Most of the grains contain granulation and sphene. Medium-high hydrothermal alteration. Temperature is 168°C (A).

AUL 39.2.7: 334.3 m — Small grains titanomagnetite (5-15 μ dimension). Medium hydrothermal alteration. Reflectivity is 22.2% for ilmenite alteration, reflectivity is 20.3-18.9% and 22.1-23.8%. Temperature is 138°C (I).

AUL 40.1.1: 337.5 m — Few small grains of titanomagnetite in class 4 deuteric oxidation. Low-medium hydrothermal alteration. Temperature is 80°C (I).

AUL 40.1.2: 337.9 m — Medium to large grains of titanomagnetite in deuteric oxidation class 4, 5 and 6. Separate ilmenite in class 5 and 6. Both titanomagnetite and ilmenite are hydrothermally altered to sphene and titanohematite. Medium-high hydrothermal alteration. Temperature is 138°C (I).

AUL 40.2.2: 338.9 m — Titanomagnetite anhedral to subhedral grains (5-15 μ dimension), altered to microcrystalline granulation phase with yellow, blue, orange and red colors. Medium-high hydrothermal alteration. Temperature is 160°C (A).

AUL 40.2.7: 339.4 m — Small-medium grains of titanomagnetite (10-25 μ dimension) in deuteric oxidation state, class 4 and 6. The grains are altered to sphene and granulation texture. Medium hydrothermal alteration. Temperature is 165°C (A).

AUL 41.1.2: 341.4 m — Elongated and tubular titanomagnetite and ilmenite up to 70 μ, in deuteric oxidation state class 5

and 6. The grains are hydrothermally altered to sphene and granulation texture. Medium-high hydrothermal alteration. Red stain in the silicates. Temperature is 178°C (A).

AUL 41.1.7: 342.1 m — Deuteric oxidation class 5 and 6 titanomagnetite and ilmenite. Medium to large subhedral to anhedral grains (30-70 μ dimension) altered sphene and granulation texture. High hydrothermal alteration. Red stain in the silicates. Some grains unaltered of ilmenite (92°C). Temperature (observed) 168°C (A). Reflectivity of ilmenite is 17.9-18.1%.

AUL 41.3.1: 346.2 m — Elongated grains titanomagnetite up to 50 μ dimension. High hydrothermal alteration. Red stain in the silicates. Temperature is 160°C (I).

AUL 41.3.2: 346.3 m — Elongated grains of titanomagnetite and ilmenite (25-60 μ dimension). High hydrothermal alteration. Red stain in the silicates. Temperature is 160°C (I).

AUL 42.2.4: 348.3 m — Class 4 and 5 deuteric oxidation in titanomagnetite and ilmenite. The grains are medium (15-30 μ dimension) and granulation after titanohematite is detected. Medium-high hydrothermal alteration. Red stain in the silicates. Temperature is 160°C (I).

AUL 42.2.7: 351.6 m — Medium titanomagnetite grains, class 4, 5 and 6 deuteric oxidation. Titanomagnetite altered to titanohematite and granulation texture. Medium hydrothermal alteration. Temperature is 160°C (I).

AUL 45.1.2: 366.5 m — Small to medium grains of titanomagnetite (10-30 μ dimension). Hydrothermally altered to sphene and granulation texture. Medium hydrothermal alteration. Reflectivity is 20.2-22.6% and 19.5% (class 4). Temperature is 160°C (I).

AUL 45.1.7: 367.1 m — Medium to large grains subhedral titanomagnetite in granulation texture state. Anhedral ilmenite also with granulation texture. Medium hydrothermal alteration. Reflectivity is 20.7% for granulation. Temperature is 160°C (I).

AUL 46.2.7: 370.8 m — Medium grains titanomagnetite and separate elongated ilmenite, both in high deuteric oxidation state, class 4, 5 and 6. The grains of titanomagnetite and ilmenite are altered to sphene and rutile. Medium hydrothermal alteration. Reflectivity of titanomagnetite alteration is 15.2-16.0% and 21.2-23.0%. Temperature is 160°C (I).

AUL 49.1.1: 382.9 m — Anhedral medium to large grains titanomagnetite and ilmenite (35-60 μ dimension). Titanohematite, rutile and sphene occur as secondary alteration phases. Medium-high hydrothermal alteration. Red stain around the opaque phases and in the silicates. Reflectivity of titanomagnetite alteration is, 15.1-16.2%, 22.9-26.1% and 19.6-18.1%. Temperature is 180°C (A).

AUL 49.1.2: 383.1 m — Medium to large grains titanomagnetite and ilmenite, up to 60 μ dimension. Both are altered to sphene, rutile and granulation texture. High hydrothermal alteration. Red stain in the silicates. Temperature is 160°C (A).

AUL 49.3.1: 385.6 m — Few grains small to medium titanomagnetite (15-25 μ). Occasional ilmenite. Low-medium hydrothermal alteration. Reflectivity is 22.9%. Temperature is 85°C. Reflectivity of ilmenite is 16.1-16.8%.

AUL 49.3.6: 387.6 — Class 3 and 4 deuteric oxidation titanomagnetite and ilmenite. The grains are medium (20-40 μ) and altered to granulation texture and sphene. Medium hydrothermal alteration. Temperature is 155°C (A).

AUL 50.1.7: 388.0 m — Medium to large grains of titanomagnetite and ilmenite. Medium hydrothermal alteration. Temperature is 150°C (H).

AUL 51.2.1: 396.3 m — Medium to large grains of titanomagnetite. Occasional ilmenite. Granulation starts in titanohematite. Medium hydrothermal alteration. Some unaltered titanomagnetite fine to medium grains with reflectivity of 16.1%. Temperature is 122°C (I).

AUL 51.2.8: 397.9 m — Small to medium grains of titanomagnetite and ilmenite in the size range of 10-35 μ. Low hydrothermal alteration. Reflectivity of ilmenite is 17.2-17.3%. Temperature is 72°C (I).

AUL 52.4.5: 402.7 m — Small to medium grains of titanomagnetite class 2-5 deuteric oxidation. Few ilmenites. Granulation texture and sphene. Medium-high hydrothermal alteration. Temperature is 160°C (A). Reflectivity of class 4 is 20.1-22.5%.

AUL 52.4.8: 403.3 m — Deuteric oxidation class 4, 5, 6 in large grains titanomagnetite and ilmenite. Both are altered to sphene, titanohematite and granulation texture. Medium hydrothermal alteration. Temperature is 160°C (A).

AUL 54.1.4: 411.1 m — Medium to large grains of titanomagnetite. Low state of deuteric oxidation, class 2 and 3. Some granulation. Low-medium hydrothermal alteration. Reflectivity of titanomaghemite is 19.0%. Temperature is 150°C (I).

AUL 54.1.5: 413.6 m — Medium to large titanomagnetite grains in low state of deuteric oxidation class 2 and 3. Low hydrothermal alteration. Temperature is 42°C (H).

AUL 54.1.9: 413.9 — Medium to large titanomagnetite grains in low state deuteric oxidation class 2 and 3. Few ilmenite. Titanomaghemite replacing titanomagnetite. Low hydrothermal alteration. Temperature is 42°C (H).

AUL 55.1.3: 415.6 m — Deuteric oxidation class 4, 5 and 6 titanomagnetite. Ilmenite, class 6 deuteric oxidation. Both ilmenite and titanomagnetite are small to medium grains with

alteration to sphene and titanohematite. Medium hydrothermal alteration. Temperature is 175°C (A).

AUL 55.1.6: 415.3 m — Medium grains titanomagnetite and ilmenite altered to sphene and granulation. Medium-high hydrothermal alteration. Red stain in silicates. Temperature is 175°C (A).

AUL 55.1.9: 418.8 m — Deuteric oxidation class 3 and 4 titanomagnetite. Ilmenite also contains class 2 deuteric oxidation. Both ilmenite and titanomagnetite altered to titanomaghemite. Low to medium hydrothermal alteration. Temperature is 97°C (I).

AUL 55.1.10: 424.1 m — Deuteric oxidation class 5 and 6 medium grains titanomagnetite, hydrothermally altered to orange, yellow sphene and titanohematite. Medium hydrothermal alteration. Temperature is 122°C (I).

AUL 57.1.3: 425.0 m — Medium to large grains (30-70 μ dimension) titanomagnetite and ilmenite class 5 and 6. Both are hydrothermally altered to titanomaghemite and pseudorutile and titanohematite with some granulation. Medium hydrothermal alteration. Temperature is 122°C (I).

AUL 57.1.6: 428.6 m — Deuteric oxidation of titanomagnetite and ilmenite class 6. Granulation texture and some titanomaghemite. Medium hydrothermal alteration. Temperature is 122°C (I).

AUL 61.3.4: 448.8 m — Deuteric oxidation of titanomagnetite and ilmenite class 4, 5 and 6. Granulation texture in both phases. The grains are large. Medium hydrothermal alteration. Temperature is 160°C (A).

AUL 61.3.8: 450.7 m — Large grains deuteric oxidation titanomagnetite, class 2 and 3. Occasional ilmenite. Low hydrothermal alteration. Temperature is 40°C (I).

AUL 62.2.3: 453.9 m — Medium grains titanomagnetite hydrothermally altered to titanomaghemite phase. Separate elongated ilmenite altered to titanohematite and rutile. Low to medium hydrothermal alteration. Temperature is 97°C (I).

AUL 66.4.3: 475.2 m — Fine to medium (5-20 μ dimension) deuteric oxidation class 6 titanomagnetite. Titanohematite, sphene and granulation are secondary phases replacing titanomagnetite. Medium hydrothermal alteration. Reflectivity of ilmenite is 22.6-26.3% and 19.8-18.5%. Temperature is 160°C (A).

AUL 66.4.7: 476.1 m — Medium to large (35-65 μ size range) titanomagnetite altered to titanomaghemite. The grains are subhedral. Anhedral ilmenite, separate and elongated (25-40 μ) altered to titanohematite and rutile. Low-medium hydrothermal alteration. Temperature is 40°C(I). Reflectivity of ilmenite is 19.6%.

AUL 68.1.3: 481.1.3 m — Medium grains titanomagnetite, class 2 deuteric oxidation. Occasional ilmenite. Medium to low hydrothermal alteration. Reflectivity is 22.7%. Temperature is 90°C (I).

AUL 68.1.7: 485.9 m — Medium to large titanomagnetite and ilmenite grains. Class 3 and 4 deuteric oxidation. Medium hydrothermal alteration. Temperature is 160°C (A).

AUL 69.7.3: 490.7 m — Large grains titanomagnetite class 4, 5 and 6, hydrothermally altered to titanomaghemite, titanohematite and granulation texture. Occasional ilmenite. Medium-high hydrothermal alteration. Reflectivity of some unaltered titanomagnetite 15.1%.

AUL 69.7.6: 491.2 m — Class 4, 5 and 6 deuteric oxidation of titanomagnetite. Medium grains (15-35 μ dimension). Occasional ilmenite class 3 and 4. Medium hydrothermal alteration. Reflectivity of ilmenite alteration is 18.6-18.8%. Temperature is 98°C (I).

AUL 71.3.7: 498.6 m — Small-medium (10-30 μ dimension) titanomagnetite and ilmenite. Medium-low hydrothermal alteration. The grains are cracked. Reflectivity of ilmenite alteration is 17.8-18.0%. Temperature is 98°C (I).

AUL 73.2.2: 508.2 m — Small grains titanomagnetite (5-15 μ) altered to sphene and titanohematite as well as granulation texture. Occastional ilmenite. Red stain in the silicates. High hydrothermal alteration. Temperature is 180°C (A).

AUL 73.2.8: 511.6 m — Titanomagnetite altered to yellow transparent sphene. Granulation texture occur. Occasional large grains of titanomagnetite contain titanomaghemite. Few grains of altered ilmenite. Most of the grains are small and in low to medium hydrothermal alteration state. Red stain in silicates. Reflectivity of ilmenite alteration is 18.1-18.3%. Temperature is 98°C (I).

AUL 74.2.3: 514.9 m — Class 4 and 5 deuteric oxidation in small-medium grains titanomagnetite and ilmenite. Both are hydrothermally altered to granulation texture. Medium-high hydrothermal alteration. Temperature is 148°C (I).

AUL 74.2.8: 516.8 m — Small-medium very high hydrothermal alteration titanomagnetite and ilmenite. Granulation texture and sphene. Red stain in silicates. High hydrothermal alteration. Temperature is 168°C (I).

AUL 75.4.3: 520.9 m — Medium to large grains titanomagnetite and ilmenite. Cracks and granulation texture. Granulation starts in titanohematite. Medium hydrothermal alteration. Temperature is 148°C (I).

AUL 75.4.7: 521.3 m — Cation deficient titanomagnetite and ilmenite. Medium grains (15-30 μ dimension). Low hydrothermal alteration. Reflectivity of titanomagnetite alteration is 21.9%. Temperatures is 98°C (I).

AUL 77.4.6: 534.1 m — Deuteric oxidation in small grains titanomagnetite and ilmenite (5-20 μ dimension). The grains are in class 5 and 6. Occasional large grains. Hydrothermal solution altered ilmenite to rutile, titanohematite and sphene. Pseudobrookite in class 6 titanomagnetite altered to sphene. Low-medium hydrothermal alteration. Some spinels with reflectivity of 16.5%. Temperature is 160°C (A).

AUL 78.1.2: 536.8 m — Deuteric oxidation in titanomagnetite and ilmenite. Class 4 and 6. Grains are small. Some alteration to titanomaghemite and pseudorutile. Low hydrothermal alteration. Reflectivity of class 5 titanomagnetite is 21.4%, 22.8-25.2% and 18.2-19.4%. Temperature is 98°C (I).

AUL 78.1.5: 541.2 m — Medium to large grains titanomagnetite and ilmenite. Ilmenite contents in this section are exceptionally high. Titanohematite phase is present. Medium hydrothermal alteration. Red stain in the silicates around the opaque phases. Reflectivity of ilmenite alteration is 18.1-18.3%. Temperature is 98°C (I).

AUL 79.1.1: 541.3 m — Deuteric oxidation in titanomagnetite and ilmenite, class 4 and 5. Medium hydrothermal alteration. The grains are small to medium (10-30 μ dimension). Temperature is 100°C (I).

AUL 79.1.2: 541.3 m — Deuteric oxidation in titanomagnetite class 4 and 5. The grains are medium in their size (20-35 μ). Il-

menite, class 3 and 5 deuteric oxidation and occur as separate elongated grains. Both ilmenite and titanomagnetite are hydrothermally altered to titanohematite, rutile and granulation phase. Medium hydrothermal alteration. Temperature is 100°C (I).

AUL 82.1.4: 562.4 m — Deuteric oxidation in titanomagnetite class 3, 4, and 6. Occasional ilmenite. Both are hydrothermally altered to titanohematite, rutile and sphene. Medium hydrothermal alteration. Temperature is 145°C (I).

AUL 82.1.8: 563.8 m — Medium grains deuteric oxidation class 4 and 5 titanomagnetite. Fair amount of separate elongated ilmenite. Both ilmenite and titanomagnetite are hydrothermally altered. Low-medium hydrothermal alteration. Reflectivity of titanomagnetite is 16.0% and 14.6-16.2%. Temperature is 105°C (I).

AUL 83.2.4: 569.9 m — Medium grains titanomagnetite and ilmenite. Low hydrothermal alteration. Reflectivity of ilmenite alteration is 18.0-18.2%. Temperature is 105°C.

AUL 83.2.7: 574.8 m — Medium grains titanomagnetite and ilmenite. The grains are cracked and granulated. Ilmenite shows little alteration. Low to medium hydrothermal alteration. Reflectivity of ilmenite alteration is 17.8-18.1%. Temperature is 105°C (I).

AUL 84.2.5: 578.8 m — Deuteric oxidation class 4 and 5 titanomagnetite and ilmenite. The grains are small and hydrotherm-

ally altered to granulation phases. Medium hydrothermal alteration. Temperature is 145°C (I).

AUL 84.2.8: 581.2 m — Small to medium grains of titanomagnetite and ilmenite. Class 4 and 5 deuteric oxidation. Both phases are hydrothermally altered to sphene and titanohematite. High hydrothermal alteration. Temperature is 180°C (A).

AUL 85.1.3: 583.5 m — Deuteric oxidation class 4, 5 and 6 titanomagnetite. Separate ilmenite class 6 deuteric oxidation. Both phases occur in medium size and hydrothermally altered to titanohematite and sphene. Medium hydrothermal alteration. Temperature is 165°C (A).

AUL 85.1.6: 587.7 m — Medium to large grains titanomagnetite and ilmenite altered to titanomaghemite and pseudorutile. Some cation deficiency. Low hydrothermal alteration. Temperature is 42°C (I).

AUL 87.2.5: 597.2 m — Small grains titanomagnetite and ilmenite, class 4 and 6. Both are hydrothermally altered to sphene, rutile and titanohematite. High hydrothermal alteration. Temperature is 178°C (A).

AUL 87.2.6: 598.3 m — Deuteric oxidation in medium grains titanomagnetite. Class 4, 5 and 6. Separate ilmenite. The phases are hydrothermally altered to granulation phases. High hydrothermal alteration. Temperature is 185°C (A).

AUL 88.2.3: 604.5 m — Small-medium grains of titanomagnetite altered to titanomaghemite and titanohematite. Medium hydrothermal alteration. Temperature is 105°C (I).

AUL 89.1.5: 607.6 m — Medium grains titanomagnetite (25-35 μ dimension), altered to titanomaghemite and titanohematite. Occasional ilmenite. Medium hydrothermal alteration. Reflectivity of ilmenite alteration is 19.3% and 20.1% for titanomagnetite. Temperature is 168°C (A).

AUL 89.1.7: 611.0 m — Deuteric oxidation of titanomagnetite and ilmenite. Class 4 and 5. The grains are medium and hydrothermally altered to titanohematite, sphene and rutile. Medium-high hydrothermal alteration. Reflectivity of titanomagnetite class 3 is 16.9%. Temperature is 168°C (A).

AUL 89.2.4: 612.3 m — Medium-large grains titanomagnetite (30-60 μ dimension), altered to titanohematite and granulation phase. Occasional altered ilmenite. Medium-high hydrothermal alteration. Temperature is 165°C.

AUL 89.2.6: 612.3 m — Medium grains titanomagnetite show granulation texture with cracks. Occasional altered ilmenite. Medium-high hydrothermal alteration. Temperature is 168°C (A).

AUL 90.1.4: 618.3 m — Deuteric oxidation of titanomagnetite and ilmenite, class 3 and 4. Small-medium grains (10-35 μ). Occasional large grains of titanomagnetite. Medium

hydrothermal alteration. Reflectivity of ilmenite alteration is 20.0%. Temperature is 175°C (A).

AUL 90.1.8: 618.3 m — Large grains titanomagnetite in the 40-70 μ size range. Deuteric oxidation class 3 and 4. Fair amount of separate ilmenite in class 2, 4 deuteric oxidation. Medium hydrothermal alteration. Temperature is 175°C (A).

AUL 92.1.1: 626.9 m — Medium grains titanomagnetite altered to titanohematite. Few ilmenite grains altered to titanohematite and rutile. Medium hydrothermal alteration. Temperature is 168°C (A).

AUL 92.1.2: 626.9 m — Few grains of titanomagnetite and ilmenite. They are hydrothermally granulated. The grains are small-medium. Medium hydrothermal alteration. Reflectivity of titanomagnetite alteration is 23.6-27.7%. Temperature is 168°C (A).

AUL 93.1.4: 635.3 m — Medium-large grains titanomagnetite altered to granulation texture. Occasional ilmenite. Medium hydrothermal alteration. Temperature is 165°C.

AUL 93.1.8: 638.9 m — The grains are in very high state of hydrothermal alteration. Difficult to identify them. High hydrothermal alteration. Temperature is 200°C (A).

AUL 94.1.3: 641.0 m — Medium to large grains subhedral to anhedral titanomagnetite. Separate elongated ilmenite. Both show granulation phases. Medium to high hydrothermal alteration. Reflectivity of ilmenite alteration is 20.2%. Temperature is 175°C (A).

AUL 94.1.8: 644.1 m — Medium to large titanomagnetite and ilmenite. Both are hydrothermally granulated. Medium-high hydrothermal alteration. Some red stain in the silicates. Temperature is 188°C (A).

AUL 95.2.3: 648.3 m — Medium grains titanomagnetite altered to titanomaghemite and titanohematite. Medium to high hydrothermal alteration. Few ilmenite. Temperature is 175°C (A).

AUL 95.2.8: 650.5 m — Medium grains titanomagnetite hydrothermally altered to granulation phase. Fair amount of ilmenite with granulation phase and sphene. Medium-high hydrothermal alteration. Temperature is 188°C (A).

AUL 96.1.3: 651.1 m — Medium to large grains of titanomagnetite and ilmenite in deuteric oxidation state, class 5 and 6. Both phases are hydrothermally altered to granulation and sphene. High hydrothermal alteration. Red stain in the silicates. Reflectivity of titanomagnetite (class 4). Temperature is 190°C (A).

AUL 96.1.6: 655.5 m — Medium to large grains of titanomagnetite and ilmenite in medium-high hydrothermal alteration state. Red stain in the silicates. Reflectivity of titanomagnetite alteration is 23.3-27.2%. Temperature is 145°C (I).

AUL 97.5.2: 660.6 m — Deuteric oxidation, titanomagnetite and ilmenite class 4 and 5. The grains are medium and all hydro-

thermally altered to granulation phases and sphene. Medium-high hydrothermal alteration. Temperature is 178°C (A).

AUL 98.2.4: 665.3 m — Titanomagnetite and ilmenite in deuteric oxidation state class 4 and 6. The grains are large and partly or wholly altered to sphene and titanohematite. Red to yellow stain in the silicates around the opaque phases. Hydrothermal alteration, high in this section. Reflectivity of titanomagnetite alteration (class 3) is 18.0% and 15.2-17.0%. Temperature is 180°C (A).

AUL 98.2.6: 665.3 m — Large grains titanomagnetite and occasional ilmenite. Both in high hydrothermal alteration state. Temperature is 178°C. Reflectivity of ilmenite alteration state. Temperature is 178°C (A). Reflectivity of ilmenite alteration is 19.2%.

AUG 98.5.1: 665.3 m — Small-medium grains titanomagnetite. No ilmenite. Low-medium hydrothermal alteration. Temperature is 105°C (I).

AUS 98.5.7: 665.8 m — Small-large grains titanomagnetite. No ilmenite. High hydrothermal alteration. Temperature is 175°C.

AUL 99.1.1: 665.9 m — Small-large grains of titanomagnetite. Occasional ilmenite. Hydrothermally altered grains to granulation phases. Medium hydrothermal alteration. Temperature is 168°C (I).

AUL 99.1.6: 668.1 m — Large grains titanomagnetite, altered to titanohematite and sphene. Medium grains of ilmenite altered to titanohematite, rutile and sphene. High hydrothermal alteration. Red stain in silicates. Reflectivity of ilmenite alteration is 20.7%. Temperature is 170°C (I).

AUL 99.2.3: 671.2 m — Small-large grains titanomagnetite. Fairly abundant, medium grains ilmenite. The grains are partly altered to titanomaghemite, titanohematite, and pseudorutile. Low-medium hydrothermal alteration. Temperature is 76°C (I).

AUL 99.2.7: 671.8 m — Small-large grains titanomagnetite (5-60 μ dimension). Few ilmenites, medium grains. Low-medium hydrothermal alteration. Temperature is 76°C (I).

AUL 100.1.2: 674.5 m — Deuteric oxidation in titanomagnetite. Class 3 and 4. Medium grains of ilmenite in class 3 and 4 deuteric oxidation. Titanohematite, rutile and sphene are abundant as secondary phases. High hydrothermal alteration. Temperature is 175°C (A).

AUL 100.1.5: 676.5 m — Small-large grains of titanomagnetite and ilmenite in high deuteric oxidation state, class 3 and 4. Both show granulation texture and sphene. High hydrothermal alteration. Temperature is 188°C (A).

AUL 102.1.7: 681.9 m — Medium to large grains of titanomagnetite. Occasional ilmenite. High granulation phase distribution with cracks. Some red stain in silicates.

Medium hydrothermal alteration. Temperature is 168°C (I).

AUL 102.1.3: 681.9 m — Anhedral medium to large grains titanomagnetite (25-65 dimension). Occasional ilmenite. All grains are in high granulation state. However, some grains are just altered to titanomaghemite. Medium hydrothermal alteration. Temperature is 105°C (I).

AUL 103.2.4: 692.2 m — Small-medium grains of titanomagnetite. Few ilmenite. Some of the grains are in high granulation state texture. Some of the grains are altered to black sphene. Medium-high hydrothermal alteration. Reflectivity of titanomagnetite alteration is 23.0-27.1%. Temperature is 145°C (I).

AUL 103.2.7: 698.8 m — Anhedral medium grains of titanomagnetite. Medium elongated grains of ilmenite. Granulation phase, titanohematite and sphene. Red-yellow stain around the opaque phases and in the silicates. Medium-high hydrothermal alteration. Reflectivity of ilmenite alteration is 20.0-18.7%, 23.0-24.6%, and 21.0-18.6%. Temperature is 105°C (I).

AUL 105.3.3: 700.7 m — Small-large grains of titanomagnetite. Separate ilmenite grains. The grains are altered to granulation state, titanohematite and sphene. Medium-high hydrothermal alteration. Temperature is 105°C (I).

AUL 105.3.6: 700.7 m — Anhedral granulated titanomagnetite and ilmenite. Secondary titanohematite and sphene are also present. Medium-high hydrothermal alteration. Reflectivity of ilmenite alteration is 20.0-18.6%, 23.4-25.3%, and 21.1-20.9%. Temperature is 120°C (I).

AUL 108.1.3: 726.2 m — Anhedral grains of titanomagnetite in granulation texture state. Separate elongated ilmenite altered to granulation texture, titanohematite, rutile and sphene. Red stain in the silicates. High hydrothermal alteration. Temperature is 180°C (A).

AUL 108.1.6: 732.7 m — Deuteric oxidation as well as hydrothermal alteration in titanomagnetite and ilmenite. Titanomagnetite is anhedral and medium in size (20-35 μ). Ilmenite is separate elongated grain up to 40 μ dimension. Red stain in the silicates. High hydrothermal alteration. Temperature is 182°C (A).

AUS 110.1.2: 734.6 m — Medium grains of titanomagnetite in granulation texture state. Medium-high hydrothermal alteration. No ilmenite. Temperature is 165°C (I).

AUS 111.2.4: 739.9 m — Few grains medium titanomagnetite in high hydrothermal alteration state. No ilmenite. Temperature is 155°C (A).

AUS 111.2.8: 744.2 m — Small-large grains titanomagnetite. Some deuteric oxidation class 4 in the large grains. Medium hydrothermal alteration, titanohematite and rutile. No ilmenite. Temperature is 120°C (I).

AUL 112.1.4: 745.5 m — Medium to large grains titanomagnetite, anhedral-subhedral forms. Occasional ilmenite. Medium-high hydrothermal alteration. Temperature is 168°C (I).

AUL 113.1.1: 753.1 m — Medium to large grains titanomagnetite and separate ilmenite, all in medium-high hydrothermal alteration state. Temperature is 175°C (A).

AUL 113.1.8: 757.1 m — Deuteric oxidation titanomagnetite and ilmenite. Titanomagnetite is in class 3 and 4 and in medium grains. Ilmenite, is anhedral up to 25 and in class 2 and 3. Low hydrothermal alteration. Reflectivity of titanomagnetite class 5 is 21.8%, 22.4-25.0%, and 18.8-20.1%. Temperature is 72°C (I).

AUL 114.1.3: 758.0 m — Medium to large grains titanomagnetite in deuteric oxidation state, class 4 and 5. Ilmenite, separate and elongated grain. Titanomaghemite and pseudo-rutile. Low hydrothermal alteration. Temperature is 72°C (I).

AUL 116.1.6: 770.2 m — Most of titanomagnetite grains are small. Occasional large grains. Few ilmenites. All the grains are in deuteric oxidation state, class 3 and 4. Low hydrothermal alteration, some medium hydrothermal alteration. Temperature is 72°C (I).

AUL 116.1.7: 776.4 m — Large grains titanomagnetite up to 70 μ dimension occasional ilmenite. Some replacement of titano-magnetite to titanomaghemite and ilmenite to il-menite type (2). Low hydrothermal alteration.

Some high hydrothermal alteration. Reflectivity of titanomagnetite alteration is 22.6%. Temperature is 72°C (I).

AUL 118.1.1: 785.3 m — Small grains of titanomagnetite and occasional large grains. Few ilmenite. All the grains are in high hydrothermal alteration. Temperature is 178°C (A).

AUL 118.1.2: 785.3 m — Mostly small grains titanomagnetite. Occasional phenocrysts. Very few ilmenite grains. The grains all in high hydrothermal alteration state. Temperature is 178°C (A).

AUL 120.1.4: 799.8 m — Small-medium grains titanomagnetite in the range of 5-25 μ. Occasional ilmenite. High hydrothermal alteration. Temperature is 190°C (A).

AUL 122.3.1: 811.9 m — Medium grains of titanomagnetite. Occasional ilmenite. The grains are in high granulation state. Medium-high hydrothermal alteration. Temperature is 168°C (A).

AUL 122.3.2: 813.2 m — Large and skeletal grains of titanomagnetite up to 80 μ size dimension. Ilmenite also in large grains (60-80). Medium to low hydrothermal alteration. Temperature is 75°C (I). Reflectivity of skeletal titanomagnetite is 16.4%.

AUL 124.1.8: 825.8 — Two generations of titanomagnetite. Small to medium size (15-25 μ) and large type (60-80 μ). Ilmenite in large grains, elongated form up to 60 μ. Medium

hydrothermal alteration. Temperature is 72°C (I). Reflectivity of ilmenite alteration is 17.0-17.2%.

AUL 129.2.1: 856.8 m — Two generations of titanomagnetite, small-medium generation and large type generation. Ilmenite occurs in large grains. Medium hydrothermal alteration. Reflectivity of ilmenite alteration is 18.1-18.4%. Temperature is 125°C (I).

AUL 129.2.2: 858.6 m — Two generations of titanomagnetite, small type and large type. Ilmenite occurs as elongated separate grains. Medium hydrothermal alteration. Reflectivity of ilmenite alteration is 18.1-18.3%. Temperature is 168°C (A).

AUL 131.1.1: 867.3 m — Skeletal and small-medium titanomagnetite. Ilmenite, medium elongated grains. Low-medium hydrothermal alteration. Reflectivity of titanomagnetite alteration is 22.0%. Temperature is 72°C (I).

AUL 131.1.8: 877.5 m — Anhedral-skeletal titanomagnetite. Some of the grains are large. Lepidocrosite occasionally. Ilmenite as separate elongated grains. Medium hydrothermal alteration. Temperature is 125°C (I).

AUL 134.1.4: 883.7 m — Anhedral-skeletal grains of titanomagnetite in class 4 deuteric oxidation. Occasional ilmenite. Medium to high hydrothermal alteration. Temperature is 125°C (I).

AUL 134.1.6: 884.3 m — Large skeletal titanomagnetite. Occasional ilmenite. Low-medium hydrothermal alteration. Temperature is 72°C (I).

AUL 135.1.3: 894.1 m — Large and small skeletal titanomagnetite grains. Occasional large ilmenite grains. Medium hydrothermal alteration. Reflectivity of ilmenite alteration is 18.0-18.2%. Temperature is 125°C (I).

AUL 135.1.5: 898.5 m — Anhedral large grains of titanomagnetite. Fairly good amount of ilmenite grains. Medium hydrothermal alteration. Temperature is 125°C (I).

AUL 136.1.5: 900.4 m — Anhedral, large grains of titanomagnetite and elongated separate ilmenite. High hydrothermal alteration. Temperature is 170°C (A).

AUL 136.1.8: 900.4 m — Few very high alteration of opaque phases. Temperature is 188°C (A).

AUL 137.1.3: 907.4 m — Skeletal and anhedral grains of titanomagnetite. Separate, elongated large ilmenite. Medium hydrothermal alteration. Reflectivity of ilmenite alteration is 18.9-19.2%. Temperature is 125°C (I).

AUL 137.1.5: 911.5 m — Skeletal grains of titanomagnetite. Ilmenite occurs in large grains. Medium hydrothermal alteration. Reflectivity of ilmenite alteration is 19.1-19.4%. Temperature is 125°C (I).

AUL 138.1.2: 913.2 m — Skeletal-medium grains of titanomagnetite. Some spinels. Occasional ilmenite. Red stain in the silicates. Medium hydrothermal alteration. Temperature is 125°C (I).

AUL 138.1.4: 917.8 m — Skeletal titanomagnetite. Medium-large grains. Fairly abundant ilmenite. Spinel occur. Low hydrothermal alteration. Reflectivity of titanomagnetite is 16.6%. Temperature is 18°C (I).

AUL 138.1.6: 917.8 m — Skeletal-anhedral titanomagnetite. Slight alteration to titanomaghemite. Few ilmenite. Low hydrothermal alteration. Temperature is 18°C (I).

AUL 138.1.10: 924.2 m — Titanomagnetite in large elongated grains and skeletal type. Occasional ilmenite. Low hydrothermal alteration. Reflectivity of titanomagnetite is 15.4%. Temperature is 18°C (I)

AUL 142.1.3: 939.7 m — Few grains titanomagnetite. High hydrothermal alteration. Temperature is 185°C (A).

AUL 142.1.6: 940 m — Skeletal and anhedral titanomagnetite. Few ilmenites. Low-medium hydrothermal alteration. Temperature is 72°C (I).

AUL 143.1.3: 947.3 m — Small skeletal and large altered titanomagnetite. Ilmenite, rare. Medium hydrothermal alteration. Pyrrhotite occur. Temperature is 125°C (I).

AUL 143.1.8: 950.2 m — Skeletal and large grains altered titanomagnetite. Ilmenite rare. Growth of magnetite and hematite. Medium hydrothermal alteration. Temperature is 125°C (I).

AUL 144.1.3: 952.8 m — Skeletal, anhedral, fairly large grains of titanomagnetite. Ilmenite, rare. Medium hydrothermal alteration. Temperature is 125°C (I).

AUL 144.1.8: 956.7 m — Large skeletal grains and anhedral of titanomagnetite and ilmenite. Medium hydrothermal alteration. Reflectivity of ilmenite alteration is 21.2-19.0%, 22.6-24.1%, and 21.7-20.7%. Reflectivity of titanomagnetite alteration is 22.0%. Temperature is 158°C (A).

AUL 146.1.6: 969.0 m — Large skeletal grains of titanomagnetite. Fairly abundant ilmenite. Low-medium hydrothermal alteration. Temperature is 78°C (I).

AUL 146.1.8: 969.8 m — Skeletal titanomagnetite grains. Occasional ilmenite. Pyrite occurs as anhedral grain. Medium hydrothermal alteration. Temperature is 125°C (I).

* Temperatures in this study are calculated as follows:

1. In the zones 600-700 m and 325-360 m, where close agreement exists between in-hole measured and isotopic calculated temperatures, the average of both is always taken. This is referred to as T(A)°C.

2. When the difference between in-hole measured and maximum isotopic calculated temperatures exceeds 20°C, either the isotopic temperature or the theoretical stability data (Verhoogen, 1962) is used as a guide. T(H)°C is the in-hole measured temperature and T(I)°C is the isotopic calculated temperature.

APPENDIX II

Rock Magnetism and Paleomagnetism

SAMPLE	DEPTH m	CURIE TEMP. °C	K[a]	Q[b]	NRM[c]	J_{200}/J_0[d]	I_o[e]	I_s[f]
AUL 1-1-1	56.7	532						
AUL 2.1.3	76.2	200-391-572						
AUL 2.1.5	99.1	232-580						
AUG 3.1.2	147.9	403-556						
AUG 5.1.1	155	360-528						
AUL 6.1.3	159.4	565						
AUL 6.1.7	165	556						
AUL 8.1.2	170.1	546	15.6	1.5	10.7	0.18	86.8	73.8
AUL 8.1.9	170.2	507	15.5	2.3	16.1	0.05	54.5	66.0
AUL 8.5.2	171.9	418-586			24.1	0.73	58.0	60.0
AUL 8.5.7	174.7	297-506-664			18.8	0.01	52.5	52.1
AUL 11.2.2	186.1		13.6	3.3	13.3	0.07	55.3	42.7
AUL 11.2.7	195.5	517	11.4	3.3	17.2	0.26	49.7	47.4
AUL 13.2.2	197.2	573						
AUL 13.4.1	199.8	506			18.5	0.33	35.9	23.5
AUL 13.4.3	199.9				20.8	0.05	53.0	51.2
AUL 14.1.1	200.9	547	8.1	3.7	13.5	0.28	38.6	34.6
AUL 14.1.5	201.2	556						
AUL 14.1.6	203.7	548	11.2	2.1	10.3	0.03	57.6	51.3
AUL 18.1.1	223.7		13.6	2.1	12.9	0.24	29.7	21.0
AUL 19.2.2	231.6	599	10.5	4.3	20.3	0.73	36.0	36.3
AUL 19.2.6	235.5	547	14.5	2.7	17.6	0.53	32.3	25.3
AUL 20.1.1	236.5		14.2	0.9	5.9	0.04	89.5	76.0
AUL 20.3.4	241.9	543	8.4	2.9	10.8	0.22	40.2	30.2
AUL 20.3.8	247.8		8.6	3.8	14.9	0.07	44.4	28.6

AUL 22.1.2	249.1	524						
AUL 22.1.7	251.1	552						
AUL 22.2.2	251.5		8.1	2.7	9.9	0.10	45.4	48.0
AUL 22.2.7	256.3		5.7	4.5	11.7	0.06	49.3	39.2
AUL 24.1.1	257.4	570						
AUL 25.6.7	266.1	512						
AUL 30.4.2	291.1		0.1	5.6	0.25	0.96	49.0	50.3
AUL 31.1.2	292.3		0.1	12.0	0.54	0.96	50.5	49.8
AUL 31.1.6	296.2		0.33	2.4	0.35	0.46	46.0	44.8
AUL 38.3.7	332.1		7.8	6.7	23.3	0.44	66.4	71.1
AUL 39.2.7	334.3	552						
AUL 40.1.1	337.5		17.0	1.7	12.8	0.13	83.0	71.5
AUL 40.1.2	337.9		23.8	1.1	11.9	0.09	72.5	60.1
AUL 41.1.2	341.4		7.4	11.8	39.3	0.25	60.6	59.4
AUL 41.1.7	342.1		11.2	3.5	17.7	0.46	67.0	68.0
AUL 42.2.4	348.3		6.5	3.0	8.7	0.61	67.6	65.3
AUL 42.2.7	351.6		11.7	1.0	5.5	0.40	64.9	63.3
AUL 45.1.2	366.5	582						
AUL 45.1.7	367.1	575						
AUL 46.2.7	370.8		20.7	2.9	26.9	0.08	77.2	75.0
AUL 46.2.8	372.1		17.1	0.75	5.8	0.66	46.1	32.6
AUL 49.1.2	383.1	551						
AUL 49.3.1	385.6	556	11.1	1.5	7.6	0.16	41.7	54.2
AUL 49.3.6	387.6	556	6.1	3.5	9.7	0.08	48.6	51.3
AUL 51.2.1	396.3	533	24.5	0.65	7.2	0.08	30.4	49.3
AUL 51.2.8	397.9		21.8	1.0	10.3	0.06	51.9	49.0
AUL 52.4.5	402.7	571						
AUL 52.4.8	403.3	566						
AUL 54.1.4	411.1	556	11.7	2.1	10.8	0.37	52.2	43.5
AUL 54.1.5	413.6	563	10.2	3.2	14.5	0.30	47.8	41.3
AUL 55.1.9	418.8	597	19.4	1.2	10.5	0.20	39.5	41.3
AUL 55.1.10	424.1		2.4	25.7	28.1	0.65	42.0	42.7

AUL 61.3.4	448.8	580						
AUL 61.3.8	450.7	564						
AUL 62.2.3	453.9	563						
AUL 62.2.7	455.8	510						
AUL 66.4.3	475.2		4.1	8.2	15.2	0.64	58.1	56.8
AUL 66.4.7	476.1	509	17.5	0.75	5.9	0.24	66.7	
AUL 68.1.3	481.8	560						
AUL 69.7.3	490.7		9.8	6.8	30.1	0.47	44.1	44.7
AUL 69.7.6	491.2		8.6	5.4	21.0	0.59	52.5	53.4
AUL 71.3.2	500.9	571						
AUL 73.2.2	508.7		8.8	3.6	14.0	0.72	52.4	51.8
AUL 73.2.8	511.6	548	14.2	0.79	5.1	0.37	66.8	44.2
AUL 75.4.3	521.3		18.6	0.56	4.7	0.39	21.2	
AUL 75.4.7	521.6	507	20.1	0.71	6.5	0.09	71.8	
AUL 77.4.6	534.1	562						
AUL 78.1.2	536.8	558	8.2	1.2	4.5	0.42	58.5	54.3
AUL 78.1.5	541.2	512	12.4	0.94	5.2	0.04	69.9	65.3
AUL 79.1.2	541.3	589						
AUL 82.1.4	562.4		8.4	2.4	9.1	0.42	68.6	78.2
AUL 82.1.8	563.8	547	11.9	1.1	5.8	0.12	56.8	68.9
AUL 83.2.4	569.9	532						
AUL 83.2.7	574.8	523						
AUL 84.2.5	578.8	576	10.7	2.6	12.6	0.44	56.8	55.4
AUL 84.2.8	581.2	596	15.7	1.1	7.6	0.36	57.1	52.6
AUL 85.1.3	583.5	580						
AUL 85.1.6	587.7	517						
AUL 87.2.6	598.3	574	9.6	4.0	17.2	0.48	59.4	60.4
AUL 87.2.8	600.2	536	15.8	1.2	8.2	0.40	64.3	58.1
AUL 88.2.3	604.5	523						
AUL 89.1.5	607.6	573	17.7	2.8	22.3	0.43	80.6	78.3
AUL 89.1.7	611.0	548	10.5	4.4	20.9	0.33	80.0	78.1

AUL 90.1.4	618.3		8.6	7.5	29.1	0.53	57.7	56.8
AUL 90.1.8	618.9	557	10.0	8.5	38.3	0.42	57.7	54.9
AUL 92.1.2	626.9	580						
AUL 93.1.4	635.3	570	18.5	1.0	8.6	0.14	61.9	60.1
AUL 93.1.8	638.9		14.3	1.6	10.4	0.26	81.7	52.2
AUL 94.1.3	641.0	551						
AUL 95.1.2	648.3	556	15.5	0.9	6.4	0.14	59.7	49.6
AUL 95.2.8	650.5		5.2	16.2	38.1	0.04	56.2	52.3
AUL 95.3.4	650.8	581						
AUL 96.1.3	651.5	570						
AUL 96.1.6	655.6	556						
AUL 97.5.1	660.5		4.6	3.0	6.2	0.58	74.9	72.2
AUL 97.5.2	665.3	560						
AUL 98.2.4	665.3	559						
AUL 98.2.6	665.6	566						
AUS 98.5.1	665.9	570						
AUL 99.1.1	666.2		8.8	1.0	4.1	0.29	54.9	27.3
AUL 99.1.6	668.1		11.5	1.2	6.3	0.35	59.0	55.9
AUL 100.1.2	674.5		1.2	7.5	4.0	0.73	58.6	56.8
AUL 100.1.5	676.5		3.0	3.3	4.5	0.66	56.7	58.0
AUL 102.1.3	681.9	570						
AUL 102.1.7	687.1	560						
AUL 103.2.4	692.2	585	8.1	2.5	8.9	0.17	68.3	55.8
AUL 103.2.7	698.8		15.1	2.0	13.4	0.10	72.1	52.8
AUL 105.3.6	700.7	554						
AUL 108.1.3	726.2	574	5.3	5.3	12.6	0.43	61.1	65.3
AUL 108.1.6	732.7		4.3	6.0	11.5	0.44	55.2	54.0
AUS 110.1.2	734.6	545						
AUL 111.2.4	739.9		15.3	0.69	4.8	0.05	50.8	53.3
AUL 111.2.8	744.2		13.9	0.97	6.1	0.11	74.0	44.9
AUL 112.1.4	745.5	560						
AUS 112.2.8	746.7	544						

AUL 113.1.1	753.1	566	4.8	11.5	24.7	0.05	59.1	59.4
AUL 113.1.8	757.1	577	9.5	5.3	22.7	0.41	51.1	53.3
AUL 116.1.7	776.4	541						
AUL 118.1.1	785.3	562						
AUL 118.1.2	785.6	555						
AUL 120.1.4	799.8	570	19.6	1.3	11.1	0.16	73.1	59.3
AUL 120.1.8	799.8	579	21.9	1.2	11.4	0.18	66.3	58.4
AUL 122.3.2	813.2	543						
AUL 124.1.2	821.7	498	13.8	2.5	15.6	0.31	63.8	56.5
AUL 124.1.8	825.8		11.0	3.0	14.7	0.20	71.8	62.7
AUL 129.2.1	856.8	580						
AUL 129.2.2	858.6	571						
AUL 131.1.1	867.3	551	6.4	3.8	11.1	0.07	59.8	71.3
AUL 131.1.8	877.5	559	5.3	8.8	21.2	0.07	74.9	72.5
AUL 134.1.6	884.3	569						
AUL 135.1.3	894.1	536	4.4	4.7	9.2	0.21	54.6	68.5
AUL 135.1.5	898.5	557	7.1	3.3	10.7	0.07	73.8	68.6
AUL 136.1.8	900.4	576						
AUL 137.1.3	907.4	554	5.4	10.3	25.2	0.15	67.2	66.6
AUL 138.1.2	913.2	570						
AUL 138.1.4	917.8	537						
AUL 138.1.6	919.8		4.6	5.1	10.5	0.08	80.8	58.1
AUL 138.1.10	924.2	550	6.3	6.0	17.1	0.04	77.0	67.8
AUL 142.1.6	940	523						
AUL 143.1.3	947.3	556	8.6	12.0	46.4	0.14	72.2	73.5
AUL 143.1.8	950.2	546	7.9	8.1	28.5	0.10	70.9	76.6
AUL 144.1.3	952.8	541						
AUL 144.1.8	956.7	573						
AUL 146.1.3	969.0		10.2	4.2	19.0	0.06	60.9	66.0
AUL 146.1.8	969.6	532	4.6	3.3	6.8	0.16	68.0	72.9

(a) Initial susceptibility (10^{-4} emu.oe^{-1}g^{-1})

(b) Konigsberger ratio (the ratio between remanent to induced magnetization, $Q = \frac{NRM}{kF}$, F is the ambient field taken as 0.45 oe for the Azores area)

(c) Natural remanent magnetization (10^{-4} emu.g^{-1})

(d) J_{200} is the magnetic intensity measured after demagnetization in 200 oe AF. J_0 is the natural remanent magnetization. The ratio J_{200}/J_0 is taken as a measure of the hardness of remanence.

(e) Natural remanent magnetization inclination.

(f) Stable inclination after demagnetization in an AF.

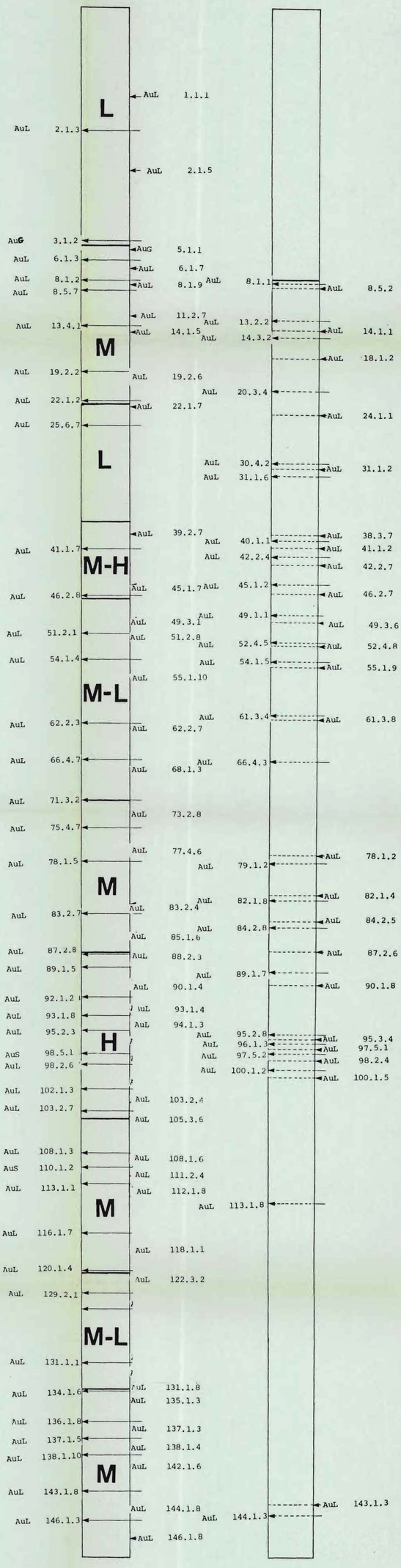

L low degree hydrothermal alteration

M medium degree hydrothermal alteration

H high degree hydrothermal alteration

M-L medium-low degree hydrothermal alteration

M-H medium-high degree hydrothermal alteration

Figure 25: Samples with hydrothermal alteration (class 1 only) in the Azores drill core.

Figure 22: Samples with deuteric oxidation in the Azores drill core.

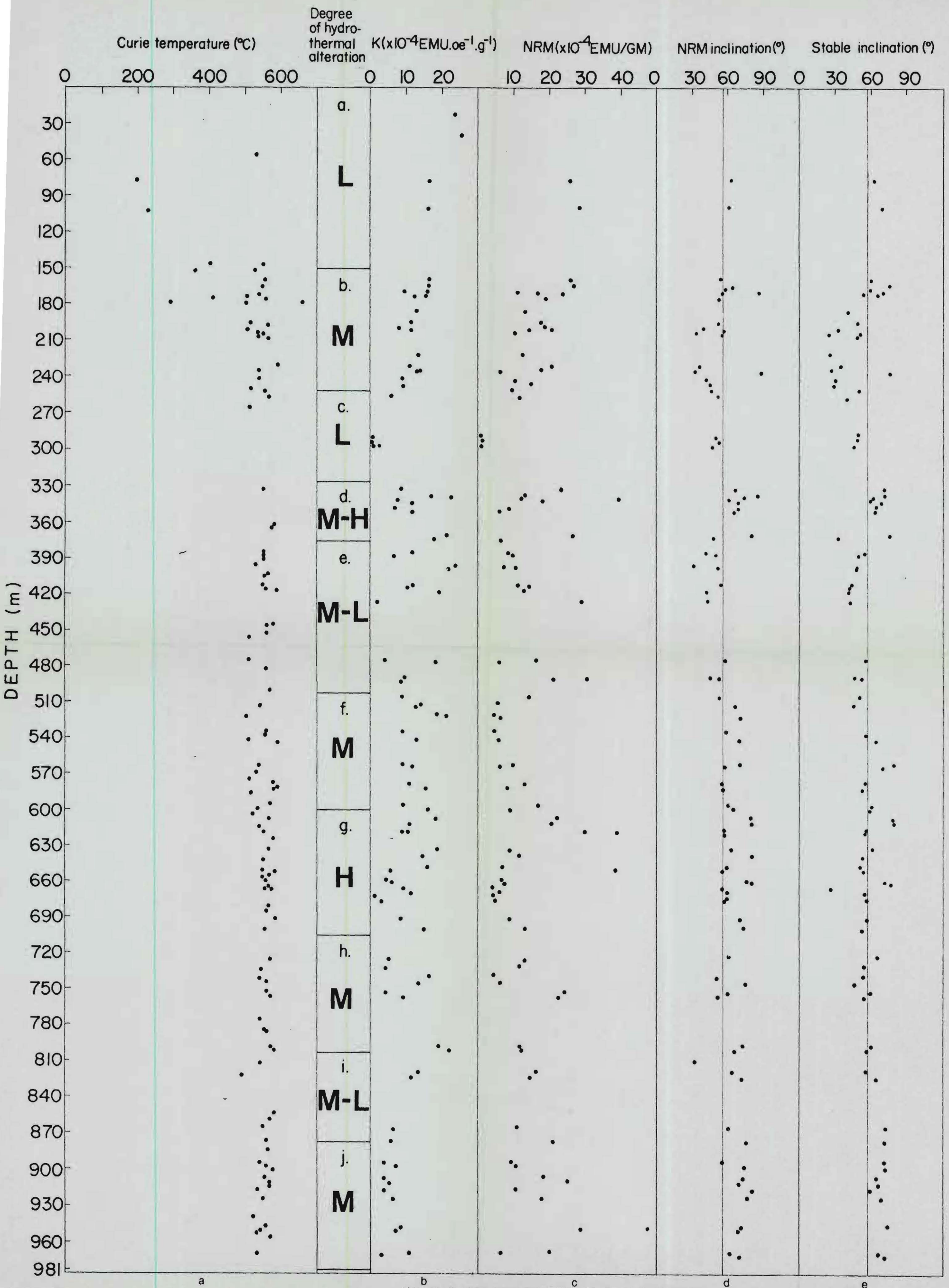

Figure 42: Correlation between Curie temperatures, Initial susceptibility, NRM intensities, NRM inclination and depth in the Azores drill core